TARTU RIIKLIKU ÜLIKOOLI TOIMETISED
UCHENYE ZAPISKI
TARTUSKOGO GOSUDARSTVENNOGO UNIVERSITETA

Scientific Notes of Tartu State University (Founded in 1893)
Issue 195

Transactions on Air Ionization and Electroaerosols
(Trudy po aeroionizatsii i elektroaerozolyam)

Vol. II

H.F. Tammet

THE ASPIRATION METHOD FOR THE DETERMINATION OF ATMOSPHERIC-ION SPECTRA

(Aspiratsionnyi metod izmereniya spektra aeroionov)

Tartu 1967

Translated from Russian

Israel Program for Scientific Translations
Jerusalem 1970

TT 68-50499

Published Pursuant to an Agreement with
THE NATIONAL SCIENCE FOUNDATION, WASHINGTON, D.C.

IPST Cat. No. 5363
UDC 551.508.941.3
621.317.792

Translated by A. Honigbaum
Edited by B. Benny

Printed in Jerusalem by Keter Press
Binding: Wiener Bindery Ltd., Jerusalem

Available from the
U.S. DEPARTMENT OF COMMERCE
Clearinghouse for Federal Scientific and Technical Information
Springfield, Va. 22151

IX/3/3

Table of Contents

The first chapter of the present monograph deals with the general theory of the aspiration method. The requirements imposed on the measuring capacitor are rendered more stringent, possibilities of measuring integral quantities with the aid of differential counters are indicated and new variants of the method of modulating the air-ion current in the measuring capacitor are suggested.

In the second chapter the systematic measurement errors are investigated and the range of application of the aspiration method determined. Empirical relationships are developed which suffice for the quantitative estimation of the essentially nonlinear edge effect. The distorting effects caused by an increase in the air-ion concentration, the asymmetry of the measuring capacitor, and the mass of air ions are calculated. A theory is developed for the resolving power of the counter which is limited by diffusion and turbulence. The last portion of the chapter deals with the adsorption of air ions at the counter inlet.

The third chapter starts with an analysis of the methods employed in measuring the air-ion current. A quantitative estimation of the counter sensitivity is carried out in order to specify the requirements for the stability of the voltage supply. The spectrum measurements under conditions of fluctuating air-ion concentrations are discussed on the basis of special observation results. Allowance is made for design calculations and the optimization of the counter parameters. The closing sections give a survey of the different designs of the aspiration counter along with a description of the SAI-TGU-66 universal aspiration counter.

INTRODUCTION

The study of ionized air and aerosols is of interest for science and technology. Ionized air and charged aerosols are employed, for example, in electrostatic precipitators, electrostatic painting, neutralization of static electricity, electrophotography, etc. The characteristics of the special air-ion distribution are studied in the physics of the atmosphere /Tverskoi,1962/. According to data of 1957 the conductivity of atmospheric air was recorded outside the USSR by 36 stations /Israël, 1957a/. Air ions are further of significance in hygiene /Minkh, 1963/ and medicine /Portnov, 1960/.

Major emphasis is laid upon the determination of the size spectrum of the submicroscopic aerosol particles. One of the most promising methods is the measurement of the electric mobilities of the particles /Fuks, 1955; Junge, 1955, 1963; Green, Lane, 1964/. The particle size spectrum is then calculated from the mobility spectrum /Metnieks, Pollak, 1961; Fuchs, 1963; Fuks, Stechkina, 1963/.

The aspiration method is the most universal and widespread method for measuring the concentration and mobility of air ions. Other methods for measuring mobility have limited application only. For the measurement of gas-ion mobilities one often uses ac methods, which are reviewed by Loeb/Loeb, 1960/. The application of ac methods is limited to the measurement of light air ions which in most cases is effected under laboratory conditions. Ac methods proved to be suitable for the measurement of the ion mobility in the rarefied upper layers of the atmosphere /Bragin, 1962, 1963/. The mass-spectrographic measurement method of the ionic composition of gases /Istonin, 1959; Narcisi, Bailey, 1956/ is applicable under rarefied-gas conditions.

The recently developed pulse method /Fedorov, 1952; Tsvang, 1956; Tsvang, Gutman, 1958/ yields interesting data on the spectral distribution of mobilities of light ions in atmospheric air /Tsvang, Komarov, 1959; Komarov, Kuzmenko, Seredkin, 1960/. For the study of the mobility spectrum of heavy ions, however, the pulse method and the ac methods are considered to be unsuitable /Komarov, Seredkin, 1960/.

Some simplified methods for air ion concentration measurement are also known /Korsunskii, Reznik, Truten', 1962a, 1965b; Chernyavskii, 1962; Tammet, 1962a/. However, these methods provide only rough approximations and are quite limited in application.

The first ideas relating to the aspiration method were published toward the end of the last century /Giese, 1882/. The work of J. J. Thomson and coworkers /Thomson, J. J., Rutherford, 1896; McClelland, 1898; Rutherford, 1899; Zeleny, 1901/ greatly contributed to the development of the aspiration method.

Notwithstanding its long history, the theory of aspiration counters has recently experienced vital impetus resulting from modern achievements in the measurement of weak currents, thus opening new possibilities for the study of air ions. The use of artifical ionization has led to the development of measurement methods at increased space charge densities and mobilities. The extension of the measurement range allows one to deal with side-effects in the measuring capacitor, which hitherto were not accounted for and which may considerably distort the measurement results. From the above considerations it thus follows that the theory of measurement methods must be rendered more rigorous.

The known devices for the air ion spectrum measurement are unsatisfactory and their sensitivity and resolving power are inadequate for many problems. For example, the structure of the distribution spectrum of atmospheric ions has hitherto not been properly investigated. It is difficult to say to what extent this situation is due to basic limitations and to what extent to the imperfection of the instruments. To estimate the adequacy of a counter design, information is required on the dependence of the functional properties of the instrument on the design parameters. Although some success has been achieved in the study of this problem /Gubichev, 1960; Komarov, 1960a, 1960b; Seredkin 1960; Siksna, Lindsay, 1961/, the available information does not suffice for detailed counter design calculations.

The present work considers measuring methods in which the precipitation of air ions in the measuring capacitor is electrometrically recorded. However, most of the results may be applied to the recording and study of the precipitated particles with the aid of optical or electronic-optical methods /Rohmann, 1923; Lipscomb, Rubin, Sturdivant, 1947; Gillespie, Langstroth, 1952; Hinkle, Orr, Dalla Valle, 1954; Litvinov, Litvinova, 1955; Sergeeva, 1958; Gillespie, 1960; Challande, David, 1960/ or with the aid of radioactive radiation /Gerdien, 1907; Wilkening, 1952; Bergstedt, 1956; Stievstadt, Papp, 1960; Matulyavichene, 1962; Styro, Matulyavichene, 1965; Fontan, Billard, Blanc, Bricard, Huertas, Marty, 1966; Wilkening, Kawano, Lane, 1966; Styro, Pestov, 1968/. The similarity between processes taking place in aspiration devices for measuring aerosols and those in devices for the electrostatic precipitation of aerosols for clean-air maintenance /Riezler, Kern 1959/ affords certain results a wider range of application.

In attempting to present the subject matter in the most systematic manner, the author has fully covered the problems related to the considered theme with the exception of some specific problems for which references are given.

The electrostatic system of units (CGSE), which is traditionally used when describing the movement of ions and charged aerosol particles in air, has been employed throughout the book.

The author would like to take the opportunity to express his gratitude to coworkers at the Air-Ionization and Electroaerosol Laboratory of the Tartu State University for their cooperation. Particular thanks go to Ya. I. Salm for his constant attention and useful remarks.

Chapter I

THE THEORY OF THE ASPIRATION METHOD UNDER IDEAL CONDITIONS

§1. AIR IONS

The fundamental views on the mechanism of electrical conductivity of air were established at the beginning of our century, mainly by Giese /Giese, 1882/ and J. J. Thomson /Thomson, J. J., Rutherford, 1896/. An extensive review of the earlier work may be found in the well-known monograph by Wiedemann /Wiedemann, 1885/.

The electrical conductivity of air is associated with the presence of charged particles capable of moving in an electric field. Elementary ionization events create positively charged ions and free electrons. However, the lifetime of free electrons and of monomolecular ions in air at atmospheric pressure is very short. Free electrons and monomolecular ions play an appreciable role only in very fast processes, for the investigation of which the aspiration method is not suitable for various reasons. Neutral molecules attach themselves to the initially charged particles and a bond is formed by electrical and molecular forces. The relatively stable particles formed in this way are called light air ions. Little is known about the internal structure of the light air ions /Israël, 1957b/. Segal /Segal, 1962/ tried to calculate theoretically the probability of formation of light air ions with different structures.

Light air ions are essential in the conductivity mechanism of atmospheric air.

Soon after the establishment of the ionic theory of air conductivity, the existence of larger charge carriers was discovered / Townsend, 1898; Lenard, 1900; Langevin, 1905a, 1905b/; these were called heavy air ions. Heavy air ions are formed as a result of the attachment of light air ions to aerosol particles contained in air. By their nature, heavy air ions are not ions in the usual sense, but solid or liquid charged particles suspended in air which remain stable even after losing their charge.

In atmospheric electric phenomena the heavy air ions act as spaced charge carriers.

Light and heavy air ions move with different velocities in an electric field. For the study of electric currents in air, the different nature of the charge carriers has no significance and it suffices to characterize the air ions in terms of their mobility only. It is therefore advisable to describe the light and the heavy air ions from a common point of view, using the general term air ions.

In the field of atmospheric electricity one usually uses the term atmospheric ions, which has the same significance and may be

considered as synonymous to the term air ions. However, to denote charged particles formed in laboratory or industry the term air ions is more suitable.

The mean velocity of an air ion in an electric field is proportional to the field strength $\vec{E}$:

$$\vec{v} = \dot{k}\vec{E}. \tag{1.1}$$

For the lightest air ions, relation (1.1) is applicable only at field strengths up to 10 kV/cm /Mitchell, Riedler, 1934; Balog, 1944/.

The mobility $\dot{k}$ of an air ion is by definition positive for positively charged and negative for negatively charged air ions. Usually, the absolute value of $\dot{k}$ is taken as the mobility of air ions. To simplify notation we shall adopt the following convention. If some quantity x has a subdot, then

$$|\dot{x}| = x. \tag{1.2}$$

Thus the letter k (without the subdot) stands for the mobility of air ions in the usual sense. The use of dotted letters for polar quantities is analogous to the vector notation: $|\vec{x}| = x$.

The largest particles that can be considered air ions are those for which gravity and inertia forces are still negligible. A sufficient condition for this is evidently

$$m \ll \frac{qE}{g + k\left|\frac{d\vec{E}}{dt}\right|}, \tag{1.3}$$

where m is the mass of the particle, g is the gravitational acceleration, and q is the absolute value of the particle charge.

This description of an air ion is satisfactory if the chemical nature and the mass of the charge carriers have no significance, as when considering processes in air. In many cases, however, the chemical nature and the mass of the particles cannot be neglected, but such problems are of secondary significance in our analysis.

The usual measuring methods give only the macroscopic parameters of ionized air. Charges of individual ions are undetectable. It is therefore advisable to characterize ionized air in terms of parameters which are independent of the air-ion charges.

Ionized air is characterized by the differential mobility distribution function of charge density, or by the differential mobility spectrum

$$\varrho(\dot{k}) = \frac{d\varrho}{d\dot{k}}, \tag{1.4}$$

where $d\varrho$ is the charge density due to air ions with mobilities between $\dot{k}$ and $\dot{k} + d\dot{k}$.

The distribution function $\varrho(\dot{k})$ is positive for positive $\dot{k}$ and negative for negative $\dot{k}$. One often uses the spectrum $\varrho(k)$, which is the absolute values of $\varrho(\dot{k})$ as defined by (1.2). $\varrho(k)$ describes only the spectrum of air ions of

one polarity. To describe spectra of air ions of both polarities one has to introduce the two functions $\varrho_+(k)$ and $\varrho_-(k)$. The mobility spectrum of air ions of both polarities is denoted by $\varrho_\pm(k)$. If air ions of only one polarity are considered, and the polarity is of no significance, the subscript $\pm$ may be omitted.

The charge density in the interval (k_1, k_2) is determined by the integral over the distribution function

$$\varrho(k_1, k_2) = \int_{k_1}^{k_2} \varrho(k)\,dk. \tag{1.5}$$

Similarly one finds the density of the negative charge $\varrho_- = \varrho(-\infty, 0)$, the density of the positive charge $\varrho_+ = \varrho(0, \infty)$ and the total charge density $\varrho = \varrho(-\infty, \infty)$.

The current density spectrum (or distribution function) in still air is expressed in terms of $\varrho(k)$ as follows.

$$\vec{j}(k) = \vec{v}\varrho(k) = k\varrho(k)\vec{E} = \lambda(k)\vec{E}. \tag{1.6}$$

We shall call $\lambda(k) = k\varrho(k)$ the conductivity spectrum. Integration of $\lambda(k)$ gives the conductivity in the interval (k_1, k_2)

$$\lambda(k_1, k_2) = \int_{k_1}^{k_2} \lambda(k)\,dk. \tag{1.7}$$

When taken between appropriate limits, this integral gives the negative conductivity $\lambda_- = \lambda(-\infty, 0)$, the positive conductivity $\lambda_+ = \lambda(0, \infty)$ and the conductivity $\lambda = \lambda(-\infty, \infty)$.

Neither the conductivity spectrum nor the integrated conductivity (for $k_1 \leqslant k_2$) can be negative. The interchange of the variables k_1 and k_2 reverses the sign of the charge density $\varrho(k_1, k_2)$ and of the conductivity $\lambda(k_1, k_2)$.

In the system of absolute values the charge density and the conductivity are positive if $k_1 < k_2$ and negative otherwise. Here k_1 and k_2 should represent mobilities of the same polarity. To describe the spectrum of air ions of both polarities, we should consider two complete sets of parameters: $\varrho_+(k_1, k_2)$ and $\varrho_-(k_1, k_2)$, $\lambda_+(k_1, k_2)$ and $\lambda_-(k_1, k_2)$. The conductivity spectrum also becomes double valued: $\lambda_+(k)$ and $\lambda_-(k)$. As in the case of $\varrho(k)$, the subscript + or − may be omitted sometimes, or written in the form $\pm$. Only when denoting polar charge densities $\varrho_\pm$ and polar conductivities $\lambda_\pm$, is the omission of the subscript admissible.

The use of the function $\lambda(k)$ facilitates the graphical presentation of the air-ion spectrum in large mobility intervals. The function $\varrho(k)$ is unsuitable to this end since it usually has large values in the region of small mobilities, and vice versa. Particular attention should be given to the graphical presentation of the conductivity spectrum on a logarithmic mobility scale. The area under the $\lambda(k)$ curve in this case is proportional to the charge density. This is explained by the relation

$$\int \lambda(k)\, d\left(\ln \frac{k}{k_1}\right) = \int \varrho(k)\,dk. \tag{1.8}$$

The arbitrary constant mobility k_1 in (1.8) is required in order to ensure correct dimensions.

Sometimes, the mobility distribution of air ions is characterized by the partial charge densities of hypothetical discrete groups. In the theory of measurement methods this approach is unjustified. The actual air-ion velocity distribution in any experimental arrangement is never strictly discrete (because of air-ion diffusion, to mention the most obvious factor). Even if the air-ion spectrum should turn out to be discrete, one must start with the assumption of a continuous distribution when setting up and evaluating observations, in order to prove discreteness. This is the best way to bring out the objective information. A discrete distribution can be considered as a particular case of a continuous one. To effect a mathematical transformation from a continuous to a discrete distribution, the function $\varrho(k)$ should be written as a sum

$$\varrho(k) = \sum_n \varrho_n \delta(k - k_n), \tag{1.9}$$

where ϱ_n are the specific densities of the air ions with mobilities k_n. Owing to the property of the delta function $\int f(k)\delta(k - k_n) = f(k_n)$ all integral expressions transform into sums which are characteristic of a discrete distribution.

In practice one often attempts to calculate the number density $n_\pm(k_1, k_2)$ of air ions. If the charge of all air ions equals one elementary charge, then

$$n_\pm(k_1, k_2) = \frac{\varrho_\pm(k_1, k_2)}{e}, \tag{1.10}$$

where e is the elementary charge.

Unfortunately the assumption $q = e$ holds only for light air ions. Heavy air ions and the even heavier, artificially created, charged aerosol particles may carry a larger charge. When this is the case, formula (1.10) does not give the actual number density but only some relative quantity. If the true mean charge of the air ions is unknown, then it would be more correct to speak of the charge density expressed in elementary charges per unit volume instead of the number density. For singly charged air ions the last quantity coincides with the number density of air ions.

§2. VELOCITY FIELD OF AIR IONS

Consider a laminar air flow and suppose that the motion of air ions is determined only by the fluid velocity and the action of the electric field. The velocity of the air ions is then

$$\vec{v} = \vec{u} + k\vec{E}, \tag{2.1}$$

where $\vec{u}$ is the fluid velocity. Equation (2.1) defines the flow lines of air ions with mobility k. In the case of steady flow the ion flow lines coincide with the trajectories of the air ions.

We now calculate the density distribution of the flow of air ions passing through some imaginary surface S.

Through a surface element $\vec{dS}$ there is a flux of charge given by

$$dI(k) = \varrho(k)\vec{v}\,\vec{dS} = \varrho(k)(d\Phi + k\,dN), \tag{2.2}$$

where $d\Phi = \vec{u}\,\vec{dS}$ is the volume rate of air flow through a surface element $\vec{dS}$ and $dN = \vec{E}\,\vec{dS}$ is the electric flux through $\vec{dS}$. The density distribution of the flow through the surface S is

$$I(k) = \iint_S \varrho(k)(d\Phi + k\,dN) = \overline{\varrho(k)}(\Phi + kN), \tag{2.3}$$

where $\overline{\varrho(k)}$ is some mean value of $\varrho(k)$ on the surface S, Φ is the air flow rate and N is the electric flux through this surface.

From formula (2.3) follow two conclusions of practical importance /Tammet, 1964b/:

1. For any flow surface of air ions with mobility k we have

$$\Phi + kN = 0, \tag{2.4}$$

since $I(k)$ through the surface of the flow always equals zero.

2. For a homogeneous distribution of air ions over some surface the density distribution of the flow through this surface is expressed by

$$I(k) = (\Phi + kN)\varrho(k). \tag{2.5}$$

Consider now the behavior of the spectrum $\varrho(k)$ in the velocity field of the air ions /Cagniard, 1943, 1944; Tammet, 1960/. Further, let us assume that the air is incompressible and neglect the recombination and generation of air ions as well as processes in which the air-ion velocity varies. On the basis of these assumptions and the law of charge conservation, the law of conservation of the charge density spectrum follows, and is given by

$$\frac{\partial \varrho(k)}{\partial t} = -\operatorname{div}\vec{j}(k). \tag{2.6}$$

Since $\vec{j}(k) = \vec{v}\,\varrho(k)$, expression (2.6) becomes

$$\frac{\partial \varrho(k)}{\partial t} = -\varrho(k)\operatorname{div}\vec{v} - \vec{v}\operatorname{grad}\varrho(k). \tag{2.7}$$

The variation of $\varrho(k)$ in a point moving along the trajectory of an air ion with velocity $\vec{v}$ is characterized by the total differential $d\varrho(k)$. This is connected with the partial derivative via the expression

$$\frac{d\varrho(k)}{dt} = \frac{\partial \varrho(k)}{\partial t} + \vec{v}\operatorname{grad}\varrho(k), \tag{2.8}$$

from which we obtain

$$\frac{d\varrho(k)}{dt} = -\varrho(k)\operatorname{div}\vec{v}. \tag{2.9}$$

Since $\operatorname{div}\vec{u} = 0$ and $\operatorname{div}\vec{E} = 4\pi\varrho$, we obtain

$$\frac{d\varrho(k)}{dt} = -4\pi\varrho\lambda(k). \tag{2.10}$$

This expression describes the phenomenon known as electrostatic dissipation /Townsend, 1898; Wolodkewitsch, 1933a, 1933b; Forster 1959; Dunskii, Kitaev, 1960; Whitby, McFarland, 1961; Kitaev, 1962/. Electrostatic dissipation is due to the mutual repulsion or attraction of air ions.

In many cases one may neglect the electric field of the space charge and assume that $\operatorname{div}\vec{E} = 0$. Then

$$\frac{d\varrho(k)}{dt} = 0. \tag{2.11}$$

This formula is a supplement to Liouville's well-known theorem on the motion of air ions. Formula (2.11) leads to a conclusion which is of great importance in the theory of the aspiration method: if one neglects generation, recombination, variation of mobility, diffusion and electrostatic interaction of air ions, then, in a laminar incompressible air flow $\varrho(k)$ is constant along the trajectory of an air ion of corresponding mobility.

A similar result first appeared in a work of Becker /Becker, 1910/. The same result was obtained and applied in a little-known work /Cagniard, 1943/ on the theory of an aspiration counter for the case of a discrete air-ion spectrum. For charged aerosols a similar result was obtained by Levin /Levin, 1957, 1959/.

When studying the motion of air ions it is sometimes advantageous to utilize the methods of the theory of similarity. To ensure similarity between the flow lines of air ions in two separate systems, then in addition to the condition of hydrodynamic and electrostatic similarity, we also require agreement between the values given by the special criterion

$$K_l = \frac{kE}{u} = \frac{kU}{ux}. \tag{2.12}$$

In this expression E denotes the characteristic field strength, u the characteristic flow velocity, U the characteristic voltage, x the characteristic dimension and k the mobility of the air ions under consideration.

§3. ARRANGEMENT OF AN ASPIRATION COUNTER AND THE PRINCIPLE OF MEASUREMENT OF THE AIR-ION SPECTRUM

The aspiration counter comprises a measuring capacitor and arrangements for drawing air through the capacitor, for supplying voltage to the

capacitor and for measuring the currents generated. One usually measures only the current through one capacitor plate, called the collector plate.

For the case of steady-state operation of the counter and a stationary spectrum $\varrho(k)$, the current through the plates is determined by conduction of the air ions.

The current flowing through the capacitor is either grounded directly or otherwise via the voltage supply or current meter. The total current flowing through the measuring capacitor may differ from zero if the mean charge densities of the air entering and leaving the capacitor are not equal to one another.

In most cases when using the aspiration counter one may assume that the motion of air ions in the capacitor is independent of the presence of other air ions in the air sample. Then the density distribution of the current $I(k)$ through the collector plate is proportional to the corresponding value $\varrho(k)$. This can be expressed in the form

$$I(k)=G\varrho(k). \tag{3.1}$$

The quantity G is here a constant depending on the structural and operational parameters of the measuring capacitor.

In what follows we shall assume that G does not depend on $\varrho(k)$ except in special cases where the interaction of air ions in the capacitor is allowed.

The current through the collector plate generated by the incoming air ions is expressed by the integral

$$I=\int_{-\infty}^{+\infty} G\varrho(k)\,dk. \tag{3.2}$$

This current can be directly measured, thus enabling the experimental determination of the dependence of the current I on the operational parameters of the counter. The function $I(\psi)$, where ψ is an arbitrarily chosen variable operational parameter, is called the characteristic of the aspiration counter. Usually a volt-ampere characteristic is used, whereby ψ denotes the voltage across the capacitor plates. Each type of counter design is characterized by a particular form of the function $G(\psi, k)$, which is the Green's function for the air-ion current through the collector plate. Expression (3.2) can be regarded as an integral equation with respect to $\varrho(k)$:

$$\left.\begin{aligned} I(\psi)&=\int_{-\infty}^{+\infty} G(\psi, k)\varrho(k)\,dk; \\ &\text{if for one polarity } G=0, \text{ then} \\ I(\psi)&=\int_{0}^{\infty} G(\psi, k)\varrho(k)\,dk. \end{aligned}\right\} \tag{3.3}$$

The physical significance of the function $G(\psi, k)$ is explained as follows. Suppose that the air sample contains air ions of mobility k_1 only. In this case $\varrho(k)=|\varrho\delta(k-k_1)$ and equation (3.3) yields $G(\psi, k_1)=I(\psi)/\varrho$. Consequently, $G(\psi, k)$ may be regarded as the counter characteristic (reduced to unit charge density) in the presence of air ions of mobility k only.

Considering counters of a given type we have to find the actual form of the function G and the method for solving equation (3.3). The solution of the integral equation (3.3) in the general case is possible only with the aid of numerical analysis, which is rather laborious.

The solution is simplified only when certain design requirements of the capacitor are fulfilled, ensuring a special form of the kernel of equation G.

These requirements, common for all aspiration counters, are listed below:

1. The measuring capacitor should possess axial symmetry.
2. There should be two openings in the outer plate of the capacitor. These openings are called the entrance and exit opening, respectively, depending on the flow direction.

The surface of the opening is defined as the imaginary surface covering the opening. The surface of the entrance opening should be such that $E = 0$ on it and the flow velocity $\vec{u}$ is directed into the measuring capacitor.

3. In the internal capacitor plates there should be no openings through which part of the air can flow.
4. All the requirements stated in the preceding paragraph should be satisfied inside the capacitor. Outside the capacitor $\varrho(k)$ should be homogeneous.

Instead of an axially symmetric capacitor, the capacitor may have the form of a sector. One often uses a parallel-plate capacitor which is a limiting case of an axially symmetric capacitor of infinite radius. In a parallel-plate capacitor a homogeneous distribution of velocities of the air flow in the longitudinal section must be ensured.

In the general theory of aspiration counters we assume the above mentioned requirements are satisfied. The effect of deviations from these requirements on the measuring results is dealt with in the second chapter.

§4. INTEGRAL COUNTER

The measuring capacitor of an integral counter comprises two plates. For the collector plate one usually chooses the inner plate /McClelland, Kennedy, 1912; Nolan, J.J., Nolan, P.J., 1930; Weger, 1953a; Siksna, 1961a/. The collector plate is connected to the current meter. A voltage U is applied across the collector and repulsing plates. The air sample is drawn into the capacitor at a volume flow rate Φ.

The integral counter is the most widely used version of the aspiration counter due to its simple design and high sensitivity. One reason for the wide use of integral counters is the simplicity of measuring integral quantities. Apart from measuring devices for ion concentration and conductivity, the integral method is applied in aerosol detectors /Sekiyama, 1959; Rich, 1959; Hasenclever, Siegmann, 1960; Siksna, 1961b/.

To determine the G-function of the integral counter, let us consider the behavior of air ions with a given mobility k in the measuring capacitor having an inner collector plate (Figure 4.1). When $Uk>0$, the air ions are repelled by the inner plate and $G = 0$. When $Uk<0$, the air ions will settle on the plate. The flow lines for air ions terminating on the inner plate enclose part of the space between the capacitor plates. This spatial

portion is limited by the flow surface which we shall call the boundary surface. The boundary surface comes into contact with the rear edge of the inner plate.

When the mobility k is sufficiently small the boundary surface does not intersect the outer plate, as shown in Figure 4.1. The electric flux through the boundary surface is then $N = 4\pi CU$, where C is the active capacitance of the measuring capacitor. The active capacitance is the capacitance of the measuring capacitor proper and differs from the capacitance of the insulated counter system, which includes the electrometer capacitance and the parasitic capacitance of the connections. Methods for determining the active capacitance are treated in §33. According to (2.4) the air-flow rate through the boundary surface equals

$$\Phi' = 4\pi CUk. \tag{4.1}$$

The flow of air ions which enter the capacitor through that portion of the entrance surface bounded by the boundary surface is Φ'_Q (2.5). Since all the air ions passing through this region settle on the inner plate, $I = \Phi'_Q$ and $G = \Phi' = 4\pi CUk$. This result was obtained for certain restricted initial conditions as early as 1903 /Riecke, 1903/. For less restricted initial conditions the problem is treated in studies carried out by Swann /Swann, 1914a, b, d/.

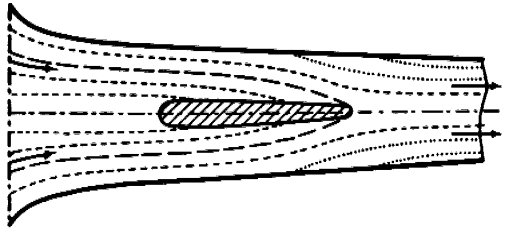

FIGURE 4.1. Flow lines in the measuring capacitor;

- - - - - - flow lines; — — — — boundary surface; · · · · · flow lines on which $q(k) = 0$; — · — · — · — entrance surface.

It should be noted that in the derivation of the expression

$$I = 4\pi CUk_Q \tag{4.2}$$

no assumptions were made on the symmetry of the measuring capacitor. Therefore expression (4.2) is also valid in the case of an asymmetric system of any geometrical configuration. Such an approach was first outlined for somewhat different conditions in the work /Kohlrausch, 1906/.

More mobile ions with a mobility k_0 will have a boundary surface that intersects the entrance surface at the outer plate. In this case $\Phi' = \Phi$.

The corresponding mobility k is called the limiting mobility. From formula (4.1) we obtain for $\Phi' = \Phi$

$$\left.\begin{aligned} k_0 &= \frac{\Phi}{4\pi CU}, \\ \text{and considering the polarity} \\ k_0 &= -\frac{\Phi}{4\pi CU} \end{aligned}\right\} \tag{4.3}$$

when $k_0 \leqslant k$, all air ions passing through the entrance surface settle and $G = \Phi$.

On the basis of the above results we may write for the air ions attracted to the collector plate

$$G = \begin{cases} 4\pi CUk & \text{for} \quad k \leqslant k_0 \\ \Phi & \text{for} \quad k_0 \leqslant k. \end{cases} \tag{4.4}$$

Similar considerations for a capacitor with an outer collector plate lead to results expressed by formulas (4.3) and (4.4).

From the above it follows that the basic formulas describing an integral counter are valid independently of the geometry of the measuring capacitor and the flow velocity distribution only when the capacitor is axially symmetric. The latter applies only to axially symmetric steady flows. Air turbulence in the capacitor is inadmissible in the general case.

The question concerning the permissible capacitor geometry and flow velocity distribution has been a matter of controversy for a long time, although the above conclusion could be reached from known results /Swann, 1914b; Cagniard, 1943, 1944; Levin, 1959/. The reason for misunderstandings lay in that the basic formulas for the integral counter were derived from the calculation of air-ion trajectories, which involved serious difficulties due to the occurrence of radial components of the flow velocity. To simplify the calculations certain assumptions on the capacitor geometry and distribution of the air-flow velocities were made. Corresponding requirements were set up with regard to counter design. Such superfluous requirements may lead to appreciable limitations when designing counters. Consider as an example Becker's well-known counter /Becker, 1909/, whereby special measures were taken to ensure a homogeneous electric field at the capacitor entrance. This, however, only complicated the design without producing any advantages /Scholz, 1931b/. Recent works propose a uniform distribution of air-flow velocities /Misaki, 1960; Paltridge, 1965/ or the absence of radial components /Hoegl, 1963b/. When choosing the capacitor dimensions, large deviations from a cylindrical geometry are considered to be inadmissible /Komarov, Seredkin, 1960/.

It should be pointed out that the calculation of air-ion trajectories is complicated and at times requires computer-programmed numerical calculations /Kraemer, Johnstone, 1955/. The solution of many basically simple problems when reduced to formulas describing the integral counter appears to be complicated when calculating trajectories /Shimizu, 1956, 1957, 1960/.

§5. SOLUTION OF THE EQUATION OF THE INTEGRAL COUNTER

Apart from depending on the mobility, the G-function of the integral counter depends on the three parameters C, U and Φ. When determining the characteristics of a counter one of the parameters is varied while the remaining ones are kept constant. Usually the voltage is varied and, less frequently, the air-flow rate /Nolan, P.J., Kenny, 1952/. The reason is that variation of the air-flow rate may have an adverse effect on the $\varrho(k)$ of the air sample.

To solve equation (3.3) it should be transformed by applying a suitable operator into a form in which the desired quantities can be eliminated by algebraic operations. In the case of the integral counter this can be achieved by a single and double differentiation with respect to ψ and the operator h_ψ

$$h_\psi = 1 - \psi \frac{\partial}{\partial \psi}. \tag{5.1}$$

The operator h_ψ is often used for the evaluation of measurements, since a convenient method—"the tangent method"— exists for determining $h_\psi I$ /Israël 1931, 1957b; Gerasimova, 1939; Imyanitov, 1957/ (see Figure 5.1).

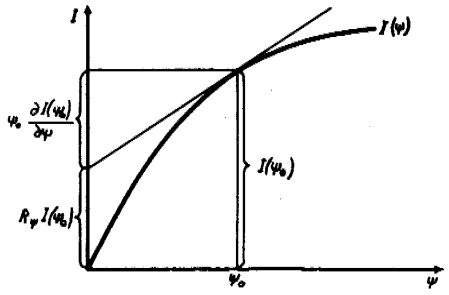

FIGURE 5.1. Determination of $h_\psi I$ by the tangent method.

In the integrand of equation (3.3) the differential operator or h_ψ acts only upon the function G. Below we list the transformations of $G(\psi, k)$ which will be used later:

$$\frac{\partial G}{\partial U} = \begin{cases} 4\pi C k & \text{for } k < k_0 \\ 0 & \text{for } k_0 < k, \end{cases} \tag{5.2}$$

$$\frac{\partial G}{\partial \Phi} = \begin{cases} 0 & \text{for } k < k_0 \\ 1 & \text{for } k_0 < k, \end{cases} \tag{5.3}$$

$$h_U G = \begin{cases} 0 & \text{for } k < k_0 \\ \Phi & \text{for } k_0 < k, \end{cases} \tag{5.4}$$

$$h_\Phi G = \begin{cases} 4\pi C U k & \text{for } k < k_0 \\ 0 & \text{for } k_0 < k, \end{cases} \tag{5.5}$$

$$\frac{\partial^2 G}{\partial U^2} = -\frac{\Phi^2}{4\pi C U^3}\delta(k - k_0), \tag{5.6}$$

$$\frac{\partial^2 G}{\partial \Phi^2} = -\frac{1}{4\pi C U}\delta(k - k_0). \tag{5.7}$$

Using expressions (5.2)—(5.7) we can readily derive formulas for calculating different parameters of ionized air in accordance with the well-known function $I(U)$ or $I(\Phi)$. The results are

$$\varrho(k_0) = -\frac{4\pi C U^3}{\Phi^2}\frac{\partial^2 I}{\partial U^2}, \tag{5.8}$$

$$\varrho(k_0) = -4\pi C U \frac{\partial^2 I}{\partial \Phi^2}, \tag{5.9}$$

$$\varrho(k_1, k_2) = \frac{h_U I(U_1)}{\Phi_1} - \frac{h_U I(U_2)}{\Phi_2}, \tag{5.10}$$

$$\varrho(k_1, k_2) = \frac{\partial I(\Phi_1)}{\partial \Phi} - \frac{\partial I(\Phi_2)}{\partial \Phi}, \tag{5.11}$$

$$\lambda(k_1, k_2) = \frac{1}{4\pi C}\left[\frac{\partial I(U_2)}{\partial U} - \frac{\partial I(U_1)}{\partial U}\right], \tag{5.12}$$

$$\lambda(k_1, k_2) = \frac{1}{4\pi C}\left[\frac{h_\Phi I(\Phi_2)}{U_2} - \frac{h_\Phi I(\Phi_1)}{U_1}\right]. \tag{5.13}$$

The use of the δ-function for the derivation of formulas (5.8) and (5.9) is not obligatory. Instead, the integral in equation (3.3) may be written as the sum of two integrals corresponding to the ranges $k \leqslant k_0$ and $k_0 \leqslant k$, respectively. Differentiating with respect to the limits of the integrals, we obtain the same results /Langevin, 1905a; Israël, 1957b/.

It is possible to derive a more general and concise notation for the solutions of the integral-counter equation /Siksna, 1950; Israël, 1957b/. In this case we take for the starting function

$$P(k_0) = \frac{I(k_0)}{\Phi}. \tag{5.14}$$

The quantity $P(k_0)$ has the dimension of charge density and will be called the conventional charge density for the limiting mobility k_0. In simplified calculations the value of P, expressed in elementary charges per unit volume, is often represented as the concentration of air ions. Thus the calculated concentration is actually a conventional quantity, since it does not correspond to any definite mobility interval. In practice, however, one often encounters conditions in which the actual character of the mobility spectrum enables us to assume

$$\varrho(k_0, \infty) \approx P(k_0). \tag{5.15}$$

This expression is used very often to calculate the concentration of light air ions.

Starting with the function $P(k_0)$, we transform equation (3.3) into

$$P(k_0)=\int_0^\infty \frac{G(k_0,k)}{\Phi}\varrho(k)\,dk. \tag{5.16}$$

Since

$$\frac{G(k_0,k)}{\Phi}=\begin{cases} k/k_0 \text{ for } & k\leqslant k_0 \\ 1 \quad \text{for } k_0\leqslant k, \end{cases} \tag{5.17}$$

equation (5.16) has only one independent operation parameter. For convenience, we take as the variable parameter the reciprocal limiting mobility $\omega=1/k_0$.

In similar fashion we obtain the formulas

$$\varrho(k_0)=-\omega^3\frac{\partial^2 P}{\partial\omega^2}, \tag{5.18}$$

$$\varrho(k_1,k_2)=h_\omega P(k_1)-h_\omega P(k_2), \tag{5.19}$$

$$\lambda(k_1,k_2)=\frac{\partial P(k_2)}{\partial\omega}-\frac{\partial P(k_1)}{\partial\omega}. \tag{5.20}$$

In the method of varying the air-flow rate, formulas (5.18)—(5.20) are inconvenient. Here it is better to start with the function

$$\Lambda(k_0)=\frac{I(k_0)}{4\pi CU}, \tag{5.21}$$

which has the dimension of conductivity and will be called the conventional conductivity at the limiting mobility k_0. The kernel of the integral equation is

$$\frac{G}{4\pi CU}=\begin{cases} k \quad \text{for } & k\leqslant k_0 \\ k_0 \quad \text{for } & k_0\leqslant k. \end{cases} \tag{5.22}$$

Calculations similar to those carried out above yield

$$\varrho(k_0)=-\frac{\partial^2\Lambda}{\partial k_0^2}, \tag{5.23}$$

$$\varrho(k_1,k_2)=\frac{\partial\Lambda(k_1)}{\partial k_0}-\frac{\partial\Lambda(k_2)}{\partial k_0}, \tag{5.24}$$

$$\lambda(k_1,k_2)=h_{k_0}\Lambda(k_2)-h_{k_0}\Lambda(k_1). \tag{5.25}$$

The integral counter is often used for measuring the polar charge density $\varrho_\pm$ and the polar conductivity $\lambda_\pm$. This is possible only under specific conditions. To measure $\varrho_\pm$ it is necessary that $\varrho(k)=0$ in the range $k<k_0$.

For the range in which $\varrho(k)=0$ an arbitrary function may be taken for G without affecting the results. Setting G equal to Φ everywhere, we obtain

$$\varrho_\pm=P_\pm=\frac{I_\pm}{\Phi}. \tag{5.26}$$

$I_\pm$ denotes current at the respective polarity.

To verify formula (5.26) k_0 must be chosen sufficiently small in order that $\varrho(k)=0$ for $k<k_0$. The condition is satisfied if upon increasing the voltage, the current I remains unaltered and upon decreasing the air-flow rate I decreases proportionally.

To measure the polar conductivity k_0 must be chosen sufficiently large in order to satisfy the condition $\varrho(k)=0$ in the range $k_0<k$. Then for all mobilities one may take $G=4\pi CUk$, which yields

$$\lambda_\pm=\Lambda_\pm=\frac{I_\pm}{4\pi CU}. \tag{5.27}$$

For the experimental verification of this formula it is necessary that the current I remains constant when increasing the air-flow rate and is proportional to the voltage when decreasing the voltage.

§6. VARIOUS INTEGRAL COUNTER TYPES

Some variants of the aspiration method possess integral characteristics. The most widespread is the method of the precondenser ascribed to Mache /Mache, 1903/, but actually proposed by McClelland /McClelland, 1898/.

The arrangement of the counter with a precondenser is shown in Figure 6.1.

When plotting the characteristics of the counter the voltage of the precondenser is varied and the current $I_2=I_2(U_1)$ through the collector plate is measured. The voltage of the main capacitor remains unaltered.

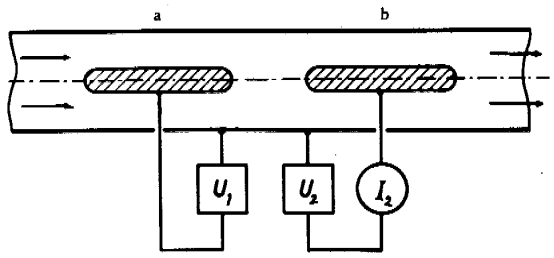

FIGURE 6.1. Counter with a precondenser:

a—precondenser; b—main capacitor; U—voltage supply; I— ammeter.

The limiting mobilities are determined as follows:

$$k_1 = -\frac{\Phi}{4\pi C U_1}, \tag{6.1}$$

$$k_2 = -\frac{\Phi}{4\pi C U_2}. \tag{6.2}$$

If $k/k_2 \leqslant 0$, then

$$G_2 = 0.$$

If $0 \leqslant k/k_2 \leqslant 1$, then

$$G_2 = \begin{cases} 0 & \text{for} \quad k/k_1 \leqslant -k/k_2 \\ -4\pi(C_1U_1 + C_2U_2)k & \text{for} \quad -k/k_2 \leqslant k/k_1 \leqslant 0 \\ -4\pi C_2U_2k & \text{for} \quad 0 \leqslant k/k_1 \leqslant 1 - k/k_2 \\ \Phi + 4\pi C_1U_1k & \text{for} \quad 1 - k/k_2 \leqslant k/k_1 \leqslant 1 \\ 0 & \text{for} \quad 1 \leqslant k/k_1 \end{cases} \tag{6.3}$$

If $1 \leqslant k/k_2$ then

$$G_2 = \begin{cases} 0 & \text{for} \quad k/k_1 \leqslant -1 \\ \Phi - 4\pi C_1U_1k & \text{for} \quad -1 \leqslant k/k_1 \leqslant 0 \\ \Phi + 4\pi C_1U_1k & \text{for} \quad 0 \leqslant k/k_1 \leqslant 1 \\ 0 & \text{for} \quad 1 \leqslant k/k_1 \end{cases}$$

The counter with a precondenser is used, as a rule, for the study of air ions with mobilities $1 \leqslant k/k_2$. In the range $0 \leqslant k/k_1$ the function G_2 of the counter with a precondenser equals the difference of the fixed parameter Φ and the function G of the standard integral counter. The value of G_2 for $1 \leqslant k/k_2$ does not depend on the polarity of the voltage U_1. This is shown in Figure 6.2, which gives a plot of the function G for a counter with a precondenser and for a standard integral counter.

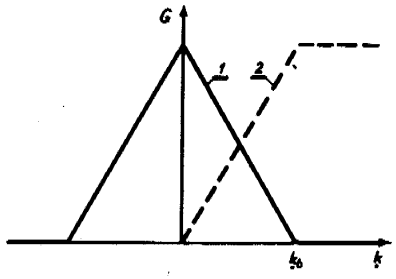

FIGURE 6.2. The G-function:

1—for a counter with a precondenser; 2—for a standard integral counter.

If in the range $0 \leqslant k/k_2 \leqslant 1$ the condition $\varrho(k) = 0$ is satisfied, then all calculations for a counter with a precondenser differ from those for a standard counter only in the sign before the derivative and the operator h_ψ.

In the opposite case the situation is somewhat more complicated. When the polarities of the voltage across the preliminary capacitor and the main capacitor are the same, partial conductivities of the type $\lambda(0, k)$ cannot be measured. It is thus recommended to plot the characteristics for opposite voltage polarities. In this case the partial conductivities are connected with the derivatives $\partial I_2/\partial U_1$ as in the case of the standard integral counter.

Some of the problems connected with the precondenser counter are treated in detail in the works /Kohlrausch, 1914; Israël, 1931; Polovko, Nichkevich, 1937; Nolan, P.J., O'Connor, 1955/.

The method of the condensation nucleus counter is closely related to the methods of the precondenser /Nolan, P.J., Deignan, 1948/. Since in the former the nonelectric quantity (concentration of condensation nuclei) is recorded, the method of the condensation nucleus counter with a precondenser will not be discussed in detail here.

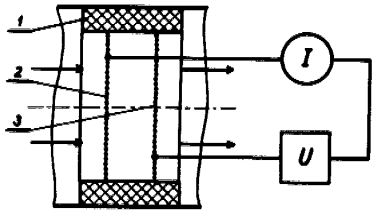

FIGURE 6.3. Counter in which air is blown through grids:

1—insulator; 2—collector grid; 3—repulsing grid.

We shall now briefly describe the method of blowing air through grids which may be used as an integral or differential method. This method was proposed in the work /Zeleny, 1898b/.

The method of blowing air through grids is not widespread /Kähler, 1903; Aselmann, 1906/, although it certainly is of interest because of the possibility of decreasing the dimensions of the measuring capacitor. The application of this method is apparently restricted to large limiting mobilities, for which it is advisable to consider a large air-flow rate with a relatively small active capacitance of the measuring capacitor.

A schematic diagram of the measuring capacitor with grids is shown in Figure 6.3.

The limiting mobility can be calculated from formula (4.3). However, more explicit is the expression

$$k_0 = \frac{u}{E}, \tag{6.4}$$

where u is the flow velocity, and E the electric field strength between the grids. The function G is given by (4.4).

The method of blowing air through grids deviates from the requirements mentioned in §3. These requirements are replaced by the condition of a

uniform electric field and air flow and the condition of total screening of the electric field by the collector grid. In the case of a wide-mesh grid the last condition is not satisfied /Loeb, 1923; Kaden, 1950, Izergin, 1958/, which should be taken into account when designing the counter. At the same time attention should be given to the adsorption of air ions, which is of particular significance in the above described method.

§ 7. DIFFERENTIAL COUNTERS OF THE FIRST ORDER

There are two types of differential counters of the first order: one has a divided electrode and the other employs a divided air flow. The method of the divided electrode was proposed by Zeleny /Zeleny 1901/. The theory of the air-ion spectrum was developed later /Blackwood, 1920; Hogg, 1939; Misaki, 1950; Tammet, 1960; Whipple, 1960; Hoppel, Kraakevik, 1965/. This method is the most widely used version of the aspiration method.

The counter with a divided electrode differs from the integral counter in that one electrode of the measuring capacitor is divided into two mutually insulated parts. During aspiration the second part serves as a collector plate, while the first part, called the forward electrode, is maintained at the same potential as the collector plate. The repulsing plate is standard. The design of such a capacitor is schematically shown in Figure 7.1. Here the inner plate is divided. As in the integral counter with an outer collector plate one can divide the outer plate, the rear part of which then becomes the collector plate. The inner part is not divided and is standard. The differential counter of the first order with a divided electrode is similar in design to an integral counter with a precondenser, but differs in its operation and the ratio of the plate capacitances.

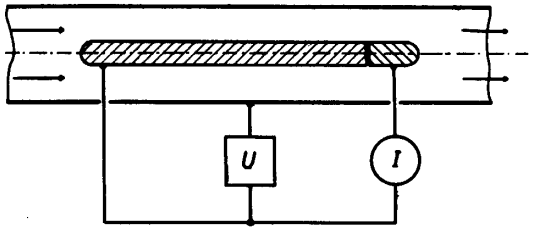

FIGURE 7.1. Differential counter of the first order with a divided electrode.

Let us now define the function G for a counter with a divided electrode. The sum of the currents through the forward and collector plates equals the current in the corresponding integral counter, the active capacitance of which is $C_1 + C_2$, where C_1 is the mutual capacitance (the absolute value of the coefficient of electrostatic induction) between the forward plate and the main plate, and C_2 is the mutual capacitance between the collector plate and the main plate.

The current through the forward plate equals the current in the integral counter with an active capacitance C_1. The current through the collector plate equals the difference of the total current and the current through the forward plate. Consequently, the G-function for the differential counter with a divided electrode corresponds to the difference of the G-function of the integral counter with an active capacitance $C_1 + C_2$ and the G-function of an integral counter with an active capacitance C_1. When describing differential counters it suffices to consider air ions of one polarity only, as in §§ 4—5. Denoting the corresponding limiting mobilities by k_a and k_b, respectively, we obtain

$$k_a = \frac{\Phi}{4\pi(C_1 + C_2)U}, \tag{7.1}$$

$$k_b = \frac{\Phi}{4\pi C_1 U}, \tag{7.2}$$

$$G = \begin{cases} 4\pi C_2 U k & \text{for} \quad k \leqslant k_a \\ \Phi - 4\pi C_1 U k & \text{for} \quad k_a \leqslant k \leqslant k_b \\ 0 & \text{for} \quad k_b \leqslant k. \end{cases} \tag{7.3}$$

The behavior of the G-function is shown in Figure 7.2.

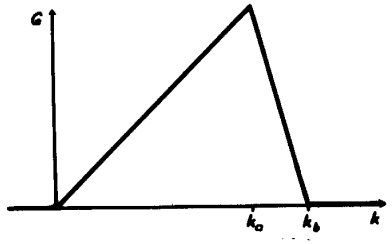

FIGURE 7.2. The G-function of a differential counter with a divided electrode.

The G-function (7.3) has the following properties:

$$h_U G = \begin{cases} 0 & \text{for} \quad k < k_a \\ \Phi & \text{for} \quad k_a < k < k_b \\ 0 & \text{for} \quad k_b < k. \end{cases} \tag{7.4}$$

$$\frac{\partial G}{\partial \Phi} = \begin{cases} 0 & \text{for} \quad k < k_a \\ 1 & \text{for} \quad k_a < k < k_b \\ 0 & \text{for} \quad k_b < k. \end{cases} \tag{7.5}$$

These properties enable the use of the differential counter of the first order with a divided electrode for measuring the partial charge density. It can be readily shown that

$$\varrho(k_a, k_b) = \frac{h_U I}{\Phi}, \tag{7.6}$$

$$\varrho(k_a, k_b) = \frac{\partial I}{\partial \Phi}, \tag{7.7}$$

where I is the absolute value of the current through the collector plate.

If the interval (k_a, k_b) is sufficiently narrow, the spectrum can be approximately defined. Using the theorem of the mean integral value, we obtain

$$\varrho(\bar{k}) = \frac{4\pi C_1(C_1 + C_2)U}{C_2\Phi^2} h_U I, \tag{7.8}$$

$$\varrho(\bar{k}) = \frac{4\pi C_1(C_1 + C_2)U}{C_2\Phi} \frac{\partial I}{\partial \Phi}. \tag{7.9}$$

In this interval the mobility $\bar{k}$ has the mean value

$$\overline{k} = \frac{(C_1 + C_2/2)\Phi}{4\pi C_1(C_1 + C_2)U} \tag{7.10}$$

and the relative half-width

$$\delta_k = \frac{C_2}{2C_1 + C_2}. \tag{7.11}$$

The smaller the ratio C_2/C_1, the smaller is the quantity δ_k and, consequently, the better the resolution of the method.

When the ratio C_2/C_1 is small, the partial conductivities can also be calculated. This follows immediately from the form of the G-function and we can write

$$\lambda(\bar{k}_1, \bar{k}_2) = \frac{1}{4\pi C_2}\left(\frac{I_2}{U_2} - \frac{I_1}{U_1}\right). \tag{7.12}$$

The mobilities $\bar{k}_1$ and $\bar{k}_2$ are defined by formulas (7.10) and (7.11) for the voltages U_1 and U_2, respectively.

The method of Misaki /Misaki, 1950/, not treated here, differs from that described above and is an independent version of the differential method with a divided electrode.

We shall now consider the differential counter of the first order in which the air flow is divided. This method is not widespread /Nolan, J.J., 1919; Nolan, J.J., Harris, 1922/. The quantitative theory is given in the work /Tammet, 1960/.

The measuring capacitor of this counter has two plates and differs from the capacitor of the integral counter only in that the capacitor inlet is divided into two parts (a circular inner and outer opening, respectively) by a coaxial tube (Figure 7.3). If the inner plate is the collector then the air sample is drawn into the capacitor at a volume flow rate Φ_2 through the outer opening. If the outer plate is the collector, the air is drawn through the inner opening. An additional flow of specially deionized air with a flow rate Φ_1 is drawn in through another opening. If the additional air flow Φ_1 were not deionized then the G-function would equal the G-function of a standard

integral counter with an air-flow rate $\Phi_1 + \Phi_2$. Assuming that the air flow Φ_2 is deionized, the G-function equals the G-function of an integral counter with an air-flow rate Φ_1. The G-function for a differential counter with a divided air flow corresponds to the difference of the G-functions for the above stated cases. Consequently,

$$G = \begin{cases} 0 & \text{for} \quad k \leqslant k_a \\ 4\pi CUk - \Phi_1 & \text{for} \quad k_a \leqslant k \leqslant k_b \\ \Phi_2 & \text{for} \quad k_b \leqslant k, \end{cases} \tag{7.13}$$

where

$$k_a = \frac{\Phi_1}{4\pi CU} \tag{7.14}$$

$$k_b = \frac{\Phi_1 + \Phi_2}{4\pi CU}. \tag{7.15}$$

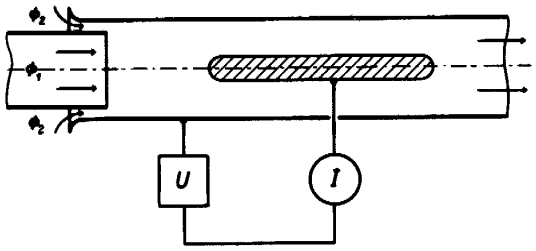

FIGURE 7.3. Differential counter of the first order with a divided air flow.

In a counter with a divided air flow one usually applies only the method of varying the voltage. Calculations similar to those for the method of the divided electrode yield

$$\lambda(k_a, k_b) = \frac{1}{4\pi C} \frac{\partial I}{\partial U}. \tag{7.16}$$

The spectrum $\lambda(k)$ is calculated from

$$\lambda(\bar{k}) = \frac{U}{\Phi_2} \frac{\partial I}{\partial U}, \tag{7.17}$$

where $\bar{k}$ lies in the interval of mean mobility

$$\overline{k} = \frac{\Phi_1 + \Phi_2/2}{4\pi CU} \tag{7.18}$$

and relative half-width

$$\delta_k = \frac{\Phi_2}{2\Phi_1 + \Phi_2}. \tag{7.19}$$

The partial charge density is calculated from the two current values $I_1(U_1)$ and $I_2(U_2)$:

$$\varrho(\tilde{k}_1, \tilde{k}_2) = \frac{I_1 - I_2}{\Phi_2}, \tag{7.20}$$

where $\tilde{k}_1$ and $\tilde{k}_2$ are determined by (7.18) and (7.19) for the voltage U_1 and U_2, respectively.

The differential version of the method in which air is blown through grids /Zeleny, 1898; Altberg, 1912; Griffiths, Awberry, 1929/ may be considered as a differential counter of the first order. The measuring capacitor of such a counter is similar to that of the integral grid counter (Figure 6.3). The difference is that in the differential method the air drawn through the net is deionized and the air ions are generated directly in the space between the grids. To generate air ions, radiation from a radioactive source or some other ionizing agency is used. This, of course, limits the application of the differential method employing grids to the laboratory.

In the theory of the differential counter with grids one should start, instead of with the function $\varrho(k)$, with the spectrum of the flow of air ions regenerated in the space between the grids. The current through the collector grid is

$$I = \int_{k_0}^{\infty} I(k)\,dk. \tag{7.21}$$

The limiting mobility k_0 is given, as in the case of the integral method, by (6.5) or (4.3). Expression (7.21) is similar to the equation of the counter having a G-function of the form

$$G = \begin{cases} 0 & \text{for} \quad k < k_0 \\ 1 & \text{for} \quad k_0 < k. \end{cases} \tag{7.22}$$

The solution of equation (7.21) is

$$I(k_0) = \frac{U^2}{ud}\frac{\partial I}{\partial U}, \tag{7.23}$$

where U is the voltage between the collector grid and the rear grid and d is the distance between the two grids.

When comparing the differential methods of the first order with the integral method, we note that in the differential method $\varrho(k)$ is calculated in terms of the first derivative of the current instead of the second derivative as in the integral method. A single differentiation is actually carried out in the experimental arrangement since either the measuring capacitor or the air flow is divided. When studying the air-ion spectrum, the differential method of the first order has appreciable advantages over the integral method. Differential counters also possess certain advantages when measuring partial charge densities. To determine the partial charge density in a given mobility interval by means of the integral method, four values of the current $I(U)$ should be known (see §29). The differential counter of the first order requires the knowledge of only two $I(U)$-values. When measuring

$\varrho(\tilde{k}_1, \tilde{k}_2)$, it is advisable to use the divided-electrode method with a relatively large C_2/C_1 ratio. When measuring $\varrho(\tilde{k}, \infty)$, the divided air-flow counter is recommended, which requires only one $I(U)$-value.

§8. DIFFERENTIAL COUNTER OF THE SECOND ORDER

The differential counter of the second order is the most perfected version of the aspiration method for the study of air-ion spectra. This method was first discussed in the works /Erikson 1921, 1922, 1924, 1929; Zeleny, 1929; Val'ta, 1929/. The quantitative theory was given by the author /Tammet, 1960/, who used a differential form of the aspiration-counter equation, which is not treated in the present book.

The measuring capacitor of a differential counter of the second order is similar to that of the differential counter of the first order with a divided electrode. However, the air is drawn in as in the case of a divided air-flow counter. The G-function for the differential counter of the second order corresponds to the difference between the G-function of the first-order differential counter with a divided electrode and air-flow rate $\Phi_1 + \Phi_2$ and the G-function for the same counter with an air-flow rate Φ_1. We denote the limiting mobilities as follows:

$$k_{aa} = \frac{\Phi_1}{4\pi(C_1 + C_2)U}, \tag{8.1}$$

$$k_{ab} = \frac{\Phi_1 + \Phi_2}{4\pi(C_1 + C_2)U}, \tag{8.2}$$

$$k_{ba} = \frac{\Phi_1}{4\pi C_1 U}, \tag{8.3}$$

$$k_{bb} = \frac{\Phi_1 + \Phi_2}{4\pi C_1 U}. \tag{8.4}$$

In the case $\Phi_2/\Phi_1 \leqslant C_2/C_1$, we have $k_{ab} \leqslant k_{ba}$, and

$$G = \begin{cases} 0 & \text{for} \quad k \leqslant k_{aa} \\ 4\pi(C_1 + C_2)Uk - \Phi_1 & \text{for} \quad k_{aa} \leqslant k \leqslant k_{ab} \\ \Phi_2 & \text{for} \quad k_{ab} \leqslant k \leqslant k_{ba} \\ \Phi_1 + \Phi_2 - 4\pi C_1 Uk & \text{for} \quad k_{ba} \leqslant k \leqslant k_{bb} \\ 0 & \text{for} \quad k_{bb} \leqslant k \end{cases} \tag{8.5}$$

In the case $C_2/C_1 \leqslant \Phi_2/\Phi_1$, we have $k_{ba} \leqslant k_{ab}$, and

$$G = \begin{cases} 0 & \text{for} \quad k \leqslant k_{aa} \\ 4\pi(C_1 + C_2)Uk - \Phi_1 & \text{for} \quad k_{aa} \leqslant k \leqslant k_{ba} \\ 4\pi C_2 Uk & \text{for} \quad k_{ba} \leqslant k \leqslant k_{ab} \\ \Phi_1 + \Phi_2 - 4\pi C_1 Uk & \text{for} \quad k_{ab} \leqslant k \leqslant k_{bb} \\ 0 & \text{for} \quad k_{bb} \leqslant k \end{cases} \tag{8.6}$$

To determine the spectrum the theorem of the mean integral value is applied to the counter equation (3.3). Since in both expressions (8.5) and (8.6) integration of the G-function yields the same result, namely

$$\int_0^{\infty} G\,dk = \frac{C_2\Phi_2(\Phi_1 + \Phi_2/2)}{4\pi C_1(C_1 + C_2)U}, \tag{8.7}$$

we obtain

$$\varrho(\tilde{k}) = \frac{4\pi C_1(C_1+C_2)U}{C_2\Phi_2(\Phi_1+\Phi_2/2)}\, I. \tag{8.8}$$

$\tilde{k}$ lies in the interval defined by the mean mobility

$$\bar{k} = \frac{(C_1+C_2)(\Phi_1+\Phi_2) - C_1\Phi_1}{8\pi C_1(C_1+C_2)U} \tag{8.9}$$

and the relative half-width

$$\delta_k = \frac{(C_1+C_2)(\Phi_1+\Phi_2) - C_1\Phi_1}{(C_1+C_2)(\Phi_1+\Phi_2) + C_1\Phi_1}. \tag{8.10}$$

Introducing the notation

$$\gamma_C = \frac{2C_1+C_2}{C_2}, \tag{8.11}$$

$$\gamma_\Phi = \frac{2\Phi_1+\Phi_2}{\Phi_2}, \tag{8.12}$$

the above expressions can be written more clearly in the form

$$\varrho(\tilde{k}) = \frac{\gamma_C+\gamma_\Phi}{2(2\Phi_1+\Phi_2)\bar{k}\delta_k} I = \frac{1+\gamma_C\gamma_\Phi}{2(2\Phi_1+\Phi_2)\bar{k}}\, I, \tag{8.13}$$

$$\bar{k} = \frac{\Phi_1}{4\pi(C_1+C_2)U(1+\delta_k)}, \tag{8.14}$$

$$\delta_k = \frac{\gamma_C+\gamma_\Phi}{1+\gamma_C\gamma_\Phi}. \tag{8.15}$$

From expression (8.13) it follows that for certain values of the mean limiting mobility and mean air-flow rate $\Phi_1+\Phi_2/2$ the current I depends on the counter parameters only via the product $\gamma_C\gamma_\Phi$. It is readily seen that when the quantity $\gamma_C\gamma_\Phi$ is not varied, the parameter δ_k has a minimum if $\gamma_C = \gamma_\Phi$. Consequently, the condition of best resolution for constant current is

$$\frac{\Phi_2}{\Phi_1} = \frac{C_2}{C_1}. \tag{8.16}$$

This expression was derived in a less strict way in the work /Tammet, 1960/.

The condition (8.16) is close to that of optimum operation, but it does not exactly coincide with the latter. The reason is that the counter sensitivity, apart from depending on the ratio $I/\varrho(k)$, depends also on the capacitance C_2. For optimum operation conditions, $C_2/C_1 < \Phi_2/\Phi_1$.

Besides the above application of the differential counter of the second order, the possibility of measuring the partial charge density or partial conductivity is of interest. This is borne out by the occurrence of the

segment $G = \Phi_2$ or $G = 4\pi C_2 U k$ in the mobility interval between k_{ab} and k_{ba}. Choosing the counter parameters in such a way that $\Phi_2/\Phi_1 \ll C_2/C_1$ or $C_2/C_1 \ll \Phi_2/\Phi_1$, one can obtain the G-function in the form shown in Figure 8.1. We shall divide the integral in equation (3.3) into terms corresponding to the linear intervals of the G-function. Most important is the integral in the interval (k_{ab}, k_{ba}), which directly gives the partial charge density or the partial conductivity. To reduce the two remaining integrals to the form of partial charge density or partial conductivity, we employ the theorem according to which in the interval (a, b) there always exists a ξ, such that

$$\int_a^b f(t)\,dt = \int_a^\xi g(t)\,dt \tag{8.17}$$

only if in the whole interval the condition

$$0 \leqslant \frac{f(t)}{g(t)} \leqslant 1 \tag{8.18}$$

is satisfied.

In the case $\Phi_2/\Phi_1 < C_2/C_1$ we obtain

$$\varrho(\tilde{k}_1, \tilde{k}_2) = \frac{I}{\Phi_2}, \tag{8.19}$$

where $\tilde{k}_1$ and $\tilde{k}_2$ lie in intervals with mean mobilities

$$\bar{k}_1 = \frac{\Phi_1+\Phi_2/2}{4\pi(C_1+C_2)U}, \tag{8.20}$$

$$\bar{k}_2 = \frac{\Phi_1+\Phi_2/2}{4\pi C_1 U}. \tag{8.21}$$

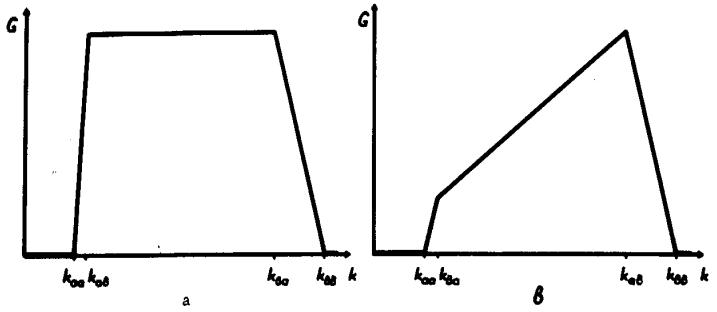

FIGURE 8.1. G-function of the second-order differential counter:

a—when $\Phi_2/\Phi_1 \ll C_2/C_1$; b—when $C_2/C_1 \ll \Phi_2/\Phi_1$.

The relative half-width of the $(\tilde{k}_1, \tilde{k}_2)$ interval is expressed by (7.19).

In the case $C_2/C_1 < \Phi_2/\Phi_1$, we obtain

$$\lambda(\tilde{k}_1, \tilde{k}_2) = \frac{I}{4\pi C_2 U}, \tag{8.22}$$

where $\tilde{k}_1$ and $\tilde{k}_2$ lie in intervals, the mean mobilities of which are given by

$$\bar{k}_1 = \frac{(C_1 + C_2/2)\Phi_1}{4\pi C_1 (C_1 + C_2) U}, \tag{8.23}$$

$$\bar{k}_2 = \frac{(C_1 + C_2/2)(\Phi_1 + \Phi_2)}{4\pi C_1 (C_1 + C_2) U}. \tag{8.24}$$

The relative half-width of the interval is given by formula (7.11).

The advantage of this new method for measuring $\varrho(k_1, k_2)$ and $\lambda(k_1, k_2)$ over other variants of the aspiration method is that it suffices to measure directly only one value of the current through the collector plate in order to obtain one value of the desired parameter. It should be mentioned that in the integral method the measuring of four and in the first-order differential method the measuring of two current values is required to obtain the same result.

§9. COUNTERS WITH SEVERAL COLLECTOR PLATES

In the following we consider counters in which the current through several plates is measured. Counters with reversible plates, for example, that are described in the work /Ortner, El Nadi, 1955/ do not belong to this group. There are many possible designs of a measuring capacitor with several collector plates. A general treatment of the problem is very involved and beyond the scope of this book. We shall therefore confine ourselves to some practical examples.

The simplest counter with two collector plates is an integral counter measuring the current through both plates. It enables the simultaneous recording of air ions of both polarities, but does not present any new possibilities of measurement.

Consider the behavior of air ions in the measuring capacitor under more general conditions. Suppose the capacitor consists of many plates to which different voltages are applied, and consider the expression for the total current through some group of plates, which we shall call the collector group. This expression is similar to that for the current in an integral counter. However, two conditions must be satisfied.

1. Air ions of one polarity only settle on the collector group and if the conductivity is sufficiently large, all air ions of this polarity will settle.

2. The boundary surface of the air ions that are being collected (the current of which is unsaturated) should separate the collector group from all the other plates, so that the electric flux through the boundary surface will correspond to the sum of the charges on the plates of the collector group.

These conditions will be called the normal conditions.

The limiting mobility of the collector group is given by

$$k_0 = -\frac{\Phi}{4\pi \sum_{n=1}^{m} Q_n}, \tag{9.1}$$

where Q_n corresponds to the charges on the plates of the collector-group plates. This is defined by the sums $\sum_l C_{n,l} U_{n,l}$, where $C_{n,l}$ and $U_{n,l}$ are respectively the mutual capacitance and the voltage between the plates with indices n and l.

The question whether the normal conditions are satisfied is complex and can be answered only in special cases.

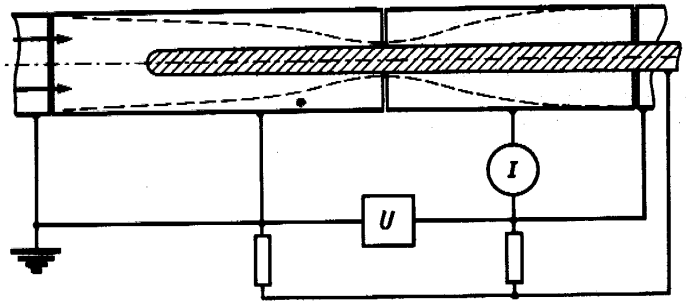

FIGURE 9.1. Example of a measuring capacitor in which the normal conditions are not satisfied.

– – – – – boundary surface for a certain mobility.

An example of a measuring capacitor in which the normal conditions are not satisfied is shown in Figure 9.1. The normal conditions are fully satisfied in the trivial case in which the potentials of all plates are equal to one another. This occurs in the differential counter with an electrode divided into several collecting plates /Israël, 1931/.

The current through the first plate of this counter is calculated in the same way as in the case of an integral counter, and the current through the remaining plates as in the case of a first-order differential counter with a divided electrode. Suppose the current is measured through the plate with index $l \neq 1$ and the plate with index $m > l$ in a capacitor designed such that $C_m = C_l$. The currents I_l and I_m are expressed by the integral (3.3) and G by equations (7.1)–(7.3), where $C_2 = C_l = C_m$ and $C_1 = \sum_{n=1}^{l-1} C_n$ for G_l and $C_1 = \sum_{n=1}^{m-1} C_n$ for G_m. The difference $I_l - I_m$ is also expressed by the integral (3.3), where $G = G_l - G_m$. The expression

$$G = \begin{cases} 0 & \text{for} \quad k \leqslant k_{ma} \\ 4\pi \sum_{n=1}^{m} C_n U k - \Phi & \text{for} \quad k_{ma} \leqslant k \leqslant k_{mb} \\ 4\pi C_l U k & \text{for} \quad k_{mb} \leqslant k \leqslant k_{la} \\ \Phi - 4\pi \sum_{n=1}^{l+1} C_n U k & \text{for} \quad k_{la} \leqslant k \leqslant k_{lb} \\ 0 & \text{for} \quad k_{lb} \leqslant k, \end{cases} \tag{9.2}$$

where k_{ma}, k_{mb}, k_{la} and k_{lb} are the limiting mobilities corresponding to the capacitances $\sum_{n=1}^{m} C_n$, $\sum_{n=1}^{m-1} C_n$, $\sum_{n=1}^{l} C_n$ and $\sum_{n=1}^{l-1} C_n$. The G-function (9.2) has the same form as the G-function of the second-order differential counter (9.6). We

can therefore apply the same method of calculation, which yields

$$\lambda(\bar{k}_1, \bar{k}_2) = \frac{I_l - I_m}{4\pi C_l U}, \tag{9.3}$$

where $\bar{k}_1$ and $\bar{k}_2$ lie in the intervals with mean velocities

$$\bar{k}_1 = \frac{\Phi\left(\sum_{n=1}^{m-1} C_n + C_l/2\right)}{4\pi U \sum_{n=1}^{m-1} C_n \sum_{n=1}^{m} C_n}, \tag{9.4}$$

$$\bar{k}_2 = \frac{\Phi\left(\sum_{n=1}^{l-1} C_n + C_l/2\right)}{4\pi U \sum_{n=1}^{l-1} C_n \sum_{n=1}^{l} C_n}. \tag{9.5}$$

The relative half-widths of the intervals are respectively

$$\delta_{k_1} = \frac{C_l}{2\sum_{n=1}^{m-1} C_n + C_l}, \tag{9.6}$$

$$\delta_{k_2} = \frac{C_l}{2\sum_{n=1}^{l-1} C_n + C_l}. \tag{9.7}$$

When studying the spectrum $\varrho(k)$ it is advisable to measure the currents through adjacent plates, the capacities of which are equal to one another. Assuming $m = l+1$, we can arrive at the results obtained above. Similarly, as in the case of the second-order differential counter, we obtain

$$\varrho(\bar{k}) = \frac{4\pi U \sum_{n=1}^{l-1} C_n \sum_{n=1}^{l} C_n \sum_{n=1}^{l+1} C_n}{\Phi^2 C_l^2} (I_l - I_{l+1}). \tag{9.8}$$

$\bar{k}$ lies in the interval with mean mobility

$$\bar{k} = \frac{\Phi \sum_{n=1}^{l} C_n}{4\pi U \sum_{n=1}^{l-1} C_n \sum_{n=1}^{l+1} C_n} \approx \frac{\Phi}{4\pi U \sum_{n=1}^{l} C_n} \tag{9.9}$$

and relative half-width

$$\delta_k = \frac{C_l}{\sum_{n=1}^{l} C_n}. \tag{9.10}$$

In formulas (9.3) and (9.8) the difference between the currents through both plates appears.

Therefore, in the case of the above-described counter, it is useful to employ one differential electrometer instead of two electrometers /Imyanitov, 1952; Zachek, 1964/. This enables us to obtain directly a count which is proportional to the desired quantity.

An interesting new counter version with two collector plates was recently proposed /Imyanitov, 1963; Imyanitov, Pavlyuchenkov, 1964; Schmeer, 1966/ for integral measurements.

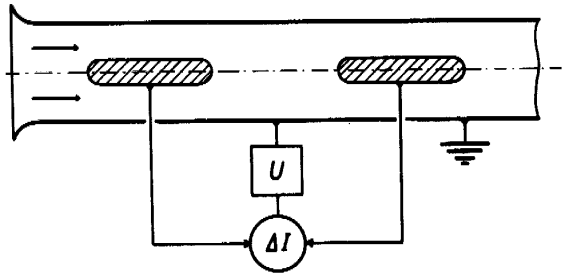

FIGURE 9.2. The counter of Imyanitov. ΔI is the differential electrometer.

A schematic diagram of the counter is given in Figure 9.2. The measuring capacitor consists of two collector plates with equal capacitances and equal voltages U. The difference $\Delta I = I_1 - I_2$ of the currents through the first and second collector plate is measured with the aid of the differential electrometer. It is readily shown that for ΔI the function G_Δ has the form

$$G_\Delta = \begin{cases} 0 & \text{for} \quad k \leqslant k_0/2 \\ (2k/k_0 - 1)\Phi & \text{for} \quad k_0/2 \leqslant k \leqslant k_0 \\ \Phi & \text{for} \quad k_0 \leqslant k \end{cases} \tag{9.11}$$

where k_0 is calculated from the active capacitance C of one inner plate. The trend of the function G_Δ is shown in Figure 9.3.

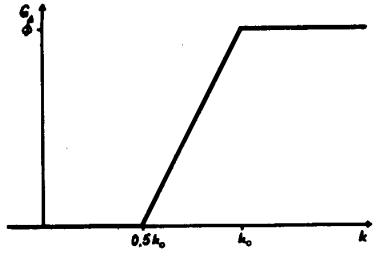

FIGURE 9.3. The G-function for the counter of Imyanitov.

Starting with expression (9.11) we can readily derive a formula useful for practical calculations:

$$\varrho[(0.75 \pm 0.25)k_0, \infty] = \frac{\Delta I}{\Phi}. \qquad (9.12)$$

To obtain one value of $\varrho(\tilde{k}, \infty)$, one count will suffice.

The differential counter of Misaki /Misaki, 1950/ may also be considered as a counter with several plates.

Let us finally consider a problem indirectly related to the present section. It appears that the normal conditions are fulfilled for the integral counter shown in Figure 9.4. The special feature of this counter is that the active capacitance of the measuring capacitor is accurately given by the formula for the capacitance of an ideal cylindrical capacitor, in spite of the fact that the electric field is of a rather complex form. Charges induced by the voltage between the forward plate and the collector plate mutually compensate one another. The normal conditions are satisfied in all capacitor designs in which some symmetrical component is connected in front of the collector plate to the outer plate. This enables the use of an annular entrance opening which is of interest in counters with a divided air flow as well as in certain specific designs of the integral counter /Reinet, 1958, 1959a/.

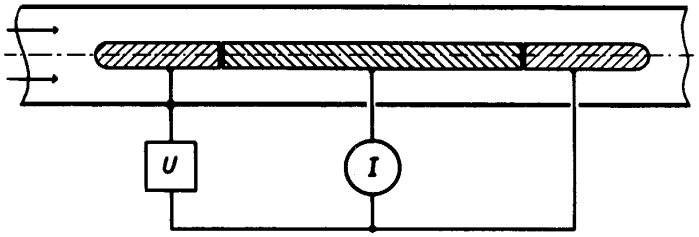

FIGURE 9.4. Measuring capacitor, the active capacitance of which can be accurately calculated from the geometrical length of the collector plate.

§10. COUNTERS WITH INTERPLATE AIR MIXING

Counters are known in which provision is made for mixing the air flow between the two inner plates of the measuring capacitor. This presents new measuring possibilities, as proposed in the works /Israël, 1949; Israël, Schultz, 1933; Gerasimova, 1941b/.

Interplate mixing of the air flow is effected by an arrangement in which the flow is first rendered turbulent and then laminar again. The mixing is facilitated by dividing the current into two branches /Israël, 1931/. Complete mixing is obtained when two measuring capacitors having plates are connected in series and separated by a grid-like screen.

Mixing of the air is unavoidably accompanied by a loss of air ions due to increased adsorption. Distortions may also arise in the case of incomplete mixing. These phenomena, which are neglected in the present chapter,

considerably reduce the practical importance of methods in which interplate air mixing is employed.

Consider a measuring capacitor with two inner plates, between which the air flow is mixed. The density spectrum of the flow of air ions passing through the first part of the capacitor is defined as the difference of the density spectrum of the incoming flow and the density spectrum of the flow of settling air ions.

$$I'(k) = (\Phi - G_a - G_b)\varrho(k), \qquad (10.1)$$

where G_a and G_b are respectively the G-functions for the inner and outer plate of the first part of the capacitor. After mixing the spectrum is given by

$$\varrho'(k) = \frac{I'(k)}{\Phi} = \left(1 - \frac{G_a + G_b}{\Phi}\right)\varrho(k). \qquad (10.2)$$

The second part of the measuring capacitor corresponds to a standard integral counter. The function G_2 for the current through the second inner plate is calculated by multiplying the G-function of a standard integral counter by the multiplicative factor of formula (10.2). Denoting the limiting mobility of the first part of the capacitor by k_1 and the limiting mobility of the second part by k_2, we obtain for the condition $k_1 \leqslant k_2$

$$G_2 = \begin{cases} \Phi \frac{k}{k_2}\left(1 - \frac{k}{k_1}\right) & \text{for} \quad k \leqslant k_1 \\ 0 & \text{for} \quad k_1 \leqslant k. \end{cases} \qquad (10.3)$$

For the condition $k_2 \leqslant k_1$

$$G_2 = \begin{cases} \Phi \frac{k}{k_2}\left(1 - \frac{k}{k_1}\right) & \text{for} \quad k \leqslant k_2 \\ \Phi\left(1 - \frac{k}{k_1}\right) & \text{for} \quad k_2 \leqslant k \leqslant k_1 \\ 0 & \text{for} \quad k_1 \leqslant k. \end{cases} \qquad (10.4)$$

In the latter case we have

$$h_{U_1} G_2 = \begin{cases} 0 & \text{for} \quad k < k_2 \\ \Phi\left(1 - \frac{k}{k_1}\right) & \text{for} \quad k_2 < k \leqslant k_1 \\ 0 & \text{for} \quad k_1 \leqslant k. \end{cases} \qquad (10.5)$$

Applying the theorem of the mean integral value we can derive

$$\varrho(\tilde{k}) = \frac{2k_1}{\Phi(k_1 - k_2)^2} h_{U_1} I_2, \qquad (10.6)$$

where $\tilde{k}$ lies in the interval with mean mobility

$$\bar{k} = \frac{k_1 + k_2}{2} \qquad (10.7)$$

and relative half-width

$$\delta_k = \frac{k_1 - k_2}{k_1 + k_2}. \qquad (10.8)$$

It should be pointed out that in the described method the condition $k_2 < k_1$ must be satisfied.

When the air flow is divided into two branches (after it has passed through the first part of the measuring capacitor), the latter are led through two respective counters with different limiting mobilities.

This enables us to determine $\varrho(k)$ from two simultaneous measurements. A detailed description of this method may be found in the works /Israël, 1931; Israël, Shultz, 1933; Israël, 1957b/.

A comparison of the above method with the usual differential methods does not reveal any advantages. On the contrary, the method of interplate air mixing is undoubtedly less accurate and less sensitive, which can be easily seen from formulas (10,6) and (7.8).

Therefore, the above method can hardly be expected to be of any practical use.

Interplate air mixing can also be effected in a standard integral counter with a precondenser. If the second capacitor operates under saturation conditions, no deviation from the usual operating conditions will occur. In the opposite case certain complications arise. A detailed treatment of this problem may be found in the works /Israël, 1931, 1957b/. Compared with the usual method of the precondenser, the method of interplate air mixing offers no advantages.

Gerasimova /Gerasimova, 1941b/ proposed a method which on first sight seemed very promising. Here the partial charge density $\varrho(0, \bar{k})$ of heavy and super-heavy ions is measured, whereby an integral counter is employed in conjunction with a precondenser and interplate air mixing. The measuring capacitors can have a relatively high limiting mobility and a simple design.

The method of Gerasimova requires that the condition $k_1 \leqslant k_2$ be satisfied. The current through the inner plate is expressed by equation (3.3), where the G-function has the form given by (10.3). Differentiation of this equation yields

$$\frac{\partial I_2}{\partial U_1} = -\frac{\Phi}{k_1 k_2 U_1}\int_0^{k_1} k^2 \varrho(k)\,dk, \tag{10.9}$$

$$h_{U_1} I_2 = \frac{\Phi}{k_2}\int_0^{k_1} k\,\varrho(k)\,dk. \tag{10.10}$$

Let us now introduce the mean square mobility of the air ions and write the integrals in the form

$$\int_0^{k_1} k^2 \varrho(k)\,dk = \overline{k^2}(0, k_1)\varrho(0, k_1), \tag{10.11}$$

$$\int_0^{k_1} k\,\varrho(k)\,dk = \overline{k}(0, k_1)\varrho(0, k_1). \tag{10.12}$$

Forming the ratio $(h_{U_1} I_2)^2 / \frac{\partial I_2}{\partial U_1}$, we obtain

$$\varrho(0, k_1) = \frac{C_1}{\Phi C_2 U_2}\,\frac{\overline{k^2}(0, k_1)}{[\overline{k}(0, k_1)]^2}\,\frac{(h_{U_1} I_2)^2}{\partial I_2 / \partial U_1}. \tag{10.13}$$

The expression $\overline{k^2}(0, k_1)/[\overline{k}(0, k_1)]^2$ cannot be determined from the measurement results, which is a serious drawback of the method. Formula (10.13) can be applied only in the case when the parameter $\overline{k^2}(0, \overline{k_1})/[\overline{k}(0, k_1)]^2$ can be estimated on the basis of previously known results. Gerasimova /Gerasimova, 1941b/ assumed $\overline{k^2}(0, \overline{k_1}) = [\overline{k}(0, k)]^2$, which leads to erroneous conclusions.

§11. MEASUREMENT OF THE SPACE CHARGE DENSITY

Many methods based on various principles are available for measuring the charge density. Those not related to aspiration methods are the Thomson method /Thomson, W., 1882, Daunderer, 1909/, the three-collector method /Daunderer, 1907/ and the Imyanitov method (related to the Thomson method) /Imyanitov, 1951; In'kov, 1958, 1965; Kitaev, 1962/, and finally the Mühleisen-Holl method /Mühleisen, Holl, 1952/ and the indirect method of calculating the charge density from the spatial distribution of the electric field and the conductivity /Hansen, 1935; Mecklenburg, Lautner, 1940/. A survey of the various methods can be found in the book /Israël, 1961/.

The aspiration device for measuring the charge density should satisfy the condition $G = \Phi$ for any mobility. Since this is impossible, we must be satisfied with the approximate fulfillment of this condition in the practical range of mobilities. In the integral counter the condition $G = \Phi$ can be fulfilled for mobilities of one polarity only. The limiting mobility should be less than the mobility of heaviest ions still contributing to the charge density. When measuring charge densities, the polar densities are recorded separately and then added. The accuracy of this method is not very high and the relative error often exceeds the relative errors of the initial measurements. Nevertheless, this method is sometimes applied in practice /Gockel, 1917; Reinet, 1958/. The simultaneous counting of air ions of both polarities can be effected by means of devices with a filter, through which the air is drawn. Here the current which flows through the filter to the ground is measured.

The operation of a fiber filter is based on air-ion adsorption. The application of the method was first described in the work /Zeleny, 1898a/. This method is considered to be one of the best methods for measuring the charge density /Mühleisen, 1957a/. The measuring filter of the device is filled with cotton wool /Becker, 1910; Obolensky, 1925/, with glass wool /Zeleny, 1898a; McClelland, 1898/, with metal shavings /Aselmann, 1906; Brown, 1930/, or with metallic grids /Krasnogorskaya, Seredkin, 1964/.

The theory of the fiber-filter method /Fuks, Stechnika, 1962/ has been little studied. To verify the effectiveness of the filter the air flow is drawn through two filters arranged in series. The filter is considered effective if the current through the second filter is sufficiently small compared to the

current through the first filter. The filter in question can be connected in series with the standard integral counter /Paltridge, 1967/. The charge density is given by an elementary formula

$$\varrho = \frac{I}{\Phi}. \tag{11.1}$$

The disadvantage of fiber filters lies in their relatively large resistance to the air flow. Accordingly, the electrostatic filter suggested by Gunn /Gunn, 1953/ is more efficient. The Gunn method is a combination of the integral-counter method and the filter method. This device is schematically shown in Figure 11.1. The G-function for such a filter has the form shown in Figure 11.2. For a sufficiently small limiting mobility the approximation $G = \Phi$ is permissible and does not depend on the mobility.

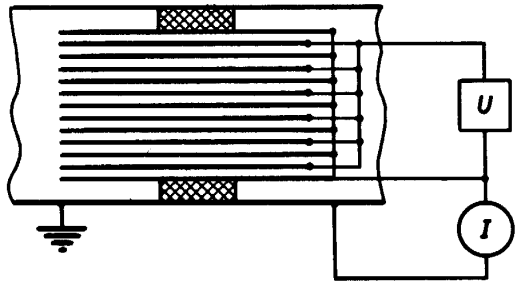

FIGURE 11.1. Gunn filter.

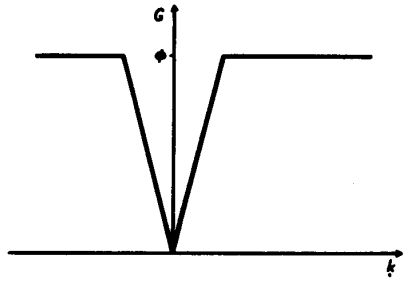

FIGURE 11.2. The G-function for the Gunn filter.

The Gunn filter usually consists of plane-parallel plates. The maximum allowable voltage between the plates should be chosen on the basis of reliability considerations. Since breakdown of the capacitor occurs at a certain value of the electric field strength E, the latter should be chosen before designing the filter. The formula for the limiting mobility (4.3) now becomes

$$k_0 = \frac{\Phi d}{EV}, \tag{11.2}$$

where d is the distance between the plates, and V is the filter volume.

§12. MODULATED COUNTERS

In the usual aspiration counters one measures a fairly weak direct current through the collector plate. Amplification and recording of such a weak direct current constitutes a difficult technical problem. For the measurement of the very weak direct current in more recent instruments it is preferable to transform the incoming signal into an alternating one, since amplification of an alternating current is much simpler.

The possibility of transforming the output signal of the measuring capacitor by introducing certain changes in the counter design was proposed quite recently /Junod, Sänger, Thams, 1962/. Apart from the outlined advantage, this method opens the way to some other new possibilities of major importance. In modulated counters it appears possible to suppress various distorting effects which often cause serious trouble in usual counters. This problem will be discussed in the following chapters.

The main advantage of the modulated counters lies in the possibility of differentiating by means of modulation techniques. This was the main reason underlying the development of modulated measuring capacitors /Junod, Sänger, Thams, 1962/.

Modulated counters record the amplitude of the alternating component of the current through the collector plate.

The modulation frequency is very low (of the order of several Hz or lower) so that the use of amplifiers is required. For simplicity, we assume that the modulation period is sufficiently large compared to the time constant of the current generated by the air ions flowing toward the collector plate of the capacitor. This enables us to forego allowance for transient processes which considerably complicate the calculation procedure.

The amplitude of the alternating current through the collector plate is given by

$$I_{\sim} = \frac{1}{2}(I_{max} - I_{min}). \tag{12.1}$$

$I_{\sim}$ can be correlated with the spectrum $\varrho(k)$ via an integral transformation similar to formula (3.3). The kernel of the integral will be denoted by $G_{\sim}$.

Let us briefly consider the specific possibilities of counters with modulated measuring and modulated precondenser. For simplicity, we assume the modulating signal is rectangular everywhere. Rectangular modulation is in most cases the most appropriate.

1. Modulation by the means of the gas flow rate. Suppose the measuring capacitor is similar to the measuring capacitor of a usual integral counter. Denote the gas flow rate during the first half-period by Φ_1, and during the second half-period by Φ_2. Assume further that $\Phi_1 < \Phi_2$ and denote the respective limiting mobilities by k_1 and k_2. The function $G_{\sim}$ is then given by

$$2G_{\sim} = \begin{cases} 0 & \text{for} \quad k \leqslant k_1 \\ 4\pi CUk - \Phi_1 & \text{for} \quad k_1 \leqslant k \leqslant k_2 \\ \Phi_2 - \Phi_1 & \text{for} \quad k_2 \leqslant k. \end{cases} \tag{12.2}$$

This expression is similar to (7.13), which represents the G-function of a first-order differential counter with a divided air current. Analysis of formula (12.2) leads correspondingly to results obtained in § 7 and expressed by formulas (7.16) and (7.20).

It may be noted that for the case $\Phi_2 = 2\Phi_1$ the function G_- assumes the same form as the function G_- of the Imyanitov counter (9.11), so that the described counter possesses the same properties as this counter.

For the case $\Phi_1 = 0$ the function G_- corresponds to the function G of an ordinary integral counter.

Two antiphase-modulated measuring capacitors may be fed by one fan. The gas flow rate through the fan will then be constant.

A disadvantage of gas flow rate modulation is the tendency of pulsating flows to become turbulent and the necessity of mechanical commutator arrangements in gas flow rate modulation.

2. Modulation of the measuring capacitor voltage. Let us denote the voltage in successive half-periods by U_1 and U_2, respectively, and assume $U_1 < U_2$. In accordance with formula (4.3) $k_2 < k_1$. The function G_- then becomes

$$2G_- = \begin{cases} 4\pi C(U_2 - U_1)k & \text{for} \quad k \leqslant k_2 \\ \Phi - 4\pi C U_1 k & \text{for} \quad k_2 \leqslant k \leqslant k_1 \\ 0 & \text{for} \quad k_1 \leqslant k. \end{cases} \tag{12.3}$$

When $U_1 = 0$, expression (12.3) corresponds to the G-function of a usual integral counter. Junod, Sänger and Thams /1962/ developed a method of double differentiation by means of a complex modulating voltage. A typical modulating voltage ensuring double differentiation is shown in Figure 12.1. Here the difference between the amplitudes of the variable high-frequency component is recorded for different half-periods of the low-frequency component.

The double differentiation method is very sensitive to fluctuations in the relative charge density.

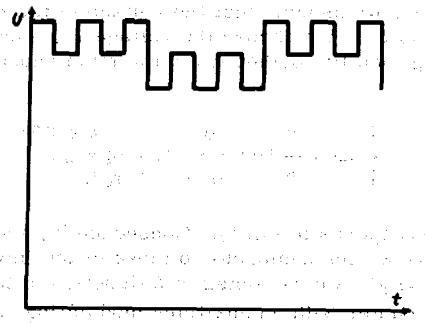

FIGURE 12.1. Modulating voltage signal ensuring double differentiation.

A serious disadvantage of this method is the necessity to accurately compensate the induced current which exceeds the measured current by

several orders of magnitude. The compensation of the induced current is effected by a bridge circuit /Junod, Sänger, Thams, 1962/, which will be described in §31.

3. Counter with a modulated precondenser. The measuring capacitor is schematically shown in Figure 12.2. The intermediate shorted screening capacitor is not necessary in principle, and merely serves to decrease the total length and to prevent a widening of the air flow after it has passed through the precondenser. Widening of the flow may cause turbulence. The auxiliary RC circuit serves to separate the alternating and direct current.

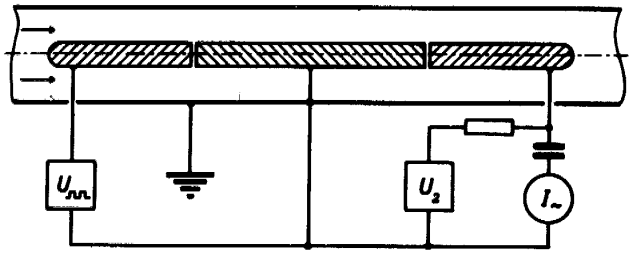

FIGURE 12.2. Counter with a modulated precondenser.

This counter has none of the shortcomings connected with the aerodynamic instability of the pulsating flow and induced current.

Counters employing a modulated precondenser offer many additional possibilities for work under various operating conditions. The function G_- is calculated as the difference of two expressions of the type (6.3). Since the general form of this function is of current interest, we shall consider only one example. Suppose the active capacitances of the preliminary and main capacitors are C_1 and C_2, respectively, and the voltage of the preliminary capacitor is 0 in the first half-period and U_1 in the second half-period. Further, we assume that the voltage of the main capacitor is constant and equals U_2. We choose the voltage U_1, such that $U_1 C_1 = U_2 C_2$. Denoting the limiting mobility of the ions in the main capacitor by k_0, we obtain

$$2G_- = \begin{cases} 0 & \text{for} \quad k \leqslant 0{,}5k_0 \\ (2k/k_0 - 1)\Phi & \text{for} \quad 0.5k_0 \leqslant k \leqslant k_0 \\ \Phi & \text{for} \quad k_0 \leqslant k. \end{cases} \tag{12.4}$$

This expression corresponds to (9.11). Consequently, the counter under consideration has properties analogous to those of the Imyanitov counter.

Choosing $U_1 C_1 = -U_2 C_2$, we can obtain a G-function of the type (4.4).

4. Differential counter with an auxiliary modulating capacitor. According to Figure 12.3 the auxiliary capacitor is located at the center of the first inner plate of the measuring capacitor. The auxiliary capacitor can be placed directly in front of the differential measuring capacitor but this would lead to complications because of the deviation from normal conditions and because of the appearance of an edge effect at the boundary between the auxiliary to the measuring capacitor.

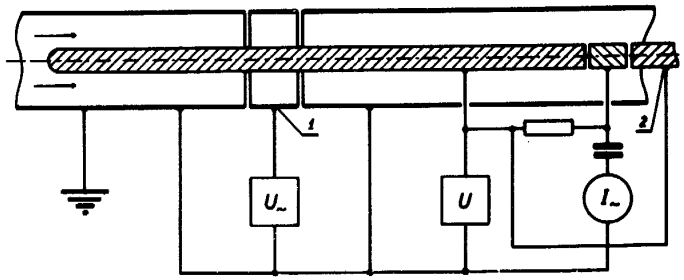

FIGURE 12.3. Differential counter with an auxiliary modulated capacitor:

1—modulated plate; 2—equipotential elongation of the inner plate intended to improve the aerodynamic properties of the measuring capacitor.

Suppose the mutual capacitance between the first inner and the entire outer plate (including the modulated plate) is C_1, the capacitance between the first inner and the modulated plate is $C_\sim$, the active capacitance of the second inner plate is C_2. Denoting the constant voltage by U and the amplitude of the alternating modulating voltage by $U_\sim$, we obtain the four limiting mobilities:

$$k_{a+} = \frac{\Phi}{4\pi[(C_1 + C_2)U + C_\sim U_\sim]}, \tag{12.4}*$$

$$k_{a-} = \frac{\Phi}{4\pi[(C_1 + C_2)U - C_\sim U_\sim]}, \tag{12.5}$$

$$k_{b+} = \frac{\Phi}{4\pi(C_1 U + C_\sim U_\sim)}, \tag{12.6}$$

$$k_{b-} = \frac{\Phi}{4\pi(C_1 U - C_\sim U_\sim)}. \tag{12.7}$$

When $k_{a-} \leqslant k_{b+}$, the function $G_\sim$ is expressed by

$$2G_\sim = \begin{cases} 0 & \text{for } k \leqslant k_{a+} \\ 4\pi[(C_1 + C_2)U + C_\sim U_\sim]k - \Phi & \text{for } k_{a+} \leqslant k \leqslant k_{a-} \\ 8\pi C_\sim U_\sim k & \text{for } k_{a-} \leqslant k \leqslant k_{b+} \\ \Phi - 4\pi(C_1 U - C_\sim U_\sim)k & \text{for } k_{b+} \leqslant k \leqslant k_{b-} \\ 0 & \text{for } k_{b-} \leqslant k. \end{cases} \tag{12.8}$$

In the case of strong modulation $k_{b+} \leqslant k_{a-}$, so that

$$2G_\sim = \begin{cases} 0 & \text{for } k \leqslant k_{a+} \\ 4\pi[(C_1 + C_2)U + C_\sim U_\sim]k - \Phi & \text{for } k_{a+} \leqslant k \leqslant k_{b+} \\ 4\pi C_2 U k & \text{for } k_{b+} \leqslant k \leqslant k_{a-} \\ \Phi - 4\pi(C_1 U - C_\sim U_\sim)k & \text{for } k_{a-} \leqslant k \leqslant k_{b-} \\ 0 & \text{for } k_{b-} \leqslant k. \end{cases} \tag{12.9}$$

* [Both this and the previous formula are denoted as (12.4) in the Russian text.]

The two last expressions are similar to formula (8.6), which describes the second-order differential counter under conditions whereby $C_2/C_1 \leqslant \Phi_2/\Phi_1$. Without further calculations it may be stated that, in principle, the above method offers the same possibilities as the second-order differential method for the conditions stated above.

When measuring the spectrum, it is advisable to choose the ratio $U_\sim/U$ equal or slightly larger than the ratio $C_2/2C_\sim$.

The voltage of the modulated plate need not necessarily have only an alternating component, as the alternating component can itself be modulated by a lower frequency component.

In the above-described method modulation by differentiation replaces the technically rather inconvenient separation of the air flow.

The possibilities of the method of modulating the precondenser are not confined to the examples considered above. Since the method is relatively new, it is difficult to indicate the practical significance of the different variants. The general theoretical calculations pertaining to the different counter variants are standard, and we shall forego any further treatment of additional variants of the method.

The theory of modulation counters must be further refined because of the need to calculate or estimate the transient processes. This problem will not be considered in the present book.

Chapter II

DEVIATIONS FROM IDEAL CONDITIONS

§13. FACTORS CAUSING DISTURBANCES AND SYSTEMATIC MEASUREMENT ERRORS

The conclusions derived from the general theory of aspiration counters are strictly valid only when the ideal conditions defined in the preceding chapter are fulfilled. In practice it is often impossible to fulfill all the conditions which lead to disturbances giving rise to systematic errors in the measuring results.

The danger of systematic errors forces us to focus our attention on the quantitative determination of these disturbances. Without such a determination it is impossible to judge whether or which disturbances appear under certain conditions. A quantitative evaluation of the disturbances is necessary for the proper choice of experimental parameters and observation methods.

More involved is the problem of applying the theory of the aspiration counter without allowing for one or another limiting requirement. The first step in the present book will be the determination of corrections eliminating the systematic errors due to small disturbances.

The measurement errors in the air-ion spectrum may be divided into three groups according to the nature of the disturbance source.

The first group comprises errors depending on the degree of perfection of the instruments employed for measuring the current, voltage, gas flow rate, etc., and errors due to the instability of the voltage supply, different contact potentials /Benndorf, 1909, 1926; Scholz, 1931a; Israël, Dolezalek, 1957/, etc. Some of these errors will be treated in Chapter III.

The second group comprises errors due to external conditions. Under ideal conditions the spectrum $q(k)$ at the counter inlet should be homogeneous and equal to the function $q(k)$ of the air sample. Deviations from this requirement may be caused by an external electric field, by a disturbance in the air movement at the measurement point, or by other factors. Of greatest practical significance is the electric field, which complicates the study of atmospheric air ionization /O'Donnel, 1952; Chalmers, 1953/. Information on the effect of the external electric field upon the measurement results may be found in a number of works /Swann, 1914d, 1923; Mackell, 1921, 1923; Norinder, 1921; Wait, 1934; Coroniti, Parziale, Callahan, Patten, 1952; Phillips, 1963; Ivanova, Kuklina, Sedunov, 1963; Zachek, 1964b; Schmeer, 1966/. The disturbance due to the external electric field may be eliminated by proper voltage regulation of the apparatus /Higazi, Chalmers, 1966/. The movement of air ions in the free atmosphere constitutes a problem which lies beyond the scope of this book, and we shall

therefore refrain from a detailed consideration of errors of the second group.

The present chapter deals with the errors of the third group which are caused by deviations from ideal conditions within the counter. The complexity of the problem compels us in most cases to consider small deviations in the first approximation. Neglecting the interaction of the disturbances, we shall be able to consider separately various deviations from the ideal conditions.

For various reasons we shall not discuss the interaction of certain disturbances of the third group. The problem of the unstable operation of the measuring capacitor is considered in detail in the works /Komarov, 1960a, 1960b/. The precipitation of air ions by inertial forces is of definite significance in conductivity measurements in clouds. This problem is dealt with in the works /Zachek, 1962, 1964a, b, 1965/. The disturbance due to inertial forces is removed in those counters having a modulated precondenser.

The effect of air-ion generation in the measuring capacitor on the measurement results is connected with the accumulation of radioactive substances on aerosols /Kurz, 1906, 1907/. The theoretical evaluation of this disturbance is involved and has so far not let to any definite results. In practice, the generation of air ions inside the measuring capacitor is determined directly from the current measurement for operating conditions corresponding to $\Phi = 0$. The effect of the radioactive substances precipitated on the plates depends basically only on the distance between the plates and increases with increasing distance. The effect of radioactive substances contained in air also depends on the distance between the plates but, in addition, is proportional to the filling time of the capacitor

$$t_0 = \frac{\pi l \left(r_2^2 - r_1^2\right)}{\Phi}. \tag{13.1}$$

Expression (13.1) applies to a cylindrical capacitor. For a parallel-plate capacitor we have

$$t_0 = \frac{lcd}{\Phi}, \tag{13.2}$$

where c is the width of the capacitor.

The disturbance due to radioactive radiation is suppressed in counters having a modulated precondenser.

The filling time of the capacitor also determines the effect of air-ion recombination in the measuring capacitor on the measurement results. The relative error in recombination and attachment of air ions to aerosol particles is limited by the inequality

$$\delta < \frac{t_0}{t_i}, \tag{13.3}$$

where t_i is the mean lifetime of the air ion. For light ions in the case of polar charge densities $t_i \approx \frac{600{,}000}{\varrho_\pm \text{ (el. charges/cm}^3\text{)}}$ (sec), where $\varrho_\pm$ is the charge density of air ions of opposite polarity.

The generation and recombination of air ions in the measuring capacitor may partly compensate one another. In the works /Vogler, 1959, 1960/ the

so-called "emission effect" is discussed. Upon decay the radioactive atom radiates α- and β-particles, the charges of which do not fully compensate one another. This gives rise to an additional current from the collector plate, upon which the radioactive substances have accumulated. According to Vogler /1959, 1960/ this current causes a considerable measurement error. An elementary quantitative evaluation shows that this statement is not valid. The "emission effect" is apparently smaller by several orders of magnitude than the effect of air ionization due to the same α- and β-particles, and can thus be of no practical significance.

§14. THE EDGE EFFECT

The edge effect results when the fringing electric field of the counter interacts with the air ions which are drawn into the measuring capacitor.

The nature of the edge effect depends on the manner in which the voltage is applied to the plates of the measuring capacitor. We shall therefore consider the different ways of applying the voltage to the measuring capacitor.

In most counters the inner plate is the collector plate. Because of certain technical advantages the collector plate is maintained at a potential close to the earth's potential. The outer plate in this case has a potential $-U$ relative to the earth. To remove the electric field outside the counter the outer plate is surrounded by a grounded screen. The diverging of the electric field around the entrance of the outer plate may be avoided with the aid of a grounded entrance cylinder. An example of the entrance cylinder of such a measuring capacitor is shown schematically in Figure 14.1.

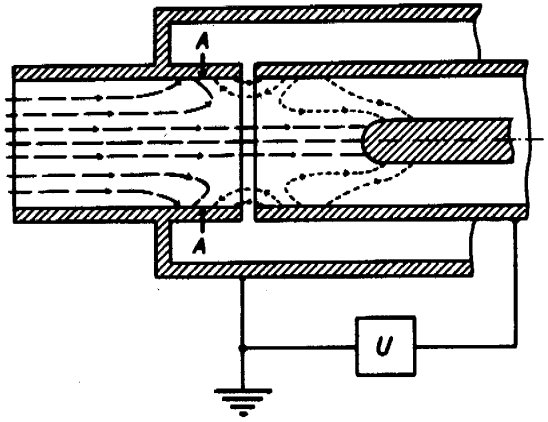

FIGURE 14.1. Example of a capacitor inlet:

– – – – – flow lines; · · · · · flow lines for which $\varrho(k) = 0$; A designates the separation region.

The edge effect in the above measuring capacitor may be analyzed from two equivalent points of view. First, if the entrance cylinder is not considered as a part of the measuring capacitor, then there exist no deviations from ideal conditions which could cause an edge effect. The edge effect is caused by the external electric field due to the potential between the outer plate and the entrance cylinder. In the second case the entrance cylinder may be considered as an additional plate of the measuring capacitor. The inlet of the measuring capacitor then corresponds to the inlet end of the entrance cylinder and the aspiration of the air to be studied will take place without any disturbances. The edge effect is the result of the settling of air ions on the plates of the inlet tube due to the influence of the electric field between the inlet tube and the external plate /Imyanitov, Zachek, In'kov, Semenov, 1960/. Both points of view are equivalent, but the latter is more convenient for theoretical quantitative calculations.

The first detailed description of the nature of the edge effect was given in /Lenard and Ramsauer, 1910/. The edge effect has subsequently been treated in a large number of works /Swann, 1914c; Itiwara, 1931; Scholz, 1931b, 1935; Gish, 1932; Israël, 1932a, 1932b; Graziadei, 1933/. The results of a detailed study on the nature of the electric fields occurring at the edge of various aspiration counters can be found in the work /Schmeer, 1966/. In his work /Israël, 1932a/ Israël proposed the quantitative theory of the edge effect—the so-called theory of the preliminary screening capacitor. According to this theory the edge effect becomes similar to the effect of the precondenser. The settling of air ions in the preliminary screening capacitor is calculated as in the case of the standard integral counter with a correspondingly small capacitance /Siksna, 1950; Israël, 1957b; Hoppel, Kraakevik, 1965/.

Let us consider the movement of the air ions of definite mobility near the inlet of the counter (see Figure 14.1). The spectrum $\varrho(k)$ at the inner surface of the inlet tube is either equal to the spectrum $\varrho_0(k)$ in the outside air, if the outward-emanating streamline of the air-ions terminates at the considered point, or to zero, if the streamline emanates from the external plate. Let us denote the mutual capacitance between the outer plate and that region of the inlet tube, where $\varrho(k) = \varrho_0(k)$, by C'. The capacitance C' depends, apart from the geometry of the electrodes, also on the location of the circle dividing the regions $\varrho(k) = \varrho_0(k)$ and $\varrho(k) = 0$ (Figure 14.1, A). If the location of the dividing circle would not depend on the operating conditions of the measuring capacitor, then the above considerations would validate the theory of the apparent precondenser. However, simple considerations show that the position of the dividing circle depends on the voltage and the air flow rate. This leads to a divergence from the known theory. When describing the edge effect, one may start with the concept of the apparent precondenser. However, the capacitance C' of the precondenser should be regarded as a function of the operation parameters of the counter. The expression for the G-function of the integral counter, taking into account the edge effect, is given by

$$G = \begin{cases} 4\pi CUk & \text{for} \quad k \leqslant k_0, \\ \Phi - 4\pi C'(U, \Phi, k)\,Uk & \text{for} \quad k_0 \leqslant k \leqslant k_0 \\ 0 & \text{for} \quad k_0 \leqslant k, \end{cases} \tag{14.1}$$

where the limiting mobilities are defined by the equations

$$k_0 = \frac{\Phi}{4\pi [C + C'(U, \Phi, k_0)] U}, \tag{14.2}$$

$$k_0' = \frac{\Phi}{4\pi C'(U, \Phi, k_0) U}. \tag{14.3}$$

Calculations according to the thus changed methods of the apparent precondenser lead to integral equations which cannot be solved in general form. This, along with the need to define initially the dependence of C' on the operating conditions of the counter, renders an exact quantitative determination of the edge effect difficult and compels us in most cases to restrict ourselves to an approximate determination.

There are counters which do not include a grounded entrance cylinder. Quantitative calculations are very involved because of the strong dependence of the edge effect on the movement of air in the vicinity of the counter and on other external factors. Generally, the character of the edge effect in this case should remain similar to that of the edge effect in counters with a grounded entrance cylinder.

Difficulties related to the edge effect required in many cases that the counter be connected in such a way that the potential of the outer plate is close to the earth's potential. As the collector plate one sometimes utilizes the inner and sometimes the outer plate. Let us first consider the counter with an inner collector plate, and the outer plate is grounded. If the counter is designed so that the inner plate is fully screened, then the air ions enter the measuring capacitor only under the influence of the air flow and the edge effect does not occur. The edge effect occurs only when the outer plate is too short and does not sufficiently screen the inner plate. In this case the electric field penetrates via the inlet into the outer space. The quantitative determination of the edge effect is difficult because of its dependence on conditions outside the counter. For a rough estimate we shall consider an approximate and simplified calculation /Tammet, 1962b/. Let us imagine a surface dividing the inner and outer space with respect to the measuring capacitor such that inside the counter the movement of air-ions proceeds in accordance with the assumptions in §2 and outside $\varrho(k)$ is uniform. There is no such surface in reality. Therefore, we shall tentatively choose an arbitrary surface at which deviations from the above-mentioned requirements are minimal. We shall seek the function G for the integral counter. Let us denote the mutual capacitance between the inner and outer plates as before by C and the capacitance of the edge effect, determining the flux of the electric field through the dividing surface, by C'. From considerations similar to those in §4 we obtain

$$G = \begin{cases} 4\pi(C + C')Uk & \text{for} \quad k \leqslant k_0 \\ \Phi + 4\pi C'Uk & \text{for} \quad k_0 \leqslant k, \end{cases} \tag{14.4}$$

where k_0 is expressed by formula (4.3). If in the corresponding ideal counter with active capacitance C the current is denoted by I_0, then we may write

$$I = I_0 + 4\pi C'U\lambda_{\pm}, \tag{14.5}$$

where $\lambda_{\pm}$ are the corresponding polar conductivities. Owing to the approximations used, (14.5) may serve only as a rough estimate of the errors caused by the edge effect. The application of this formula for the determination of corrections /Tammet, 1962b/ is not justified.

In counters with an outer collector plate the source of voltage is connected between the inner plate and ground. The potential of the outer plate is close to that of the earth. To prevent interference the counter is always screened. If the outer plate is sufficiently long in comparison to the inner one, then the counter with the outer collector plate will experience no edge effect. In the opposite case, an edge effect caused by the precipitation of air ions on the entrance tube occurs (Figure 14.2). The measuring capacitor of the integral counter is similar to that of the first-order differential counter with a divided capacitor and differs from it only by the quantitative ratio of the plate capacitances. This enables us to utilize formula (7.3) for the description of the edge effect. C_1 is the capacitance between the inner plate and the entrance tube and C_2 is the capacitance between the outer and inner plates. In practice the limiting mobility usually exceeds the mobility of the most mobile air ions. This simplifies calculations and the correction for the edge effect may be determined by the formula

$$I = I_0 - 4\pi C_1 U\lambda_{\pm}, \tag{14.6}$$

where I_0 is the current induced by the air ions in the corresponding ideal counter with active capacitance $C_1 + C_2$.

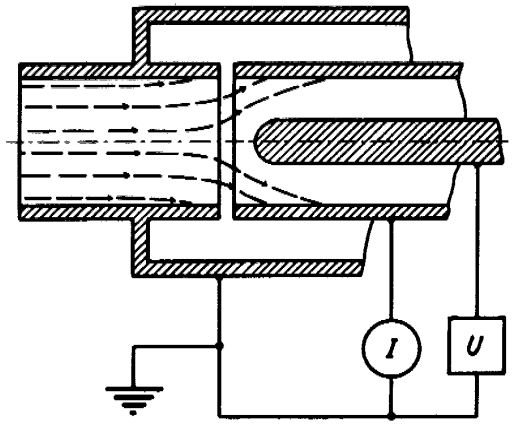

FIGURE 14.2. Edge effect in a counter with an outer collector plate.

If the counter is attached to a free balloon, then we cannot determine the way in which the counter plates are connected merely on the basis of whether the outer plate is grounded or not. No attention was given to the edge effect under these conditions /Kroenig, 1960; Mühleisen, Fischer, 1961/. A qualitatively correct description of the edge effect for the case of an isolated counter is given in the work /Schmeer, 1966/.

Neglect of the edge effect may be unjustified. The precipitation of air ions in the measuring capacitor charges the isolated system which may give rise to an edge effect similar to that in a counter, the outer plate of which is maintained at a certain voltage.

Consider a simplified example. Suppose a counter attached to a free balloon collects all the air ions from the passing air. If the space charge of the air is, for example, positive, then the apparatus acquires a positive charge Q. The charge Q may be expressed by the product of the apparatus capacitance C_s and the voltage $Q = C_s U_s$. This charge induces an edge effect which causes the current from the positive air ions measured by the counter to decrease by a value which is approximately proportional to the voltage U_s and the polar conductivity λ_+. We shall denote the decrease in the current generated by positive air ions by $4\pi C' U_s \lambda_+$, where C' corresponds to the capacitance of the edge effect. The apparatus will receive a current generated by negative air ions equal to $4\pi C_s U_s \lambda_-$. Assuming that the inner plate of the measuring capacitor is sufficiently screened by the outer plate, we obtain from the current balance condition the relationship

$$U_s = \frac{\Phi \varrho}{4\pi (C_s \lambda_- + C' \lambda_+)}, \tag{14.7}$$

where Φ is the air flow rate through the counter and ϱ is the space charge density. If the edge effect is not considered when measuring ϱ_+, we obtain the relative error

$$\delta = \frac{\varrho C' \lambda_+}{\varrho_+ (C_s \lambda_- + C' \lambda_+)}. \tag{14.8}$$

When measuring the current generated by air ions, the polarity of which is opposite to that of the space charge, the edge effect is not observed.

The edge effect does not affect the measurement results of polar conductivity obtained by means of the apparatus attached to a free balloon.

The above simplified example explicitly shows the nature of the edge effect in the case of an isolated counter. A more vigorous and general treatment of the problem will not be attempted. Because of the involved calculations this would hardly be of practical interest.

§15. RESULTS OF THE EXPERIMENTAL INVESTIGATION OF THE EDGE EFFECT

The problem of the edge effect is significant in the case when the outer plate of the measuring capacitor is maintained at a certain potential relative to the earth. To estimate the edge effect the capacitance C' must be known in each specific case as a function of the operation parameters of the measuring capacitor. The capacitance C' is preferably represented as a function of the similarity criteria. The flow field of air ions in the inlet section of the counter depends on the Reynolds number and the dimensionless number K_l, considered in §2. Below we shall use the following expressions for these criteria:

$$\mathrm{Re} = \frac{\Phi}{\pi \nu r}, \tag{15.1}$$

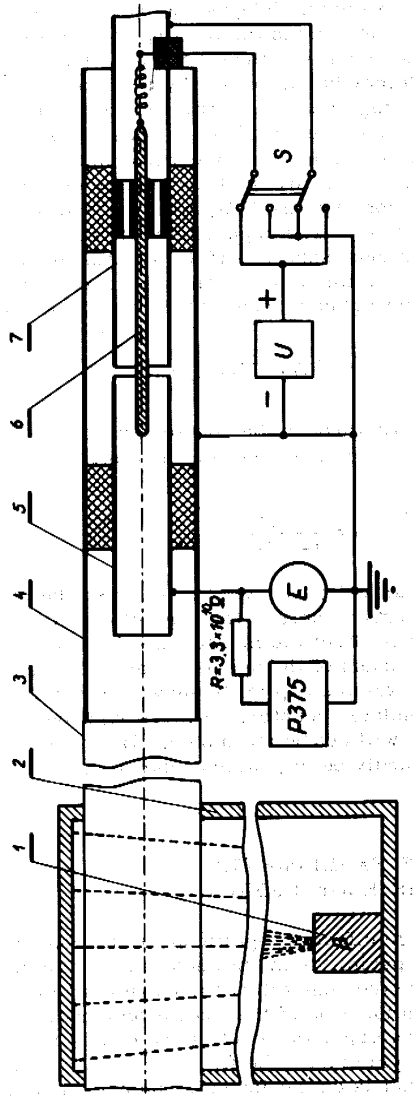

FIGURE 15.1. Arrangement for studying the edge effect:
1 – Sr^{90} preparation; 2 – chamber shielded against β-radiation; 3 – paper tube; 4 – cylindrical screen; 5 – first hollow cylindrical electrode; 6 – inner electrode; 7 – second hollow cylindrical electrode; E – electrometer (null indicator).

$$K_I = \frac{kr}{k_0 C} = \frac{4\pi Ukr}{\Phi}, \qquad (15.2)$$

where ν is the kinematic viscosity of air, r is the radius of the outer plate or the entrance tube (specified for each specific case), k_0 is the limiting mobility, C is the active capacitance of the measuring capacitor, U is the voltage between the outer plate and the entrance tube. The theoretical determination of the function $C' = C'(\mathrm{Re}, K_I)$ is difficult because of the laborious calculations, since the flow field of the air ions is determined only by numerical methods. Therefore, experiments were carried out with the aim of determining the capacitance of the edge effect of typical capacitor inlet units.

Experiments were performed with the aid of a device in which the electrode arrangement could be varied (Figure 15.1). Artificially ionized, unpurified laboratory air was used. In order to achieve a laminar flow, the air was drawn into the apparatus from a chamber having a volume of 0.1 m^3 through a special laminarizing arrangement (not shown in figure). The air ions were generated by β-radiation from the Sr^{90} preparation. The age of the air ions at the deposition point was about one second. Positive air ions, the mobilities of which were distributed over a narrower interval, appeared to predominate (Figure 15.2). The polar charge density was about 10^5 e.s.u./cm^3, which does not give rise to any appreciable disturbances. The current generated by the air ions was compensated by a current through a resistor (3.3×10^{10} ohm) connected to a precision potentiometer of the type P375; as a null-indicating device a dynamic recording electrometer was used to record the residual voltage. In this way an air-ion current instability of no higher than 0.2% was ensured. The decisive requirement for obtaining such a stability was the complete suppression of turbulence in the air-ion generation zone.

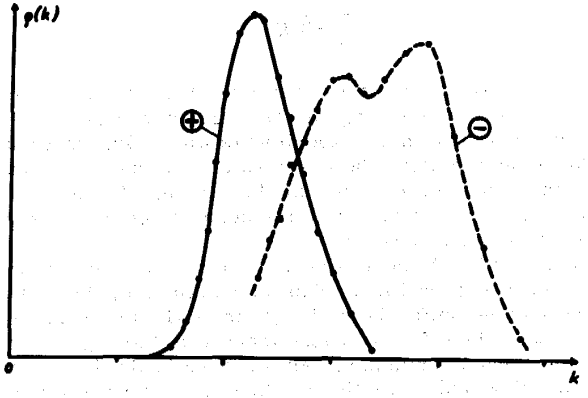

FIGURE 15.2. Spectra of positive and negative air ions according to measurement results obtained in § 21.

The geometry of the electrodes and the position of the switch S (Figure 15.1) correspond to the usual integral counter with an outer collector plate in which the edge effect does not occur. With the aid of such an arrangement the characteristic $I = I(U)$ of an integral counter, corresponding to the

constant active capacitance C, was determined. The measurement was performed by means of an ac bridge.

After turning the switch the edge effect current was measured. The first hollow cylindrical electrode, which previously served as the collector plate of the counter, now plays the role of the entrance tube and the second hollow cylindrical electrode becomes the outer plate. The direct measurement of the edge-effect current flowing to the entrance tube ensures greater accuracy than in the case of measuring the current through the inner plate of the counter. This is particularly important when the ratio of the edge-effect current to the saturation current is small. In order to alter the geometry of different entrance arrangements, exchangeable parts which could be placed on the electrodes were used. In a corresponding manner the geometry of the inner electrode was varied. The capacitance C' of the edge effect is calculated from

$$C'U' = CU, \qquad (15.3)$$

where U' is the voltage at which the edge-effect current equals the current generated by the air ions in the integral counter with an active capacitance C at a voltage U. Expression (15.3) is valid if all air ions have the same mobility. The dispersion of the air-ion spectrum smoothes the function $C' = C'(K_I)$, averaging out values of C' at neighboring points in accordance with the spectrum $\lambda(k)$. Such smoothing is essential only in the case of a strongly nonlinear behavior of the function $C' = C'(K_I)$, which is not observed in reality. The characteristics $I' = I'(U')$ of the edge effect were plotted for different values of the Reynolds number. The results are obtained in the form of the function $C' = C'(I'/I_0)$, where I' is the edge-effect current and I_0 is fluctuating current corresponding to the precipitation of all passing air ions. The parameter I'/I_0 is related to K_I as follows:

$$\frac{I'}{I_0} = \frac{C'}{r} K_I. \qquad (15.4)$$

The measurement results are shown in Figure 15.3 and the geometry of the corresponding entrance arrangements is given in Figure 15.4. The length of the entrance tube in all experiments was 9.5r. In Figure 15.3 the parameter I'/I_0 is plotted along the abscissa and the inclined straight lines correspond to the values of K_I shown in the figure. The errors due to the instrument itself and the instability of the current generated by the air ions range from one to several percent.

The decrease in C' with increasing K_I, for all entrance arrangements, is clearly evident in Figure 15.3. This is explained by the fact that an increase in the voltage shifts the dividing circle (Figure 14.1) toward the incoming air flow. The effective capacitance C' of the edge effect depends primarily on the Reynolds number. An increase in Re flattens the velocity profile of the air flow and shifts the dividing circle toward the outer plate. Even if the critical value of the Reynolds number is exceeded, the flow in the entrance arrangement will remain laminar; since in the wider tube of the air-ion generator the Reynolds number is less than the critical value and in the short entrance tube turbulence has no time to develop. Quantitative data on the dependence of C' on Re (Figure 15.3) are valid only for an entrance tube of length 9.5 r. For smaller lengths of the entrance tube the same values of C' are obtained for a smaller Re, and vice versa. The dependence of C' on the flow profile is clearly seen in curves 4 and 6,

corresponding to entrance arrangements with identical electrode geometry but differing from each other by the air-flow direction and the function of electrodes. A section consisting of a tube of smaller diameter was attached in one case to the first cylindrical electrode and in the other case to the second hollow cylindrical electrode (Figure 15.1). The inner electrode was removed. The air flow in the entrance arrangement in the first case diverges and in the second case converges. In the converging flow the velocity distribution is more uniform, causing larger values of C' than in the case of the diverging flow. In the asymmetric entrance arrangement, whereby the cross section of the entrance tube and the outer plate are equal (Figure 15.4 d without an inner plate), a similar change in the direction of the air flow and a change in function of the electrodes did not alter the effective capacitance within the limits of accuracy of the experiment.

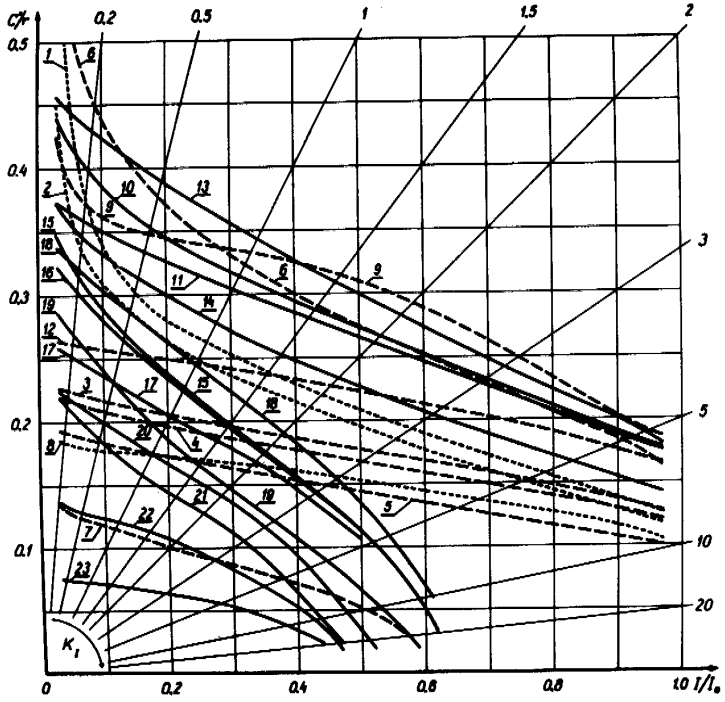

FIGURE 15.3. Edge-effect capacitance of different entrance arrangements. Below, the type of entrance arrangement (Figure 15.4) and the values of the parameters are listed according to the number of the curve:

1—c, Re = 2500; 2—c, Re = 250; 3—e, Re = 2500; 4—e, Re = 1000; 5—e, Re = 250; 6—e, with a reversed air flow, Re = 1000; 7—f, Re = 1000; 8—d, Re = 1000; 9— g, Re = 1000; values obtained from curve 9 should be doubled (the scale of curve 9 is halved); 10 —a, d/r = = 0.05 or d/r = 0.1 (results practically coincide), Re = 1000; 11—a, d/r = 0.2, Re = 1000; 12—a, d/r = 0.5, Re = 1000; 13—a, d/r = 0.1, Re = 2500; 14—a, d/r = 0.1, Re = 250; 15—b, d/r = = 0.05, r_1/r = 0.234, Re = 1000; 16— b, d/r = 0.1, r_1/r = 0.234, Re = 1000; 17—b, d/r = = 0.2, r_1/r = 0.234, Re = 1000; 18—b, d/r = 0.1, r_1/r = 0.234, Re = 2500; 19—b, d/r = = 0.1, r_1/r = 0.234, Re = 250; 20 = b, d/r = 0.1, r_1/r = 0.65, Re = 1000; 21—b, d/r = = 0.05, r_1/r = 0.83, Re = 1000; 22—b, d/r = 0.1, r_1/r = 0.83, Re = 1000; 23—b, d/r = 0.2, r_1/r = 0.83, Re = 1000.

Curve 8 in Figure 15.3 indicates that the entrance arrangement shown in Figure 15.4d used to eliminate the edge effect /Becker, 1909; Furman, 1960/ is ineffective, which was already convincingly pointed out earlier /Scholz, 1931b/. The edge effect is not removed, and is in fact increased when providing the entrance device with a grid (Figure 15.4g), which was erroneously proposed for the prevention of the edge effect /Imyanitov, Zachek, Inkov, Semenov, 1960/. This may be seen when comparing curves 9 and 10 in Figure 15.3. In the investigated device a grid with a mesh width of 0.15 r and a wire diameter of 0.034 r was used.

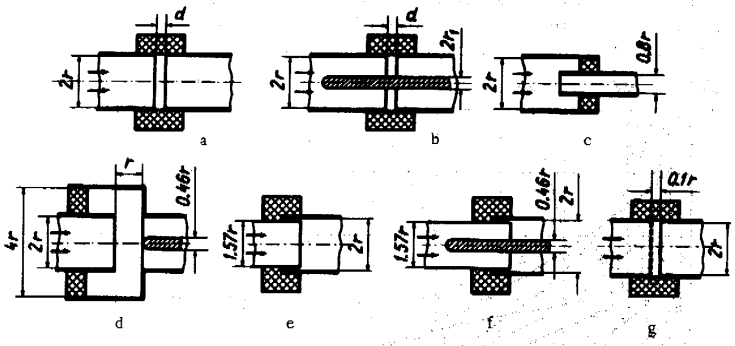

FIGURE 15.4. Entrance arrangements.

The edge-effect current of entrance arrangements f /Scholz, 1931b/ and b, in which the inner plate protrudes into the entrance tube, approaches some limit which is a certain fraction of the saturation current as the voltage is increased. This is reflected in the rapid decrease of C' when I'/I_0 approaches some limiting value (Figure 15.3, curves 7 and 15—23).

§16. EFFECT OF SPACE CHARGE ON MEASUREMENT RESULTS

The space charge of the air induces an electric field which may distort the electric field of the measuring capacitor. The electric field of the space charge causes an electrostatic dispersion of the air ions in the measuring capacitor.

Allowance for the distortion of the electric field of the measuring capacitor was made as early as 1906 /Franck, 1906; Becker, 1910/. The problem is considered in more detail in the work /Siksna, Metnieks, 1953; Siksna, Lindsay, 1961/. Here the intensity and the potential of the electric field in a cylindrical capacitor with a uniformly distributed charge density was calculated. In the first of the above works an error occurs which is corrected in the second work.

The effect of the space charge on the flow of air ions between the plates of the measuring capacitor is very complex. An attempt to calculate rigorously the effect of the space charge in the general theory of aspiration

counters does not give the desired results owing to the mathematical difficulties. When the charge density is large, the processes in the measuring capacitor acquire a nonlinear character and the function G starts to depend on $\varrho(k)$. An analytical solution of the counter equation is impossible and a numerical solution is not feasible because of the laborious calculations.

The piecewise-linear character of the function G, necessary for a simple solution of the counter equation, is retained if the distribution of the space charge between the plates of the measuring capacitor is uniform and does not depend on the operation parameters of the counter. Such a case will be considered in the present section /Tammet, 1962b, 1963a/. This is of some practical interest because the described situation may take place when measuring conductivities and studying the spectrum of light ions in air, the space charge of which is caused by heavy ions. The results obtained in the general case will suffice to obtain a rough estimate of the errors.

As a simplification, suppose that:

1) the measuring capacitor is an ideal cylindrical capacitor or an ideal parallel-plate capacitor;

2) the air flow field in the capacitor is uniform;

3) the charge density in the capacitor is distributed uniformly and does not depend on the voltage between the plates.

The charge Q of the collector plate is composed of the charge CU, dependent on the voltage between the plates, and the charge Q', induced by the space charge. We denote the equilibrium voltage of the collector plate by U'. If $U = U'$, then the charge $CU + Q'$ of the collector plate equals zero, and consequently $Q' = -CU'$, so that

$$Q = C(U - U'). \tag{16.1}$$

We can write the relationship

$$U' = a\varrho, \tag{16.2}$$

where a is a constant of the measuring capacitor.

To find the actual expression for the constant a, we must know the electric field of the measuring capacitor under the assumption $Q = 0$. The equation describing the electric field in a cylindrical capacitor has the form

$$\frac{1}{r}\frac{d(rE)}{dr} = 4\pi\varrho, \tag{16.3}$$

where r is the distance of the considered point from the capacitor axis. The solution of this equation for the boundary condition $E(r_1) = 0$ is

$$E_1(r) = 2\pi\varrho\left(r - \frac{r_1^2}{r}\right). \tag{16.4}$$

For the boundary condition $E(r_2) = 0$, we obtain

$$E_2(r) = -2\pi\varrho\left(\frac{r_2^2}{r} - r\right). \tag{16.5}$$

The voltage U' is determined by the integral of $E(r)$ over the interval (r_1, r_2). Calculating the corresponding integrals enables us to find the specific expressions for the constant a. In the case where the collecting electrode is the inner plate, we obtain

$$a = a_1 = \pi\left(r_2^2 - r_1^2 - 2r_1^2 \ln\frac{r_2}{r_1}\right). \tag{16.6}$$

In the case of the outer collector plate, the relevant expression is

$$a = a_2 = \pi\left(2r_2^2 \ln\frac{r_2}{r_1} - r_2^2 + r_1^2\right). \tag{16.7}$$

A similar calculation for a parallel-plate measuring capacitor yields

$$a = a_0 = 2\pi d^2, \tag{16.8}$$

where d is the distance between the plates.

The dependence of the constant a on the ratio of the radii of the plates of the cylindrical capacitor is shown in Figure 16.1.

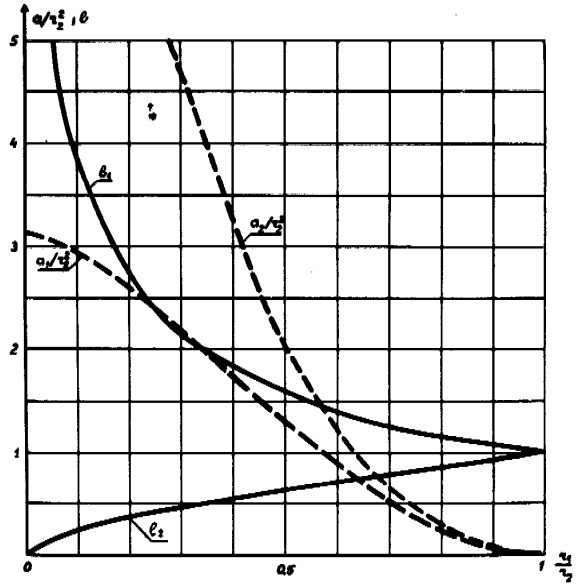

FIGURE 16.1. Dependence of the constants a and b on the ratio of the radii of the plates of the cylindrical capacitor.

Consider the behavior of a discrete group of air-ions with mobility k and partial charge density ϱ' in the measuring capacitor.

The variation of ϱ' with time is described by equation (2.10), which has, in the case of an unaltered charge density ϱ, the solution

$$\varrho' = \varrho_0' \exp(-4\pi\varrho k t), \tag{16.9}$$

where ϱ_0 is the initial value of ϱ' at the instant $t = 0$.

If ϱ' and Q have the same sign and the limiting surface does not intersect the second plate, then the function G can be found by integrating the current density $j' = kE\varrho'$ over the entire collector plate area and dividing the result by ϱ_0':

$$G = -kE\int\int_S \exp(-4\pi\varrho k t)\, dS. \tag{16.10}$$

t is the time required for the air ion to move from the beginning of the measuring capacitor to the point where it is precipitated. Denoting the distance from the beginning of the capacitor to this point by x, we obtain

$$t = \frac{x}{l} t_0. \tag{16.11}$$

We bear in mind the relationship

$$EdS = \frac{4\pi C(U - U')}{l}\, dx. \tag{16.12}$$

After integrating, we have

$$G = -\frac{C(U - U')}{\varrho t_0}\left[1 - \exp(-4\pi\varrho k t_0)\right]. \tag{16.13}$$

We shall introduce the concept of the characteristic mobility, defined by the expression

$$k' = \frac{1}{4\pi\varrho t_0}. \tag{16.14}$$

The characteristic mobility plays a similar role with regard to the electric field generated by the space charge as the limiting mobility with regard to the electric field induced by the voltage between the plates. Let us now write the function G for the entire interval of mobilities $(-\infty, \infty)$:

$$G = \begin{cases} 0 & \text{for} \quad k/k_0 \leqslant 0 \\ -4\pi C(U - U')k'\left[1 - \exp\left(-\frac{k}{k'}\right)\right] & \text{for} \quad 0 \leqslant k/k_0 \leqslant 1 \\ \Phi & \text{for} \quad 1 \leqslant k/k_0. \end{cases} \tag{16.15}$$

The limiting mobility k_0 is determined by the equality of the expressions of G in the interval $0 \leqslant k/k_0 \leqslant 1$ and $1 \leqslant k/k_0$:

$$-4\pi C(U - U')k'\left[1 - \exp\left(-\frac{k_0}{k'}\right)\right] = \Phi. \tag{16.16}$$

Eliminating k_0, we obtain

$$k_0 = k' \ln \frac{U - U'}{U + \left(\frac{t_0\Phi}{aC} - 1\right)U'}. \tag{16.17}$$

The term $t_0\Phi/aC$ is a dimensionless constant of the geometrical shape of the capacitor. To simplify the notation, we set

$$b = \frac{t_0\Phi}{aC} - 1. \tag{16.18}$$

It is easily verified that for a parallel-plate capacitor $b = 1$. For a cylindrical capacitor with an inner collector plate, we have

$$b = b_1 = \frac{a_2}{a_1} \tag{16.19}$$

and for an outer collector plate

$$b = b_2 = \frac{a_1}{a_2}. \tag{16.20}$$

The dependence of the constant b on the ratio r_1/r_2 is given in Figure 16.1.

Now that we have introduced b, we can express the characteristic mobility by

$$k' = \frac{\Phi}{4\pi CU'(1 + b)}. \tag{16.21}$$

We now write the formula for the limiting mobility

$$k_0 = k' \ln \frac{U - U'}{U + bU'}. \tag{16.22}$$

The last expression, notwithstanding its concise form, is inconvenient in the case of small U'/U-values. Although in the limit $U' \to 0$ the expression (16.22) transforms into the usual formula of the limiting mobility (4.3), a direct calculation is indeterminate. An evaluation of the errors arising when not allowing for the influence of the space charge is quite complicated. It is often more convenient to use the following expansion

$$k_0 = -\frac{\Phi}{4\pi CU}\left[1 + \sum_{n=1}^{\infty} \frac{\sum_{m=0}^{n} (-b)^m}{n+1}\left(\frac{U'}{U}\right)^n\right]. \tag{16.23}$$

For a parallel-plate capacitor this becomes

$$k_0 = -\frac{ud^2}{lU}\left[1 + \sum_{n=1}^{\infty} \frac{1}{2n+1}\left(\frac{U'}{U}\right)^{2n}\right]. \tag{16.24}$$

Considering the result obtained, it should be noted that the limiting mobility is indefinite in the interval $(U', -bU')$. In this interval the argument of the natural logarithm in the expression (16.22) has negative values and the series (16.23) and (16.24) do not converge. The dependence $1/k_0$ on U is shown in Figure 16.2. The behavior of k_0 is explained by the existence of a field strength inversion in the measuring capacitor if U is contained in the same interval. If $U=U'$, then the inversion layer reaches the surface of the collector plate; if $U=-bU'$, then it reaches the surface of the second plate. Since the air ions of any mobility cannot penetrate the inversion layer, there can be no limiting mobility for $U \in (U', -bU')$. If k_0 is indefinite, the function G has the form

$$G=\begin{cases} 0 & \text{for} \quad k/k' \leqslant 0 \\ -4\pi C(U-U')k'\left[1-\exp\left(-\frac{k}{k'}\right)\right] & \text{for } 0 \leqslant k/k'. \end{cases} \tag{16.25}$$

The equation of the counter is solved under the assumption $U \bar{\in} (U', -bU')$. We apply to the function G of the form (16.15) the modified operator h':

$$h'_U = 1-(U-U')\frac{\partial}{\partial U}, \tag{16.26}$$

which gives

$$h'_U G=\begin{cases} 0 & \text{for} \quad k/k_0 \leqslant 1 \\ \Phi & \text{for} \quad 1 \leqslant k/k_0 \end{cases} \tag{16.27}$$

From the last expression we obtain the formula for calculating the partial charge density:

$$\varrho(k_1, k_2)=\frac{h'_U I(U_1)}{\Phi_1}-\frac{h'_U I(U_2)}{\Phi_2}. \tag{16.28}$$

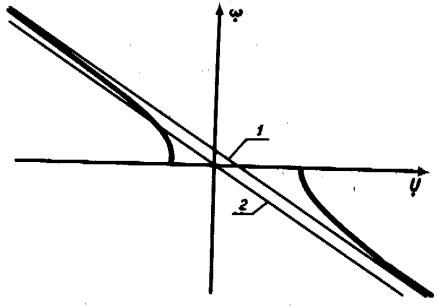

FIGURE 16.2. Dependence $\omega = 1/k_0$ on voltage: 1 – asymptote of the function $\omega(U)$; 2 – $\omega(U)$ for $\varrho = 0$.

The geometric interpretation of the operator h'_U is given in Figure 16.3.

The second derivative of the function G has the form

$$\frac{\partial^2 G}{\partial U^2}=-\frac{\Phi^2}{4\pi C(U-U')^2|U+bU'|}\delta(k-k_0). \tag{16.29}$$

Hence, we obtain the formula for the spectrum

$$\varrho(k_0)=-\frac{4\pi C(U-U')^2|U+bU'|}{\Phi^2}\frac{\partial^2 I}{\partial U^2}, \quad U \neq U'. \tag{16.30}$$

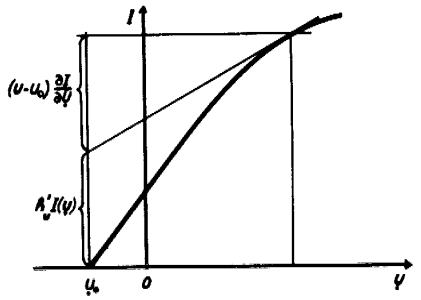

FIGURE 16.3. Determination of $h'_U I(U)$ by the method of tangents.

We note that all the above formulas were derived under the limiting conditions stated at the beginning of this section. If these conditions are not fulfilled, the results obtained merely suffice to effect a rough evaluation of the errors arising when not allowing for the space charge. Most characteristic of the distorting effect of the space charge is the error in the limiting mobility which can be conveniently estimated with the aid of the expansion (16.23). In the first approximation the error is determined by the absolute value of the first term of the sum

$$\delta'_k=\frac{|b-1|a\varrho}{2U}. \tag{16.31}$$

If the ratio of the radii of the plates of the cylindrical capacitor is small, we should consider also the second term which gives the correction

$$\delta''_k=\frac{(b^2-b+1)a^2\varrho^2}{3U^2}. \tag{16.32}$$

For a parallel-plate capacitor the error is expressed in the first approximation by

$$\delta'_k=\frac{4\pi^2\varrho^2 d^4}{3U^2}. \tag{16.33}$$

A simple computation shows that under conditions of natural atmospheric ionization, it is usually justifiable to neglect the effect of the space charge. The error in the limiting mobility becomes appreciable only in exceptional cases.

The effect of the space charge should always be accounted for in the case of artificial ionization. When designing a counter for measurement under

conditions of increased space charge density, it is useful to choose the smallest possible value for $r_2 - r_1$. As follows from (16.31) and (16.33) a decrease in the difference $r_2 - r_1$ enables an effective decrease in the counter sensitivity to the distorting effect of the space charge.

Additional errors arise from variations in the space charge density with time /Komarov, 1960a, 1960b/: A change in the charge density causes a variation in the induced charge Q'. The induced current is superimposed on the measured conduction current due to the air ions. A detailed calculation of the induced current is given in the works /Komarov, 1960a, 1960b/. Below we shall consider only the most simple case in which the space charge is induced by air ions, the mobility of which is considerably less than the limiting mobility. We can thus disregard the effect of the electric field of the measuring capacitor on the charge density. It should be noted that in this case variations in charge density present a serious problem, since the charge density may be of the same (or even larger) order of magnitude as the polar charge density of the precipitated air ions. When calculating the induced current, we start with the fact that the uniform space charge of the air filling the capacitor induces a charge $aC\varrho$ on the collector plate.

Taking into account the incoming as well as the outgoing charges, we obtain

$$I'(t) = \frac{aC}{t_0}[\varrho(t) - \varrho(t - t_0)], \tag{16.34}$$

where $\varrho(t)$ is the charge density at the beginning of the capacitor.

The error due to the induced current decreases as the current averages out with time and depends on the inertia of the recording instrument. The mean value of the induced current in the time interval Δt is

$$\bar{I}' = \frac{aC}{\Delta t}(\bar{\varrho}_1 - \bar{\varrho}_2), \tag{16.35}$$

where $\bar{\varrho}_1$ and $\bar{\varrho}_2$ are the charge densities between the plate of the measuring capacitor at the initial and final instants, respectively.

§17. MEASUREMENT METHODS BASED ON THE UTILIZATION OF THE ELECTRIC FIELD OF THE SPACE CHARGE

When the space charge density is appreciable, certain additional possibilities of measurement arise. For example, expression (16.2) points to the possibility of directly measuring the density of the space charge /Tammet, 1963a/. The voltage U' may be determined experimentally, since the potential of the insulated inner plate gradually approaches the value U'. The density of the space charge is calculated from the formula

$$\varrho = \frac{U'}{a}. \tag{17.1}$$

The above method for determining the charge density is similar to the well-known method of Thomson and may be considered as a modification thereof.

In the case of unipolar ionization the direct determination of U' involves large experimental errors. The equilibrium voltage of the inner plate may considerably exceed U' which is explained by the adsorption of ions. To prevent this U' should be determined by the extrapolation of the current intensity in the voltage interval $(U', -bU')$. The extrapolation is simplified by the fact that no limiting mobility exists in the indicated voltage range and the current intensity depends linearly on the voltage.

In many counters the current is determined from the accumulation of charge on the characteristic capacitance of the measuring capacitor. For such counters the following methods of practical determination of U' can be proposed. First, a rough intuitive estimation of U' is made on the basis of the observed voltage variation of the insulated inner plate. We choose a voltage U_1 which should be close to $-bU'$. Now we charge the inner plate to the potential U_1 or higher. We insulate the inner plate and determine the time Δt, which is the time required for the voltage to change from U_1 to 0. Then we follow the subsequent variation of the voltage and determine U_2, which is attained by the inner plate during the time interval Δt after passing through 0. U' is calculated in accordance with

$$U' = \frac{U_1 U_2}{U_1 + U_2}. \tag{17.2}$$

The derivation of this formula is based on a law whereby the voltage changes exponentially:

$$U = U'[1 - \exp(-\alpha t)], \tag{17.3}$$

where α is the unknown constant. Writing the corresponding expression for $t = -\Delta t$ and $t = \Delta t$, we obtain equations which can be solved by formula (17.2).

The above method of measuring the charge density widens the range of application of small-ion counters for the study of artificially ionized air. Under conditions of unipolar ionization it is possible for the small-ion counter to determine, apart from the partial density of small ions, also the partial charge density of large ions and even the mean mobility of large ions. The last quantity is calculated according to

$$\bar{k}(0, k_1) = \frac{\lambda(0, k_1)}{\varrho - \varrho(k_1, \infty)}. \tag{17.4}$$

Komarov /1960b/ developed a method in which the charge density is measured by a recording of the induced charge. The measuring capacitor is provided with a precondenser capable of collecting all air ions from the passing air. At the beginning of the measurement the voltage is disconnected from the precondenser and the main measuring capacitor is filled with a space charge. By measuring the induced charge $aC\varrho$, the charge density can be calculated. If the conductivity of the air is not too high and the induced charge is recorded by a low-inertia instrument, the diffusion of air ions does not constitute a negative influence in this method.

The last method of measuring the charge density can be combined with the earlier-described method of recording the equilibrium voltage. This

ensures the continuity of observations utilizing both the advantages characteristic of the method of equilibrium voltage and the rapid response characteristic of the method of induced charge. There is no need for a precondenser. This synthesis is possible owing to modern electrometers which effect compensation by means of feedback of the parasitic capacitance and render the effective capacity of the insulated system equal to the active capacitance of the measuring capacitor. In this case the voltage caused by the induced charge coincides with the equilibrium voltage. After switching on the instrument the insulated inner plate gradually acquires an equilibrium charge which then rapidly follows the variations in the charge density. However, along with the positive quality of the described arrangement, we must allow for the serious disadvantage caused by the effect of adsorption of air ions on the measuring results. The method is applicable if a sufficiently symmetric conductivity of the air sample can be assumed. To render the conductivity symmetric the air sample can be irradiated with radioactive radiation.

Tammet /1963a/ proposed a method for studying the air-ion spectrum based on the precipitation of air ions in the electric field of the space charge. The characteristics $I = I(\Phi)$ of the integral counter can be experimentally determined at $U = 0$. Because of limited applicability and the complexity in evaluating the observations this method is of no practical significance. Here, the manner in which the air-ion mobility is measured in the case when all air ions have the same mobility k may be of some interest. The equation of electrostatic dispersion then assumes the form

$$\frac{d\varrho}{dt} = -4\pi k\varrho^2. \tag{17.5}$$

The solution of this equation is

$$\varrho = \frac{\varrho_0}{1 + 4\pi k\varrho_0 t}, \tag{17.6}$$

where ϱ_0 is the value of ϱ at $t = 0$.

The current through the collector plate at $U = 0$ is calculated by integrating the current density over the surface area of the plate. In this case, we obtain

$$EdS = \frac{4\pi Ca\varrho}{l}\,dx, \tag{17.7}$$

hence the expression for the current may be written

$$I(0) = \frac{4\pi Cak}{l}\int_0^l \varrho^2(x)\,dx. \tag{17.8}$$

Integrating, we obtain

$$I(0) = \frac{4\pi Ca\varrho_0^2 kk'}{k + k'}, \tag{17.9}$$

where k' is determined correspondingly by the initial charge density. Eliminating k from the expression (17.9), we have

$$k = \frac{\Phi^2 I(0)}{4\pi CaI^*[I^* - (1+b)I(0)]}, \tag{17.10}$$

where $I^* = \varrho_0\Phi$ is the saturation current.

§18. THE ELECTRODE EFFECT

In still air, a space charge layer is formed in the vicinity of the charged electrodes which enhances the electric field strength at the electrode surface. This phenomenon may play a significant role in the aspiration counter if the air is sufficiently strongly ionized. Suppose that the density of the free space charge of the air sample equals 0 or is infinitesimal.

In the measuring capacitor the electric field separates the polar charges and consequently a layer of free space charge appears at both plates. The charge distribution in the measuring capacitor when measuring the conductivity is shown in Figure 18.1. Simple considerations lead to the conclusion that in this case the electrode effect is greatest. The determination of the electrode effect is in general involved. The problem is somewhat simplified when assuming a large limiting mobility because of the small thickness of the space charge layer in comparison to the distance between the plates. For simplicity, let us further suppose that the air contains positive air ions of mobility k_+ only and negative air ions of mobility k_- only.

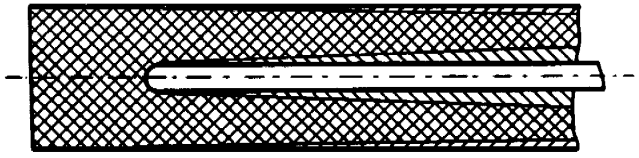

FIGURE 18.1. Distribution of charges causing the electrode effect. Hatching in one direction designates space filled with air ions of one polarity; hatching in the other direction shows the space filled with air ions of the opposite polarity.

The space charge in the vicinity of the surface of the inner plate induces an additional charge Q' on the latter. Since the charge of the inner plate in the absence of the electrode effect is $Q = CU$, the relative error in measuring the conductivity is

$$\delta = \frac{Q'}{CU}. \tag{18.1}$$

The induced charge Q' can be considered to be approximately equal to the charge in the layer of the space charge adjacent to the plate. The space charge formed on one plate primarily induces an additional charge on the same plate and only slightly affects the charge on the other plate. This

conclusion is readily verified with the aid of the well-known Ramo-Shockley theory.

To estimate the electrode effect the volume of the space charge layer must be calculated. This volume depends primarily on the velocity distribution of the air flow in the measuring capacitor. The hydrodynamic problem of air flow in a cylindrical capacitor has not been solved. The exact flow profile is known only for two boundary cases. In a potential flow the velocity distribution is uniform. For a high flow rate and a sufficiently short capacitor the air flow approaches a potential flow in the entire capacitor /Misaki, 1960; Hoegl, 1963b/. In a long measuring capacitor and for a low flow rate the flow approaches a steady laminar flow. The profile of the steady laminar flow is described by the formula /Lamb, 1947; Targ, 1951/

$$u(r)=\frac{2\Phi\left(\frac{r_2^2-r_1^2}{\ln\frac{r_2}{r_1}}\ln\frac{r}{r_1}+r_1^2-r^2\right)}{\pi\left(r_2^2-r_1^2\right)\left(r_2^2+r_1^2-\frac{r_2^2-r_1^2}{\ln\frac{r_2}{r_1}}\right)}. \tag{18.2}$$

Under intermediate conditions the actual flow differs considerably from the above two profiles. In this case more exact results are obtained when using the boundary layer theory.

If the conditions

$$\left.\begin{aligned}\sqrt{\nu t_0}&\ll r_2-r_1\\ \sqrt{\nu t_0}&\ll r_1\end{aligned}\right\} \tag{18.3}$$

are satisfied, the boundary layer at the plate is then similar to that at a flat plate. The flow velocity in the vicinity of the surface is /Loitsyanskii, 1959/

$$u(y)=0{,}332y\sqrt{\frac{u_0^3}{\nu x}}, \tag{18.4}$$

where y is the distance from the surface, x is the distance from the beginning of the plate and u_0 is flow velocity far from the plate.

When the air flow is potential, the calculation of the error δ is simple. The volume of the space charge layer at both plates is in the first approximation given by

$$V'=2\pi t_0 k_{\mp} CU. \tag{18.5}$$

Using (18.1), we obtain

$$\delta=2\pi t_0 k_{\mp}\varrho_{\pm}. \tag{18.6}$$

In these and in the following formulas the upper sign in the subscript will refer to the case $k_0>0$ (the voltage of the collector plate is negative), the lower sign to the case $k_0<0$ (U is positive).

In the center of the boundary layer the radial component of the flow velocity must be considered. To avoid mathematical difficulties we start

with the expression for the air flow rate through the dividing surface of the space charge layer which is defined in the first approximation by

$$\Phi'(x)=k_{\mp}N(x)=4\pi C(x)k_{\mp}U. \tag{18.7}$$

This expression describes the region of the surface of the space charge layer from the beginning of the plate to the point corresponding to the coordinate x. On the other hand, $\Phi'(x)$ is defined by (18.4):

$$\Phi'(x)=\pi r_c y u(y)=0.332\,r_c y^2\sqrt{\frac{u_0^3}{\nu x}}, \tag{18.8}$$

where r_c is the radius of the collector plate and y the thickness of the space charge layer at the point with coordinate x. From expressions (18.7) and (18.8) we can readily derive the equation for the surface of the space charge layer as follows:

$$y=2.46\left(\frac{k_{\mp}U}{r_c\ln\frac{r_2}{r_1}}\right)^{1/3}\left(\frac{\nu}{u_0^3}\right)^{1/4}x^{3/4}. \tag{18.9}$$

The volume of the space charge layer is given by the integral

$$V=2\pi r_c\int_0^l y(x)\,dx. \tag{18.10}$$

The expression for the error may be written in the form

$$\delta=2\pi t_0 k_{\mp}\varrho_{\pm}\sqrt{\frac{k_0}{k_{\mp}}}Y. \tag{18.11}$$

Actual calculations for the case of an inner collector plate yield

$$Y=Y_1=\sqrt[4]{\frac{780\nu l r_1^2}{(r_2^2-r_1^2)\Phi}} \tag{18.12}$$

and for the case of an outer collector plate

$$Y=Y_2=\sqrt[4]{\frac{780\nu l r_2^2}{(r_2^2-r_1^2)\Phi}}. \tag{18.13}$$

A similar calculation for the parallel-plate capacitor leads to the same formula (18.11), where

$$Y=Y_0=\sqrt[4]{\frac{62\nu l}{u_0 d^2}}. \tag{18.14}$$

The formulas obtained are applicable if the thickness of the boundary layer exceeds the thickness of the space charge layer. For the case of an inner collector plate the last condition is written as follows:

$$\left(\frac{k_0}{k_\mp}\right)^2 > \frac{(r_2^2 - r_1^2)\Phi}{4\pi r_1^2 \nu l}, \tag{18.15}$$

for the case of an outer collector plate

$$\left(\frac{k_0}{k_\mp}\right)^2 > \frac{(r_2^2 - r_1^2)\Phi}{4\pi r_2^2 \nu l} \tag{18.16}$$

and for the case of a parallel-plate capacitor

$$\left(\frac{k_0}{k_\mp}\right)^2 > \frac{u_0 d^2}{\nu l}. \tag{18.17}$$

The assumption of a steady laminar profile complicates the problem. However, the calculations can be simplified by the approximation

$$u(y) = \frac{du(r_c)}{dy}\, y, \tag{18.18}$$

since we are interested only in the thin layer of air in the vicinity of the plate. At the surface of the inner plate, we obtain

$$\frac{du(r_1)}{dy} = \frac{2\Phi\left(\dfrac{r_2^2 - r_1^2}{r_1 \ln \frac{r_2}{r_1}} - 2r_1\right)}{\pi(r_2^2 - r_1^2)\left(r_2^2 + r_1^2 - \dfrac{r_2^2 - r_1^2}{\ln \frac{r_2}{r_1}}\right)} \tag{18.19}$$

and at the surface of the outer plate

$$\frac{du(r_2)}{dy} = \frac{2\Phi\left(2r_2 - \dfrac{r_2^2 - r_1^2}{r_2 \ln \frac{r_2}{r_1}}\right)}{\pi(r_2^2 - r_1^2)\left(r_2^2 + r_1^2 - \dfrac{r_2^2 - r_1^2}{\ln \frac{r_2}{r_1}}\right)}. \tag{18.20}$$

Under the above assumptions the equation for the surface of the space charge layer is simply

$$y = \left[\frac{2k_\mp U}{r_c \ln \frac{r_2}{r_1} \frac{du(r_c)}{dy}}\right]^{1/3} x^{1/3}. \tag{18.21}$$

The calculation of the error δ leads to the formula (18.11) where Y for the case of an inner collector plate has the form

$$Y = Y_1' = \sqrt{\frac{32r_1\left(r_2^2 + r_1^2 - \dfrac{r_2^2 - r_1^2}{\ln \frac{r_2}{r_1}}\right)}{9(r_2^2 - r_1^2)\left(\dfrac{r_2^2 - r_1^2}{r_1 \ln \frac{r_2}{r_1}} - 2r_1\right)}}. \tag{18.22}$$

For the case of an outer collector plate

$$Y = Y_2' = \sqrt{\frac{32r_2\left(r_2^2 + r_1^2 - \dfrac{r_2^2 - r_1^2}{\ln \frac{r_2}{r_1}}\right)}{9(r_2^2 - r_1^2)\left(2r_2 - \dfrac{r_2^2 - r_1^2}{r_2 \ln \frac{r_2}{r_1}}\right)}}. \tag{18.23}$$

For a parallel-plate capacitor we obtain

$$Y = Y_0' = 0.77. \tag{18.24}$$

When estimating the electrode effect the conditions (18.3) and (18.15), (18.16) or (18.17) must first be verified. If these conditions are fulfilled, formula (18.12), (18.13) or (18.14) must be applied. In the opposite case, formulas (18.22)–(18.24) are used. Note that these formulas give the largest possible errors corresponding to a large limiting mobility. When k_0/k is small the errors are considerably smaller.

In the naturally ionized air of the air layer near the ground the electrode effect plays a significant role only in exceptional cases. The electrode effect constitutes a negative influence for stratospheric measurements. The possibility of distortions due to the electrode effect should always be taken into account when studying air with artificially produced ions of increased mobility.

To render the theory more rigorous the electrode effect and the effects of air-ion recombination should be simultaneously considered, since these distortions arise under the same conditions and may partly compensate one another. It is also advisable to allow for the electrostatic dispersion of air ions in the space charge layer.

§19. DIFFUSION OF AIR IONS

Diffusion is a consequence of the thermal motion of air ions which is of a random nature. The equation of motion $\vec{v} = \vec{u} + \vec{k}\vec{E}$, used in the preceding sections without reservations, is in fact merely the equation of the mean expected motion of the air ions. The actual trajectories of the air ions form a diverging beam about the mean trajectory defined by the above equation.

The first attempt to quantitatively estimate the effect of diffusion in an air-ion counter /Mache, 1903/ was unsuccessful because of erroneous

theoretical premises. In the work /Becker, 1910/ the starting principles and the qualitative characterization of diffusion are correct, but rough approximations used in calculations lead to serious disagreement with experimental data. More satisfactory is the evaluation of the random displacement of an air ion directly from formulas of the theory of Brownian motion /Zeleny, 1929/.

There are two methods which enable a mathematical description of the diffusion of air ions: the method of calculating the diffusion flow on the basis of the Fick equation and the statistical method used in the statistical theory of Brownian motion. The second method is the more appropriate for our purposes.

The influence of the diffusion of air ions in the measuring capacitor can be described in two ways. In the first case, the diffusion is already allowed for in the expression for the function G. The function G in this case loses its piecewise linear behavior (Figure 19.1), which complicates the solution of equation (3.3). In the second case, the effect of diffusion is represented as a transformation of the function $\varrho(k)$ into the function of the apparent distribution $\varrho^*(k)$, whereby the former trend of the function G is retained. The considerations below are based on this approach.

As a consequence of diffusion, an air ion of mobility k precipitates in the measuring capacitor at that point where, in the absence of diffusion, air ions of some other mobility k_1, which is the apparent mobility of the air ion under consideration, would precipitate. We shall denote the probability that an air ion of mobility k possesses an apparent mobility between k_1 and $k_1 + dk$ by $W(k, k_1)dk$. If the actual spectrum of air ions is characterized by the function $\varrho(k)$, then the apparent distribution is

$$\varrho^*(k_1) = \int_{-\infty}^{+\infty} W(k, k_1)\, \varrho(k)\, dk. \qquad (19.1)$$

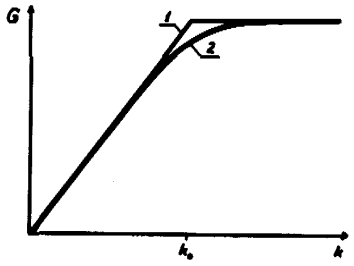

FIGURE 19.1. The function G of an integral counter:

1—ideal case; 2—when diffusion of air ions takes place.

The function $W(k, k_1)$ completely determines the effect of the diffusion of air ions on the measuring results. If this function is known, then formula (19.1) may be taken to define the actual spectrum $\varrho(k)$ on the basis of the

function $\varrho^*(k)$, calculated without allowance for the effect of diffusion. The solution of the integral equation (19.1) is rather involved. One is usually satisfied with the result $\varrho(k) \approx \varrho^*(k)$. The function $W(k, k_1)$ is used in this case only to estimate the errors caused when diffusion is disregarded.

Consider the simplest case of measuring the mobility of an air ion. Suppose that the air ion moves in a uniform electric field of field strength E, and its mobility is inferred from the distance d traversed by the air ion in the direction of the electric field during time t. The mean value of this distance is

$$\bar{d} = kEt = \sqrt{kUt}, \qquad (19.2)$$

where U is the voltage between the mean end point and starting point of air-ion motion. According to the theory of Brownian motion, the random difference $d - \bar{d}$ obeys a normal distribution with mean square deviation

$$\sigma_d = \sqrt{2Dt}, \qquad (19.3)$$

where D is the diffusion coefficient of the air ions. The diffusion coefficient is linked to the mobility via the relationship

$$D = \frac{KTk}{q}, \qquad (19.4)$$

where K is Boltzmann's constant, T is the absolute temperature and q is the charge of the air ion.

The measured value of the mobility is proportional to the distance d, so that the measured mobility also obeys a normal distribution. The relative mean square deviation s_k of the mobility equals the relative mean square deviation s_d of the distance. With the aid of expressions (19.2), (19.3) and (19.4) we obtain

$$s_k = \frac{\sigma_k}{k} = \frac{\sigma_d}{\bar{d}} = \sqrt{\frac{2KT}{qU}}. \qquad (19.5)$$

The function W in this case has the form

$$W(k, k_1) = \frac{1}{\sigma_k \sqrt{2\pi}} \exp\left[-\frac{(k-k_1)^2}{2\sigma_k^2}\right]. \qquad (19.6)$$

From formula (19.5) it follows that the relative error of the mobility measurement depends on the ratio of the mean energy of thermal motion of the air ion to the mean work of displacement of the air ion in the electric field. This fact is of special physical significance, which is fully disclosed only when approaching the problem from the point of view of the kinetic theory. Although there is no direct need for this, we shall briefly follow the simplified derivation of formula (19.5) based on kinetic considerations.

Suppose that the probability distribution of the air-ion velocity at the initial instant is determined only by thermal motion. Consider a short time interval t, in which no collisions of the air ion with molecules occur. Owing to thermal motion the air ion traverses during this time in the direction

of one coordinate axis, a distance whose mean value equals zero and whose mean square deviation is

$$\sigma_d = \sqrt{\frac{KT}{m}}\, t, \tag{19.7}$$

where m is the mass of the air ion. Under the influence of the electric field the air ion acquires the additional velocity qEt/m and traverses the distance

$$d = \frac{qEt^2}{2m} = \sqrt{\frac{qU}{2m}}\, t, \tag{19.8}$$

where U is the voltage drop over the distance d. Calculation of the ratio σ_d/d leads to formula (19.5).

If during the time t one collision occurs, then the latter subdivides the time interval t into two parts, t_1 and t_2. The dispersion of the thermal displacement of the air ions in the interval t_1 is $\sigma_1^2 = \frac{KT}{m} t_1^2$ and in the interval t_2, $\sigma_2^2 = \frac{KT}{m} t_2^2$. The colliding air ion retains on the average a fraction α of the initial momentum. The covariation of the thermal displacements of the air ion in the time intervals t_1, t_2 is therefore $\alpha \frac{KT}{m} t_1 t_2$. The dispersion of the thermal displacement in the interval t is correspondingly expressed by the sum

$$\sigma_d^2 = \frac{KT}{m}(t_1^2 + 2\alpha t_1 t_2 + t_2^2). \tag{19.9}$$

The displacement of the air ion due to the electric field is in the first time interval $d_1 = Eqt_1^2/2m$ and in the second time interval $d_2 = Eq(\alpha t_1 t_2 + t_2^2/2)/m$. The total displacement is then

$$d = \frac{Eq}{2m}(t_1^2 + 2\alpha t_1 t_2 + t_2^2) = \sqrt{\frac{qU}{2m}}\sqrt{t_1^2 + 2\alpha t_1 t_2 + t_2^2}\, t_2^2. \tag{19.10}$$

The ratio σ_d/d is expressed, as previously, by formula (19.5). On the basis of similar arguments we can verify that expression (19.5) holds for an arbitrary number of collisions.

In the aspiration method the time of movement of the air ions is inferred from the drift of the air ion with the air flow. Since diffusion occurs also in the direction of the air flow, this introduces an additional error into the measurement result.

Consider the determination of the mobility in a homogeneous electric field. Here and in subsequent derivations in this section we shall assume that the flow velocity $\vec{u}$ and the field strength $\vec{E}$ of the electric field are perpendicular to one another. If the air ion traverses over a certain time a distance x in the direction of the air flow and a distance y in the direction of the electric field, then its mobility is determined by the relation

$$k = \frac{u}{E}\frac{y}{x}. \tag{19.11}$$

The ratio y/x has no statistical moments, since at $x = 0$ there exists a finite probability density. In order to retain clarity of presentation we shall refrain from full mathematical rigor and introduce certain new concepts. The ratio $\bar{y}/\bar{x}$ will be called the conditional mean of the ratio y/x. The sum $s_y^2 + s_x^2$, which equals the relative variance of the linearized form of the ratio y/x, will be called the conditional relative variance of the ratio y/x. We shall assume that random deviations are considerably less than the mean values of x and y. Then the distribution function of the ratio $\bar{y}/\bar{x}$ practically coincides with the distribution function, whose variance equals the conditional variance of the ratio y/x. For the sake of brevity, we shall omit in the following the word conditional in the definitions "conditional mean" and "conditional variance."

In a homogeneous field $\sigma_x = \sigma_y$ and $s_x = \frac{y}{x} s_y$. The standard deviation σ_u is defined by formula (19.5). Setting $y/x = kE/u$, we obtain

$$s_k = \sqrt{\frac{2KT}{qU}\left(1 + \frac{k^2E^2}{u^2}\right)}. \tag{19.12}$$

The above result may be directly applied to evaluate the effect of diffusion in a counter with a parallel-plate measuring capacitor.

The method of the apparent distribution of mobilities enables us to describe similarly the effect of the diffusion of air ions in the measuring capacitor for the case of an integral as well as a differential counter. In both cases the measurement results depend on the behavior of the critical air ions, which move close to the limiting surface for the mobility k_0.

In a counter with a parallel-plate measuring capacitor, we have for the critical air ions $x = l$ and $y = d$. Accordingly,

$$s_k = \sqrt{\mu \frac{2KT}{qU}}, \tag{19.13}$$

where

$$\mu = 1 + \frac{d^2}{l^2}. \tag{19.14}$$

In the case of a inhomogeneous field matters become more complicated in the coaxial capacitor. We shall make an approximate calculation, whereby we consider the movement of an air ion over short successive segments for which one may use formula (19.12) with sufficient accuracy. The movement of the air ion is determined by the ratio of the air-flow rate and the electric flux $k = \Phi/N$ through the flow surface. If the flow surface consists of successive segments through which the flow rates and electric fluxes are Φ_n and N_n respectively, and the considered air-ions possess different apparent mobilities k_n, in each of those segments we may then write for each segment $k_n = \Phi_n/N_n$. For the entire flow surface the apparent mobility is given by

$$k = \frac{\sum_n \Phi_n}{\sum_n N_n} = \frac{\sum_n N_n k_n}{N}. \tag{19.15}$$

Consequently, the variance of the mobilities is determined by the sum

$$\sigma_k^2 = \frac{\sum_n N_n^2 \sigma_{kn}^2}{N^2}. \tag{19.16}$$

When the critical air ions move through the entire measuring capacitor, $N = 4\pi CU$. For a short segment of the axially symmetric flow surface, we have

$$N_n = 2\pi r_n E_n l_n, \tag{19.17}$$

where l_n is the length of the relevant segment along the capacitor axis. Determining σ_{kn} in accordance with (19.12), and bearing in mind that

$$U_n = \frac{E_n^2 k_n l_n}{u_n}, \tag{19.18}$$

we obtain

$$\sigma_k^2 = \frac{KT}{2q C^2 U^2} \sum_n k_n \left(r_n^2 u_n^2 + r_n^2 E_n^2 k_n^2\right) t_n, \tag{19.19}$$

where $t_n = l_n/u_n$ is the time of passage through the segment l_n.

In the above expression a certain mean mobility may be placed before the summation sign. Thus, assuming the mean mobility is equal to k_0, the expression for s_k can be written in the form of (19.13), where μ is given by

$$\mu = \frac{\pi}{C\Phi}\left(\sum_n r_n^2 u_n^2 t_n + k_0^2 \sum_n r_n^2 E_n^2 t_n\right). \tag{19.20}$$

In this expression it is advisable to switch from summation to integration. A physical interpretation makes this transition seem rather incorrect because of the nonpermissible increase in the variance σ_{kn}^2. The integration should be considered only as a means of effecting an approximate calculation. The final expression of the parameter μ for the axially symmetric measuring capacitor with transverse fields $\vec{u}$ and $\vec{E}$ is

$$\mu = \frac{\pi t_0}{C\Phi}\left[\int_0^1 r^2(\vartheta) u^2(\vartheta)\, d\vartheta + k_0^2 \int_0^1 r^2(\vartheta) E^2(\vartheta)\, d\vartheta\right]. \tag{19.21}$$

The relative time ϑ is defined as

$$\vartheta = \frac{t}{t_0}, \tag{19.22}$$

where the time of passage of the air ion through the capacitor is assumed to be equal to the filling time of the capacitor.

In the absence of radial components of the air flow velocity, we obtain for a cylindrical capacitor

$$r^2(\vartheta) = r_2^2 - \left(r_2^2 - r_1^2\right)\vartheta \tag{19.23}$$

or

$$r^2(\vartheta) = r_1^2 + \left(r_2^2 - r_1^2\right)\vartheta. \tag{19.24}$$

The product rE is constant:

$$rE = \frac{U}{\ln \frac{r_2}{r_1}}. \tag{19.25}$$

In the case of uniform distribution of flow velocities integration is simple and yields

$$\mu = \left(\frac{r_2^2 - r_1^2}{2l^2} + \frac{r_2^2 + r_1^2}{r_2^2 - r_1^2}\right)\ln \frac{r_2}{r_1}. \tag{19.26}$$

For a velocity distribution described by (18.2), integration likewise involves no difficulties, but the resulting formula is awkward and inconvenient. The value of the parameter μ depends only slightly on the profile of the flow velocity, so that formula (19.26) suffices for practical considerations.

The dependence of the parameter μ on the ratios l/r_2 and r_1/r_2 is given in Figure (19.2).

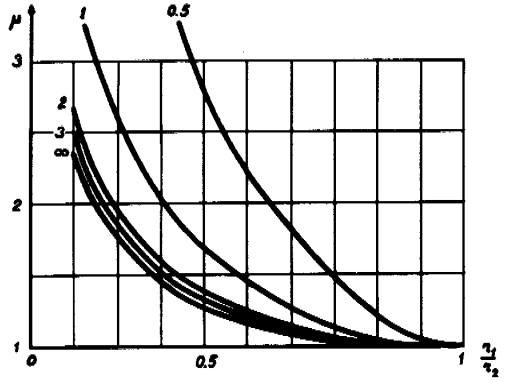

FIGURE 19.2. Dependence of the parameter μ on the dimensions of a cylindrical capacitor. The numbers above the curves denote the values for the ratio l/r_2.

The expression obtained for s_k differs from that given in the work /Tammet, 1962b/, where an unjustified simplification is used. The difference in the results, however, becomes marked only for large values of the ratio r_2/r_1, which are seldom encountered in practice.

Apart from the distortions treated in the present section, diffusion leads to the absorption of air ions. The problem will be dealt with below.

§20. TURBULENT MIXING OF AIR IN A MEASURING CAPACITOR

In the theory of the aspiration method, it is usually assumed that the air flow in the measuring capacitor possesses a laminar character. Sometimes this condition is not satisfied and the air flow in the capacitor is more or less turbulent. The estimation of distortions caused by turbulence is of great interest, since these distortions constitute a decisive factor when choosing the flow rate for the aspirated air. Unfortunately, the effect of turbulence on the measurement results is the most complicated and least studied problem in the theory of the aspiration counter. In early works /Gish, 1933a, 1933b; Wait, 1934; Graziadei, 1935/ only ill-founded, hypothetical propositions on the effect of turbulence on the current generated in the integral counter were made. In these works the absence or presence of turbulence in the measuring capacitor was judged on the basis of the Reynolds number. This, however, leads to doubtful results. Only in the works /Israël, 1931; Wolodkewitsch, Dessauer, 1931b/ was the appearance of turbulence determined by observing a smoke trace in a transparent model of the capacitor. This method of studying the nature of the flow was recently also applied with success /Faucher, 1958; Misaki, 1960; Matulyavichene, 1962/. In the work /Misaki, 1960/ the smoke-trace method was modified to serve as a quantitative measure for determining the flow profile. Israël /Israël, 1931/ showed that turbulence reduces the current generated in the integral counter by approximately 5—10%. This result is disputed in another work /Reimers, 1940/, where, on the basis of experimental data and theoretical considerations, it is maintained that the character of the air flow in the measuring capacitor in no way affects the measurement results. Insufficient accuracy of the experiments and ill-founded theoretical considerations are evidence that this assertion is unreliable.

The most detailed experimental work in the study of turbulent mixing was performed by Yaita and Nitta /Yaita, Nitta, 1955/. The character of the flow was studied with the aid of a thermistor probe. Accordingly, it was found that the effect of turbulence is manifested in the dispersion of the air-ion mobilities. The quantitative results are limited to a few examples in which the characteristics of an integral counter are compared under different operating conditions in a parallel-plate capacitor.

Tammet /Tammet, 1962b/ estimated the intensity and regularity of turbulent mixing from data based on atmospheric turbulence /Richardson, 1926; Teverovskii, 1949/. Ill-founded initial assumptions rendered the results of this work erroneous.

The turbulent mixing of air disperses the air-ion trajectories in the same way as in the case of thermal diffusion. According to (19.1) this leads to a smoothing of the spectrum $\varrho(k)$. In the following calculations we shall neglect thermal diffusion.

The turbulent flow field may be resolved into the mean field $\vec{u}_0$ and the field of turbulent fluctuations $\vec{u}_t$. The field $\vec{u}_0$ is time-independent and has properties which should be characteristic of the flow field in the measuring capacitor of the counter. Deviations from ideal operating conditions of the counter are caused by the additional field $\vec{u}_t$. The mean value of $\vec{u}_t$ is equal to zero by definition, so that turbulent pulsations do not affect the mean

distance traversed by the air ion over a given period. Consequently, in the first approximation turbulent mixing will not distort the mean values of the measured mobilities. This is confirmed by experimental results described in the following section.

As in the preceding paragraph we shall assume that the fields $\vec{E}$ and $\vec{u}_0$ are perpendicular to one another. Consider the movement of an air ion during the short time interval t_n. The time t_n should be sufficiently small, so that the inhomogeneity of the electric field and the mean air velocity along the trajectory of the air ion can be neglected. The time t_n should also be small compared to the Lagrangian microscale of turbulence. The mean displacement of the air ions in the direction during the time t_n is $\bar{x}_n = u_0 t_n$; the variance of this displacement is $\sigma_x^2 = \overline{u_{tx}^2} t_n^2$. Correspondingly, the displacement along the electric field is $\bar{y}_n = kEt_n$, and the variance is $\sigma_y^2 = \overline{u_{ty}^2}\, t_n^2$. The apparent mobility of an air ion is proportional to the ratio y_n/x_n. Remembering that the ratio $\overline{u_t^2}/u_0^2$ usually does not exceed 100, the relative variance of the apparent mobility can be calculated as follows:

$$s_k^2 = s_x^2 + s_y^2 - 2R_{x,y}s_x s_y \tag{20.1}$$

where $R_{x,y}$ is the correlation coefficient between u_{tx} and u_{ty}. Since the coordinate axes of the correlation are at right angles, $R_{x,y}$ is small remote from the plates. When moving from one plate of the measuring capacitor to the other, $R_{x,y}$ changes sign and, when averaged, is practically equal to zero. Suppose $R_{x,y} = 0$. Then

$$s_k = \varepsilon \sqrt{1 + \frac{u_0^2}{k^2E^2}}. \tag{20.2}$$

ε is a certain mean intensity of turbulence. Assuming that $\overline{u_{tx}^2} = \overline{u_{ty}^2} = \overline{u_{txy}^2}$, ε is expressed by

$$\varepsilon = \frac{\sqrt{\overline{u_{txy}^2}}}{u_0}. \tag{20.3}$$

If the air ion has different apparent mobilities k_n in the successive time intervals t_n, then the apparent mobility determined from the movement of air ions over a longer time interval can be calculated by formula (19.15). When determining the dispersion of the apparent mobility, we must allow for the characteristics of the turbulent diffusion /Batchelor, 1953; Frenkiel, 1953; Pai, 1957; Monin, Yaglom, 1965, 1967/. In the case of the thermal diffusion, the deviations of the apparent mobility from the mean $k_n - \bar{k}$ in successive time intervals could be considered as independent, but in the case of the turbulent diffusion, the situation is more involved. The deviations $k_n - \bar{k}$ and $k_m - \bar{k}$ are correlated with one another. Denoting the correlation coefficient between the above deviations by $R_{n,m}$, we obtain the following expression for the variance:

$$\sigma_k^2 = \sum_n \sum_m R_{n.}\ \frac{N_n N_m}{N^2}\ \sigma_{kn}\sigma_{km}. \tag{20.4}$$

We now utilize formula (19.17), and, after replacing t_n by dt, we switch from summation to integration:

$$\sigma_k^2 = \frac{4\pi^2}{N^2}\int_0^{t_0}\int_0^{t_0} R(t_1,t_2)r(t_1)E(t_1)u_0(t_1)\sigma_k(t_1)\times$$
$$\times r(t_2)E(t_2)u_0(t_2)\sigma_k(t_2)\,dt_1dt_2. \qquad (20.5)$$

$R(t_1, t_2)$ is the Lagrangian correlation function of the apparent mobility along the trajectory of the air ion.

To simplify the notation, we change over to the relative time scale and introduce the dimensionless quantity

$$w(\vartheta) = \frac{2\pi r(\vartheta)E(\vartheta)u_0(\vartheta)t_0}{N}. \qquad (20.6)$$

The relative variance of the apparent mobility of the critical air ion in the measuring capacitor is now given by

$$s_k^2 = \int_0^1\int_0^1 R(\vartheta_1,\vartheta_2)w(\vartheta_1)w(\vartheta_2)s_k(\vartheta_1)s_k(\vartheta_2)\,d\vartheta_1d\vartheta_2. \qquad (20.7)$$

Let us now carry out the calculation for a cylindrical measuring capacitor, assuming that the field $\vec{u_0}$ is homogeneous. It can be readily shown that in this case $w(\vartheta) = 1$. The expression for $R(\vartheta_1, \vartheta_2)$ is unknown, which compels us to confine ourselves to an approximate solution. We place the correlation function $R(\vartheta_1, \vartheta_2)$ before the integral sign, using the mean-value theorem. The corresponding mean value will be denoted by $\bar{R}$ and will be called the relative effective scale of turbulence in the measuring capacitor. Thus, we place before the integral sign the effective turbulent intensity $\bar{\varepsilon}$, which is the corresponding mean value of the quantity $\varepsilon(\vartheta)$. As a result, we obtain

$$s_k = \mu_t\bar{\varepsilon}\sqrt{\bar{R}}, \qquad (20.8)$$

where

$$\mu_t = \int_0^1 \sqrt{1+\frac{u_0^2(\vartheta)}{k_0^2E^2(\vartheta)}}\,d\vartheta. \qquad (20.9)$$

Integration yields for the cylindrical measuring capacitor

$$\mu_t = \frac{r_2^2-r_1^2}{6l^2}\left\{\left[1+\frac{4l^2r_2^2}{(r_2^2-r_1^2)^2}\right]^{3/2} - \left[1+\frac{4l^2r_1^2}{(r_2^2-r_1^2)^2}\right]^{3/2}\right\} \qquad (20.10)$$

Figure 20.1 shows curves plotted in accordance with the above formula.

A similar calculation for the parallel-plate capacitor leads to the same formula (20.8). However, the parameter μ_t is now expressed by

$$\mu_t = \sqrt{1+\frac{l^2}{d^2}}. \qquad (20.11)$$

In (20.8) the quantities $\bar{R}$ and ε remain undefined. Therefore, the above calculations do not yield any direct practical results, but merely serve the purpose of creating a qualitative picture of the effect of the turbulent mixing in the measuring capacitor. Formula (20.8) may be used for a quantitative estimation only in the absence of more accurate data. In the case of a completely turbulent flow in the cylinders ε is of the order of about 1/20 /Hinze, 1959/, and the relative scale $\bar{R}$ may be estimated from the ratio of $r_2 - r_1$ and the length of the trajectory of the critical air ions.

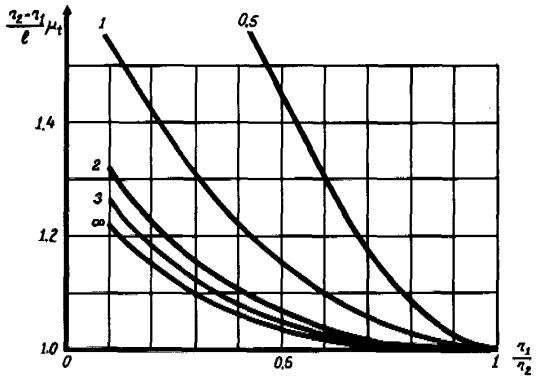

FIGURE 20.1. Dependence of the parameter μ_t on the dimensions of the cylindrical capacitor. Numbers above the curves correspond to values of the ratio l/r_2.

In principle, the quantity $\bar{\varepsilon}\sqrt{\bar{R}}$ may be estimated more accurately when using the well-known semiempirical theories of turbulence and the available data obtained in experimental investigations of turbulent flow in tubes and channels /Pai, 1957; Hinze, 1959; Gkhosh, 1968/. However, this leads to rather involved calculations and the accuracy obtained is still doubtful. In addition to this, the initial data necessary for such calculations are known only in a limited number of cases. We are thus compelled to prefer another approach, for example, the direct experimental investigation of the effect of turbulent mixing of air in the measuring capacitor.

Finally, we note that turbulent mixing as well as diffusion of air ions has practical significance, particularly in the study of the air-ion spectrum. The effect of turbulence on the current generated in the integral counter is not very strong and causes only a slight reduction in the latter. The error reaches a maximum if the air contains air ions of mobility $k = k_0$ only. The relative error in this case is determined approximately by the formula

$$\delta_I = \frac{1}{2} + \frac{s_k}{\sqrt{2\pi}}\left[1-\exp\left(-\frac{1}{2s_k^2}\right)\right] - \frac{1}{2}\operatorname{erf}\left(\frac{1}{\sqrt{2}\,s_k}\right). \qquad (20.12)$$

For $s_k < 30\%$ a sufficient accuracy in ensured by the simplified formula

$$\delta_I \approx 0.4s_k. \qquad (20.13)$$

Of practical significance is also the effect of turbulent mixing on the adsorption of air ions /Siksna, Metnieks, 1953; Zachek, 1964b/.

§21. RESULTS OF THE EXPERIMENTAL INVESTIGATION OF THE EFFECT OF TURBULENCE

The main purpose of the experiments described below is to study the character of the dependence of the mobility dispersion on turbulence, on the parameters and operating conditions of the measuring capacitor, as well as on the air conditions at the counter inlet. Together with this, the task of the compiling data for a rough quantitative estimate of the effect of turbulent mixing on the measurement results was kept in mind.

The following requirements were imposed on the experimental counter:

1. The counter should have a high resolving power, so that the smoothing of the spectrum by turbulent mixing can be detected and quantitatively measured. The smoothing of the spectrum should be prevented because of the adsorption of air ions.
2. So as not to complicate the aerodynamical properties of the counter inlet, methods requiring the separation of the air flow should not be employed.
3. The design of the counter should ensure the possibility of using interchangeable inner plates of different lengths and radii, while maintaining the radius of the outer plate.

These requirements compel us to select the principle of the first-order differential counter with a divided capacitor and an outer collector plate. The arrangement of the measuring capacitor is schematically shown in Figure 21.1. The inner plate may be optionally displaced toward the inlet opening or in the opposite direction, allowing us to regulate the effective length of the measuring capacitor. The effective length was determined by a calculation method which will be described in §33.

Another suitable method for the experimental investigation of turbulent mixing in the measuring capacitor is the use of an integral counter with an oppositely charged precondenser (Figure 9.1). Here, operating conditions can be used, whereby the current generated in the main capacitor occurs only in the case of dispersion of the apparent mobilities of the air ions. In the present book, the last method was not used because it was judged to be less suitable under the condition that there was no preliminary information on the character of turbulent mixing in counters.

The circuit diagram and the air path of the counter used here are shown in Figure 21.2. The voltage was applied to the inner plate by a P82 potentiometer from the VS-22 rectifier, which ensured a highly stable voltage up to 4000 volts. The voltage of the inner plate was measured with the aid of an M502 voltmeter (accuracy ± 0.1 V). The current through the collector plate was measured by the method described in §15. The air-flow rate was measured with the aid of a gas counter of the type GKF or RS-40, which were previously calibrated with the aid of a calibrated 0.6-m^3 container filled with water. Sudden changes in the air flow due to the gas counter were smoothed with the aid of a drum having a rubber cover and an effective volume of about 1 m^3. The correction for the pressure difference, which became marked at high flow rates, was allowed for. To calculate the correction the temperature difference in the system was measured.

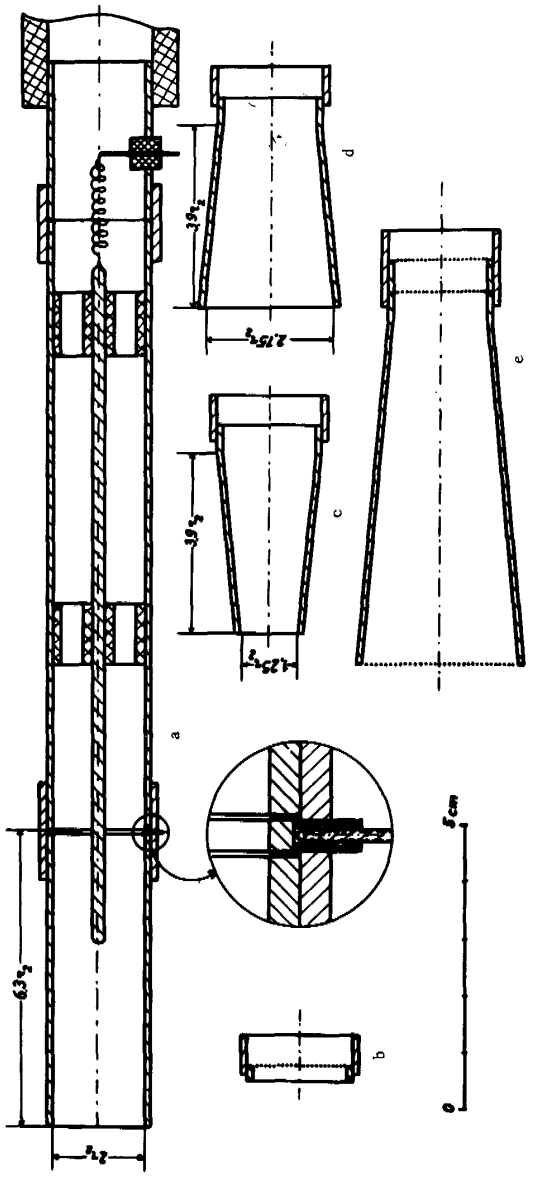

FIGURE 21.1. a—measuring capacitor; b—nozzle with grid ($k = 0{,}055\ r_1$, $r_0 = 0{,}0085\ r_2$); c—diffuser nozzle; d—nozzle; e—laminarizing nozzle with three grids.

A highly stable source of air ions was necessary in order to perform the experiment. The ion generator must be sufficiently powerful, so that the ionization of air drawn into the measuring capacitor does not depend appreciably on the flow rate. The age of the generated air ions at the inlet of the counter should be not less than half a second, so that the spectrum $\varrho(k)$ will have enough time to stabilize and will not change while the air is passing through the measuring capacitor. In addition to this, it is necessary to create a turbulent field at the inlet of the counters which corresponds to conditions encountered in the atmospheric layer near the ground. The turbulent field must be sufficiently stable. Keeping the above-mentioned requirements in mind, a special ion generator was designed and built (see Figure 21.3). The air ions are generated in equal quantities for both polarities. The maximum obtainable polar charge density was 170,000 e.s.u./cm^3. The ionizing power is regulated by placing aluminum disks under a radioactive preparation. The mean linear air velocity in the ion generator was 2.15 m/sec, and the flow rate 0.245 m^3/sec. The turbulent intensity can be reduced by letting the air flow through a grid placed at the outlet of the ion generator. The turbulent intensity was not measured, since a suitable instrument was not available.

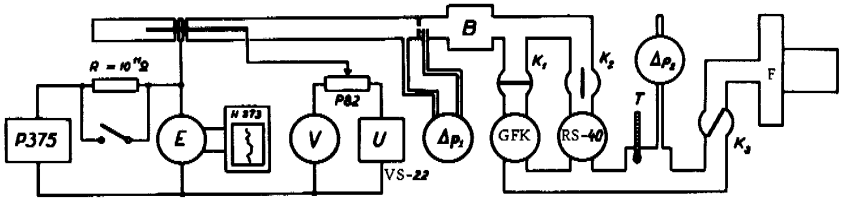

FIGURE 21.2. Circuit diagram of the counter. E—dynamic electrometer; Δp_1—differential manometer of the flow meter; B—shock drum; K_1 and K_2—two-way stopcocks of the flowmeters; K_3—control stopcock; F—fan operating at $\Delta p = 600\,\text{kg/m}^2$.

The air-ion spectrum was determined for Re = 1200, $l/r_2 = 2.5$ and $r_2/r_1 = 8.4$. The counter was provided with a laminarizing unit consisting of a nozzle and grids. Preliminary experiments showed that such conditions ensured a resolving power close to the best possible resolving power which can be obtained upon varying the operating conditions of the described counter. The results of the spectrum are given in Figure 15.2. Further measurements were carried out with positive air ions, the spectral distribution of which is quite close to a normal Gaussian distribution. This specifically applies to the left-hand part of the spectral distribution, which cannot be distinguished from the normal distribution curve with a relative variance $s_k^2 = 0.016$. Preliminary experiments also showed that the character of the spectral distribution remains similar to a normal distribution even when turbulence occurs in the counter.

These preliminary results greatly simplified the experimental layout for further experiments. To find the dispersion it is not necessary to determine the spectrum in detail. Instead, the method described below was used.

We shall determine the voltage U^*, which for laminar air flow satisfies the condition

$$I(U^*) = I(U^*/2). \tag{21.1}$$

Assuming a normal distribution of mobilities with a relative variance of $s_k^2 = 0.016$, we obtain

$$U^* = 0{,}984\,\frac{\Phi}{4\pi\bar{C}\bar{k}}, \tag{21.2}$$

where $\bar{C} = C_1 + C_2/2$ is the mean effective capacitance and $\bar{k}$ is the mean mobility. Since the accuracy in determining the mean effective capacitance is relatively low, the value of U^* was accurately adjusted for each electrode geometry. To do this, four measurements were performed at the respective voltages U_a, U_b, $U_a/2$, $U_b/2$, where U_a and U_b were chosen close to U^*. The exact value of U^* was determined from the measurement results by means of graphical solution of equation (21.1). For a change in the flow rate, while maintaining the electrode geometry unaltered, U^* was calculated from the relationship $U_2^*/\Phi_2 = U_1^*/\Phi_1$.

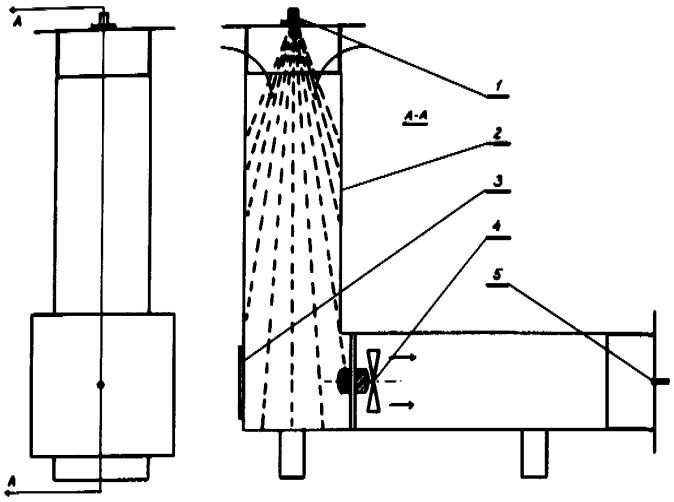

FIGURE 21.3. Ion generator. 1—preparation Sr^{90} (10 mCi); 2—air channel; 3—door; 4—fan; 5—measuring capacitor of the counter.

To determine the variance the current was measured at voltages $U_1 = 0.8\,U^*$ and $U_2 = 1.3\,U^*$, respectively. From these measurements the auxiliary value

$$Z = \frac{I(U_2)}{I(U_1)}, \tag{21.3}$$

was calculated, which is related to the relative variance of the spectrum. Assuming a normal distribution, we obtain

$$Z = 1.625 \frac{\operatorname{erf}\frac{1}{\sqrt{2}\,s_k} - \operatorname{erf}\frac{0.2185}{\sqrt{2}\,s_k} - \sqrt{\frac{2}{\pi}}\,s_k\left[\exp\left(-\frac{0.0477}{2s_k^2}\right) - \exp\left(-\frac{1}{2s_k^2}\right)\right]}{\operatorname{erf}\frac{1}{\sqrt{2}\,s_k} - \operatorname{erf}\frac{0.2700}{\sqrt{2}\,s_k} - \sqrt{\frac{2}{\pi}}\,s_k\left[\exp\left(-\frac{0.0729}{2s_k^2}\right) - \exp\left(-\frac{1}{2s_k^2}\right)\right]}. \qquad (21.4)$$

The dependence $s_k^2 = s_k^2(Z)$, plotted in accordance with (21.4), is shown in Figure 21.4. The parameter Z appears to be quite a sensitive indicator of small changes in the variance of the spectrum.

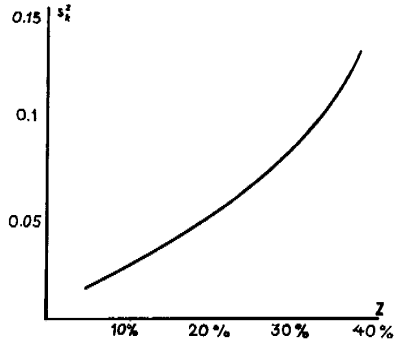

FIGURE 21.4. Graph of function $s_k^2(Z)$

Note that the auxiliary value Z depends essentially on the behavior of air ions, the mobility of which is less than the mean mobility. As mentioned above, the assumption of a normal distribution of mobilities is valid in the range in question. This is sufficient reason to assume that the accuracy of the described method is satisfactory. Considerable deviations from a normal distribution may arise only in the case of particularly large variances. Therefore, the standard deviations, obtained with the aid of the described method and which exceed 20—30%, are inaccurate and have rather the character of some conditional parameter.

As an example, Figure 21.5 shows the characteristics of a counter for relative variances of 0.016 and 0.100. The points U^*, U_1, U_2 and the method for the graphical solution of equation (21.1), can be seen in the figure.

When smoothing the spectrum successively with the aid of certain smoothing functions, the relative variances of the spectrum and the smoothing functions are cumulative, so that the relative variance of the apparent spectrum becomes

$$s_k^2 = s_{k0}^2 + s_{k\Delta}^2 + s_{kd}^2 + s_{kt}^2, \qquad (21.5)$$

where $s_{k\Delta}^2$ is due to the finite length of the collector plate; s_{kd}^2 is due to the thermal diffusion of air ions; s_{kt}^2 is due to turbulent mixing; and s_{k0}^2 is due to the actual spectral distribution and to unmentioned smoothing factors which play a secondary role.

The variance $s_{k\Delta}^2$ is determined from formulas (7.6) and (7.11). After carrying out the relevant calculations, we obtain

$$s_{k\Delta}^2 = \frac{1}{12}\left(\frac{\Delta l}{l}\right)^2. \qquad (21.6)$$

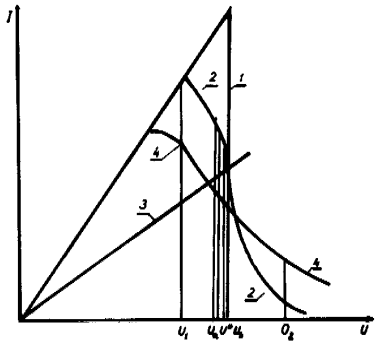

FIGURE 21.5. Counter characteristics: 1—for $s_k^2 = 0$; 2—for $s_k^2 = 0.016$; 3— $I(U/2)$ for $s_k^2 = 0.016$; 4— $I(U)$ for $s_k^2 = 0.1$.

The variance s_{kd}^2 is calculated in accordance with formulas (19.13) and (19.26). The variance s_{k0}^2 must be determined experimentally. To do this, operating conditions must be attained for which $s_{kt}^2 = 0$. The laminarizing nozzle shown in Figure 21.1 helped to prevent turbulence. The electrode geometry was specified by the ratios $l'/r_2 = 3.8$, $l/r = 2.5$, and $r_3/r_1 = 8.4$. The dependence $s_k^2 = s_k^2$ (Re) was determined with the aid of an earlier described method.

The Reynolds number Re was calculated from

$$\mathrm{Re} = \frac{\Phi}{\pi\nu r_2}. \qquad (21.7)$$

The results are listed in Table 21.1.

These results enable us to assume that at Re $\leqslant$ 1400 there is no turbulent mixing of air in the counter. To verify this, several experiments at Re = 1400 were carried out. First, the ion generator was provided with a grid which reduced the level of internal turbulent fluctuations. In the experiment without a laminarizing nozzle, the value of s_k^2 decreased from 0.2 to 0.09. With the laminarizing nozzle, we obtained $s_k^2 = 0.0163$ in both cases. Hence, it follows that external turbulence does not penetrate through the laminarizing nozzle. Secondly, a tube of length $29\,r_2$ was mounted between the measuring capacitor and the laminarizing nozzle.

This also did not alter the variance s_k^2. Consequently, no turbulence occurs inside the capacitor.

The described experiments at the same time constitute an experimental verification of the theory of the diffusion dispersion of mobilities. The results listed in the first three columns of Table 21.1 agree well with the theoretical conclusions (§19), on the basis of which the variances s_{kd}^2 were calculated.

TABLE 21.1

Re	570	1115	1400	1920	2980	5030
s_k^2	0.0183	0.0165	0.0163	0.0189	0.0207	0.0211
$s_{k\Delta}^2$	0.0002	0.0002	0.0002	0.0002	0.0002	0.0002
s_{kd}^2	0.0039	0.0019	0.0016	0.0012	0.0008	0.0004
$s_{k0}^2 + s_{kt}^2$	0.0142	0.0144	0.0145	0.0177	0.0199	0.0205

A series of basic measurements was carried out over the shortest possible time interval in order to prevent marked variations in the external conditions. The experiments were performed in a basement which rendered the test easier. Over a period of six days, which was the time necessary for the measurements, the air temperature varied from 21° to 24°, the relative humidity from 42% to 52% and the atmospheric pressure from 756 mm to 766mm Hg. Each day, prior to carrying out the measurements, the exact value of U^* and the variance s_{k0}^2 were determined.

The values of s_{k0}^2 were 0.0141, 0.0145, 0.0144, 0.0144, 0.0149 and 0.0144, respectively. The relative standard deviation of the parameter s_{k0} from the mean value was 0.9%. This value characterizes the stability of the relative spectral distribution of air ions for the described conditions.

The length l' of the frontal section was varied by mounting tubular sections between the measuring capacitor and entrance nozzle. The results are graphically shown in Figure 21.6.

From the curves in Figure 21.6, it immediately follows that s_{kt} depends strongly on the turbulence of the air entering the counter. For intermediate lengths of the frontal sections the external turbulence and the entrance conditions of the air play a decisive role in the turbulent smoothing of the spectrum.

Another interesting result is that in a counter without a laminarizing nozzle and without tubular sections (curve 1, Figure 21.6) s_{kt} decreases with increasing air flow rate, even at high values of Re. This emphasizes the incompatibility of the traditional viewpoint on the problem of preventing turbulence in counters. The observed "reciprocal" dependence of s_{kt} on Re is fully explicable. Small-scale turbulent pulsations penetrate with the aspirated air into the measuring capacitor. The turbulent intensity at the beginning of the measuring capacitor is determined by the ratio of the mean

square value of the fluctuation and the mean airflow velocity. Consequently, the turbulent intensity decreases with increasing flow velocity.

In the described experiments the intensity of the turbulence penetrating from the outside considerably exceeds the turbulent intensity of the steady flow in the tube. The initial turbulence gradually diminishes as air flows through the measuring capacitor. In the long tubular attachment the initial turbulence decreases considerably and the variance s_{kt}^2 depends only slightly on the conditions under which the air enters into the counter. These conclusions are borne out by the behavior of curves 9—12, Figure 21.6.

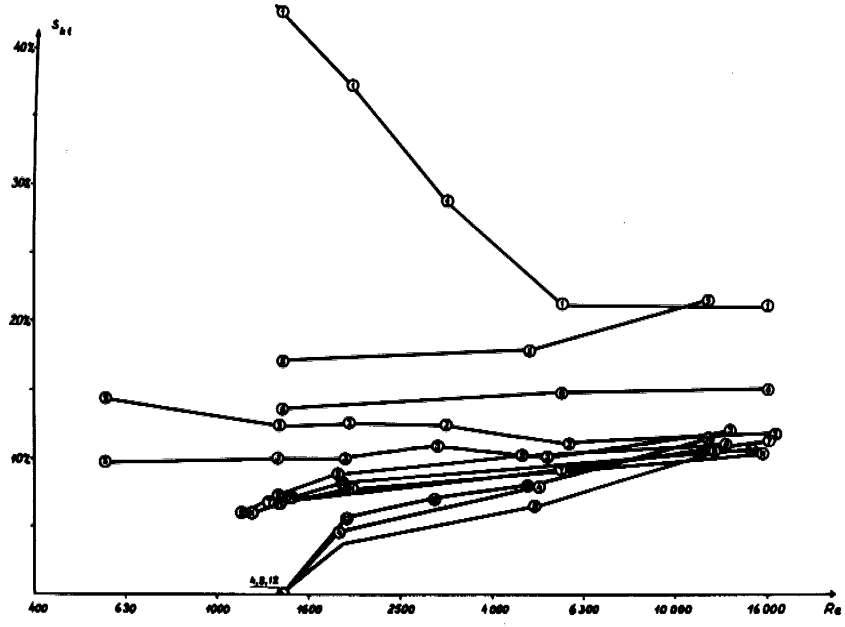

FIGURE 21.6. Turbulent dispersion of mobilities. The type of nozzle (Figure 21.1) and the value of the ratio l'/r_2 (in parentheses) are given for the respective curves:

1—without nozzle (3.8); 2—d (3.8); 3—b (3.8); 4—e (3.8); 5—c (14.3); 6—without nozzle (14.3); 7—d (14.3); 8—e (14.3); 9—c (33); 10—without nozzle (33); 11—d (33); 12—e (33).

The effect of the conicity of the entrance section of the measuring capacitor appears to be extremely strong. In the widening flow (nozzle, Figure 21.2, c) particularly vigorous turbulence is generated, which in the above experiment exceeds even the level of the external turbulence. In the case of a short cylindrical entrance section the parameter Z reached values up to 65%, which does not permit calculating the variance with the aid of the applied method. Therefore, the corresponding data do not appear in Figure 21.6. On the contrary, the convergent channel section strongly

suppresses the external turbulence. This is in good agreement with the well-known results of a study on the stability of converging and diverging currents /Loytsyanskii, 1959/.

An effective means for the suppression of turbulence in the measuring capacitor is the use of a grid attached to the inlet (curves 1 and 3, Figure 21.6).

The dependence of s_{kt} on the effective length of the measuring capacitor was studied for the conditions Re = 1400, $r_2/r_1 = 8.4$; $(l'+l)/r_2 = 17$. The air was drawn into the counter via a converging channel. The measuring results are shown in Table 21.2.

TABLE 21.2

l/r_2	1	2.5	6
s_{kt}^2	0.0037	0.0057	0.026
$\overline{\varepsilon}\sqrt{\overline{R}}$	0.035	0.022	0.019

The values of the parameter $\overline{\varepsilon}\sqrt{\overline{R}}$ are calculated from experimental data according to formula (20.8). The decrease of $\overline{\varepsilon}\sqrt{\overline{R}}$ with increasing length of the measuring capacitor is explained by the decrease of $\sqrt{\overline{R}}$. The mean turbulent intensity $\overline{\varepsilon}$ increases slightly with the length l because of the decrease in the length l' of the frontal section. For comparison, we note that for an inner plate with $l/r_2 = 2.5$ under the same conditions the following values were obtained: for $l'/r_2 = 3.8$, $\overline{\varepsilon}\sqrt{\overline{R}} = 3.6\%$; for $l'/r_2 = 14.5$, $\overline{\varepsilon}\sqrt{\overline{R}} = 2.2\%$; for $l'/r_2 = 33$, $\overline{\varepsilon}\sqrt{\overline{R}} = 1.8\%$.

The measurement results in the case of long and intermediate frontal sections, and large Reynolds numbers agree well with a rough determination of the parameter $\overline{\varepsilon}\sqrt{\overline{R}}$ according to the method described at the end of the preceding section.

A number of experiments was performed to clarify the effect of the geometry of the end of the inner plate on the turbulent mixing. The results of these experiments are mostly of a qualitative nature and we shall therefore refrain from stating any values. In the case of a thin plate ($r_2/r_1 = 8.4$), no considerable influence of the geometry of the end of the inner plate was observed. For the ratio $r_2/r_1 = 2.7$ turbulence started at a lower flow rate and the variance s_{kt} of the mobility due to turbulence was larger when the end of the inner plate had the form of a transversely truncated hollow cylinder. No differences were observed between the results obtained with an inner plate having a flat, semispherical and semiellipsoidal end, respectively.

For $r_2/r_1 = 1.17$ a considerable dependence of turbulent mixing on the geometry of the end of the inner plate was observed. The intensity of turbulent mixing increases in the following order of plate-end geometries: semiellipsoidal, semispherical and flat.

The investigation of the dependence of s_{kt} on the ratio r_2/r_1, with the aid of the above experimental arrangement, proved successful, since upon changing the radius of the inner plate the transition conditions of air from the section with a circular cross section to the section with an annular cross section are not preserved, which essentially affects the character of the flow. This introduces an uncertainty into the measurement results which does not allow us to make any concrete statements.

§22. LONG MEASURING CAPACITOR WITH A TURBULENT AIR FLOW

In the preceding sections the mobility dispersion due to turbulence is assumed to be relatively small. Without this assumption the problem becomes considerably more complex. There exists, however, a very simple solution of the problem in the limiting case of very strong turbulent mixing in a long measuring capacitor. This solution is of practical importance since it determines the upper limit of distortions which can be caused by turbulence.

In the limiting case of a long capacitor with vigorous air mixing, the function $\varrho(k)$ between the plates can be considered to be independent of the radial coordinate of the point under consideration. $\varrho(k)$ will be a function of the distance x of this point from the beginning of the measuring capacitor.

The equation describing the characteristics of the integral counter under these conditions was derived already in the work /Becker, 1910/. Below we shall consider this equation in a somewhat altered form. Let us first suppose that the air contains air ions of mobility k only. For a short section of the cylindrical measuring capacitor we can write

$$dI = 4\pi U \lambda_{\pm}\, dC = \Phi \frac{k}{k_0} \varrho(x) \frac{dx}{l}, \tag{22.1}$$

where k_0 is given by (4.3).

$\varrho(x)$ decreases in this section by the value $dI(x)/\Phi$. Consequently, the equation for $\varrho(x)$ has the form

$$\frac{d\varrho(x)}{dx} = -\frac{k\varrho(x)}{k_0 l} \tag{22.2}$$

Integrating this equation for the condition $\varrho(0) = \varrho_0$, we obtain

$$\varrho(x) = \varrho_0 \exp\left(-\frac{kx}{k_0 l}\right). \tag{22.3}$$

The current through the collector plate of the counter is computed by the integral

$$I = \frac{\Phi k}{k_0 l} \int_0^l \varrho(x)\, dx. \tag{22.4}$$

The function G is defined as the ratio I/Q_0. Integrating, we obtain

$$G = \Phi\left[1 - \exp\left(-\frac{k}{k_0}\right)\right]. \tag{22.5}$$

In Figure 21.1 the curve of the function G for the above case is compared with the curve for an ideal counter.

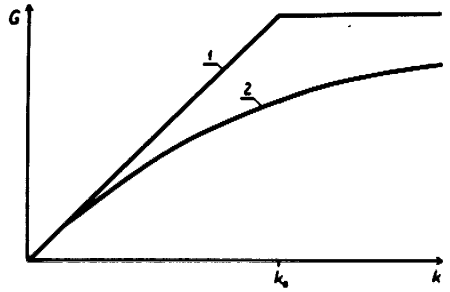

FIGURE 22.1. Function G of an integral counter:

1—laminar flow; 2—complete mixing.

The obtained form of the function G is inconvenient for solving equation (3.3). The study of the spectrum of air ions under these conditions is senseless and we shall therefore consider only the errors arising in the calculation of the polar conductivities and the polar charge densities, using the well-known formulas derived under the assumption of laminar flow. The greatest distortions in the conductivity will arise when the mobility of all the air ions is equal to the maximum mobility k_{max} of air ions actually encountered. To ensure that the relative error will not exceed the value δ, a sufficiently large limiting mobility should be chosen. The minimum permissible values k_0, calculated according to the divergence between the G-functions in (22.5) and (4.4), respectively, are listed in Table 22.1. When measuring the polar charge density, one should start with the minimum value k_{min} of the encountered mobility and restrict k_0 to a sufficiently small value. The permissible limit of the value k_0 for different δ-values is also shown in Table 22.1.

As can be seen from the results, turbulent mixing constitutes a negative influence when measuring polar conductivities.

Allowance for the true form of the curve $q(k)$ ensures less stringent restrictions. It is easy to show that for the condition

$$k_0 \geqslant k_{max} \tag{22.6}$$

we obtain

$$\delta_\lambda = \frac{\int_0^\infty \frac{k}{2k_0}\left(1 - \frac{1}{3}\frac{k}{k_0} + \frac{1}{12}\frac{k^2}{k_0^2} - \frac{1}{60}\frac{k^3}{k_0^3} + \ldots\right)\lambda(k)\,dk}{\int_0^\infty \lambda(k)\,dk}. \tag{22.7}$$

Correspondingly, for the condition

$$k_0 \leqslant k_{min} \tag{22.8}$$

we obtain

$$\delta_q = \frac{\int_0^\infty \exp\left(-\frac{k}{k_0}\right) q(k)\,dk}{\int_0^\infty q(k)\,dk}. \tag{22.9}$$

TABLE 22.1

Permissible error	Permissible k_0	
	Measurement of $\lambda_\pm$	Measurement of q_*
1%	$k_0 \geqslant 50\ k_{max}$	$k_0 \leqslant k_{min}/4.6$
2%	$k_0 \geqslant 24.6\ k_{max}$	$k_0 \leqslant k_{min}/3.9$
5%	$k_0 \geqslant 9.7\ k_{max}$	$k_0 \leqslant k_{min}/3$
10%	$k_0 \geqslant 4.7\ k_{max}$	$k_0 \leqslant k_{min}/2.3$
20%	$k_0 \geqslant 2.2\ k_{max}$	$k_0 \leqslant k_{min}/1.6$

However, complete mixing, as assumed in the above calculations, is never attained in practice. The experimental verification of the manner in which the air ions settle in a long capacitor with a turbulent air flow was carried out with the setup described in §21. The parameters of the counter were: $r_2/r_1 = 2.7$, $l/r_2 = 17$, $l'/r_2 = 18$, $\mathrm{Re} = 15{,}500$. The air was drawn into the measuring capacitor through a convergent channel.

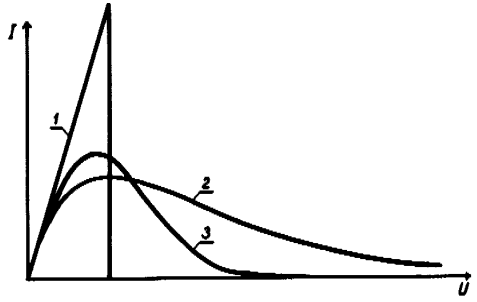

FIGURE 22.2. Characteristics of a differential counter:

1—laminar flow; 2—complete mixing; 3—according to experimental results.

In the case of complete air mixing the function G of the first-order differential counter with a divided capacitor has the form

$$G = \Phi \frac{C_2}{C_1} \frac{k}{k_0} \exp\left(-\frac{k}{k_0}\right). \qquad (22.10)$$

The above formula holds if the ratio C_2/C_1 is small. In the experiment described, $C_2/C_1 = 0.007$, which justifies the approximation employed.

The experimental results are given in Figure 22.2. For comparison, the figure shows the characteristics of a counter for laminar flow conditions and those of a counter for conditions of complete mixing (formula (22.10)).

§23. THE ASYMMETRY OF THE MEASURING CAPACITOR AND THE EFFECT OF GRAVITATION ON AIR IONS

The intricacy of a cylindrical measuring capacitor depends on how accurately the inner plate is centered. To determine the required accuracy, we must know the dependence of the arising errors on the eccentricity of the cylindrical plates.

Consider an asymmetrical measuring capacitor of an integral counter. For small voltages the limiting surface intersects the inlet cross section, and the function G equals $4\pi CUk$, i.e., it does not differ from the function G of a symmetrical counter. An increase in the voltage causes the limiting surface to intersect the second plate. However, because of the asymmetry, the limiting surface will not enclose the entire flow. Here, the function G is then less than $4\pi CUk$, but also less than Φ. Only a further increase in the voltage causes the limiting surface to enclose the entire air flow, and the function G attains the value of Φ. An approximation of the function for an asymmetrical measuring capacitor is shown in Figure 23.1.

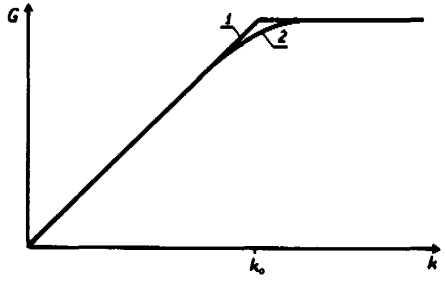

FIGURE 23.1. Function G of an integral counter:

1—for a symmetrical capacitor; 2—for an asymmetrical capacitor.

The effect of the asymmetry of the measuring capacitor on the measurement results can be described also by the method of the apparent spectral

distribution used in §19 and §20. In equation (3.3) the undistorted form of the function G is preserved and the distortions are described as the dispersion of the apparent mobilities. It can be readily verified that the interval of dispersion of the apparent mobilities coincides with the interval of mobilities in which the function G is distorted.

We shall carry out the calculation for a cylindrical capacitor in which the axes of the plates are parallel but displaced by a distance Δr. For simplicity, we make two approximations: 1) we assume that the profile of the air flow is homogeneous, 2) we also assume that $\Delta r \ll r_2 - r_1$, and then carry out the corresponding calculations in the first approximation.

The transverse cross section of the capacitor with an off-center inner electrode is shown in Figure 23.2. The electric field in the capacitor coincides with the field of two charged filaments at distances f_1 and f_2, respectively, from the axis of the outer plate /Landau, Lifschitz, 1957/.

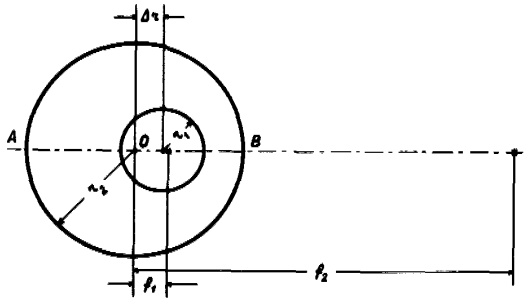

FIGURE 23.2. Cross section of an asymmetrical capacitor.

The distances f_1 and f_2 are defined by

$$\left.\begin{aligned} f_1 f_2 &= r_2^2 \\ (f_1 - \Delta r)(f_2 - \Delta r) &= r_1^2 \end{aligned}\right\}. \qquad (23.1)$$

In the first approximation f_1 and f_2 are expressed in simple fashion by

$$f_1 = \frac{r_2^2}{r_2^2 - r_1^2}\,\Delta r, \qquad (23.2)$$

$$f_2 = \frac{r_2^2 - r_1^2}{\Delta r}. \qquad (23.3)$$

Consider the field along the line OA (Figure 23.2). The distance from the axis O of the outer plate will be denoted by r. The field strength is given by

$$E = 2Q\left(\frac{1}{r + f_1} - \frac{1}{r + f_2}\right). \qquad (23.4)$$

where Q is the charge per unit length of the capacitor. Taking into account expressions (23.2) and (23.3), and neglecting second-order small quantities, we obtain

$$E = \frac{2Q}{r\left[1 + \frac{r^2 + r_2^2}{r\left(r_2^2 - r_1^2\right)}\Delta r\right]} \tag{23.5}$$

The apparent mobility of an air ion is inversely proportional to the time t required for the air ion to pass from one plate to the other. If no radial components of the air-flow velocity occur, then

$$t = \int_{r_1 - \Delta r}^{r_2} \frac{dr}{kE(r)}. \tag{23.6}$$

Calculation yields

$$t = \frac{1}{4kQ}\left\{\left(r_2^2 - r_1^2\right) + \Delta r\left[2r_1 + \frac{2\left(r_2^3 - r_1^3\right)}{3\left(r_2^2 - r_1^2\right)} + \frac{2r_2^2}{r_2 + r_1}\right]\right\}. \tag{23.7}$$

The relative deviation of the apparent mobility from the value at $\Delta r = 0$ is determined by the ratio of the two components in formula (23.7). This ratio is expressed by

$$\delta_k = \frac{8\Delta r\left(r_2^3 - r_1^3\right)}{3\left(r_2^2 - r_1^2\right)^2}. \tag{23.8}$$

It is not difficult to carry out a similar calculation for an air ion moving along the line OB. In this case, the time of passage of the air ion is shortened and the absolute value of the relative deviation of the apparent mobility due to the asymmetry can be determined, in the first approximation, by the same formula (23.8).

For air ions moving in other longitudinal cross sections of the measuring capacitor, the deviation of the apparent mobility will be less than in the above cases. Therefore, formula (23.8) in the first approximation defines the limits of the dispersion of the apparent mobilities resulting from the asymmetry of the measuring capacitor.

The distortion of the flow profile due to the asymmetry causes an additional dispersion of the apparent mobilities. In a flat channel the mean flow velocity at unaltered pressure is proportional to the square of the distance between the walls. Therefore, one can write for the flow across the lines OA and OB

$$\delta_{\bar{u}} < \frac{2\Delta r}{r_2 - r_1}. \tag{23.9}$$

It is readily shown that the error limited by condition (23.9) is always less than the error determined by expression (23.8). Hence, we conclude that the distortion of the flow profile cannot effect more than a twofold increase

in the distortion limits of the mobilities determined by (23.8). In actual fact, the distortion limits of the mobilities increase considerably less.

The problem of asymmetry has special significance in the case of a parallel-plate measuring capacitor. Only an infinitely wide parallel-plate capacitor strictly fulfills the symmetry requirements.

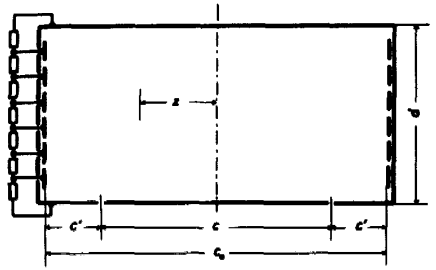

FIGURE 23.3. Cross section of a parallel-plate measuring capacitor.

The electric field of a parallel-plate capacitor may be rendered more homogeneous by means of the method applied in the work /Fontell, 1932/. This method is explained in Figure 23.3.

To prevent distortions it is a prerequisite that the profile of the collector plate is identical in all longitudinal sections of the capacitor. The measuring capacitor should be sufficiently wide so that side walls do not distort the air flow over the collector plates.

In the case of high flow velocity the required distance between the edge of the collector plate and the side wall (Figure 23.3) can be determined on the basis of boundary flow theory. As is well known /Kochin, Kibel, Roze, 1963/, the relative distortion of the flow velocity in the vicinity of the wall is less than 2δ, if the distance from the wall exceeds $\Psi(\delta)\sqrt{\nu x/u_0}$. Some values of the function $\Psi(\delta)$ are listed in Table 23.1.

TABLE 23.1

δ	0.1%	0.2%	0.5%	1%	2%	5%	10%	20%
Ψ	5.7	5.4	4.9	4.5	4.3	3.4	2.7	1.9

According to the above it is sufficient to assume

$$c' = \Psi(\delta)\sqrt{\nu t_0}. \tag{23.10}$$

Independently of the fulfillment of this condition one observes an increase in the flow velocity along the axis of the capacitor, since the widening boundary layer pushes the air toward the center /Yaita, Nitta, 1955/.

At low flow velocities formula (23.10) can yield excessively large values for the distance c', since it does not allow for the effect of the lower and

upper walls. The exact calculation of this effect is only possible for a steady laminar flow. The movement of air ions in a parallel-plate capacitor with a steady laminar flow is treated in the work /Lipscomb, Rubin, Sturdivant, 1947/. We shall use the formula derived in this work for determining the distance x', within which the air ion entering at the edge of the plate is precipitated.

$$x' = \frac{2u_a d^2}{3kU}\left[1 + \frac{32}{\pi^3 \operatorname{ch}\frac{\pi c_0}{2d}}\left(1 + \frac{32}{\pi^3 \operatorname{ch}\frac{\pi c_0}{2d}}\right)\left(1 - \frac{3}{\pi}\operatorname{ch}\frac{\pi z}{d}\right) + \ldots\right]. \qquad (23.11)$$

Here, u_a is the flow velocity in the center of the rectangular channel, c_0 is the width of the channel and z the distance from the central vertical longitudinal cross section (Figure 23.3). In practice, the inequality $c_0/d > 1$ always exists. In the case $z = 0$ the expression in brackets nearly equals unity. For the half-width of the interval of dispersed mobilities we obtain the formula

$$\delta_k \approx \frac{48}{\pi^4 \operatorname{ch}\frac{\pi c_0}{2d}}\left(1 + \frac{32}{\pi^3 \operatorname{ch}\frac{\pi c_0}{2d}}\right)\left[\operatorname{ch}\frac{\pi\left(\frac{c_0}{2} - c'\right)}{d} - 1\right] \qquad (23.12)$$

To simplify calculations, we give in Figure 23.4 curves which enable us to find a satisfactory value for c', when δ_k and c_0/d are known.

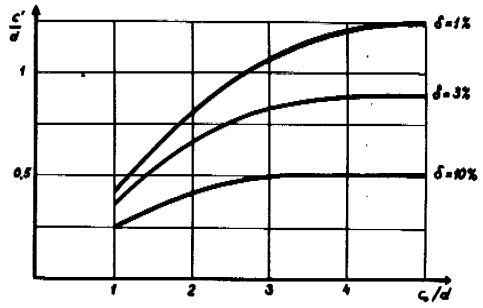

FIGURE 23.4. Curves for finding a satisfactory value for c' at developed laminar flow.

In design calculations of a counter δ_k should be determined in accordance with both formula (23.10) and formula (23.12), and the smaller of the two values selected.

In the case of charged aerosol particles additional distortions may be caused by gravity. The determination of the gravitational effect is quite simple. There exist several different ways for doing this and it is advisable to consider each one separately. For simplicity, we shall assume the flow profile to be uniform in all cases.

In a horizontally oriented cylindrical capacitor the gravitational effect is quite similar to the effect of the asymmetry of the measuring capacitor.

In the first approximation the relative half-width of the interval of dispersed mobilities is given by

$$\delta_k = \frac{2mg\left(r_2^3 - r_1^3\right)\ln\frac{r_2}{r_1}}{3qU\left(r_2^2 - r_1^2\right)}, \qquad (23.13)$$

where m is the mass of the particles.

In a horizontally oriented parallel-plate capacitor the apparent mobilities of air ions of equal mass mobility are not dispersed, but shifted toward one direction. The relative shift is expressed by

$$\delta_k = \frac{mgd}{qU}. \qquad (23.14)$$

In a vertically oriented capacitor the apparent mobilities are also shifted toward one direction. For a cylindrical capacitor we obtain

$$\delta_k = \frac{mg\left(r_2^2 - r_1^2\right)\ln\frac{r_2}{r_1}}{2qUl}, \qquad (23.15)$$

and for a parallel-plate capacitor

$$\delta_k = \frac{mgd^2}{qUl}. \qquad (23.16)$$

Of some interest is the situation in which a parallel-plate capacitor is placed on its side, so that the direction of both the air flow and the electric field are horizontal. In this case distortions are completely eliminated, if the condition

$$c' > \frac{mgd^2}{qU} \qquad (23.17)$$

is fulfilled.

§24. ADSORPTION OF AIR IONS

Gerasimov /Gerasimov, 1941b/ showed that losses of air ions due to adsorption should always be considered when designing inlet devices for an aspiration counter.

Adsorption here applies to the settling of air ions owing to diffusion and attractive electrical image forces. Before calculating the adsorption, we should specify the respective roles of the above two mechanisms.

Consider air ions with mobility k and charge q, distributed uniformly at the initial instant $t = 0$ near the plane conducting wall. If only the diffusion mechanism of adsorption were acting, then in time t as many air ions would settle as are contained in a layer whose thickness equals the mean Brownian displacement of the air ions /Fuks, 1955/. This thickness is given by

$$y_d = \sqrt{\frac{4KTkt}{\pi q}}. \qquad (24.1)$$

When only the image-force mechanism is active, the corresponding layer thickness is

$$y_q = \sqrt[3]{\frac{3qkt}{4}}. \qquad (24.2)$$

The more dominant of the two mechanisms is indicated by the relation

$$\frac{y_d}{y_g} = \sqrt[6]{\frac{1024K^3T^3kt}{9\pi^3 q^5}}. \qquad (24.3)$$

We shall clarify this expression by setting $T = 283°K$:

$$\frac{y_d}{y_q} = 37\sqrt[6]{\frac{k\ (\text{cm}^2/\text{V}\cdot\text{sec})\ t\ (\text{sec})}{[q\ (\text{elem.ch.})]^5}} \qquad (24.4)$$

It appears that in most cases the image-force mechanism of adsorption is of no practical significance. This mechanism may become dominant only for artificially charged aerosol particles. In the following, we shall ignore the image-force mechanism of adsorption.

In the theory of adsorption it is useful to exploit the similarity between the problem at hand and that of heat transfer. The diffusion equation differs from the equation of thermal conductivity only in that the temperature is replaced by the concentration of impurities and that the heat conductivity coefficient is replaced by the diffusion coefficient. The flow of material to the surface where it is adsorbed is proportional to the initial impurity concentration. In calculations, it is convenient to use the ratio Φ_A of these two proportional quantities which we shall call the adsorption flow rate. In analogy to the Newton formula from the theory of heat transfer, we write

$$\Phi_A = \zeta S, \qquad (24.5)$$

where S is the area of the adsorbing surface and ζ is the coefficient of adsorption, which in our case replaces the coefficient of heat transfer.

In order to apply the formulas of heat transfer to problems of adsorption, the specific heat capacity and the density of the material should equal unity, the Prandtl number Pr should be replaced by the Schmidt number $\text{Sc} = \nu/D$ and the Nusselt number Nu by a special adsorption criterion

$$K_A = \frac{\zeta r}{D}, \qquad (24.6)$$

where r is the determining parameter.

Let us first consider the adsorption of air ions when the air is flowing through wire grids. The use of wire grids in the inlet unit presents certain advantages, since with the aid of grids one can screen disturbing electric fields and suppress turbulent pulsations of the incoming flow. The only drawback is that these grids adsorb a certain portion of the air ions.

We assume that the mesh width of the grid is sufficiently wide, so that the adsorption on the grid wires can be compared to that on separate wires.

The heat transfer of a separate wire is described by the empirical equation /Ulsamer, 1932; Gröber, Erk, Grigull, 1958/

$$\text{Nu} = 0.91\ \text{Re}^{0.385}\ \text{Pr}^{0.31}, \qquad (24.7)$$

where the diameter of the wire is taken to be the determining parameter. Formula (24.7) was derived from experimental data for the ranges $0.2 < \text{Re} < 50$ and $6 < \text{Pr} < 1240$, respectively /Davis, 1924/. These values of the Prandtl number correspond to singly charged air ions with mobilities ranging from 0.005 to 1 $\text{cm}^2/\text{volt}\cdot\text{sec}$. The Reynolds number rarely exceeds 50. When $50 < \text{Re} < 10,000$, we should use the formula /Ulsamer, 1932/

$$\text{Nu} = 0.60\ \text{Re}^{0.5}\ \text{Pr}^{0.31}. \qquad (24.8)$$

Formula (24.7), as applied to the problem of air-ion adsorption, becomes

$$\zeta = 0.6\ \frac{u^{0.385} D^{0.69}}{r_0^{0.615} \nu^{0.075}}, \qquad (24.9)$$

where r_0 is the wire radius.

The relative adsorption is determined by the ratio

$$A = \frac{\Phi_A}{\Phi}, \qquad (24.10)$$

where Φ is the air-flow rate.

If a grid is mounted on the inlet of a cylinder of radius r, then that portion of the cross-sectional area covered by wires is given by

$$S = \frac{4\pi^2 r_0 r^2}{h}, \qquad (24.11)$$

where h is the mesh width.

For the relative adsorption we then obtain

$$A = 15\ \frac{r_0^{0.385} r^{1.23} D^{0.69}}{\Phi^{0.615} h \nu^{0.075}}. \qquad (24.12)$$

For normal external conditions

$$A = 0.4\ \frac{[r_0\ (\mu\text{m})]^{0.385} [r(\text{cm})]^{1.23} [k\ (\text{cm}^2/\text{V}\cdot\text{sec})]^{0.69}}{[\Phi(\text{cm}^3/\text{sec})]^{0.615} h(\text{mm})} \qquad (24.13)$$

In the case $ur_0 > 25\nu$, we start with formula (24.8) and obtain

$$A = 0.11\ \frac{[r_0\ (\mu\text{m})]^{0.5} r(\text{cm})\ [k\ (\text{cm}^2/\text{V}\cdot\text{sec})]^{0.69}}{[\Phi(\text{cm}^3/\text{sec})]^{0.5} h(\text{mm})} \qquad (24.14)$$

Formula (24.13) was verified experimentally. The air was ionized with ions of both polarities by the ion generator described in §21. The mean mobility of the air ions was 1.2 $\text{cm}^2/\text{volt}\cdot\text{sec}$. The relative adsorption was determined by comparing the flows obtained in the integral counter with and without a grid. The counter was operated under saturation conditions.

The radius of the outer plate was 0.8 cm. The results are listed in Table 24.1.

The agreement between the experimental data and the calculated values is somewhat rough. However, when designing a counter, formula (24.13) is sufficiently accurate for a preliminary estimation of the errors.

TABLE 24.1

h (mm)	r_0 (μm)	Φ (cm³/sec)	A	
			experimental	(24.13)
0.44	67	220	19%	15%
0.44	67	510	13%	9%
0.44	67	1000	9%	6%
0.785	145	220	10%	11%
0.785	145	510	7%	7%
0.785	145	1000	5%	4%

There exist no suitable empirical formulas in the theory of heat transfer which can be applied here for calculating the adsorption of air ions in the inlet cylinder of the counter. The available formulas /Mikheev, 1956/ apply only to long cylinders. For short cylinders some results are known for the specific case Pr = 0.71. The use of these data in calculating the air-ion adsorption is unjustified for a number of reasons. We shall attempt, therefore, to calculate theoretically the relative adsorption of air ions in the inlet cylinder on the basis of certain simplifying assumptions.

In the work /Siksna, Metnieks, 1953/ this problem is solved under conditions of uniform air flow in the cylinder. Simple calculations yield

$$A = 4\frac{l'^{0.5}}{\Phi^{0.5}}D^{0.5}, \tag{24.15}$$

where l' is the length of the inlet cylinder.

The assumption of a uniform flow profile is somewhat loose, since adsorption takes place in the near-wall layer, where the flow velocity differs considerably from the mean flow velocity. Calculation shows that the layer thickness $Ar/2$, calculated from formula (24.15), is considerably less than the thickness of the boundary layer. According to a preliminary assessment, adsorption takes place completely within the boundary layer where the velocity profile is nearly linear (see formula (18.4)). Accordingly, the following calculations will be carried out on the basis of this assumption.

In still air the adsorption is described by expression (24.1). Hence,

$$\zeta = \frac{2D}{\pi y_d}. \tag{24.16}$$

Here, y_d denotes the equivalent layer thickness from which the air ions are adsorbed. In the boundary layer, ζ is somewhat less than in still air for the same value of y_d. This difference, however, cannot be large. For simplicity, we shall also use (24.16) to describe the adsorption from the boundary layer.

The airflow rate in a layer of thickness y_d is given by

$$\Phi = 0.166\, c y_d^2 \sqrt{\frac{u_0^3}{\nu x}}, \tag{24.17}$$

where c is the width of the strip in question (for the entire tube $c = 2\pi r$) and x is the distance from the beginning of the cylinder. The adsorption flow rate is calculated with the aid of the integral

$$\Phi_A = c\int_0^x \zeta(x')\,dx'. \tag{24.18}$$

Comparing expressions (24.17) and (24.18), we obtain

$$\frac{y_d^2(x)}{\sqrt{x}} = \frac{D}{0{,}83\pi}\sqrt{\frac{\nu}{u_0^3}}\int_0^x \frac{dx'}{y_d(x')}. \tag{24.19}$$

The solution of the above equation is

$$y_d = 1.97\frac{\nu^{1/8}D^{1/3}}{u_0^{1/2}}x^{1/2}. \tag{24.20}$$

Now it is easy to calculate the flow rate Φ_A from formula (24.17) or (24.28). The relative adsorption is given by

$$A = 2.3\frac{l'^{1/2}D^{2/3}}{\Phi^{1/3}\nu^{1/6}}. \tag{24.21}$$

At room temperature and normal pressure we have

$$A = 0.27\frac{[l'(\text{cm})]^{1/2}[k(\text{cm}^2/\text{V}\cdot\text{sec})]^{2/3}}{[\Phi(\text{cm}^3/\text{sec})]^{1/2}} \tag{24.22}$$

The following condition must be fulfilled in order to apply formula (24.12):

$$r \gg \sqrt{\nu t_0'}, \tag{24.23}$$

where t_0' is the filling time of the preliminary cylinder. At the same time it must be ensured that y_d does not exceed the thickness $2\sqrt{\nu t_0'}$, within the limits of which formula (18.4) is sufficiently accurate. The last condition is fulfilled if $Sc > 1$. For normal external conditions it suffices that $k < 6\ \text{cm}^2/\text{volt}\cdot\text{sec}$.

Comparing formulas (24.15) and (24.21), we see that the former gives values which are $1.74\,Sc^{1/6}$ times greater than those of the latter. The error produced upon applying formula (24.16) merely effects a decrease in this ratio. The deviation between formulas (24.15) and (24.12) in the case of the most highly mobile air ions corresponds to a factor of two; for slightly mobile air ions this factor is considerably larger.

In the work /Siksna, Metnieks, 1953/ experimental data are given which coincide well with formula (24.15). This, however, is doubtful, since theoretical considerations speak in favor of formula (24.21).

The controversial character of the problem stimulated further investigation. The methods employed in the relevant experiments were generally the same as those described in the work /Siksna, Metnieks, 1953/. It should be noted, however, that these methods are not fully free from external distorting influences, and do not guarantee high accuracy. A slightly modified version of the setup shown in Figure 15.1 was used. Air ions were generated not by radioactive irradiation but by corona discharge. The ionization was unipolar positive. The mean air-ion mobility $\bar{k} = 1.2\ cm^2/volt \cdot sec$ was determined by the integral counter method with the aid of the same arrangement. The cylinder connected to the electrometer had an inner radius of 0.845cm and a length of 4.0 cm. It was possible to lengthen the cylinder by an additional cylindrical segment of the same radius and of length 8.0 cm. Before measuring the adsorbed flow, the inner plate was removed.

The experimental results presented in Table 24.2 clearly speak in favor of formula (24.21). At large Reynolds numbers the experimental data deviate sharply from the calculated ones (this may be due to turbulence).

The problem of air-ion adsorption from the turbulent flow is more complex and precludes a simple theoretical approach. The use of empirical formulas of the theory of heat transfer to calculate the turbulent adsorption is unjustified, since owing to the extremely short time intervals the image-force mechanism of air-ion capture can no longer be neglected. The adsorption of aerosol particles from the turbulent flow in the measuring capacitor of a counter was estimated in the work /Zachek, 1964b/.

TABLE 24.2

l' (cm)	Φ $\left(\frac{cm^3}{sec}\right)$	$Re = \frac{\bar{u}r}{\nu}$	ϱ_+ $\frac{elem.ch.}{cm^3}$	A		
				experimental	(24.21)	(24.15)
4	137	340	20,000	4%	5%	12%
4	257	640	30,000	3%	4%	9%
4	372	930	30,000	3%	3%	7%
4	1010	2500	40,000	6%	2%	4%
4	1790	4500	40,000	5%	1.5%	3%
12	96	240	20,000	13%	11%	25%
12	220	550	30,000	7%	7%	16%
12	416	1040	40,000	6%	5%	12%
12	1010	2500	40,000	8%	3%	8%
12	1750	4400	40,000	7%	2.5%	6%

The adsorption changes the spatial distribution of air ions over the entrance cross section of the measuring capacitor. Therefore, air-ion adsorption in the inlet cylinder is not only manifested in the measurement results of the polar charge densities, but also in the results of the spectral distribution analysis. Counters with inner and outer collector plates behave differently with respect to adsorption. The effect of adsorption on the function G of the integral counter is shown in Figure 24.1. The measurement results of the conductivity are distorted only in the case of the outer collector plate. However, connecting a counter with an outer collector plate has the advantage that the air-ion adsorption in the inlet cylinder does not affect the measurement results of the spectral distribution. In the case of an inner collector plate, the usual methods of data processing give a distorted apparent spectral distribution. In this case the mobilities not only exhibit dispersion but the mean mobility undergoes a shift as well. The relative decrease in the mean mobility equals the relative adsorption A. The dispersion limits of the apparent mobilities are in effect also limited by the value A.

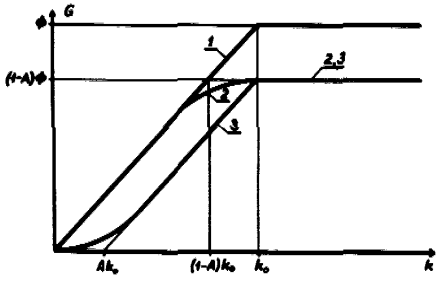

FIGURE 24.1. Function G of an integral counter:

1—in the absence of adsorption; 2—for an inner collector plate; 3—for an outer collector plate.

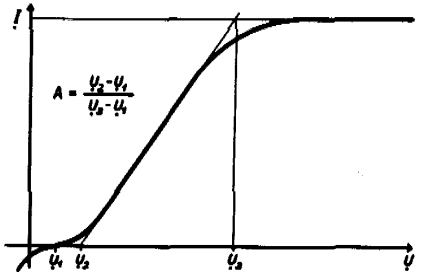

FIGURE 24.2. Determination of the relative adsorption from the characteristics of an integral counter with an outer collector plate:

U_1 — contact potential.

A plot of the function G in the case of an outer collector plate enabled us to determine the relative adsorption A from the experimental curve $I = I(U)$. The essential feature of the suggested method is clearly illustrated in Figure 24.2. This method is in some respects more appropriate than the method of measuring the adsorbed flow of unipolar air ions, and can be recommended for further experimental work on the study of the adsorption of air ions in the inlet cylinder.

Chapter III

PARAMETERS AND DESIGN PRINCIPLES OF ASPIRATION COUNTERS

§ 25. CLASSIFICATION OF COUNTER CIRCUIT ARRANGEMENTS

There are many ways in which the measuring capacitor, electrometer and voltage supply can be connected to the counter circuit. The principal circuit arrangement determines the different properties of the counter, and, consequently, the specific choice of a circuit is of great practical importance.

Below, we shall consider the circuit arrangements of integral counters only. However, all considered circuits are also feasible for differential counters.

To provide a basis for the circuit classification it is advisable to specify criteria determining the properties of the counter and to effect a subdivision of all circuits into several groups according to each criterion.

First, we shall subdivide the circuits into two groups, i.e., respectively corresponding to parallel and series connection of the electrometer into the circuits. In the parallel arrangement (Figure 25.1a) the entire voltage of the voltage supply is applied to the electrometer. The current through the collector plate is determined from the rate at which the voltage decreases at the electrometer. This arrangement was utilized in the well-known counter of Ebert/Ebert, 1901, 1905/. The high voltage supplied to the electrometer renders it necessary to use a coarse instrument of low sensitivity. In contemporary counters the series arrangement is used almost without exception (Figure 25.1b). Here it is possible to employ a sensitive electrometer and to carry out the measurements on the basis of the charge accumulation method as well as by the method of the voltage drop across a resistance connected in parallel to the electrometer. The series arrangement was implied in the first two chapters of the present work.

The parallel arrangement is usually referred to in the literature as the circuit based on the "discharge method," and the series arrangement – that based on the "charging method." However, these names are not always used consistently. In some cases the series arrangement was called the circuit based on the "discharge method" /Nolan, J.J., Nolan, P.J., 1935; Reinet, 1958, 1959a/.

The inconsistency in the terminology "charge method" and "discharge method" is partly due to the fact that these names do not describe the essential feature of the method and are, consequently, rather arbitrary. In fact, as charge accumulates, the measuring capacitor discharges in

both methods, and the electrometer in the series arrangement can be charged or discharged depending on the initial charge.

Sometimes the parallel arrangement is called the circuit with the low-sensitivity electrometer, and the series arrangement the circuit with the high-sensitivity electrometer.

Secondly, we shall subdivide all circuit arrangements into three groups depending on the ground connection. If the point c is grounded (Figure 25.1), we have a circuit with a grounded repulsive plate. In this circuit the edge effect causes an increase in the current through the collector plate. When grounding the point a, we obtain a circuit with a grounded collector plate. In this case the edge effect causes a decrease in the current through the collector plate. Grounding the circuit at point b gives a circuit arrangement with an intermediate grounded point, which is the most general arrangement and which includes the two preceding schemes as limiting cases /Tammet, 1962b/.

Sometimes the "charging method" and the "discharge method" are distinguished according to the choice of the ground connection, i.e., the first applies to the method of the grounded repulsive plate and the second to the method of the grounded collector plate.

Thirdly, the circuit arrangements are subdivided according to the geometry of the measuring capacitor. Here, there are also three principal variants: the cylindrical capacitor with an inner collector plate, the parallel-plate capacitor, and the cylindrical capacitor with an outer collector plate.

The classification scheme shows the classification of the circuit arrangements of counters.

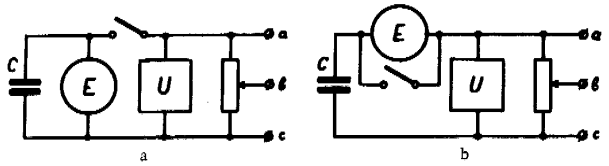

FIGURE 25.1. Principal circuit arrangements of a counter:

C – measuring capacitor; E – electrometer; U – voltage supply.

Of the 18 possible circuit arrangements, only the five indicated by lines in classification scheme 25.1 are applied in practice. Let us briefly consider these variants.

1. The parallel arrangement. Since only one variant of the parallel arrangement has practical application, there is no need to specify further the name. The usual name "discharge method" can be applied only to the parallel arrangement, although in the literature this is not always the case. The use of the parallel arrangement was described already in the first papers on the study of the electrical conductivity of air/Wiedemann, 1885; Elster, Geitel 1899/. The most widely known counters are those of Ebert/Ebert 1901, 1905; Lutz, 1909/ and Gerdien/ Gerdien, 1905a, 1905b/. In the parallel arrangement the instability of the voltage supply cannot affect the measuring result, since the voltage supply is turned off

during the charge accumulation cycle. However, because of the low sensitivity of the electrometer, this advantage has no practical value. Currently, the parallel arrangement is rarely used and is mainly of historical significance.

Classification scheme 25.1

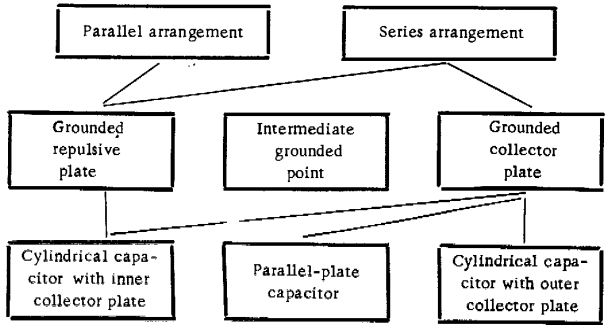

2. The series arrangement with a grounded outer plate. The inner plate is the collector plate. To prevent ambiguity, the classification according to the "discharge method" and "charging method" should not be used here. The series arrangement with the grounded outer plate was used already in the first aspiration counter /Thomson, J.J., Rutherford, 1896; McClelland, 1898; Rutherford, 1899/. Later, it gained wider application /Nordmann, 1904a, 1904b; Baranov, 1925; Israël, 1931; Nolan, J.J., Nolan, P.J., 1935; Weiss, Steinmauer, 1937; Schaffhauser, 1952; Gubichev 1955; Reinet, 1958, 1959a; Hock, Schmeer, 1962/. In some of the above works the series arrangement with the grounded outer plate was erroneously regarded as a new method. The series arrangement with a grounded outer plate readily enables the suppression of the edge effect and has been used over the last years.

3. The series arrangement with a grounded inner collector plate. This is usually called the arrangement based on the "method of charging." The series arrangement with the grounded inner collector plate is the most widespread. Among the first works in which this arrangement was described, we shall cite the following: /Zeleny, 1901; Kähler, 1903; Bloch, 1904; Becker, 1909; Lenard, Ramsauer, 1910; Swann, 1914c/. A disadvantage of this arrangement lies in the complications which result from the edge effect.

4. The series arrangement with a grounded outer collector plate enables us to suppress the edge effect. However, it is relatively seldom used /McClelland, Kennedy, 1912; Nolan, J.J., Nolan, P.J., 1930, 1931; Weger, 1935a; Israël, 1937; Siksna, 1961a/.

5. The parallel-plate measuring capacitor was used exclusively in the series arrangement with a grounded collector plate. The parallel-plate capacitor was employed in differential counters /Nolan, J.J., 1919; Erikson, 1921, 1922, 1924, 1929; Nolan, J.J., Harris, 1922; Chapman, 1937; Daniel, Brackett, 1951; Hewitt, 1957/. In integral counters the parallel-plate capacitor was seldom used /McClelland, Kennedy, 1912; Nolan, J.J., Boylan, Sachy, 1925; Beckett, 1961/.

Of some interest are also the series arrangement with a grounded repulsive plate in a parallel plate capacitor and the three variants of the series arrangement with an intermediate grounded point. The remaining nine possible variants of the principal circuit arrangements are of no practical significance whatever.

§ 26. CURRENT MEASUREMENT BY THE CHARGE ACCUMULATED IN A CAPACITOR

The current through the collector plate of an integral counter is usually of the order of $10^{-14}-10^{12}$ A. In differential counters one sometimes must record currents not exceeding $10^{-16}-10^{-15}$ A. Direct methods of current measurement via the magnetic field effects do not ensure the required sensitivity. Consequently, in aspiration counters indirect measurements are used which are based on the conversion of the measured current into voltage, which is then recorded by means of an electrometer. The circuit diagram for converting the current into voltage, when connecting the electrometer in series with the measuring capacitor, is shown in Figure 26.1. Let us combine the internal capacitance of the measuring capacitor, the electrometer capacitance and parasitic capacitances and denote this as the total capacitance C_0. In the same way the resistance R_0 includes all the leakage resistances in parallel with the electrometer.

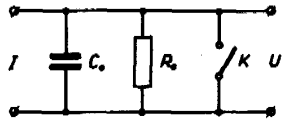

FIGURE 26.1. Circuit diagram for converting current into voltage.

Let the switch K be opened at time $t=0$. Assuming that the current I is constant, we shall represent the time dependence of the voltage by

$$U = IR_0\left[1-\exp\left(-\frac{t}{\tau}\right)\right], \qquad (26.1)$$

where $\tau = R_0C_0$ is the time constant. Of practical importance are only two segments of the function $U(t)$: the initial segment $t \ll \tau$, in which $U \approx \frac{I}{C_0}t$, and the steady-state segment $\tau \ll t$, in which $U \approx IR_0$. Correspondingly, the current measurement method based on the charge accumulated in a capacitor and the current measurement method via the voltage drop across a resistance are distinguished.

In the method of charge accumulation the resistance R_0 should be as large as possible. The largest value of R_0 is restricted by the leakage resistance R_p of the insulators. Since the current is calculated via

$$I = \frac{UC_0}{t}, \qquad (26.2)$$

the occurrence of the resistance R_p causes an error, the relative value of which in the first approximation is $t/2\tau$. If the electrometer is characterized by the limiting error ΔU in the voltage, then the limit of the relative error of current measurement is

$$\delta_I = \frac{t}{2R_pC_0} + \frac{C_0\Delta U}{It}. \tag{26.3}$$

Here it is assumed that the exact value of the capacitance C_0 is known.

The charge accumulation time t is chosen in such a way that the required measurement accuracy is achieved. The shorter of the two solutions of equation (26.3) is

$$t = R_pC_0\delta_I\left(1 - \sqrt{1 - \frac{2\Delta U}{IR_p\delta_I^2}}\right) = \\ = \frac{C_0\Delta U}{I\delta_I}\left[1 + \frac{1}{2}\left(\frac{\Delta U}{IR_p\delta_I^2}\right) + \frac{1}{2}\left(\frac{\Delta U}{IR_p\delta_I^2}\right)^2 + \ldots\ldots\right]. \tag{26.4}$$

A measurement with an error not larger than δ_I will be possible only under the condition

$$I \geqslant \frac{2\Delta U}{R_p\delta_I^2}. \tag{26.5}$$

Formula (26.5) determines the lower limit of current measurement for the given electrometer sensitivity.

In the limiting case $R_p \gg 2\Delta U/I\delta_I^2$, the charge accumulation time is given by

$$t = \frac{C_0\Delta U}{I\delta_I}, \tag{26.6}$$

and in the case $R_p = 2\Delta U/I\delta_I^2$

$$t = R_pC_0\delta_I = 2\frac{C_0\Delta U}{I\delta_I}. \tag{26.7}$$

The last formula determines the larges possible charge accumulation time for a given measurement accuracy.

The electrometer sensitivity depends largely on factors which are of a technical nature. There exists, however, a lower error limit, determined by thermal fluctuations. The determination of thermal fluctuations should be carried out separately for two measuring methods, i.e., for the fixed-zero and the zero-drift method.

In the method of the fixed zero only one electrometer reading is taken. The initial instant $t = 0$, $U = 0$ is taken as the instant at which the switch is opened. After opening the switch a residual charge will remain in the capacitance C_0, which is included in the measurement results. This is a serious disadvantage of the fixed-zero method. A proper switch design helps to decrease the charge generated by the contacts /Shulman, Shepsenvol, 1950; Polonnikov, 1960/, but the thermal noise level still remains the decisive factor for the limit of this charge. The variance of the thermal voltage jumps when opening the switch is simply

$$\sigma_U^2 = \frac{KT}{C_0}. \tag{26.8}$$

Since this quantity equals the variance of the steady random process of the R_pC_0 circuit, the voltage variance at $I = 0$ is determined by expression (26.8) independently of the time after the switch is opened.

Using expression (26.2), we obtain the mean-square error of the measured current

$$\sigma_I = \frac{\sqrt{KTC_0}}{t}. \tag{26.9}$$

In practical applications ($T = 288°K$) this formula becomes

$$\sigma_I(a) = \frac{6.3 \cdot 10^{-17}\sqrt{C_0(\text{nF})}}{t(\text{sec})} \tag{26.10}$$

In the zero-drift method two readings are taken: U_1 at the instant t' and U_2 at the instant $t + t'$ after opening the switch. The current is calculated from the ratio $I = C(U_2 - U_1)/t$. To determine the error we consider the case $I = 0$. The variance of the difference $U_2 - U_1$ is $\sigma^2_{U_2-U_1} = \sigma^2_{U_2} + \sigma^2_{U_1} - 2R_{1,2}\sigma_{U_1}\sigma_{U_2}$, where $R_{1,2}$ is the correlation coefficient between the voltages U_1 and U_2. For the thermal noise of the RC circuit /Lebedev, 1958/ we obtain

$$R_{1,2} = \exp\left(-\frac{t}{\tau}\right). \tag{26.11}$$

The variances $\sigma^2_{U_1}$ and $\sigma^2_{U_2}$ are expressed by formula (26.8). The mean-square error of the current measurement equals the ratio $C_0\sigma^2_{U_2-U_1}/t$. With the approximation $t \ll \tau$, calculation yields

$$\sigma_I = \sqrt{\frac{2KT}{R_pt}}. \tag{26.12}$$

For actual calculations ($T = 293°K$) this formula is written in the form

$$\sigma_I(a) = \frac{9 \cdot 10^{-17}}{\sqrt{R_p(\text{Tohm})t(\text{sec})}} \tag{26.13}$$

In the zero-drift method the voltage sensitivity of the electrometer depends on the charge accumulation time. The last term of expression (26.3) which is inversely proportional to time vanishes. We must therefore reassess some of the statements made at the beginning of the present section. Solving the problem of the minimum error δ_I, we obtain the charge accumulation time ensuring the greatest current sensitivity in the zero-drift method

$$t = \frac{2}{3}R_pC_0\delta_I. \tag{26.14}$$

The minimum value of the current measured at 99% confidence level with an error not greater than δ_I is

$$I_{min} \approx \frac{6}{R_p \delta_I^{1.5}} \sqrt{\frac{KT}{C_0}}. \qquad (26.15)$$

In practice ($T = 287°K$), the last formula has the form

$$I_{min}(a) \approx \frac{3.8 \cdot 10^{-13}}{R_p(\text{Tohm})\sqrt{C_0\,(\text{nF})}\ (100\,\delta_I)^{1.5}} \qquad (26.16)$$

The above expressions determine the theoretical limit of current measurement only when neglecting the correction for leakage. When this correction is included, it is possible to measure a weaker current. However, at present, even the limit defined by formula (26.15) is not reached in practice because of the occurrence of distorting factors of another origin, for example, the additional current generated by the insulators of the electrometer and the measuring capacitor.

A comparison of the thermal noise in the methods of the fixed and the drifting zero points to marked advantages of the latter. For example, under the conditions $C_0 = 100$ nF, $R_p = 10^{16}$ ohm, $t = 100$ sec, the mean-square error due to thermal fluctuations is $6.3 \cdot 10^{-18}$A for the fixed zero and $9 \cdot 10^{-20}$A for the drifting zero.

In some cases the pulse method is used /Schulman, Shepsenvol, 1950; Arabadzhi, Rudik, 1963/, which is sometimes called the integration method. In the pulse method the zero is fixed. The charge accumulates on the capacitance C_1, which is not connected to the electrometer. The variance of the accumulated charge under the operating conditions $I = 0$ is KTC_1. At the end of the cycle the capacitance C_1 is connected in parallel with the input RC circuit of the electrometer, which records the voltage pulse. If the input capacitance of the electrometer is C_2, then the variance of its fluctuating charge prior to connecting capacitance is KTC_2. The sum of the variances of the charges on C_1 and C_2 coincides with the variance of the steady-state process of the circuit after connecting the capacitance C_1 to the electrometer. Consequently, the variance of the measured current does not depend on the time during which a voltage reading is performed, provided this time is considerably smaller than the time constant of the electrometer input. The mean-square error is expressed by formula (26.9), assuming $C_0 = C_1 + C_2$.

The advantage of the pulse method is that the electrometer can be used with a relatively small input resistance without limiting the current sensitivity. The disadvantage lies in the necessity of choosing the charge accumulation time beforehand without knowing the value of the measured current. In other respects the pulse method is similar to the usual method of charge accumulation with a fixed zero.

§ 27. CURRENT MEASUREMENT BASED ON THE VOLTAGE DROP ACROSS A RESISTANCE

In this method the operating conditions correspond to $t \gg \tau$. The current is calculated from Ohm's law $I = U/R$. In order to ensure

measurement accuracy and to shorten the voltage stabilization time, a special shunt resistance R, considerably smaller than the leakage resistance R_p of the insulators, is inserted into the circuit.

In the preceding section we neglected the error in the determination of the capacitance C_0. With regard to the leakage resistance R this was unjustified. The stability and measurement accuracy of high resistances employed in counters are smaller than the stability and measurement accuracy of small capacitances by more than one order of magnitude. The relative error δ_R is included in the error of the measurement results. To simplify the error calculation, we shall introduce the special notation $\delta_I' = \delta_I - \delta_R$ for the error due to other causes. In the case at hand this error is given by

$$\delta_I' = \frac{\Delta U}{IR} + \exp\left(-\frac{t}{\tau}\right). \qquad (27.1)$$

The measurement can be performed if

$$I > \frac{\Delta U}{R\delta_I'}. \qquad (27.2)$$

The time lost for obtaining a reading is

$$t = \tau \ln \frac{1}{\delta_I' - \frac{\Delta U}{IR}}. \qquad (27.3)$$

It is advisable to select the resistance R in such a way that this time is minimized. Suppose that ΔU does not depend on the resistance R. The solution of the extremum problem $dt/dR = 0$ can be written in the form

$$R_{opt} = \frac{\Delta U}{I\delta_I'} f_{opt}(\delta_I'). \qquad (27.4)$$

$f_{opt}(\delta_I')$ cannot be expressed in terms of elementary functions. Some values found by numerical methods are listed in Table 27.1.

In the interval $2 \cdot 10^{-5} < \delta_I' < 0.45$ the function $f_{opt}(\delta_I')$ is approximated with an error less than 1% by the expression

$$f_{opt} \approx 1.180 + 0.79\ \delta_I' - \frac{0.00048}{0.005 + \delta_I'}. \qquad (27.5)$$

At optimum resistance and for the initial condition $U_{t=0} = 0$ the measurement time is

$$t = \frac{C_0 \Delta U}{I\delta_I'} \frac{f_{opt}(\delta_I')}{f_{opt}(\delta_I') - 1}. \qquad (27.6)$$

Comparing the above expression with formula (26.6), we can see that the measurement time in the method of the voltage drop across a resistance is at least $f_{opt}/(f_{opt} - 1)$ times larger than the measurement time in the method of charge accumulation. Several values of the function $f_{opt}/(f_{opt} - 1)$

are listed in Table 27.1. The above statement holds if $U_{t=0} = 0$. However, the stabilization time of a reading having the required accuracy exceeds the measurement time in the method of charge accumulation also in the case of a sudden change in the current.

TABLE 27.1

$\delta_I'(\%)$	t_{opt}	$\frac{t_{opt}}{t_{opt}-1}$	$\delta_I'(\%)$	t_{opt}	$\frac{t_{opt}}{t_{opt}-1}$	$\delta_I'(\%)$	t_{opt}	$\frac{t_{opt}}{t_{opt}-1}$
0	1	∞	0.3	1.13	9.0	5	1.21	5.8
0.001	1.07	15.2	0.5	1.14	8.4	10	1.26	4.9
0.005	1.08	13.5	1	1.15	7.6	20	1.34	4.0
0.02	1.09	12.0	1.5	1.16	7.2	30	1.41	3.4
0.1	1.11	10.2	2	1.17	6.9	40	1.49	3.0
0.2	1.12	9.4	3	1.19	6.3	50	1.60	2.7

In order to determine the limiting accuracy of the method of the voltage drop across a resistance, we shall consider the thermal fluctuations of the current. Let us suppose that the output signal of the electrometer is smoothed by an integrating RC circuit having a time constant τ_2. In the absence of such a circuit, we must set $\tau_2 = 0$. The insertion of the output smoothing circuit increases the inertia but at the same time decreases the effect of thermal fluctuations on the measurement result, which in certain cases may be advantageous. The mean-square fluctuation of the recorded current, derived from the signal fed into the electrometer, is given by

$$\sigma_I = \sqrt{\frac{KTC_0}{\tau_1(\tau_1+\tau_2)}}, \tag{27.7}$$

where τ_1 is the time constant of the input circuit. In practice, this formula takes on the following form ($T = 288°K$):

$$\sigma_I(a) = 6.3 \cdot 10^{-17} \sqrt{\frac{C_0(\text{nF})}{\tau_1(\text{sec})\,[\tau_1(\text{sec}) + \tau_2(\text{sec})]}} \tag{27.8}$$

A comparison of formulas (27.8), (26.9) and (26.12) shows that the sensitivity limit of the method of the voltage drop across a resistance is of the same order of magnitude as the sensitivity limit of the method of charge accumulation with a fixed zero but is lower than the sensitivity of the zero-drift method.

When using the output of the integrating circuit, the problem of selecting the optimum ratio of the time constants τ_1 and τ_2 arises. This problem

should be solved in such a way that for a given thermal noise level σ_I a minimum stabilization time of the reading can be achieved with an error δ. The error is determined from the equation of the transient process

$$\left.\begin{aligned} \delta &= \frac{\tau_1}{\tau_1-\tau_2}\exp\left(-\frac{t}{\tau_1}\right) - \frac{\tau_2}{\tau_1-\tau_2}\exp\left(-\frac{t}{\tau_2}\right);\ \tau_1 \neq \tau_2 \\ \delta &= \left(1+\frac{t}{\tau_1}\right)\exp\left(-\frac{t}{\tau_1}\right);\ \tau_1 = \tau_2 \end{aligned}\right\}. \tag{27.9}$$

The problem of determining the optimum operation conditions reduces to finding the minimum of the function

$$\delta(\alpha) = \frac{(1-\alpha)\exp\left(-\frac{\vartheta}{\sqrt{1-\alpha}}\right) - \alpha\exp\left(\frac{\vartheta\sqrt{1-\alpha}}{\alpha}\right)}{1-2\alpha}, \tag{27.10}$$

where

$$\alpha = \frac{\tau_2}{\tau_1+\tau_2} \tag{27.11}$$

and

$$\vartheta = \frac{\sigma_I}{\sqrt{KTC_0}}\ t. \tag{27.12}$$

The optimum value of the parameter α is determined by a numerical solution of the corresponding equation. Some results obtained in these calculations are listed in Table 27.2.

TABLE 27.2

δ	α_{opt}	$\vartheta_{\alpha=\alpha_{opt}}$	$(\Delta\vartheta/\vartheta)_{\alpha=0}$	$(\Delta\vartheta/\vartheta)_{\alpha=0.5}$
0.02%	40%	7.5	14%	5%
0.13%	37%	6.0	11%	7%
0.43%	34%	5.0	9%	8%
1.2 %	30%	4.2	6%	10%
2.8 %	25%	3.4	4%	12%
4.7 %	20%	3.0	2%	15%
9.3 %	10%	2.4	0.5%	19%
13.5 %	0%	2	0%	24%

The table also gives the relative increase in the current stabilization time as compared with the optimum operating conditions at $\alpha = 0$ and $\alpha = 0.5$.

Despite the inertia and the lower sensitivity, the method of measuring the voltage drop across a resistance is often more convenient than that of charge accumulation. This is explained by the fact that in the former case, simple, continuous current recorders can be used. In the

method of charge accumulation an intricate commutation device is required for automatic current recording. The method of charge accumulation with a drifting zero is preferable if a particularly high accuracy or sensitivity is desired. Another advantage of the method of charge accumulation still remains to be pointed out. Commutation of the input circuit ensures in each cycle automatic compensation of the zero drift of the electrometer. In the method of the voltage drop across a resistance the zero drift is very troublesome, so that more stringent requirements must be imposed on the electrometer.

§ 28. SENSITIVITY OF THE INTEGRAL COUNTER

The often used determination of the sensitivity of the measuring instrument as well as the number of scale divisions in a measurement unit is not fully satisfactory. To render this determination more precise one should, in addition, indicate the ratio of a scale division to the possible errors in the measurement result. In essence, the sensitivity of an instrument is uniquely determined by the distribution of measurement errors for small values of the measured quantity. Here, we shall characterize the sensitivity by means of the standard deviation σ_x of the measurement result when the value of the measured quantity x is zero. The term "sensitivity" is taken to mean the ratio of a unit of the measured quantity σ_x or some other quantity which increases with decreasing σ_x. There is no need for a quantitative determination of the sensitivity.

Measurement errors in the absence of air ions are due to several factors:

1) errors in the electrometer readings (instrument error);
2) induced current when measuring the voltage or the capacitance of the measuring capacitor;
3) current noise due to the properties of the insulators.

The errors in the electrometer readings are due to thermal fluctuations and imperfection of the electrometer. The thermal fluctuations of the current were considered in the preceding sections. The imperfection of the electrometer causes an additional error in the voltage, the standard deviation of which will be denoted by σ_{UE}. The latter is a function of time. However, in practical calculations it can be assumed, for simplicity, to be constant.

In the method of charge accumulation with a fixed zero we must, in addition, allow for charges of nonthermal origin, which arise when the contacts are disconnected. The variance of this charge σ_{Qk}^2 is determined by the design of the switch and by internal disturbances.

The variation of the voltage applied to the measuring capacitor induces a current producing a distorting effect /Weger, 1935b/. The same applies to the instability of the capacitance of the measuring capacitor. If the plates of a parallel-plate capacitor are not perfectly parallel, a relative change in the capacitance

$$\delta_C = \frac{\Delta d}{d} \tag{28.1}$$

is induced, where Δd is the variation in the interplate distance. When one of the axes of a cylindrical capacitor is displaced by dr, we obtain

$$\delta_C \approx \frac{2\Delta\, r dr + (dr)^2}{(r_2^2 - r_1^2)\ln\frac{r_2}{r_1}}, \tag{28.2}$$

where Δr is the initial separation between the axes. From expression (28.2) it follows that the stability of the capacitance of a cylindrical capacitor depends strongly on the accuracy of centering the cylindrical plates.

A distorting induced current is also caused by a random variation in the dielectric constant of the air flowing through the measuring capacitor. The induced current is generated also by the rapid drift in the contact potential between the plates of the measuring capacitor. The last two factors are of second-order significance and will not be considered in the following discussion.

The effect of random variations in the supply voltage can be partly compensated by means of special connections. It is therefore useful to introduce the concept of the equivalent fluctuation voltage, which in compensated circuits is correspondingly smaller than the fluctuating component of the voltage supply. When determining the equivalent fluctuation voltage it is advisable to allow simultaneously for the random variations in the capacitance of the measuring capacitor, since relative variations in the capacitance are equivalent in their effect to equal relative variations in the voltage applied to the measuring capacitor.

In the method of charge accumulation the variance of the mean induced current per cycle is

$$\sigma_{IU}^2 = \frac{C^2 U^2 s_{\Delta UC}^2(t)}{t^2}, \tag{28.3}$$

where C is the effective capacitance of the measuring capacitor and $U^2 s_{\Delta UC}^2(t)$ is the variance of the changes in the equivalent fluctuation voltage during time t. The relative variance $s_{\Delta UC}^2(t)$ can be expressed in the form

$$s_{\Delta UC}^2(t) = 2s_{UC}^2[1 - R_{UC}(t)], \tag{28.4}$$

where s_{UC}^2 is the variance of the ratio of the equivalent fluctuating voltage to the mean voltage of the measuring capacitor, and $R_{UC}(t)$ is the correlation coefficient between the equivalent fluctuation voltages at the initial and final instant of the cycle.

The capacitance C_p attenuates the variations in the voltage by a factor of $C/(C + C_p)$ and increases the capacitance of the differentiating circuit. Taking into account the above information, we obtain the expression for the variance of the induced current in the method of the voltage drop across a resistance

$$\sigma_{IU}^2 = \frac{C^2 U^2 s_{\tau UC}^2(\tau)}{\tau^2}, \tag{28.5}$$

where $\tau = RC_0$.

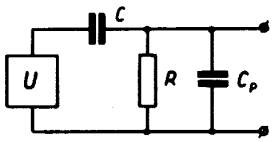

FIGURE 28.1. Circuit arrangement for transferring the fluctuation voltage.

The dependence of $s^2_{\tau UC}(\tau)$ on the correlation function of the fluctuation voltage is very involved. If the effective fluctuation voltage is differentiated with respect to time, then within the limits of small τ and t the induced current is calculated from $I_i = C\frac{dU}{dt}$ and then $s^2_{\tau UC}(t) = s^2_{\Delta UC}(t)$. Within the limits of large values of the time we have $s^2_{\tau UC}(t) = s^2_{UC} = \frac{1}{2} s^2_{\Delta UC}(t)$. In both limiting cases the expression

$$2s^2_{\tau UC}\left(\frac{t}{\sqrt{2}}\right) = s^2_{\Delta UC}(t) \tag{28.6}$$

is valid and can be used for a rough estimation of the ratio of $s_{\tau UC}$ and $s_{\Delta UC}$.

The stability of different voltage sources can be studied experimentally with the aid of the circuit shown in Figure 28.2. The capacitance C must be stable and can have a sufficiently large value, which facilitates the measurements. The additional $R_1C_1 \gg \tau$ circuit is intended to eliminate errors connected with the leakage of the capacitor C. $s_{\tau U}(\tau)$ is determined by the ratio of the instrument reading U_I and the voltage U.

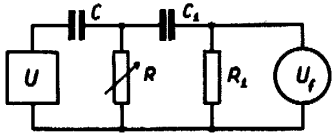

FIGURE 28.2. Circuit arrangement for the determination of $s_{\tau U}(RC)$:

U – voltage source to be investigated;
U_I – instrument for measuring the ultra-low frequency voltage.

The current disturbance generated by the insulators is practically independent of the operating conditions of the measuring capacitor. Experiment shows that this current is inversely proportional to the resistance R_p of the insulators. We shall therefore denote the variance of the insulator current by σ^2_{UR}/R^2_p. The quantity σ_{Up} is usually of the order of a tenth of a volt. During short time intervals the insulator current is so strongly correlated that it may be assumed to be constant.

Leakage through the insulator between the plates will be ignored, since this leakage is fully averted when the insulator is properly designed. Similarly, the errors due to the retarded polarization of the insulators after voltage commutation can be completely eliminated.

When determining the sensitivity one should use as the measured value either the conditional charge density $P = I/\Phi$ or the conditional conductivity $\Lambda = I/4\pi CU$. The variance of the conditional charge density is

$$\sigma^2_P = \frac{\sigma^2_I}{(4\pi k_0 CU)^2}. \tag{28.7}$$

The variance of the conditional conductivity is

$$\sigma^2_\Lambda = k^2_0 \sigma^2_P. \tag{28.8}$$

In order to determine σ^2_I we take the sum of the variance of all the above-considered current disturbances. The following results are obtained.

1. Method of charge accumulation with a fixed zero and the pulse method:

$$\sigma^2_P = \frac{1}{(4\pi k_0 t)^2}\left[s^2_{\Delta UC}(t) + \frac{\sigma^2_{QK} + C^2_0\sigma^2_{UE} + KTC_0}{C^2U^2} + \frac{\sigma^2_{UR}t^2}{C^2U^2R^2_p}\right]. \tag{28.9}$$

2. Method of charge accumulation with a drifting zero:

$$\sigma^2_P = \frac{1}{(4\pi k_0 t)^2}\left[s^2_{\Delta UC}(t) + \frac{C^2_0\sigma^2_{UE}}{C^2U^2} + \frac{2KTt}{C^2U^2R_p} + \frac{\sigma^2_{UR}t^2}{C^2U^2R^2_p}\right]. \tag{28.10}$$

3. Method of the voltage drop across a resistance:

$$\sigma^2_P = \frac{1}{(4\pi k_0 t)^2}\left[s^2_{\tau UC}(\tau) + \frac{C^2_0\sigma^2_{UE} + KTC_0}{C^2U^2} + \frac{\sigma^2_{UR}t^2}{C^2U^2R^2_p}\right]. \tag{28.11}$$

Under certain conditions the above expressions can often be simplified by neglecting one of the terms.

For the condition $t \approx \tau$ formulas (28.10) and (28.11) yield sensitivity values close to one another, since the thermal noise is usually overlapped by the remaining disturbances.

§ 29. CALCULATION OF AIR-ION SPECTRAL CHARACTERISTICS

The partial charge densities, partial conductivities and the spectrum $\varrho(k)$ can be determined from direct measurement only by means of the appropriate calculations. In most of the formulas given in the first chapter, not only air-ion current values are encountered, but also the derivatives of the current with respect to one of operation parameters. This complicates the evaluation of the observations, since the usual measurement methods do not enable us to obtain the continuous function $I(\psi)$, but only a number of isolated points $I(\psi_1), I(\psi_2), \ldots\ldots, I(\psi_n)$.

The graphical methods for determining the quantities expressed in terms of the operator h_ψ were briefly described in § 4. The derivative of the current with respect to ψ can be determined from the curve $I(\psi)$. More detailed information on the graphical method can be found in the literature /Gerasimova, 1939; Imyanitov, 1957; Israël, 1957b/. Complications arise if the curve $I(\psi)$ is to be plotted for the discrete points $I(\psi_n)$ It is somewhat arbitrary to plot a smooth curve. Israël /Israël, 1957b/ pointed out this problem by the question "break point or bend?" To obtain reliable results, the limits of arbitrariness introduced by the evaluation of the observations should be precisely determined. In graphical methods this is quite difficult, as can be seen from the treatment of the nature of the spectrum of heavy air ions in the works /Nolan, J.J., 1916; Blackwood, 1920; Nolan, P.J., 1921; Nolan, J.J., 1923; Nolan, J.J., Sachy, 1927; Boylan, 1931/, and, more recently, /Fuks, 1955; El Nadi, Farag, 1960, 1961/.

The graphical method is inconvenient if the mobility range is large. In practice, one often has to evaluate data on the spectrum of air ions with extreme mobilities with a ratio of 10,000 or more, while on one graph it is difficult to represent a spectrum with a width larger than one order of magnitude. The attempt to give up the linear scale when plotting curves proved unsuccessful, and the ill-considered use of a logarithmic mobility scale /Hoegl, 1963b/ led only to errors.

Interesting ideas on the use of a logarithmic scale may be found in the work /Aoki, Kato, 1954/. However, these ideas still did not enable us to find a method which was less time consuming.

The evaluation of the observations may also be carried out by numerical methods, which were applied in the determination of the partial charge density of light ions /Baranov, 1925; Baranov, Stschepotjewa, 1928; Shchepotieva, 1929/, and recently in the evaluation of spectrum measurements /Hoppel, Kraakevik, 1965/.

The main advantage of numerical methods is that they enable us to estimate the errors in the measurement results, and to determine accurately the uncertainty limits which arise due to the fact that the function $I(\psi)$ is given by a series of points. There are also no difficulties in the case of a large mobility interval. In numerical methods the derivatives are determined from formulas of finite increments. The use of interpolation methods would be unjustified, since nothing besides continuity can be assumed concerning the behavior of the function $\varrho(k)$ /Tammet, 1962d/. Physical considerations also give reason to assume the continuity of the function $I(\psi)$ and its derivatives. Let us stipulate that the points I_n are chosen in a monotonic sequence. If ψ is the voltage, then we shall consider ψ_n with one polarity only. Under these assumptions the following assertions are valid /Tammet, 1962d/:

a) in the interval (ψ_1, ψ_2) there always exists a $\psi = \xi_1$, such that

$$\frac{\partial I(\xi_1)}{\partial \psi} = \frac{I_2 - I_1}{\psi_2 - \psi_1} \tag{29.1}$$

(Lagrange formula);

b) in the interval (ψ_1, ψ_2) there always exists a $\psi = \xi_2$, such that

$$h_\psi I(\xi_2) = \frac{\psi_2 I_1 - \psi_1 I_2}{\psi_2 - \psi_1}; \tag{29.2}$$

c) in the interval (ψ_1, ψ_2) there always exists a $\psi = \xi_3$, such that

$$\xi_3 h_\psi I(\xi_3) = 2\psi_1\psi_2 \frac{\psi_2 I_1 - \psi_1 I_2}{\psi_2^2 - \psi_1^2}; \tag{29.3}$$

d) in the interval (ψ_1, ψ_2) there always exists a $\psi = \xi_4$, and in the interval (ψ_3, ψ_4) a $\psi = \xi_5$, such that

$$\frac{\frac{\partial I(\xi_4)}{\partial \psi} - \frac{\partial I(\xi_5)}{\partial \psi}}{h_\psi I(\xi_4) - h_\psi I(\xi_5)} = \frac{(\psi_4 - \psi_3)(I_2 - I_1) - (\psi_2 - \psi_1)(I_4 - I_3)}{(\psi_4 - \psi_3)(\psi_2 I_1 - \psi_1 I_2) - (\psi_2 - \psi_1)(\psi_4 I_3 - \psi_3 I_4)}; \tag{29.4}$$

e) if ψ_2 is contained in the interval (ψ_1, ψ_3), then this interval contains a $\psi = \xi_6$, such that

$$\xi_6^3 \frac{\partial^2 I(\xi_6)}{\partial \psi^2} = 2\psi_1\psi_2\psi_3 \frac{(\psi_3 - \psi_2) I_1 - (\psi_3 - \psi_1) I_2 + (\psi_2 - \psi_1) I_3}{(\psi_3 - \psi_2)(\psi_3 - \psi_1)(\psi_2 - \psi_1)}. \tag{29.5}$$

With the aid of formulas (29.1) – (29.5) we can calculate all the characteristics, which in the first chapter were expressed in terms of the derivatives of the functions $I(\psi)$ or $P(\psi)$. Formula (29.4) also makes it possible to calculate the mean mobility

$$\bar{k}(k_1, k_2) = \frac{\int_{k_1}^{k_2} k\varrho(k)\,dk}{\int_{k_1}^{k_2} \varrho(k)\,dk} = \frac{\lambda(k_1, k_2)}{\varrho(k_1, k_2)}. \tag{29.6}$$

Below calculation formulas are given for the integral counter and the first-order differential counter in the case of the voltage variation method. The uncertainty of the argument in the formulas of finite differences is interpreted as the error in the measured mobilities. The mobility determined only on the basis of the interval will be denoted by k. The mean mobility of the interval will be denoted by $\bar{k}$ and the maximum relative error corresponding to the uncertainty limits δ_k.

a) The integral counter; calculation of partial charge densities, charge mobilities, and mean mobilities. The voltages U_n are chosen in increasing order: $U_1 < U_2 < U_3 < U_4$.

$$\varrho(\tilde{k}_2, \tilde{k}_1) = \frac{(U_2 - U_1)(U_4 P_3 - U_3 P_4) - (U_4 - U_3)(U_2 P_1 - U_1 P_2)}{(U_2 - U_1)(U_4 - U_3)}, \tag{29.7}$$

$$\lambda(\tilde{k}_2, \tilde{k}_1) = \frac{\Phi[(U_4 - U_3)(P_2 - P_1) - (U_2 - U_1)(P_4 - P_3)]}{4\pi C(U_4 - U_3)(U_2 - U_1)}, \tag{29.8}$$

$$\bar{k}(\tilde{k}_2, \tilde{k}_1) = \frac{\Phi[(U_4 - U_3)(P_2 - P_1) - (U_2 - U_1)(P_4 - P_3)]}{4\pi C[(U_2 - U_1)(U_4P_3 - U_3P_4) - (U_4 - U_3)(U_2P_1 - U_1P_2)]}, \quad (29.9)$$

$$\bar{k}_2 = \frac{\Phi(U_3 + U_4)}{8\pi CU_3U_4}, \quad (29.10)$$

$$\bar{k}_1 = \frac{\Phi(U_1 + U_2)}{8\pi CU_1U_2}, \quad (29.11)$$

$$\delta_{k_2} = \frac{U_4 - U_3}{U_4 + U_3}, \quad (29.12)$$

$$\delta_{k_1} = \frac{U_2 - U_1}{U_2 + U_1}. \quad (29.13)$$

b) The integral counter; calculation of the spectrum $\varrho(k)$. We assume that the condition $U_1 < U_2 < U_3$ is satisfied.

$$\varrho(\tilde{k}) = \frac{8\pi CU_1U_2U_3[(U_3 - U_1)P_2 - (U_3 - U_2)P_1 - (U_2 - U_1)P_3]}{\Phi(U_3 - U_1)(U_3 - U_2)(U_2 - U_1)}, \quad (29.14)$$

$$\bar{k} = \frac{\Phi(U_1 + U_3)}{8\pi CU_1U_3}. \quad (29.15)$$

$$\delta_k = \frac{U_3 - U_1}{U_3 + U_1}. \quad (29.16)$$

In order to obtain the most uniform information for all the investigated mobility intervals and to simplify calculations it is advisable to choose, when possible, the points U_n in a well-defined order. To calculate $\varrho(k_1, k_2)$, $\lambda(k_1, k_2)$ and $\bar{k}(k_1, k_2)$, the U_n should be chosen in pairs, which enable a more distinct determination of the limits of the interval $(\bar{k}_1, \bar{k}_2)$. Here, the ratio U_{n+1}/U_n has for all even numbers one value and for all odd numbers a different value. The smaller of the two ratios determines the error in the mobility, and their product the width of the interval (k_2, k_1). To determine the spectrum $\varrho(k)$ it is expedient to choose U_n with a constant ratio U_{n+1}/U_n. The values of $\varrho(k)$ are calculated on the basis of each three successive U_n, which in the case of m points of the function $P(U)$ always gives $m-2$ points of the function $\varrho(k)$. The relevant calculation formulas are:

a) Choosing

$$\frac{U_4}{U_3} = \frac{U_3}{U_1} = \alpha \quad (29.17)$$

and

$$\frac{U_4}{U_2} = \frac{U_3}{U_1} = \beta, \quad (29.18)$$

we obtain

$$\varrho(\tilde{k}_2, \tilde{k}_1) = \frac{\alpha(P_3 - P_1) - (P_4 - P_2)}{\alpha - 1}, \quad (29.19)$$

$$\lambda(\tilde{k}_2, \tilde{k}_1) = \frac{\Phi[\beta(P_2 - P_1) - (P_4 - P_3)]}{4\pi CU_3(\alpha - 1)}, \quad (29.20)$$

$$\bar{k}(\tilde{k}_2, \tilde{k}_1) = \frac{\Phi}{4\pi CU_3} \frac{\beta(P_2 - P_1) - (P_4 - P_3)}{\alpha(P_3 - P_1) - (P_4 - P_2)}, \quad (29.21)$$

$$\bar{k}_2 = \frac{\Phi(1 + \alpha)}{8\pi CU_4}, \quad (29.22)$$

$$\bar{k}_1 = \frac{\Phi(1 + \alpha)}{8\pi CU_2}, \quad (29.23)$$

$$\delta_{k_2} = \delta_{k_1} = \frac{\alpha - 1}{\alpha + 1}. \quad (29.24)$$

b) Choosing U_1, U_2 and U_3, such that

$$\frac{U_{n+1}}{U_n} = 1 + \delta, \quad (29.25)$$

we obtain

$$\varrho(\tilde{k}) = \frac{4\pi CU_3}{\Phi\delta^2}\left[(2P_2 - P_1 - P_3) + \frac{\delta}{2 + \delta}(P_3 - P_1)\right], \quad (29.26)$$

$$\bar{k} = \frac{\Phi\left(1 + \delta + \frac{1}{1 + \delta}\right)}{8\pi CU_2} \approx \frac{\Phi}{4\pi CU_2}, \quad (29.27)$$

$$\delta_k = \frac{(1 + \delta)^2 - 1}{(1 + \delta)^2 + 1} \approx \delta. \quad (29.28)$$

c) The first-order differential counter with a divided capacitor. $U_2/U_1 = \alpha > 1$.

$$\varrho(\tilde{k}_a, \tilde{k}_b) = \frac{\alpha I_1 - I_2}{(\alpha - 1)\Phi}, \quad (29.29)$$

$$\bar{k}_a = \frac{(\alpha + 1)\Phi}{8\pi(C_1 + C_2)U_2}, \quad (29.30)$$

$$\bar{k}_b = \frac{(\alpha + 1)\Phi}{8\pi C_1U_2}, \quad (29.31)$$

$$\delta_{k_a} = \delta_{k_b} = \frac{\alpha - 1}{\alpha + 1}, \quad (29.32)$$

$$\varrho(k) = \frac{8\pi C_1(C_1 + C_2)U_2}{C_2\Phi^2} \frac{\alpha I_1 - I_2}{\alpha^2 - 1}, \quad (29.33)$$

where

$$k = \frac{(\alpha C_1 + C_1 + \alpha C_2)\Phi}{8\pi U_2C_1(C_1 + C_2)}, \quad (29.34)$$

$$\delta_k = \frac{\alpha(C_1 + C_2) - C_1}{\alpha(C_1 + C_2) + C_1}. \qquad (29.35)$$

When laying out the measurement program, it should be kept in mind, that the errors in the measurement result increase when increasing the accuracy in the mobility determinations by decreasing the constants α and δ. The problem of determining the measurement error will be considered in the following sections. When studying atmospheric ionization with the aid of an integral counter of average sensitivity and accuracy /Reinet, 1956/, the ratios $\alpha = 2$ and $\beta = 5$ are the most suitable. In accordance with the recommendation of the present author such ratios were used in multiannual observations of atmospheric ionization, carried out in Tartu by P. K. Prüller /Prüller, Reinet, 1966/. The evaluation of the observation data was carried out according to formulas (29.19) and (29.21) with the aid of a small desk calculator.

The question of the amount of work necessary to evaluate the observation data should be solved separately for each case with allowance for the actual conditions. One should also consider the possibility of programming the data on a computer, which can considerably increase the efficiency of the computation method. In some cases a graphical method and in other cases a numerical method may appear more convenient. As an example, a comparison of graphical and numerical methods was carried out for the calculation of partial charge densities in an integral counter. The series of limiting mobilities was as follows: 1; 0.5; 0.1; 0.05; 0.01; 0.005; 0.001; 0.0005; 0.0001; 0.00005 $(\frac{cm^2}{V \cdot sec})$. The partial charge densities were calculated in five ranges $\varrho[(0.75 \pm 0.25)\frac{cm^2}{V \cdot sec}, \infty]$, $\varrho[(0.075 \pm 0.025)\frac{cm^2}{V \cdot sec}$, $(0.75 \pm \pm 0.25)\frac{cm^2}{V \cdot sec}]$, etc. The computations were performed by a laboratory assistant, who had no previous experience in the evaluation of observation data by either method. In the numerical method a VMP-2 calculator was employed. To get used to both methods a full working day was spent on each of them. A time check of the control tasks showed that the evaluation of the observation data by means of the graphical method took 2.5 times as long as the evaluation of the same amount of data by the numerical method.

§ 30. ASSESSMENT OF RANDOM ERRORS IN MEASURING THE CHARACTERISTICS OF THE AIR-ION SPECTRUM

Errors in the characteristics of the air-ion spectrum are larger than the errors produced when measuring the conditional charge density. Not only are the direct observation errors significant, but also the instability of the air-ion spectrum during the measurement period. The last factor is irrelevant when the points $I(k_n)$ are taken simultaneously.

The demands imposed upon the accuracy of the error determination are not too high, so that certain simplifying assumptions can be made. Suppose that the parameters of the measuring capacitor are exactly known. If necessary, the omitted error can be separately estimated and added to the result.

Consider the error determination for integral counters. The variance of the errors of the measured quantity x is composed of two terms $\sigma_x^2 = \sigma_I^2 + \sigma_\varrho^2$, where σ_I characterizes the instrument error, and σ_ϱ the error due to fluctuations of the air-ion spectrum with time. To estimate σ_I we assume that the air-ion spectrum is stable. Errors inherent in the instruments are practically independent of one another. Neglecting systematic errors, we can estimate the error in the conditional charge density from formulas (28.9 – 28.11). Assume, for simplicity, that all the P_n appearing in one formula are equal to one another and are denoted by $\bar{P}$. With these assumptions the calculation of the variance σ_I^2 is simple when evaluating the observation data according to formulas (29.19), (29.20) and (29.26).

The fluctuation of the air-ion spectrum with time has the result that the series of successive measurement values $P_1, P_2, \ldots, P_n, \ldots$ do not represent the function $P(U_n)$ for any definite time interval. When estimating σ_ϱ, we assume that the ratio α appearing in formula (29.19) is close to unity. This enables us to estimate the variance of the fluctuations of the differences $\alpha P_1 - P_2$ and $\alpha P_3 - P_4$ from the variances of the differences $P_n - P_{n+1}$, where P_n and P_{n+1} corresponds to the same limiting mobility. Let us adopt the notation $s_\Delta = \sigma_{(P_n - P_{n+1})}/\bar{P}$. To determine s_Δ special supplementary measurements must be performed in which the same time conditions are observed as in the main observation series.

In the same way the variance of the fluctuations of the differences $2P_2 - P_1 - P_3$ appearing in formula (29.26) can be estimated. The corresponding relative standard deviation will be denoted by $s_{\Delta\Delta} = \sigma_{(2P_n - P_{n-1} - P_{n+1})}/\bar{P}$.

Owing to the above simplifications, the formulas for estimating the errors can be written in a simple form, which is convenient for practical calculations. Evaluating the observation data according to formulas (29.19) and (29.20), we obtain

$$\sigma_{\varrho(\bar{k}_1,\ \bar{k}_2)} \approx \frac{\sqrt{2(\sigma_P^2 + \alpha^2\sigma_P^2 + \bar{P}^2 s_\Delta^2)}}{\alpha - 1}, \qquad (30.1)$$

$$\sigma_{\lambda(\bar{k}_1,\ \bar{k}_2)} \approx \frac{k_2\sqrt{(1+\beta^2)(2\sigma_P^2 + \bar{P}^2 s_\Delta^2)}}{\alpha - 1}. \qquad (30.2)$$

Here, we make the additional assumption that the errors in the differences $P_2 - P_1$ and $P_4 - P_3$ are independent of one another and have equal variances. $\bar{P}$ is some mean value of the relative charge densities P_1, P_2, P_3, P_4.

For the evaluation of the observation data according to formula (29.26), assuming that the parameter δ is small, we obtain

$$\sigma_{\varrho(\bar{k})} \approx \frac{\sqrt{6\sigma_P^2 + P_2^2 s_{\Delta\Delta}^2}}{\bar{k}\delta^2}. \qquad (30.3)$$

In first-order differential counters the calculation is similar in all respects. In the differential methods of the second order the estimation of errors is the most simple, since the quantity to be determined is found from the result of one measurement, and, consequently, the fluctuating component of the error drops out.

In practice, the integral method is most often used. Here, the fluctuation of the relative charge intensity is the principal factor determining the measurement accuracy. Random oscillations of the current through the collector plates of the counter were treated in a large number of works /Shepherd, 1932; Baranov, Kravchenko, 1934; Shaffhauser, 1952; Schilling, Carson, 1953; Dessauer, Graffunder, Laub, 1955–1956; Sagalyn, Faucher, 1956, 1957; Siksna, Lindsay, 1961; Siksna, Eichmeier, 1961; Siksna, Schmeer, 1961; Prüller, Reinet, 1966/. However, the authors of these works confined themselves only to citing examples of recordings of the conditional charge density and devoted most of their attention to analyzing the underlying causes of the fluctuations, while leaving the problem of quantitative laws untouched. Only in the work /Collin, Groom, Higazi, 1966/ are quantitative data presented which characterize the relaxation of the autocorrelation function.

To obtain quantitative data on the fluctuations of the conditional charge density of atmospheric air, observations were carried out with the aid of a high-speed counter specially designed for this purpose. This counter was connected in accordance with the circuit arrangement with a grounded inner plate. The parameters and operating conditions of the measuring capacitor are determined by the following parameters: $r_2 = 14$ cm, $r_1 = 2.3$ cm, $l = 45$ cm, $\Phi = 1.5$ m^3/sec, $U = 2$ kV, $k_+ = 5$ cm^2/V·sec. The voltage supply consisted of a stabilized VS-22 rectifier with an additional integrating RC filter ($R = 2$ Mohm, $C = 100\ \mu$F). The absence of disturbances due to random voltage oscillations was established by measurement with the air flow switched on. The filling time $t_0 = 0.02$ sec of the measuring capacitor allows us to assume that the effect of fluctuations of the space charge density on the measurement results is negligibly small. This was verified by special measurements for the operating conditions $U = 0$. The current through the inner plate of the measuring capacitor was measured by the method of the voltage drop across a resistance. A high-speed dynamic electrometer was used. The time constant of the transient process was $\tau = 0.4$ sec. Recording was performed with the aid of the EPP-09M2 electronic potentiometer with a full-scale deflection time of 1 sec. In the experiments, the data of which are given below, the chart speed was 1.33 mm/sec.

The counter was installed in a cabin located not far from Tartu, which is located in the territory of the actinometric station of the Institute of Physics and Astronomy of the AN ESSR. During the experiments wind blew over flat terrain stretching approximately half a kilometer from the cabin. The city was located on the lee side.

The air was sampled at a height of 5 m and was led into the counter through a vertical, wooden channel with a square cross section and a length of 2.6 m. The width of the channel narrowed down from 60 cm at the upper end to 45 cm at the counter inlet. The air was exhausted on the lee side at a distance of 12 m from the counter.

The measurements were performed on July 26 and August 1 and 2, 1963 The positive conductivity was the object of measurement. The trend of the recording was practically independent of the polarity. For a detailed evaluation data of two measurement periods were considered. In the first measurement period – from 19 to 21 hours (local solar time) on August 1 – the intensity of the fluctuations was nearly maximum. The meteorological conditions were as follows: cloudless sky; westerly wind, 2–2.5 m/sec (at a height of 8 m); air temperature at a height of 2 m about 25°C; surface temperature of the soil approximately the same; relative humidity about 50%; pressure 761 mm Hg. During the second measurement interval – from 1 to 2 hours on August 2 – the intensity of the fluctuations was minimum. The meteorological data were: cloudless sky; westerly and southwesterly wind, 2.5–3 m/sec; air temperature at a height of 2 m about 18°C; soil temperature 14°C; relative humidity about 80%; pressure 761 mm Hg. The low intensity of the fluctuations of the conductivity under these conditions was due to a sharp temperature inversion, which led to a decrease in the intensity of the turbulence mixing of the near-ground air layer. The mean conductivity during the second measurement period was two times smaller than during the first period.

The theory of the fluctuation of the air-ion concentration in the atmosphere has not yet been developed. It can be assumed that turbulent mixing /Csanady, 1967/ is the main cause of rapid fluctuations. The initial nonuniformity of the concentration can be explained in terms of the electrode effect.

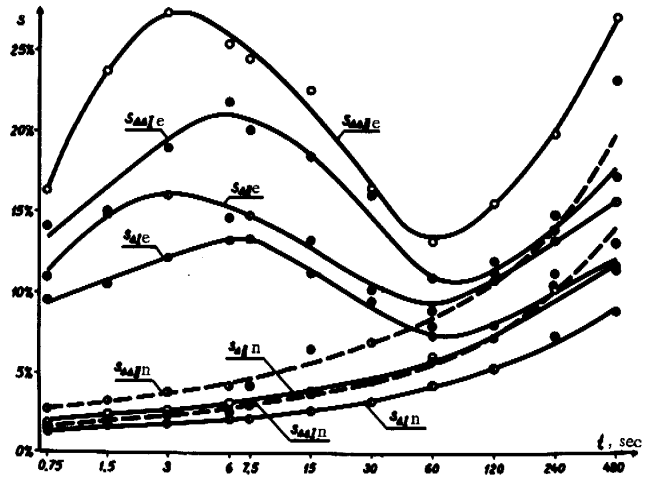

FIGURE 30.1. Results of the investigation of the conductivity of atmospheric air. The subscripts e and n denote the results of evening and night observations.

In the following, the observations taken over the two described measurement periods will be briefly referred to as evening and night observations.

The observation results were evaluated as follows. After recording, the mean conductivities were determined for the consecutive times 0.75, 1.5, 3, 6, 12, 24, 48 sec and 7.5, 15, 30, 60, 120, 240, 480 sec. For the series averaged over $t = 0.75$ sec, $t = 1.5$ sec, etc., each of the 768 sec/t values of mean conductivity were calculated for the evening and the night observations. For the series averaged over $t = 7.5$ sec, $t = 15$ sec, etc., each of the 7680 sec/t values of mean conductivity were calculated for the evening observations and each of the 3840 sec/t values were calculated for the night observations. From the obtained data s_Δ and $s_{\Delta\Delta}$ were determined for different averaging times. The calculations were carried out for two time conditions. For time condition I the differences of the mean conductivities of neighboring averaging intervals were determined. This corresponds to the method of charge accumulation for the condition that the cycles follow one another directly without any time loss during switching. For time condition II the difference of the mean mobilities were determined in unit intervals. This corresponds to conditions under which the time loss during switching of the circuit is the same as the time required for charge accumulation.

The results are graphically represented in Figure 30.1.

Data referring to the averaging time 0.75 sec are somewhat distorted due to the inertia of the recorder.

From the results of the described experiments we arrived at a number of conclusions. As expected, the dependence of $s_{\Delta\Delta I}$, $s_{\Delta II}$ and $s_{\Delta\Delta II}$ on the averaging time basically reiterates the function $s_{\Delta I}(t)$. $s_{\Delta I}$, $s_{\Delta II}$, $s_{\Delta\Delta I}$ and $s_{\Delta\Delta II}$ refer to time condition I and time condition II, respectively. The following relationship holds with slight deviations

$$s_{\Delta II}(t) = 1.26\, s_{\Delta I}\left(\frac{3}{2}t\right). \qquad (30.4)$$

The last result was found from an analysis of the values of the ratio $2s_{\Delta II}(t)/[s_{\Delta I}(t) + s_{\Delta I}(2t)]$. The curve of the frequency of deviations of this ratio from the coefficient of formula (30.4) is given in Figure 30.2, which shows all the results obtained for the averaging times from 3 to 25 sec and from 7.5 to 240 sec.

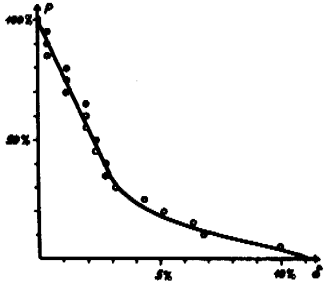

FIGURE 30.2. Error frequency curve of formula (30.4):

p — frequency of errors, exceeding δ.

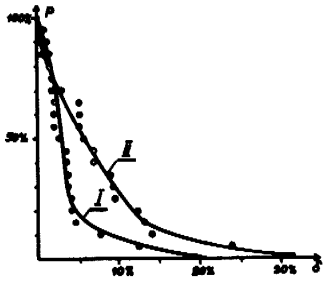

FIGURE 30.3. Error frequency curve of formula (30.5). Roman numerals on the curves denote the operation conditions.

Similar reasoning leads to the formula

$$s_{\Delta\Delta}(t) = s_\Delta(t)\sqrt{4 - 1.6\,\frac{s_\Delta^2\left(\frac{3}{2}t\right)}{s_\Delta^2(t)}}. \qquad (30.5)$$

The frequency of deviations of the experimental values from formula (30.5) is plotted in Figure 30.3.

It is of practical interest to study the dependence of s_Δ on the averaging time. If the fluctuations are small, s_Δ increases monotonically with an increase in the averaging time; this increase is due to the slow fluctuations of the conductivity caused by the variation of the meteorological conditions. Under strong fluctuations, a totally different variation trend of $s_\Delta(t)$ is observed: the curve passes through a maximum for an averaging time between 5 and 10 sec, and through a minimum for an averaging time between 60 and 120 sec, the maximum-to-minimum ratio of the s_Δ-values being equal to 1.9 in our case. The knowledge of the variation trend of $s_\Delta(t)$ is necessary for the correct selection of the charge accumulation time. The results obtained show that the tendency to select a charge accumulation time shorter than a minute seems questionable; it would be better to use a time from one to three minutes. These conclusions are tentative, since they are based on limited data. It seems desirable to include special measurements for the study of the function $s_\Delta(t)$ when planning observatory observations of the ionization of atmospheric air.

The quantitative results obtained in the experiments show that under conditions of small fluctuations (during the night temperature inversion) it is possible to measure the spectrum of light ions by the integral method with a standard deviation of 20% for a half-width of 15% of the mobility uncertainty range. The suitability of night conditions for the study of the spectral distribution of air ions was also mentioned in the paper /Norinder, Siksna, 1953/. Under unsuitable conditions the standard deviation will not drop below 30%, even for a half-width of 30% of the mobility uncertainty range. The detailed study of the spectrum $\varrho(k)$ becomes practically meangingless in this case.

The conclusions made so far are true only insofar as the values found for P_n or $\varrho(k_1, k_2)$, $\lambda(k_1, k_2)$ and $\varrho(k)$ are not subsequently averaged over successive measurements series. If such an averaging is carried out, a higher accuracy is theoretically possible. The reasoning with regard to the selection of the charge accumulation time becomes likewise meaningless. It can, in fact, be easily shown that when the results of n measurement series are averaged, an n-fold reduction in the charge accumulation time will always lead to a reduction in the influence of the fluctuations of P_n on the final result.

The above analysis pertains to the charge accumulation method. In the case of the method of the voltage drop across a resistance, the measurement results will be affected more strongly by the fluctuations of the conventional density. The use of this method for the study of the spectral distribution of air ions by an integral or first-order differential counter is therefore not to be recommended.

A rough estimate of the effect of fluctuations on the result of a measurement by the voltage drop method can be obtained on the basis of the approximate equivalence of the times t and 1.7τ, indicated in the paper /Kagan, 1964/.

§ 31. ELIMINATION OF THE EFFECT OF RANDOM VOLTAGE FLUCTUATIONS ON THE MEASUREMENT RESULTS

The sensitivity of a counter connected in series is limited by the instability of the power source. The dependence of the sensitivity of an integral counter on random fluctuations was examined in § 28. A quantitative analysis leads to the conclusion that the stability of the standard electronic voltage stabilizers is insufficient for measuring the polar charge density of heavy air ions under conditions of natural ionization atmospheric air. A somewhat better stability is achieved by using high-quality batteries, for which $s_{\Delta U}(100\ \text{sec})$ is of the order of 10^{-5}. For $k_0 = 0.0001\ \frac{\text{cm}^2}{\text{V}\cdot\text{sec}}$ and $t = 100$ sec, σ_r, caused by the voltage fluctuations, exceeds 50 elementary charges/cm^3, which is frequently inadmissible. To increase the power stability, it is necessary to use batteries of larger dimensions and weight, which are bulky and inconvenient. It seems therefore preferable to eliminate the effect of the supply voltage fluctuations by means of special circuit arrangements.

The connection of the counter to a bridge circuit (see Figure 31.1) is a known method of compensating the current induced by a change in the supply voltage. Since the type of ground connection used can depend on the specific conditions, no ground connection is indicated in Figure 31.1. The utilization of the bridge circuit in the aspiration counter was already described in /Erikson, 1921/. The bridge circuit can be used with equal success in both the integral and the differential measuring methods. The integral counter is examined below.

In this circuit (Figure 31.1) the electrometer is inserted on the diagonal of the bridge formed by the resistances R_1, R_2 and the capacitances of the measuring capacitor C, and the additional compensation capacitor C_1. Assuming that all the parasitic capacitances are connected in parallel to the electrometer, we have the equilibrium condition

$$\frac{C_1}{C} = \frac{R_1}{R_2}. \tag{31.1}$$

When this condition is satisfied, a change in the circuit supply voltage will not affect the electrometer reading.

The use of a bridge circuit is convenient when the sensitivity increase resulting from the decrease in the variance $s^2_{\Delta UC}$, determined in the bridge circuit by the stability of the bridge equilibrium, exceeds the sensitivity loss caused by the insertion of the shunt capacitance C_1. To increase the sensitivity, the capacitance C_1 should be small. This requires, however, a high supply voltage U_s, which exceeds by a factor of $(1 + C/C_1)$ the voltage of the measuring capacitor.

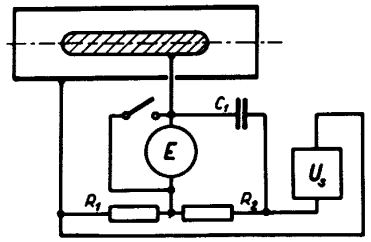

FIGURE 31.1. Counter connection in a bridge circuit.

Consider the problem of the determination of the optimum capacitance $C_{1\,opt}$ (the capacitance giving the minimum error σ_p) corresponding to a given supply voltage U_s of the bridge circuit. The problem has a simple solution only if all the errors except the electrometer error σ_{UE} are neglected. Then

$$C_{1\,opt} = \sqrt{C(C_0 - C_1)}, \tag{31.2}$$

where one starting magnitude is the total capacitance of the isolated system, excluding the capacitance of the compensation capacitor $(C_0 - C_1)$. The influence of the other sources of errors can be estimated in the first approximation

$$C_{1\,opt} \approx (1 + \delta)\sqrt{C(C_0 - C_1)}. \tag{31.3}$$

The expressions for δ are

1) in the method of charge accumulation with fixed zero and the pulse method

$$\delta = \frac{R_p^2\sigma_{QK}^2 + t^2\sigma_{UR}^2 + KT[(C_0 - C_1) + \sqrt{C(C_0 - C_1)}]R_p^2}{2R_p^2\sigma_{UE}^2(C_0 - C_1)[C + \sqrt{C(C_0 - C_1)}]}, \tag{31.4}$$

2) in the method of charge accumulation with drifting zero

$$\delta = \frac{t^2\sigma_{UR}^2 + 2KTR_p t}{2R_p^2\sigma_{UE}^2(C_0 - C_1)[C + \sqrt{C(C_0 - C_1)}]}, \tag{31.5}$$

3) in the method of the voltage drop across a resistance

$$\delta = \frac{\tau^2\sigma_{UR}^2 + KT[(C_0 - C_1) + \sqrt{C(C_0 - C_1)}]R_p^2}{2R_p^2\sigma_{UE}^2(C_0 - C_1)[C + \sqrt{C(C_0 - C_1)}]}. \tag{31.6}$$

The first approximation is adequate for all practical purposes, if $\delta \ll 1$.

The compensation capacitor C_1 must have a high insulation resistance, since leakage causes additional measurement errors. If the admissible value of this error is ΔP, the leakage resistance R_{C_1} must satisfy the condition

$$R_{C_1}C_1 \geqslant \frac{1}{4\pi k_0 \Delta P}. \tag{31.7}$$

The self-discharge time constant of high-quality solid-dielectric capacitors is $10^6 - 10^7$ sec. This is usually insufficient, and special air capacitors have to be used. As in the case of C_1 it is also possible to use the capacitance of the other measuring capacitor, which is not discharged. As a result several other parasitic phenomena are simultaneously compensated /Komarov, Kuz'menko, 1960; Komarov, Kuz'menko, Seredkin, 1961/.

The induced current is best compensated by a differential electrometer, in which the compensating signal can be phase-synchronized with the voltage variation. No voltage division is necessary, and the total voltage of the supply source can be applied to the measuring capacitor, which increases the counter sensitivity. The shunting effect of the compensating capacitor is likewise eliminated. The described circuit differs from the ordinary series circuit in that the other input of the electrometer is connected to the power source via an additional circuit, having the same transfer function as the circuit transmitting the voltage fluctuations through the measuring capacitor to the first input of the electrometer /Jonassen, 1962/.

This principle of compensating power supply fluctuations has been most successfully used in the Imyanitov counter, described in § 10. In this counter compensation is effected without any additional components, using only the symmetry of the system consisting of two measuring capacitors.

Another possibility for eliminating the errors caused by power source instability consists in replacing the power source in the counter circuit by a special reference-voltage capacitor, charged beforehand by the power source /Tammet, 1962b, 1963b/. The condition for a constant self-discharge time of the reference-voltage capacitor coincides with condition (31.7) for the compensation capacitor of the bridge circuit. The capacitance of the reference-voltage capacitor does not shunt the measuring system, and the power source voltage is fully utilized. Furthermore, in this design it is possible to use an ordinary electrometer without differential input. This method, however, possesses a shortcoming. It becomes impossible to effect continuous recording of the current over a long period.

In circuits with a grounded collector plate the reference-voltage capacitor can be connected between the repulsive plate and earth. The capacitance must exceed in this case tens of times the capacitance of the measuring capacitor; otherwise the measurement results will be distorted by the influence of the current generated by air ions of the opposite polarity settling on the repulsive plate. The high capacitance of the reference-voltage capacitor and the higher requirements imposed upon the insulator of the repulsive plate complicate the design of the corresponding counter.

The method of the reference-voltage capacitor is more suitable in the circuit with a grounded outer plate. It is convenient to switch the position between the electrometer and the power source. The reference-voltage capacitor is then connected between the inner plate of the measuring capacitor and the electrometer input (Figure 31.2). During measurements switch K_1 is opened only after the opening of switch K_2, and is closed before the closing of switch K_2. The circuit in Figure 31.2 can be considered from two points of view. If the capacitor C_2 is considered as

the power supply, the circuit then belongs to the series circuit arrangement. The capacitor C_2 can, however, also be considered as an additional element of the electrometer, which, owing to the presence of the dividing capacitor, enables the application of a high direct voltage without impairing the sensitivity to changes in the voltage. According to this interpretation the circuit in Figure 31.2 would seem to belong to the parallel circuit arrangement of the counter. Ignoring this question, we shall designate the circuit in Figure 31.2 as the circuit with a dividing capacitor; this name reflects the function of the capacitor C_2.

The requirement imposed upon the insulation of the dividing capacitor coincides with requirement (31.7).

The capacitance of C_2 is best taken several times larger than the capacitance of the measuring capacitance and electrometer connected in series. A considerable sensitivity loss results when this condition is not fulfilled.

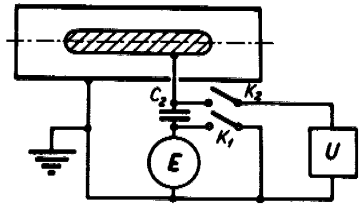

FIGURE 31.2. Circuit arrangement of the counter with a dividing capacitor.

In the circuit of Figure 31.2 the parasitic capacitance C_p is split into the capacitance C_p', consisting of the capacitance of the electrometer and the capacitance of the mounting, and the capacitance C_p'', connected in parallel with switch K_2. In view of the presence of the capacitance C_p'', the dependence of the electrometer readings on random fluctuations of the power source is not completely eliminated, but is only reduced by a factor of C_p''/C. The removal of the capacitance C_p'' is practically impossible, since to ensure the required insulation of the inner plate it is necessary to use two insulating layers with a conducting layer sandwiched between them and connected to the power source. This screens the insulator from the electric field. Otherwise, a considerable leakage and disturbances caused by the retarded polarization of the insulators after power switching is unavoidable.

The influence of the power source instability is completely eliminated in the combined circuit represented in Figure 31.3. The equilibrium condition here differs from condition (31.1) in that the capacitance C is replaced by C_p''. It thus follows that the capacitance of the compensation capacitor C_1 in the bridge circuit with dividing capacitor can be relatively small. The counter sensitivity in this arrangement is therefore higher than in the usual bridge circuit. The bridge circuit with dividing capacitor is particularly convenient for a counter with an interchangeable inner plate of the measuring capacitor, since the balance condition is independent of the effective capacitance.

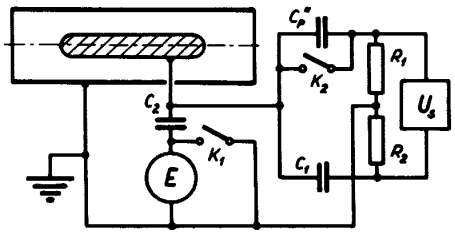

FIGURE 31.3. Combined counter circuit arrangement.

The influence of slow fluctuations in the supply voltage is automatically eliminated in all the modulating counters.

§ 32. PREVENTION OF THE EDGE EFFECT

The edge effect is most simply prevented in counters connected in accordance with the circuit having a grounded outer plate or the circuit with a grounded outer collector plate.

Consider first the circuit with a grounded outer plate. To estimate the edge effect, we use formula (14.5). Since this formula is very approximate, the admissible relative error δ must be specified with sufficient allowance. The effective capacitance of the edge effect must satisfy the inequality

$$C' \leqslant \frac{\delta}{L} C, \tag{32.1}$$

where L is the maximum expected value of the dimensionless ratio $\lambda_2 \Phi / k_0 l(k_0)$.

In order to fulfill condition (32.1) it is necessary to select a sufficiently large distance l' between the end of the inner plate and the plane of the input end of the outer plate perpendicular to the capacitor axis. Experiments on a suitable model were conducted in order to study the dependence of the capacitance C' on the distance l'. The measured parameter was the capacitance C^* between the inner plate of the coaxial capacitor and a large metallic disk placed in the plane of the input end of the outer plate. The disk had an opening at its center coinciding with the inlet opening of the outer plate. The disk was insulated from the outer plate by a thin plexiglass ring. The function $C^* = C^*(l')$ was determined for six replaceable inner plates of different diameter for different end configurations. The The ratio r_2/r_1 had the following values: 1.09, 1.42, 2.09, 3.62, 8.2, 21. The measurement results for a flat end of the inner plate are represented by the empirical formula

$$l' = r_2[\log(r_2/3C^*) - 0.6\log(r_2/r_1)]. \tag{32.2}$$

Formula (32.2) intentionally effects a systematic overestimation of the values of l', since errors in the other direction are more dangerous. The error in the distance l', calculated by this formula, does not exceed $0.1(l' + r_2)$, if $l'/r_2 > 0.5$ and $r_2/r_1 < 20$.

Experiments conducted with inner plates having other end configurations led to similar results, thus making it possible to use formula (32.2) with a certain correction. In the case of an inner plate with a semielliptical end (ratio of the axes 2:1) it is necessary to subtract from the value of l', determined by formula (32.2), the correction $r_1/2$, if $r_2/r_1 \geqslant 2$, or $r_1/4$, if $r_2/r_1 < 2$. For a semispherical end the correction will be $r_1/3$, if $r_2/r_1 \geqslant 2$, and $r_1/5$, if $r_2/r_1 < 2$.

The experimentally confirmed logarithmic relationship expressed by formula (32.2) was theoretically predicted by Grinberg /Grinberg, 1948/. On the basis of these considerations the range of application of formula (32.2) was extended to large ratios l'/r_2, although experimental checks were carried out only up to $l'/r_2 = 3$. The procedure for a quantitative estimate of the length l' is also discussed in the paper /Schmeer, 1966/.

The definition of the capacitance C' is similar to the definition of the capacitance C^*, so that in the design calculation of the counter it is possible to start from the approximation $C' \approx C^*$ and to calculate the required length of the inlet cylinder by formulas (32.1) and (32.2). In the empirical determination of the edge effect current, two- and threefold deviations from the relationship $C' = C^*$ were observed in some counters. However, due to the logarithmic relationship this error is compensated by a small reserve in the length l'.

A sufficiently large length l' contributes also to the damping of external aerodynamic disturbances in the inlet portion of the capacitor. This problem has been little studied, and no specific recommendations can be given. The length l' should not be too large, since this increases the errors caused by the adsorption of air ions.

In the circuit with a grounded outer collector plate the capacitance of the edge effect C_1 has definite significance and can be measured by the usual methods without any additional assumptions. To remove the edge effect, the capacitance C_1 must be selected according to condition (32.1). The dependence of C_1 on l' was studied by model measurements similar to those described above. The measured parameter was the capacitance between the inner plate and the inlet tube of the cylindrical measuring capacitor. The radii of the outer plate and the inlet tube were equal, and the gap between them was equal to $0.05\, r_2$. The experiments were conducted for six values of the ratio r_2/r_1 between 1.09 and 21. The end of the inner plate was provided with replaceable nozzles of different configurations. An empirical formula was established on the basis of the results calculated from (32.2) in such a way that the error cannot take on negative values:

$$l' = r_2[\log(r_2/2C_1) - 0.6\log(r_2/r_1)]. \tag{32.3}$$

The formula represented corresponds to an inner plate with a flat end. The accuracy and applicability limits of this formula are of the same order as formula (32.2). In the case of an inner plate with a semiellipsoidal or semispherical end it is necessary to introduce the same corrections as for formula (32.2).

The required length l' is reduced if a metallic grid is attached to the inlet opening of the outer plate. The screening effect of the grid can only

approximately be estimated by computation methods. On the basis of the known formula of the screening effect of a grid in a parallel-plate capacitor /Kaden, 1950/ it is possible to suggest the following approximate formula for estimating the permeability of a grid transverse to the coaxial capacitor axis:

$$\frac{C_1}{C_{10}} \approx \frac{2h}{3r_2} \log \frac{h}{2\pi r_0}, \qquad (32.4)$$

where C_{10} is the capacitance in the absence of the grid, h the mesh width and r_0 the wire radius.

The coefficient of formula (32.4) was selected empirically. For a grid with $h/r_2 = 0.1$ and $r_0/r_2 = 0.0043$ the measured values of the permeability were up to 15% lower than the values calculated by the formula (for $l'/r_2 > 0.5$). For a grid with $h/r_2 = 0.08$ and $r_0/r_2 = 0.0163$ the permeability is up to 30% lower than the calculated value, owing to the large ratio r_0/h.

Having provided the measuring capacitor with a grid, one should not forget the danger of air-ion adsorption. The dependence of the parameter AC_1/C_{10} on the wire radius is of interest for the selection of the grid size. The calculation shows that AC_1/C_{10} decreases monotonically with a decrease in the wire radius, provided that $h > 6\ r_0$. It is therefore possible to recommend the utilization of the thinnest possible wire, which makes it possible to ensure a smaller adsorption of air ions at a given permeability.

This is illustrated by the following example. If we were to reject the utilization of a grid in the counter described in § 36, the outer plate would have to be lengthened by 30% in order to preserve the previous capacitance of the edge effect.

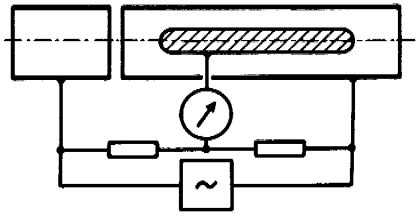

FIGURE 32.1. Bridge for measuring C_1/C.

Corrections for the edge effect can be introduced in the counter with a grounded outer collector plate. For this it is necessary to know the capacitance C_1 with an accuracy higher than that given by formulas (32.3). and (32.4). The ratio C/C_1 is most conveniently measured by an ac bridge (Figure 32.1). When a correction is introduced, it is desirable to fulfill the condition $C/C_1 > k_{max}/k_{min}$, where k_{max} and k_{min} are respectively the maximum and minimum mobilities of the air ions. On the basis of (14.6) we find

$$P(k_0) = P'(k_0) + \frac{C_1}{C} \frac{k_1}{k_0} P(k_1), \qquad (32.5)$$

where $P'(k_0)$ is the value of the conventional charge density distorted by the edge effect, and k_1 is the limiting mobility, exceeding k_{max}.

The suppression of the edge effect is more difficult in counters with a grounded inner collector plate. If the measuring capacitor is not equipped with electrostatic shielding, the edge effect can be estimated from the data given in § 15 of this book. It is not necessary to use electrostatic shielding in all conductivity measuring counters, in which it suffices to determine the critical discharge from the sum of the effective capacitance and the capacitance C' in order to prevent the edge effect. In counters for measuring the partial charge densities the utilization of electrostatic shielding is usually unavoidable.

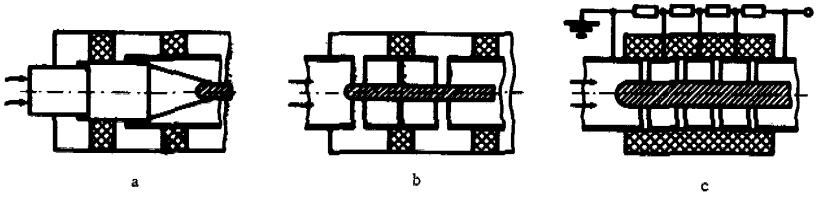

FIGURE 32.2. Electrostatic shields.

The best-known electrostatic shield is due to Swann /Swann, 1914 c/. A drawback of the usual design of the Swann shield (Figure 32.2a) is the air flow expansion upon entering the measuring capacitor, which contributes to the formation of turbulence. The improved variant of the Swann shield, represented in Figure 32.2b /Reimers, 1940; Komarev, Kuz'menko, Seredkin, 1961/, has eliminated this drawback.

In the measuring capacitor with a Swann shield part of the air ions settle on the shield. If the effective capacitance of the measuring capacitor is included the capacitance C' of the respective input device (Figure 15.4e corresponds to Figure 32.2a, and Figure 15.4b to figure 32.2b). The conduction current in the counter with a Swann shield is not strictly linear, but this is of practical importance in rare cases only. The correction C' is usually relatively small and can be considered constant. The effective capacitance of the measuring capacitor is substantial only for air ions of mobility lower than the limiting mobility, and therefore only the range $I/I_0 \leqslant C'/C$ must be allowed for when estimating C' by Figure 15.3.

The Swann shield must reduce the electric field, which penetrates the former until the capacitance C' satisfies condition (32.1). The problem of the longitudinal penetration of an electric field between two coaxial cylindrical surfaces has not been solved. The pattern of field reduction is known only in limiting cases, when the radius of the inner plate is equal to zero or is close to the radius of the outer plate (Grinberg, 1943; Kaden, 1957). In both cases the field strength drops according to a near-exponential law. Using the known theoretical premises and the quantitative relationships established on the basis of the experiments described in connection with formulas (32.2) and (32.3), we suggest the following approximate formula for estimating the necessary length of the Swann shield:

$$l_S = [0.75(r_2 - r_1) + 0.25(r_2 - r_1)^2/r_2]\log(r_2 L/2C\delta). \qquad (32.6)$$

If the inner plate does not penetrate into the shield, we must take $r_1 = 0$. Formula (31.6) has not been checked by direct experiments, and it should therefore be used with certain caution. We have stated it here because no other methods exist for calculating the Swann shield.

The electrostatic shield with transition rings /Komarov, 1961/ is not connected with the inner plate of the measuring capacitor and only slightly increases the parasitic capacitance. The effective capacitance of a measuring capacitor with such a shield (Figure 32.2c) is constant. The determination of the number and length of the transition rings must be effected experimentally, in view of the difficulties involved in the theoretical calculation. The shield calculation is simplified if the length of an individual ring exceeds several times the distance $r_2 - r_1$. In this case the ratio of the first (starting from the air inlet) ring to the voltage of the outer plate must be limited by the value $C\delta/C'L$, where C' is the capacitance of the edge effect of the corresponding input device without shield (Figure 15.4b) for $l/l_0 \approx \delta$. The ratio of voltages of adjacent rings, and also the ratio of the voltage of the outer plate to the voltage of the last ring, must be smaller than C_n/C', where C_n is the capacitance between the transition ring and the inner plate. The shield with transition rings is structurally the most convenient for counters with a small ratio of the radii of the measuring capacitor plates.

A similar electrostatic shield was used in the counter with a divided air flow /Yunker, 1940/, but the efficiency of the shield was in this case much lower, due to the absence of the screening effect of the inner plate. The edge effect capacitance in this shielding is determined by the relationship

$$C' = \frac{S}{4\pi l_Y}, \qquad (32.7)$$

where S is the cross-sectional area of the air flow in the shield, and l_Y the shield length.

§ 33. METHODS OF DETERMINATION OF THE EFFECTIVE CAPACITANCE OF THE MEASURING CAPACITOR

The effective capacitance of the measuring capacitor can be either calculated or measured. While calculation is obviously the only means available in the design stage, measurement represents a more accurate procedure, and is accordingly used after the completion of the counter in order to refine the calculated value.

The capacitance of a coaxial capacitor is calculated by the formula

$$C = \frac{l}{2\ln\frac{r_2}{r_1}}, \qquad (33.1)$$

where l is the capacitor length, r_2 the radius of the outer plate, and r_1 the radius of the inner plate. The capacitor length is determined with an accuracy of the order of r_2, which is frequently insufficient /Swann, 1914b/. The manufacture of a coaxial capacitor of the correct length is possible by using equipotential elongations of the inner plate. An equipotential elongation of the input end of the measuring capacitor is admissible only when measuring the conductivity /Cagniard, Lévy, 1946/, a fact restricting the possibilities of this method.

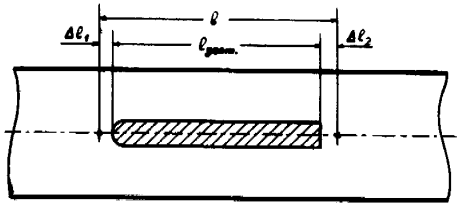

FIGURE 33.1. Effective length of the measuring capacitor.

In § 9 we described a measuring capacitor whose effective capacitance can be accurately calculated (Figure 9.4); this capacitor has, however, a very complex structure.

Formula (33.1) can be considered to be valid in the case of the standard measuring capacitor as well, provided the quantity l is understood as the corresponding effective length /Tammet, 1964a/. In the case of a sufficiently long measuring capacitor, the difference between the effective length and the geometrical length of the inner plate is independent of the plate length, and is uniquely determined by the configuration of the capacitor ends. It is possible to set the points of the effective ends of the inner plate in such a way that the effective length is equal to the distance between them. This is illustrated in Figure 33.1. The effective length is the sum of the geometrical length and the corrections Δl for the two ends.

In the case of equipotential elongation the correction $\Delta l = 0$. The corrections Δl for the other most widely used configurations of the inner plate end were determined by means of model measurements. The experimental setup for these measurements is schematically shown in Figure 33.2. The capacitance between electrodes 3 and 2 is measured by means of a bridge. Electrode 1 serves as an equipotential elongation of plate 3. The electric field is similar to the field in an ideal coaxial capacitor, since the gap between electrodes 2 and 1 was made small. After the removal of electrode 1 from the capacitor, the measured capacitance changed by ΔC. From this we determine the correction for the inner plate which includes the end effect:

$$\Delta l = 2\Delta C \ln\frac{r_2}{r_1}. \qquad (33.2)$$

Such measurements were conducted for six different ratios of r_1/r_2: 0.048, 0.123, 0.276, 0.479, 0.702, and 0.916.

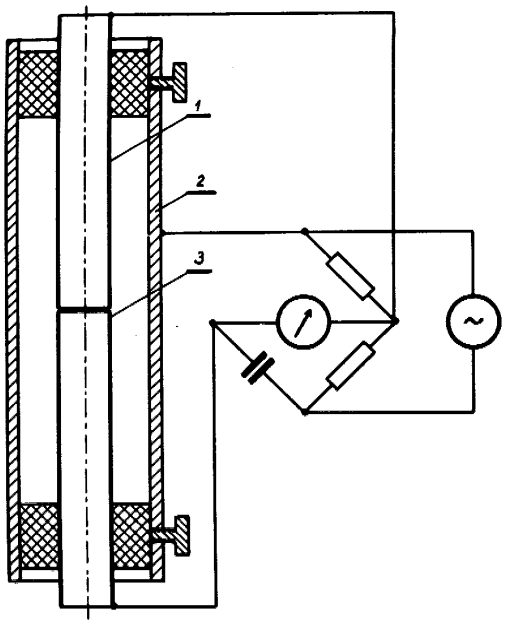

FIGURE 33.2. Arrangement for determining the corrections for the length of the coaxial capacitor:

1 — equipotential elongation; 2 — outer plate; 3 — inner plate.

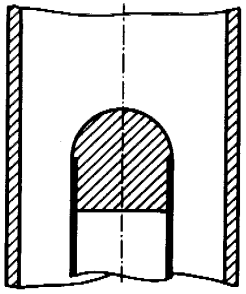

FIGURE 33.3. End of the inner plate with cap.

In order to determine the correction Δl for other configurations of the inner end plate, the change in the capacitance caused by mounting a suitable cap on the end of electrode 3 (see Figure 33.3) was measured. The corrections for an inner plate with a flat end were directly determined by the same method as that used for an inner plate with a hollow end.

The measurement results are plotted in Figure 33.4. The error of curves 1—2 does not exceed 0.01, and that of curves 3—6 does not exceed $0.015 \pm 0.03\ |\Delta l|/r_2$.

The applicability of the curves is restricted by the conditions $l' > 3r_2$ and $l_0 > 3(r_2 - r_1)$, where l' is the distance of the end of the inner plate from the end of the cylindrical portion of the outer plate, and l_0 is the length of the cylindrical portion of the inner plate. According to experimental data given by Schmeer /Schmeer, 1966/, the dependence of ΔC on l' is practically unnoticeable already at $l' = 2r_2'$.

The capacitance of a parallel-plate measuring capacitor is calculated by the standard formulas.

The capacitance of a measuring capacitor with an outer plate and an inner plate can be approximately calculated by the formula

$$C \approx \frac{r_1 l}{2(r_2'' - r_2')}\left[\frac{\ln\frac{r_2''}{r_1}}{\ln\frac{r_2'}{r_1}} + \left(1 + \frac{1}{4}\ln\frac{r_2' r_2''}{r_1^2}\right)\ln\frac{r_2''}{r_2'} + \sum_{n=3}^{\infty}\frac{1}{n \cdot n!}\left(\ln^n\frac{r_2''}{r_1} - \ln^n\frac{r_2'}{r_1}\right)\right], \qquad (33.3)$$

where r_2' is the radius of the outer plate at the thin end and r_2'' at the wide end.

When determining the length of a conic measuring capacitor it is necessary to take into account the corrections for the configuration of the end of the inner plate. With a small error it is possible to use the data of Figure 33.4, taking as r_2 the radius of the outer plate at the end under consideration.

The method which requires the least time for the approximate calculation of the capacitance with an arbitrary plate geometry was described in the paper /Pflügel, 1969/.

The direct measurement of the effective capacitance of the measuring capacitor is complicated by the necessity of eliminating the parasitic capacitances connected in parallel to the measuring capacitor. If this is possible, the parasitic capacitances should be connected in parallel to the null indicator of the bridge. This is achieved in the circuit shown in Figure 33.2, where the capacitance between electrodes 1 and 3 is eliminated. It can happen that the design of the measuring capacitor prevents the realization of such a connection. The effective capacitance can be measured in this case only by means of special methods. One such method is the following. A screen covering the whole inner surface of the outer plate of the measuring capacitor, but insulated from the latter, is manufactured from paper and foil. By connecting the capacitance between the inner plate and the screen in parallel to the null indicator, it is possible to measure the parasitic capacitance C_p. The screen is then

removed, and the total capacitance is measured in the usual way. The effective capacitance is the difference between the total and parasitic capacitances: $C = C_0 - C_p$.

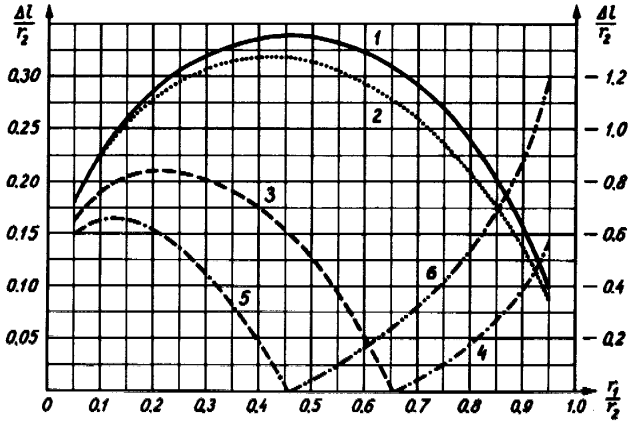

FIGURE 33.4. Curves for determining corrections for the length of the measuring capacitor. The left vertical scale corresponds to curves 1, 2, 3, and 5; the right scale to curves 4 and 6. The curves correspond to the following configurations of the end of the inner cylinder:

1 — plane transverse to the capacitor axis; 2 — transversely cut-off end of a hollow cylinder with wall thickness 0,05 r_2; 3 and 4 — semisphere; 5 and 6 — semi-ellipsoid with major semi-axis equal to the diameter of the inner plate (ratio of the axes 2:1).

§ 34. PRINCIPLES OF THE SELECTION OF THE PARAMETERS AND OPERATING CONDITIONS OF THE INTEGRAL COUNTER

The limiting mobility or the limiting mobility range which must be covered by adjusting the voltage or flow rate must be specified before starting the counter design. The effective capacitance of the measuring capacitor is assumed to be constant for a specific counter, since the adjustment of the effective capacitance is technically difficult and usually not expedient in practice. The specified limiting mobility range can be covered for different selections of the effective capacitance and voltage and flow rate ranges. It is the task of the designer to find the optimal solution.

This problem is complex and cannot be solved in a general form. We shall accordingly restrict ourselves to several particular aspects of practical importance.

We start by examining the dependence of the counter sensitivity on the basic parameters C, Φ, and U for the case of a fixed limiting mobility. Let

the electrometer parameters and the relative instability $S_{\Delta UC}$ or $S_{\tau UC}$ be given. The analysis is based on formulas (28.9) – (28.11). It is easily seen that the sensitivity has an upper limit, determined by the following expressions:

$$\sigma_{P_{min}} = \frac{s_{\Delta UC}(t)}{4\pi k_0 t}, \tag{34.1}$$

when the current is measured by the charge accumulation method, and

$$\sigma_{P_{min}} = \frac{s_{\tau UC}(\tau)}{4\pi k_0 \tau}, \tag{34.2}$$

when it is measured from the voltage drop across a resistance. In order to approach this limit we must increase indefinitely both the flow rate and the voltage.

The flow rate and voltage scale is determined by the absolute critical values Φ_{cr} and U_{cr}, which are the minimum values of these parameters, at which the increase of one of them leads to the limit $\sigma_P^2 = 2\sigma_{P_{min}}^2$. In the charge accumulation method with fixed zero and the pulse method we have

$$\Phi_{cr} = \frac{4\pi k_0}{s_{\Delta UC}(t)} \sqrt{\sigma_{QK}^2 + C_p^2 \sigma_{UE}^2 + KTC_p + \frac{\sigma_{UR}^2 t^2}{R_p^2}} \tag{34.3}$$

and

$$U_{cr} = \frac{\sigma_{UE}}{s_{\Delta UC}(t)}. \tag{34.4}$$

In the charge accumulation method with a drifting zero

$$\Phi_{cr} = \frac{4\pi k_0}{s_{\Delta UC}(t)} \sqrt{C_p^2 \sigma_{UE}^2 + \frac{2KTt}{R_p} + \frac{\sigma_{UR}^2 t^2}{R_p^2}}, \tag{34.5}$$

where U_{cr} is expressed, as before, by formula (34.4).

Here and in what follows we give only the formulas corresponding to the charge accumulation methods. The corresponding expressions for the voltage drop across a resistance are obtained (within the limits of this section) by replacing t by τ, $s_{\Delta UC}$ by $s_{\tau UC}$ and σ_{QK} by 0 in the formulas describing the charge accumulation method with fixed zero and the pulse method.

The effective capacitance does not have an absolute critical value, since for any value of C the unbounded increase of Φ and U leads to the limit $\sigma_P = \sigma_{P_{min}}$.

In practice, the maximum flow rates and voltages are limited by technical considerations. The maximum sensitivity is achieved if the flow rate and the voltage have the highest admissible values and the effective capacitance is selected in accordance with these values. There is no sense in considerably exceeding the critical values of the flow rate and the voltage, although this might be possible in practice.

This recommendation does not apply if the corresponding effective capacitance is beyond the specific technical possibilities. The procedure

in such a case is to select the highest admissible effective capacitance and voltage, and then to determine the flow rate.

The behavior of the function $\sigma_p = \sigma_p(C)$ for a fixed voltage is of interest for the rational selection of the effective capacitance. An unlimited increase in the effective capacitance leads to the value

$$\lim_{C\to\infty}\sigma_p = \frac{\sqrt{\frac{\sigma_{UE}^2}{U^2}+s_{\Delta UC}^2(t)}}{4\pi k_0 t}. \tag{34.6}$$

σ_p^2 attains a double limiting value for the critical value of the effective capacitance $C = C_{crU}$. We obtain

$$C_{crU} = \frac{C_p\sigma_{UE}^2+\frac{KT}{2}}{\sigma_{UE}^2+U^2s_{\Delta UC}^2(t)} + \sqrt{\left(\frac{C_p\sigma_{UE}^2+\frac{KT}{2}}{\sigma_{UE}^2+U^2s_{\Delta UC}^2(t)}\right)^2+\frac{\sigma_{QK}^2+C_p^2\sigma_{UE}^2+KTC_p+\frac{\sigma_{UR}^2t^2}{R_p^2}}{\sigma_{UE}^2+U^2s_{\Delta UC}^2(t)}} \tag{34.7}$$

in the charge accumulation method with fixed zero and the pulse method, and

$$C_{crU} = \frac{C_p\sigma_{UE}^2}{\sigma_{UE}^2-U^2s_{\Delta UC}^2(t)} + \sqrt{\left(\frac{C_p\sigma_{UE}^2}{\sigma_{UE}^2+U^2s_{\Delta UC}^2(t)}\right)^2+\frac{C_p^2\sigma_{UE}^2+\frac{2KTt}{R_p}+\frac{\sigma_{UR}^2t^2}{R_p^2}}{\sigma_{UE}^2+U^2s_{\Delta UC}^2(t)}} \tag{34.8}$$

in the charge accumulation method with drifting zero.

The dependence of the sensitivity on the effective capacitance for a fixed flow rate is of interest for the selection of the parameters of light-ion counters and conductivity-measuring counters. In order to increase the sensitivity it is then necessary to reduce the effective capacitance, while simultaneously increasing the voltage. The sensitivity displays here a dependence on C which is the converse of the preceding case. It is possible in this case as well to indicate a critical capacitance $C_{cr\Phi}$, for which σ_P^2 attains the double limiting value $\lim_{C\to 0}\sigma_P^2$.

In the charge accumulation method with fixed zero and the pulse method we obtain

$$C_{cr\Phi} = \sqrt{2C_p^2+\frac{\sigma_{QK}^2+2KTC_p}{\sigma_{UE}^2}+\left(\frac{KT}{2\sigma_{UE}^2}\right)^2+\left(\frac{\Phi s_{\Delta UC}(t)}{4\pi k_0\sigma_{UE}}\right)^2+\left(\frac{\sigma_{UR}t}{\sigma_{UE}R_p}\right)^2} - \frac{KT}{2\sigma_{UE}^2} - C_p. \tag{34.9}$$

In the charge accumulation method with a drifting zero we have

$$C_{cr\Phi} = \sqrt{2C_p^2+\left(\frac{\Phi s_{\Delta UC}(t)}{4\pi k_0\sigma_{UE}}\right)^2+\left(\frac{\sigma_{UR}t}{\sigma_{UE}R_p}\right)^2} - C_p. \tag{34.10}$$

The counter calculation for the given range of the limiting mobility (k_{min}, k_{max}) is more complex. The counter operating conditions will be described by functions of the limiting mobility. To simplify the calculations, the counter sensitivity can be characterized by the following criterion:

$$\eta = \sigma_p^2(k_{min}) + \Theta^2\sigma_p^2(k_{max}), \tag{34.11}$$

where the parameter Θ is taken equal to the mean ratio $P(k_{min})/P(k_{max})$ is selected on the basis of other considerations. Obviously, for $k_0 = k_{min}$ it is efficient to use the maximum admissible voltage U_{max}, and for $k_0 = k_{max}$ the maximum admissible flow rate Φ_{max}. In the entire range of the limiting mobility the highest sensitivity is achieved when one of these parameters has the maximum admissible value, while the other parameter is determined according to the required limiting mobility. The effective capacitance of the measuring capacitor must be determined from the values U_{max}, Φ_{max} and from some mean value of the limiting mobility. As a function of the effective mobility the criterion η has a minimum, which determines the optimum value C_{opt} of the capacitance.

The condition of the minimum of η leads to the equation of the optimum capacitance

$$1+\frac{C_{opt}}{C_1} = \frac{C_{opt}^3}{C_3^3}+\frac{C_{opt}^4}{C_4^4}, \tag{34.12}$$

where the coefficients C_1, C_3, and C_4 are determined by the following expressions:

1) in the charge accumulation method with fixed zero and the pulse method

$$C_1 = \frac{\sigma_{QK}^2+C_p^2\sigma_{UE}^2+KTC_p+\frac{\sigma_{UR}^2t^2}{R_p^2}}{C_p\sigma_{UE}^2+\frac{KT}{2}}, \tag{34.13}$$

$$C_3^3 = \frac{C_1}{\left(4\pi k_{min}\Theta\frac{U_{max}}{\Phi_{max}}\right)^2}, \tag{34.14}$$

$$C_4^4 = \left(C_p+\frac{KT}{2\sigma_{UE}^2}\right)C_3^3; \tag{34.15}$$

2) in the charge accumulation method with a drifting zero

$$C_1 = C_p+\frac{2KTt}{\sigma_{UE}^2R_pC_p}+\frac{\sigma_{UR}^2t^2}{\sigma_{UE}^2R_p^2C_p}, \tag{34.16}$$

C_3 is expressed in terms of C_1 by formula (34.14)

$$C_4^4 = C_pC_3^3. \tag{34.17}$$

We recall that expressions (34.3), (34.4), (34.6), (34.7), (34.9), and (34.13) – (34.15) can be used in the method of the voltage drop across a resistance, provided we write $\sigma_{QK}=0$ and replace t by τ and $s_{\Delta UC}$ by $s_{\tau CU}$.

If the specific values of the coefficients C_1, C_2 and C_4 are known, equation (34.12) is easily solved by a numerical or graphical method. In the case of a numerical solution it is possible to set $C_{opt}\approx C_4$ in the first approximation.

The above method of calculating the effective capacitance is illustrated below by a particular example with typical values of the parameters. Let us take the following initial values: $k_{min}=0.00033$ cm^2/V·sec, $\Theta=10$, $t=100$ sec, $C_p=10$ cm, $R_p=9\times10^{14}$ ohm, $\sigma_{UR}=300$V, $U_{max}=300$ V, $\Phi_{max}=1000$ cm^3/sec. When using a mechanical electrometer with $\sigma_{UE}=3$ mV, we find $C_{opt}\approx 43$ cm. For a limiting mobility of 1 cm^2/V·sec we obtain $\sigma_p\approx 10$ elementary charges/cm^3, and for the limiting mobility 0.00033 cm^2/V·sec, $\sigma_p\approx 200$ elementary charges/cm^3. Observe that for these initial conditions it is altogether impossible to reduce σ_p below 160 elementary charges/cm^3 for $k_0=0.00033$ cm^2/V·sec by means of an increase in the effective capacitance. If a dynamic electrometer with $\sigma_{UE}=0.3$ mV is used, the optimum capacitance $C_{opt}\approx 90$ cm, and for $k_0=1$ cm^2/V·sec we obtain $\sigma_p\approx 3$ elementary charges/cm^3, for $k_0=0.00033$ cm^3/V·sec $\sigma_p\approx 25$ elementary charges/cm^3. The increase in the optimum capacitance with an increase of the electrometer sensitivity is due to the allowance for the current generated by the insulator. For $\sigma_{UR}=0$ the solution of the problem considered is $C_{opt}\approx 40$ cm, regardless of the electrometer sensitivity.

Specific determinations show that the effective capacitance of the measuring capacitor of many known wide-range counters, selected on the basis of intuitive considerations, is close to the optimum value calculated by the above method. In counters with mechanical electrometers there is a tendency to select a superfluously high effective capacitance, as shown on the basis of the simplified formula of counter sensitivity by /Gubichev, 1960/.

The method described for calculating the optimum effective capacitance should not be considered an absolute and rigorous method. The determination of the optimality on the basis of the minimum of the criterion is in a sense arbitrary and does not reflect all the aspects of the problem. No property of the counter besides the sensitivity was taken into account in the deductions made. The value obtained for C_{opt} should therefore be considered a tentative value, subject to subsequent refinement when selecting the size of the measuring capacitor.

The design calculation of the measuring capacitor is confronted with a number of unsolved and little-studied problems. It is necessary in the first place to solve the problem of adequately neutralizing the distortions linked with the turbulent mixing of air. Two procedures are available to achieve this end. One of them consists in a sufficient decrease of the ratio $l/(r_2-r_1)$. It is then possible to work at $Re>Re_{cr}$, and, as a result, to select a very high air-flow rate and to achieve a high counter sensitivity. This procedure has been little studied, although it seems promising for measurements in the range of high limiting mobilities. A rough estimate

of the maximum ratio $l/(r_2-r_1)$ of the measuring capacitor of the integral counter with turbulent air flow can be made via the formula

$$\frac{l}{r_2-r_1}\leqslant 1000\,\delta^2, \tag{34.18}$$

where δ is the admissible error of the conditional density. The formula was derived on the basis of theoretical considerations and the empirical values at Re = 10,000—16,000, described in the preceding chapter.

The high resolving power necessary for the study of the spectral distribution of air ions according to mobilities is attained only if the turbulent mixing in the measuring capacitor has been sufficiently suppressed. The procedure for reducing the errors connected with the turbulence has likewise been insufficiently studied, although the elimination of the turbulence has been the aim in almost all designs of aspiration counters. To remove turbulent mixing in the measuring capacitor it is necessary to suppress the turbulent fluctuations in the air entering the measuring capacitor, and at the same time to ensure a laminar flow inside the capacitor. The turbulence of the incoming air flow can be suppressed by means of a wire grid /O'Donnel, Hess, 1951; Yaita, Nitta, 1955/. The efficiency of turbulence damping by blowing the air through the grid is calculated by the standard formulas /Batchelor, 1955/ or laminarizing grids /Styro, Matulyavichene, 1965; Dolezalek, Oster, 1965/. However, the use of grids is limited due to the adsorption of air ions. The turbulence can be suppressed to a certain extent by means of an inlet suction nozzle, such as was used in Gerdien's counter /Gerdien, 1905a/. The turbulence is also damped at low Reynolds numbers in a long inlet pipe.

To ensure laminar flow conditions inside the measuring capacitor, the Reynolds number should be sufficiently low. In the determination of the Reynolds number for an annular pipe it is expedient to select $r_2-r_1^2/r_2$ as the characteristic dimension /Lonsdale, 1923/, which ensures the coincidence of the values of the Reynolds number $Re=\Phi/\pi\nu r_2$ for the measuring capacitor and the inlet pipe. The above characteristic dimension was also used in the preceding chapter (formula 21.7). The critical value of the Reynolds number is a function of the ratio r_2/r_1. The data available on this function are not adequate. The only conclusion which can be drawn from the sparse data available /Schiller, 1932; Schlichting, 1959 /is that Re_{cr} increases with a decrease in the ratio r_2/r_1. In some papers /Funder, 1939; El Nadi, Bessa, 1958; Hoegl, 1963b/ the critical value of the quantity $\Phi/\pi\nu(r_2+r_1)$ is taken as constant. This, however, is a very rough approximation. The estimate $(Re=\Phi/\pi\nu r_2)_{cr}\approx 1100(1+r_1/r_2)$ is true only for large values of r_2/r_1, while for low values of this ratio it seems questionable.

Attention should be given to the role played by bars transverse to the flow in the creation of the turbulence /Tammet, 1962c/. If it is impossible to avoid the use of bars, they should be streamlined /Komarov, Kuz'memko, Seredin, 1961/ or made as thin as possible. No turbulence will form behind a cylindrical wire if $r_0<0.01(r_2-r_1)$. This estimate was derived on the basis of the known value of the critical Reynolds number for transverse flow past a cylinder /Landau, Lifshitz, 1954/.

To improve the aerodynamic properties of the measuring capacitor, the outer plate can be made conical. As is known, in a converging flow the laminar flow conditions are preserved for considerably higher flow rates than in a flow of uniform cross section /Loitsyanskii, 1959/.

Experiments on the stability of an air flow in a converging capacitor with flat plates are described in the paper /Hoppel, 1968/ and confirm the above statements. In this study the properties of a conical measuring capacitor were also investigated.

At very low flow rates, air mixing due to heat convection constitutes a problem.

The problem of the maximum admissible field intensity in the measuring capacitor has so far not been solved. A drop in the counter reliability has been observed above 1000 V/cm. This drop is due to the frequent entanglement of microscopic filaments and motes in the capacitor, which leads to the appearance of local discharges and leaks. Obviously, the admissible intensity depends on the linear velocity of the air flow. The value $E_{max} = 1000$ V/cm /Gerasimova, 1939/ corresponds to moderate flow velocities; the increase in the velocity shifts this limit toward higher values. However, the function $E_{max} = E_{max}(u)$, which is highly significant for a substantiated design calculation of the counter, has hardly been studied. The radius of the inner plate must be selected according to E_{max}, and it is expedient to set it equal to the larger of the two solutions of the equation.

$$r_1 \ln \frac{r_2}{r_1} = \frac{U_{max}}{E_{max}}. \tag{34.19}$$

This equation can be solved graphically or numerically.

In the region of high mobilities it is necessary to allow for diffusion, which limits the attainable resolving power of the counter. If, in accordance with /Komarov, Seredkin, 1960; Eichmeier, 1967, 1968/, we determine the resolving power from the relationship

$$R = \frac{k}{\Delta k}, \tag{34.20}$$

where Δk is the minimum difference of the mobilities of two discrete groups of air ions, for which the empirical curve $q(k)$ has two maxima, the resolving power has an upper bound

$$R_d = \frac{1}{2s_{kd}} = \frac{1}{2}\sqrt{\frac{1}{\mu}\frac{qU}{2KT}}. \tag{34.21}$$

The parameter μ was determined in § 19. To increase the limiting resolving power, it is necessary to ensure a sufficiently high value of the voltage, reducing, if necessary, the effective capacitance.

The design calculation for the measuring capacitor on the basis of these considerations is far from perfect. Although there exist some elements of quantitative calculations, the most crucial solutions are based on intuitive considerations, such as the assessment of the value of the initial parameters, and the compromise between accuracy and cost considerations.

The best substantiated method of complete calculation of the optimum design of a counter is based on the minimum cost principle /Tammet, 1963a/. The idea behind one of the variants of calculation by this method consists in the following. Consider a multidimensional space in which the coordinates are determined by the design parameters of the counter. To every point of this space corresponds a specific counter design. Let the functional characteristics of the counter (sensitivity, accuracy, range of limiting mobilities, resolving power, weight, size, etc.) be specified. Set up formulas expressing these characteristics as functions of the design parameters. By substituting the specified values of the functional characteristics into these expressions we obtain equations defining the multidimensional surface of the designs satisfying the specified values. It is possible, in principle, to set up a formula giving the development and manufacturing cost as a function of the design parameters. The optimum design is defined by the coordinates of the point of minimum cost on the surface of the designs satisfying the specified values.

Although designers always solve this problem intuitively, a rigorous mathematical solution is very difficult and laborious. The rapid improvement of the theoretical solutions of individual counter components, such as the electrometer and the power stabilizer, considerably complicates the establishment of cost formulas. The realization of an overall calculation of the optimum design can be useful only when the counter is designed for mass production.

§35. BRIEF SURVEY OF THE DESIGNS OF AIR-ION ASPIRATION COUNTERS

The existing aspiration counters are of the most varied designs. Almost every investigator using the aspiration method of air-ion study introduced some changes in the counter design. The survey given below has no pretentions of completeness. For relatively detailed technical descriptions of the counters we refer to the original papers. Some data on the different counters can also be found in survey papers /Kähler, 1929; Gerasimova, 1939; Torreson, 1949; Imyanitov, 1957; Israël, 1957b; Beckett, 1961; Siksna, 1961a; Minkh, 1963; Knoll, Eichmeir, Schön, 1964/.

The first designs of aspiration counters were described in the papers of J. J. Thomson and his pupils, mentioned in the introduction of this book. We shall briefly describe one of these instruments /McClelland, 1898/, which is of considerable practical interest. This counter is equipped with a cylindrical measuring capacitor with a grounded outer cylinder. The radius of the outer cylinder is 0.85 cm. The counter has two inner cylindrical plates, connected to the electrometer and the power source according to the circuit diagram in Figure 6.1. Both inner plates have a radius of 0.2 cm and are 6.5 cm long. Each of them is fastened to an ebonite insulator by means of a thin transverse bar. The insulator is placed in such a way that its surface is protected from the direct effect of the air flow. The first inner plate is connected to the stabilized power source. The second inner plate is connected to one pair of quadrants of the highly sensitive quadrant electrometer.

The other pair of quadrants is connected to the stabilized power source. Before measurement, both pairs of quadrants are shorted by means of a suitable key. The current is measured by the charge accumulation method. The air is drawn through the measuring capacitor and flowmeter by a water-jet pump. The air-flow rate was 270 cm^3/sec. This instrument was used in laboratory studies.

The scientific and technical level of the instrumentation used by the first investigators of the natural ionization of atmospheric air was much lower than the level attained in the works of the Thomson school. Of greatest historical importance are the instruments of Ebert/Ebert, 1901, 1905/ and Gerdien /Gerdien, 1903, 1905, 1905b/. These two counters are connected according to the parallel circuit arrangement and equipped with electrometers of low sensitivity. The size and operation conditions of the measuring capacitor of the Ebert counter are given by the following figures: $r_2 = 1.46$ cm, $r_1 = 0.25$ cm, $l = 40$ cm, $\Phi = 2000$ cm^3/sec, $U = 200$ V. The Ebert counter was described with negligible alterations in the papers /Lutz, 1909; Speranskii, 1926; Chernyavskii, 1937, 1957/. Gerdien's counter was first intended for conductivity measurement. Its basic parameters are the following: $r_2 = 8$ cm, $r_1 = 0.75$ cm, $l = 24$ cm, $\Phi = 9000$ cm^3/sec. Some features of the Gerdien counter are described in the paper /Hewlett, 1914/.

Subsequently, the method of connecting the counter in series became more widespread. The most important design of the early period is the heavy-ion counter of Langevin and Moulin /Langevin, Moulin, 1907/. This counter employs a highly sensitive quadrant electrometer. The design of the inner-plate insulators are of interest; they are provided with an intermediate metallic layer for protection against leakage. The design of counter insulators with a protective ring was earlier described in the paper /Kähler, 1903/. Measurements by means of the Langevin and Moulin counter have been automized, the electrometer readings being recorded on photographic paper placed on a slowly revolving drum. Another system for the automatic recording of electrometer readings was described still earlier in the paper /Benndorf, 1906/. The evaluation of the recordings of the Benndorf electrograph can be simplfied by using simple apparatus /Tamm, 1960/.

The design of the measuring capacitor of the Langevin-Moulin counter has been used with unessential modifications in the studies /Gockel, 1917; Hess, 1929/.

The next most important improvement in the design of aspiration counters was described in the paper of Swann /Swann, 1914c/, who invented the electrostatic shield.

In the designs of the heavy-ion counter of Langevin and Moulin and the light-ion counter of Swann a level was reached which was comparable to contemporary integral counters equipped with mechanical electrometers. Many known counters and automatic recorders /Kähler, 1930; Torreson, Wait, 1934; Wait, Torreson, 1934; Hogg, 1934; Lutz, 1934, 1936; Grieger, 1935; Greinacher, Klein, 1937; Gerasimova, 1937, 1939, 1941a; Leckie, 1938; Funder, 1939, 1940; Salles, 1942; Reinet, 1956; Saks, 1956; Neaga, Antonescu, 1958/ differ from those described above only by a different combination of the design elements and secondary improvements. Important features of the above-mentioned studies are the use of the method of current measurement from the voltage drop across

a resistance /Wait, Torreson, 1934/, the improvement of the air-supply system and the arrangement of a measuring capacitor with an inlet which opens from below /Hogg, 1934; Leckie, 1938/, the utilization of a flow rate /Grieger, 1935/, the realization of automatic voltage commutation of the measuring capacitor according to a specified program /Saks, 1956/.

The counters described in the works /Thellier, 1933, 1936, 1941; Vasiliu, Calinicenco, Onu, 1954; Vasiliu, Calinicenco, Mateiciuc, 1956/. differ by the utilization of the compensation method of current measurement, in which the electrometer serves as a null indicator.

A peculiar design of the measuring capacitor with increased effective capacitance for a standard size of the instrument is described in the papers /Wolodkewitsch, Dessauer, 1931b; Litvinov, 1938, 1941/.

The paper /Wigand, 1919/ describes the only known attempt to employ an Einthoven galvanometer for the measurement of the current in the counter. In order to increase the current, a large number of measuring capacitors are connected in parallel. Such a method for attaining a high effective capacitance was described earlier in the paper /Kennedy, 1913/. Lately, the parallel connection of several measuring capacitors is again finding application /Mühleisen, 1957b; Hock, Schmeer, 1962; Hoegl, 1963a; Siksna, Eichmeier, 1966/.

An ingenious principle is the operation principle of a simple automatic indicator of ionization anomalies, described in the paper /Milin, Berezina, In'kov, 1954/.

The recent advance in the development of new designs of aspiration counters is due to the application of sensitive cathode electrometers /Godefroy, 1949; Mühleisen, 1957; Dolezalek, 1962a; Hock, Schmeer, 1962; Mendenhall, Fraser, 1963; Hock, 1967/ and dynamic electrometers /Kilinski, 1949, 1953; Callahan, Coroniti, Parziale, Patten, 1951; Curtis, Hyland, 1958; Kraakevik, 1958; Salvador, Masson, 1958; Adkins, 1959; Komarov, Seredkin, 1960; Jonassen, 1962; Saks, 1963; Reinet, Tammet, Salm, 1963; Hoegl, 1963; Reinet, Tammet, Salm, 1967/. A substantial advantage of the cathode and dynamic electrometers consists in the possibility of effecting automatic recording with the aid of the ordinary recording electronic measuring instruments.

In the work /Sozin, 1965/ an instrument is described for measuring the conductivity gradient. In this device a differential cathode electrometer is used.

When the electrometer possesses a high sensitivity, the instability of the power source is of considerable importance. It is necessary in many cases to use bridge and compensation circuits /Komarov, Kuz'menko, 1960; Jonassen, 1962; Reinet, Tammet, Salm, 1963; Kitaev, Kloiz, 1963/. The bridge circuit with a dividing capacitor is also used in the counter designed by the author. The arrangement of the measuring capacitor of this counter is represented in Figure 35.1. The use of an electrometer was described in the paper /Saks, 1963/. A weak flow of specially dried air is blown through the insulated casing. This method of preserving the quality of insulation was treated earlier in the work /Chapman, 1937/.

Although contemporary electrometers enable a nearly complete elimination of leakage via the insulators, quality insulation is still a prerequisite for the suppression of the noise generated by the insulators.

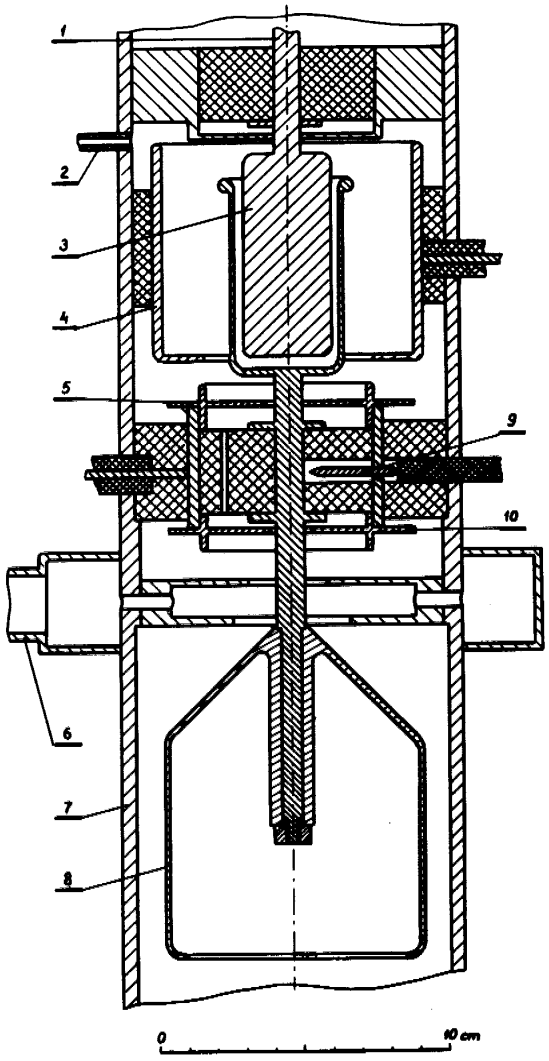

FIGURE 35.1. Schematic diagram of the measuring capacitor of the counter with combined circuit arrangement:

1 — branch to the electrometer; 2 — connecting branch for feeding dried air into the chamber of the insulators; 3 — cylinder of the dividing capacitor; 5 and 10 — screens of the insulator; 6 — branch for pumping out the air; 7 — outer cylinder; 8 — inner cylinder; 9 — switch K_2.

Teflon insulators have an extremely high resistance and are ideally moisture proof, but possess a high emf noise. The best insulating properties are exhibited by sapphire. A perfected design of sapphire insulators for a measuring capacitor is described in the paper /Gunn, 1965/. When designing counters for operation under extremely severe meteorological conditions it is also useful to consider the designs which have been developed for insulating field measuring devices of the collector type /Dolezalek, 1956, 1961; Gadomski, 1965/.

Currently, major effort is being put into the development of universal portable counters intended for the study of various artificial sources of air ions in addition to the study of the natural ionization of atmospheric air. The Israël counter /Israël, 1929/, which is manufactured to this day by Spindler and Choier (F. R. G.), can be considered as the first of the contemporary portable counters. The Israël counter uses two measuring capacitors — one for positive and one for negative air ions. When necessary, the measuring capacitors can be connected in series. The air-flow rate is low and the voltage of the measuring capacitor is relatively low. The two measuring capacitors are of the same size: $r_2 = 3.4$ cm, $r_1 = 2.6$ cm, $l = 50$ cm. A drawback of the Israël counter is the edge effect — the counter is connected according to the arrangement with a grounded inner collector plate and does not possess an electrostatic shield. The counters of Bogoyavlennyi /Lesgaft, 1938/ and Tverskoi /Tverskoi, Otto, 1962/ have similar properties. The latter is described in the paper /Styro, Yurgelionis, 1956/. The Tverskoi counter is equipped with one measuring capacitor for light ions and one for heavy ions. Flow rates of up to 600 cm^3/sec and voltages of up to 300 V are used. The effective capacitance of the measuring capacitor for light ions is 4 cm, and that of the measuring capacitor for heavy ions 105 cm. The instrument dimensions are 80×32×18 cm, and its weight is 16 kg. The simplified Tverskoi counter /Grachev, 1959/, intended for the measurement of light ions only, is even more compact.

Many designs of portable counters were developed by the group of collaborators of the Tartus State University under the direction of Reinet /Reinet, 1959b, 1962a, 1962b, 1963/. In the SAG-2M counter a mechanical electrometer of the type SG-1M is used. The edge effect is suppressed, since the measuring capacitor is connected according to the circuit arrangement with a grounded outer plate. In order to suppress the effect of random fluctuations of the supply voltage on the measurement results a bridge circuit is used. The design of the insulators prevents leakage and parasitic polarization phenomena. The dimensions of the measuring capacitor are $r_2 = 1.95$ cm, $r_1 = 0.95$ cm, $l = 63$ cm. The maximum voltage of the measuring capacitor is 300 volts, the maximum flow rate 600 cm^3/sec. The outside dimensions of the instrument are 85×43×33 cm; the weight is 31 kg.

The dynamic electrometer is used in the counter of Komarov, Kuzmenko and Seredkin /Komarov, Kuzmenko, and Seredkin, 1961/. The dimensions of the measuring capacitors of this counter are chosen on the basis of

theoretical calculations. The edge effect is suppressed by using an electrostatic shield. An improved variant of the bridge circuit was utilized. The rigid design of the measuring capacitors which enables the instrument to be used aboard aircraft deserves attention. The counter of Komarov, Kuzmenko and Seredkin is one of the most highly perfected contemporary counters. However, it is unique and is not manufactured industrially. A counter of the type SI-62 /Kitaev, Kloiz, 1963/ is manufactured in the Soviet Union. The design of this counter consists of elements of the counters of Reinet and of the counter of Komarov, Kuzmenko and Seredkin. The SI-62 counter is provided with two measuring capacitors connected according to the circuit arrangement with a grounded inner collector plate. The dimensions of both capacitors are identical: $r_2 = 1.9$ cm, $r_1 = 1.2$ cm, $l = 58$ cm. The voltage of the measuring capacitor can reach 250 volts and flow rates of up to 1500 cm/sec can be attained. The air-ion current is measured with the aid of a mechanical or cathode electrometer. The weight is 85 kg and the outside dimensions of the instrument are relatively large. A particular feature of the SI-62 counter is the presence of a portable measuring capacitor, which can be installed at a distance of up to 5 m from the remaining parts of the instrument. Royco Instruments, California, manufactures a model 411 light-ion counter and the model 412 counter, having a minimum limiting mobility of 0.0064 $cm^2/V \cdot sec$. The instruments manufactured by Royco are distinguished by the flat geometry of the plates of the measuring capacitor. Kathrein, West Germany, manufactures a model 8310 ionometer, which is characterized by a high sensitivity. The limiting mobility is fixed (0.9 $cm^2/V \cdot sec$). The inner plate of the cylindrical measuring capacitor of the model 8310 counter is tubular. 14% of the air flows through the inner plate and is not utilized for measurements. The demands laid down in § 3 are not satisfied. However, in the instrument model 8310 this does not cause any distortions.

A very compact recording counter of light ions is described in the paper /Giorgi, 1963/.

Several other extremely simplified designs of portable counters with small outside dimensions are known /Grachev, 1962; Derekhaov, 1962/. Their use is limited to checking the operation of artificial air-ion generators, used in medicine and industry. Several models of simplified counters are described in the paper /Livshitz, Moiseev, 1965/.

Special demands are made upon the design of counters for the study of the ionization of the free atmosphere. Counters intended for use aboard aircraft /Wigand, 1914, 1921; Gish, Sherman, 1935; Callahan, Fraucher, 1954; Coroniti, 1960; Kranopevtsev, 1966; Paltridge, 1966/ differ only slightly from standard counters. A particular feature of some instruments /Zachek, 1965/ is the use of special devices to effect a decrease in the compensation of the flow of particles which settle due to inertial forces. Counters used in radiosondes attached to free balloons should operate automatically and weigh not more than a few kilograms. In such counters one utilizes the natural ventilation, arising in a vertically mounted capacitor when the balloon ascends. Owing to the strict technical

demands, radiosondes merely enabled the simplest measurement in the range of high limiting mobilities/Venkiteshwaran, Gupta, Huddar, 1953; Koenigsfeld, 1955, 1957; Venkiteshwaran, 1958; Hatakeyama, Kobayashi, Kitaoka, Uchikawa, 1958; Woessner, Cobb, Gunn, 1958; Mühleisen, Fischer, 1958; Jones, Maddever, Sanders, 1959; Kroening, 1960; Coroniti, Mazarek, Stergis, Kotas, Seymour, Werme, 1954; Uchikawa, 1963, 1966; Paltridge, 1965; Takeuti, Ishikawa, Iwata, 1966; Pavlyuchenkov, 1966/. In the paper /Kroening, 1960/ a mechanical electrometer is used which at the same time serves as an automatic switch /Neher, 1953/. In all the remaining counters for radiosondes different variants of cathode electrometers are used and more rarely dynamic electrometers.

In the paper /Bordeau, Whipple, Clark, 1959/ a counter intended for use aboard a meteorological rocket is described.

In all the counters considered above the integral measuring method is used. Differential methods were used much more rarely. Apart from designs mentioned in the first chapter of the present work, the first-order differential counters described in the papers /De Broglie, 1909; Nolan, P. J., 1926; Young, 1926, Gagge, Moriyama, 1935; Misaki, 1961/ and second-order differential counters described in the papers /Chapman, 1937; Yunker, 1940; Daniel, Brackett, 1951; Hewitt, 1957; Hoegl, 1963a, b/ should be mentioned. The insulator design described in the work /Chapman, 1937/ is worthy of attention. In order to ensure a large leakage resistance under conditions of high humidity of the investigated air an auxiliary flow of dried air is used, which flows around the insulator. The counter described in the work /Hewitt, 1957/ is based on a special principle. In this instrument, the measured air ions do not settle in the capacitor, but are drawn through a narrow slit and are collected in an adsorbent filter which is connected to the electrometer. Here, disturbances caused by the instability of the voltage source are suppressed. This approach is utilized also in the paper /Wnitby, Clark, 1966/.

To measure the space charge density, the method of the adsorption filter is most widespread. Apart from instruments mentioned in the first chapter, space charge counters are described in the papers /Dowling, Haughey, 1922; Wolodkewitsch, Dessauer, 1931a; Pluvinage, 1946; Beau, Blanquet, L., Blanquet, P., 1953; Beau, Blanquet, L., Blanquet, P., Fourton, 1956; Gonsior, 1957; Makhotkin, Sushchinskii, 1960; Moore, Vonnegut, Mallahan, 1961; Arabadzhi, Rudik, 1963; Bent, 1964/. The instrument described in the last paper is distinguished by a highly perfected insulator design and high sensitivity (air-flow rate 3000 cm^3/sec) /Arabadshi, Rudik, 1963/. The highest sensitivity in charge density measurements was attained in the study /Moore, Vonnegut, Mallahan, 1961/, where a filter is described which is capable of letting through an air flow with a flow rate of up to 0.7 m^3/sec.

§36. DESCRIPTION OF A UNIVERSAL INTEGRAL AIR-ION COUNTER

The counter described below (SAI-TGU-66) was designed and built by the staff of the Tartu State University under the direction of the author.

This counter is the last model of a series of constantly improved counters SAI-TGU-64, SAI-TGU-65, SAI-TGU-65 m.

The design was implemented with the aim of ensuring small outside dimensions of the instrument and operating convenience.

The measuring capacitor of the counter is connected according to the circuit with a grounded outer collector plate. The design specifications of the measuring capacitor were calculated accordingly (Figure 36.1). The capacitor is mounted vertically with the entrance opening facing upward. The outer plate (7) is connected to the voltage source via a lower terminal. The terminal is connected to the inner plate by means of a lead, drawn tightly along the axis of the grounded supporting tube. The centering system of the inner plate (8) has 6 degrees of freedom. After all the adjustments are made the system is secured with the aid of epoxy glue. The outer plate (5) is carefully insulated.

The lead of the outer plate through the annular insulator (6) is not shown in the figure. In order to suppress turbulent mixing the outer plate is given a conical form. The conicity is not large and amounts to 1:50. The cross section of the air flow is narrowed down by 30% along the entire length of the inner plate. The inlet opening of the inner plate (2) is covered by a grid (3) of mesh width $h = 2$ mm and made of wire of $r_0 = 50\mu$. The grid shields the conical inlet tube against the inner plate. Apart from this, the grid prevents the entry of insects into the measuring capacitor, guards against accidental touching of the inner plate, which is maintained at high voltage, and suppresses to some extent the turbulence of the incoming air. At a flow rate of 4500 cm^3/sec the adsorption of light ions on the grid is 2 – 3%.

The measuring capacitor can be readily disassembled. After unscrewing the upper shielding tubes (4) the outer plate together with the plastic annular insulator (6) are easily taken out. When it is necessary to separate the inner plate, it suffices to unscrew one bolt and to lift up the plate. After dismounting, all insulators and the plate surfaces are accessible for cleaning. In order to clean the grid of adhering particles, one can hold the removed outer plate upside down (with the grid facing downward) under a water tap with a strong, wide, foamy stream. The grid and the plate of the measuring capacitor are made of aluminum alloys. The capacitance of the measuring capacitor is 51 pF. The effective capacitance of the precondenser is 1 pF. The inner plate of the measuring capacitor (1) is removable and the entrance tube is the outer plate (2).

The block diagram of the counter is shown in Figure 36.2. At the input of the electrometer a dynamic capacitor C_2 is used which modulates the constant signal with a frequency of 425 Hz. The dynamic, small-size capacitor designed by O. V. Saks ensures a modulation coefficient of 0.4 under these operating conditions. The alternating component of the voltage is transmitted from the dynamic capacitor to the amplifier through a double dividing capacitor C_3, C_4. The dividing capacitor has a special design with a guard ring, preventing the self-discharge of the capacitor C_3 on the surfaces of the insulator. The dielectric of the dividing capacitor is a

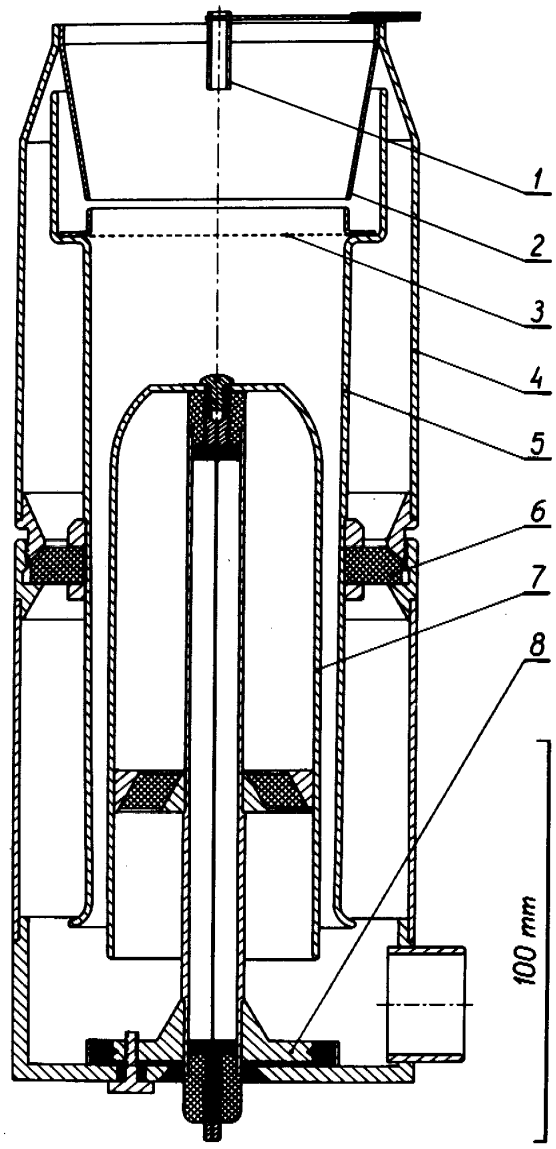

FIGURE 36.1. Measuring capacitor of the SAI-TGU-66 counter.

fluoroplastic film. The constant-voltage signal is amplified 10,000-fold from the dynamic capacitor to the output of the amplifier. From the divider $R_a - R_b$, a 40—120-fold feedback is applied to the input through the resistance R_s. At full scale the voltage across the terminals of the resistor R varies from 70 to 228 millivolts. The voltage between the outer plate and air is only 1.5 millivolts. The electrometer operates as an analog amplifier with a potentially grounded input. The current generated by the air ions is compensated by the current through the resistance R. This system of feedback renders the measurement accuracy practically independent of the drift of the amplifying coefficients of the tubes and also effects a 40—120-fold reduction in the leakage resistance caused by the shunting effect of the insulators of the outer plate.

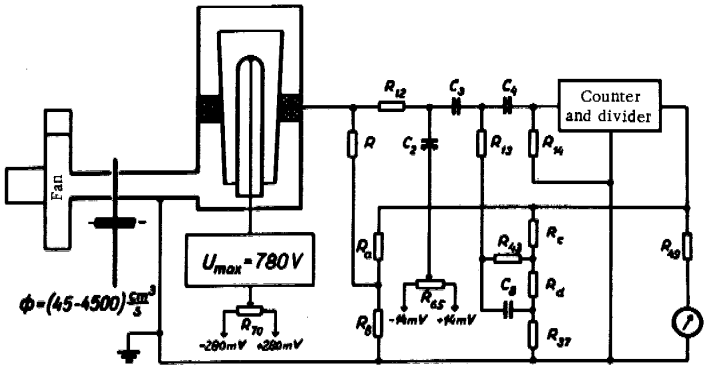

FIGURE 36.2. Block diagram of the SAI-TGU-66 counter.

The shunting effect of the leakage resistance under such conditions is not dangerous. Dirt accumulation becomes marked already at leakage resistance, the shunting effect of which is not felt.

The resistance R is connected depending on the measuring range of the conditional charge density. The largest value is $R=10^{12}$ ohm; the smallest is $R=10^{7}$ ohm.

Feedback is also utilized for the control of the degree of smoothing of the recording of the conditional charge density with time. The smoothing is carried out by an integrating circuit, consisting of resistances R, R_{12}, and the capacitor C_3. An additional feedback signal from the divider $R_c - R_d - R_{37}$ is applied through the capacitor C_3. The auxiliary circuit $R_{43}C_8$ serves for the stabilization of the transient process. The time constant of the transient process depends on the position of the switches, reversing the outlet of the divider $R_c - R_d$ and the resistance R. In the case $R=10^{12}$ ohm the shortest time required to attain 90% of full scale is 35 sec. The largest time constant of smoothing is 1500 sec. In the case $R \leqslant 3.3 \cdot 10^{9}$ ohm these quantities are 2 and 140 sec, respectively.

The potentiometer R_{65} serves to determine the zero of the electrometer. The potentiometer R_{70} serves for the compensation of the contact potential between the plates of the measuring capacitor.

Figure 36.2 shows the block diagram of the air path, consisting of the measuring capacitor, the switch of the diaphragm and the fan. By switching in the calibrated diaphragms flow rates of 45, 142, 450, 1420, or 4500 cm^3/sec can be achieved.

The entire circuit diagram of the counter is shown in Figure 36.3. Data of the circuit are listed in the specifications at the end of the present section.

The power transformer of the counter operates under conditions of ferroresonance, which ensures the stabilization of all voltages in the circuit. The voltage of the inner plate of the measuring capacitor is stabilized in addition by a 2-step stabilizer using SG-303S and SG-301S voltage regulators. The output voltage regulators V_5 and V_6 operate under optimum current conditions (about 14 μA), thermal insulation and mechanical shock absorbers. The attenuator $R_{88} - R_{91}$ and the divider $R_{78} - R_{87}$ are built from stable microwire resistors.

The amplifier of the electrometer consists of an amplification of the alternating current at the pentode V_1, a phase detector at the pentode with two grids V_2, and a series-ballanced amplifier of constant current at the double triode V_4. The pentode V_3 serves as an oscillator for the dynamic capacitor. The magnetizing current for the winding W is stabilized by a 12-fold negative feedback of the constant-current oscillator.

The counter is supplied by an external automatic blocking system, consisting of a relay Rel connected via the bridge $D_6 - D_9$, a limiter $D_2 - D_5$ and the pulse-linked capacitors C_9 and C_{33}. The relay Rel consists of a standard 2-way polarizing relay of the type RP-4. If the moving contact of the relay is in the left-hand position, then the input of the electrometer is shorted. The position of the relay Rel may be judged from the signal lamp L_1. The relay is operated by hand with the aid of the switch S_0. Automatic triggering of the relay occurs in the case of a constant 160% overload of the electrometer when a pulse signal appears on the grid of the tube V_4. The pulse signal arrives on the grid V_4 via a capacitor C_{33} when the voltage of the measuring capacitor is reversed. The high-speed external blocking system prevents high voltages from reaching the outer plate of the measuring capacitor, which in the case of improper operation of the instrument could polarize the insulator and put the instrument out of order for a long time.

The operation of the counter is very simple, since in order to determine the limiting mobility and the range of the conditional concentration, the reading on the counter is merely multiplied.

Let us state some other data on the SAI-TGU-66 counter.

1. The limiting mobility has all told 50 nominal values, determined by the switches. These values are: 8; 6.3; 5; 4; 3.2; 2.5; 1.6; 1.26; 1; 0.8; 0.63; .....; 0.00016; 0.000123; and 0.0001 ($cm^2/V \cdot sec$). The maximum voltage of the measuring capacitor is 780 volts.

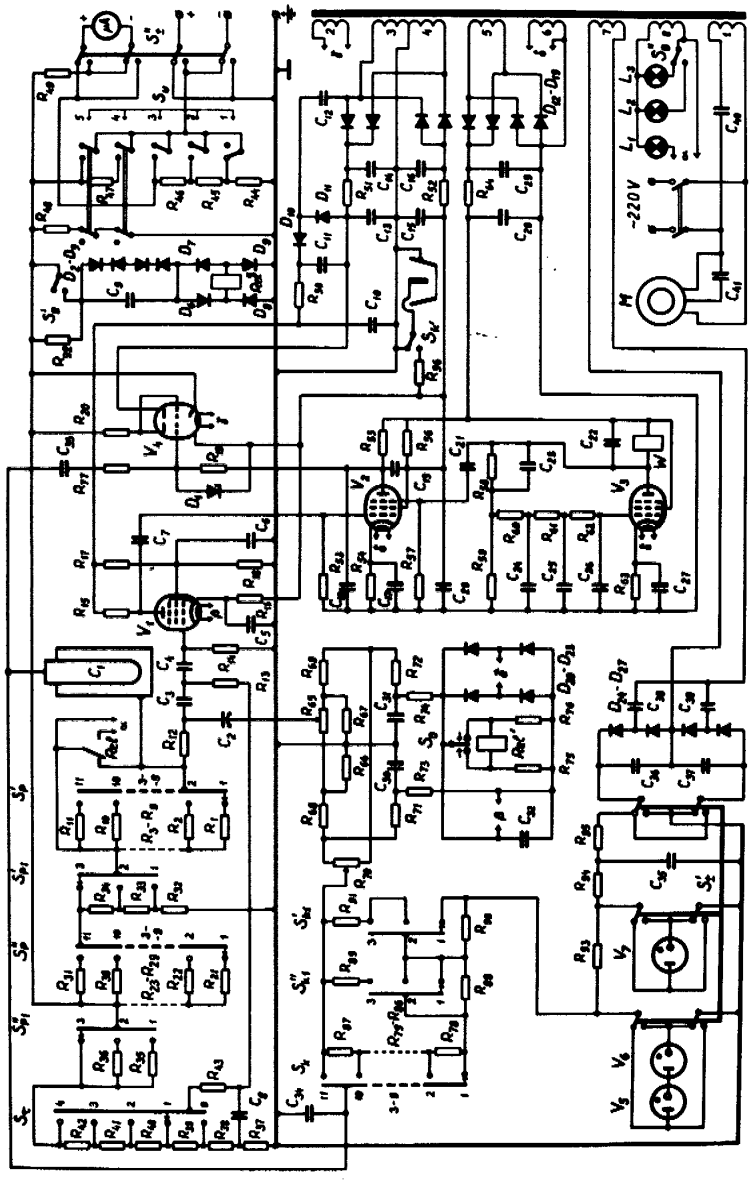

FIGURE 36.3. Circuit diagram of the SAI-TGU-66 counter.

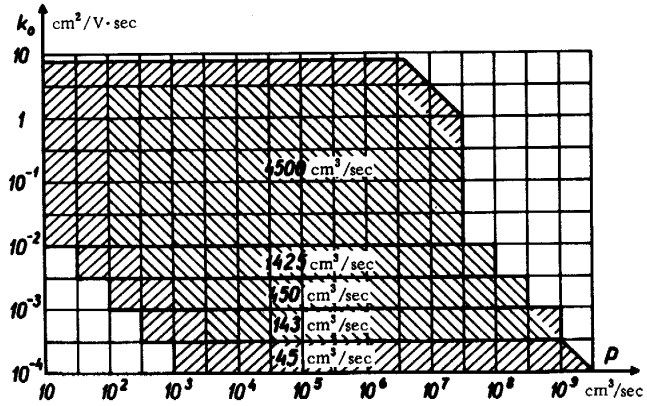

FIGURE 36.4. Measurement limits of the SAI-TGU-66 counter. The hatchings in the other direction correspond to the region in which marked distortions are possible.

2. There are 35 possible ranges of the conventional concentration of the charge with upper limits 100; 200; 316; 632; 1000; ..... 10^9, 2×10^9, 3.16×10^9 (elementary charges/cm³).

3. The actual measurement limits are shown in Figure 36.4.

4. $s_{\tau UC}$ (40 sec) $\approx 10^{-6}$; $\sigma_{UE} \approx 40$ μV; $\sigma_{UR}/R_p \approx 10^{-16}$ A.

5. For light ions $\sigma_p < 10$ elementary charges/cm³, for $k_0 = 0.0005$ cm²/V·sec $\sigma_p < 400$ elementary charges/cm³.

6. The constant of the edge effect is $C/C_1 = 25{,}000$.

7. The counter is provided with a preliminary capacitor having an electric switch. The limiting mobility of the preliminary capacitor at $\Phi = 142$ cm³/sec is 0.12 cm²/V·sec.

8. To the counter we can connect a potentiometric recorder with an input of 10, 100, or 150 mV, or a recording voltmeter with 15V full-scale deflection and a current consumption up to 5 mA. There is also a standard current output up to 5 mA for a load of 2.4 kohm for automatic control devices.

9. The mean measurement error is not higher than 5%.

10. The outside dimensions of the counter (in portable state) are 45 × 23 × 33 cm; the weight does not exceed 12 kg. The required power is not more than 45 watts.

The counter is illustrated in Figure 36.5.

Design specifications for Figure 36.3

I. VACUUM-TUBE AND SEMICONDUCTOR ELEMENTS

V_1 and V_3	V_2	V_4	V_5 and V_6	V_7	$L_1 - L_3$
6Zh 1 P	6Zh 2P	6 N 14P	SG-301 S	SG-303 S	LN3.5—0.28

$D_1 - D_5$	$D_6 - D_{19}$	$D_{20} - D_{23}$	$D_{24} - D_{27}$
D 810	D 226 B	D 7 A	AVS-1-220

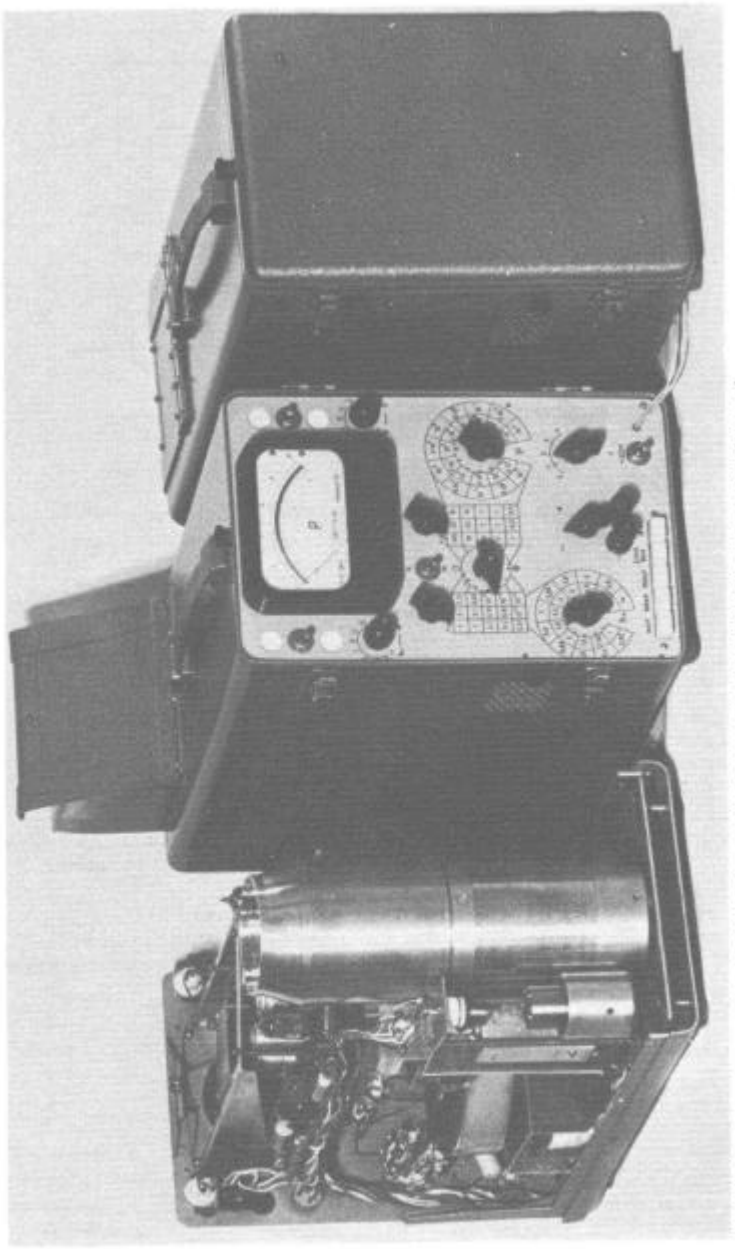

FIGURE 36.5. Three forms of the SAI-TGU-66 counter (with cover removed, in working state, in portable state).

II. CAPACITORS

No.	C	Type	No.	C	Type
1	51	Measuring	22	0.07	KBGI – 200 V
2	25	Dynamic	23	0.05	MBM – 160 V
3	20	Dividing	24	2000	KSO – 500 V
4	40	"	25	2000	"
5	0.25	MBM – 160 V	26	2000	"
6	0.05	"	27	20.0	K50 – 3 – 25 V
7	2000	KSO – 500 V	28	20.0	KE – 2 – 150 V
8	1.0	MBM – 160 V	29	50.0	"
9	1.0	"	30	20.0	K50 – 3 – 6 V
10	0.25	MBM – 500 V	31	20.0	"
11	5.0	KE – 2 – 300 V	32	400.0	ETO – 15 V
12	0.25	MBM – 500 V	33	390	POV – 10 kV
13	20.0	K50 – 3 – 160 V	34	390	"
14	50.0	"	35	0.1	MBM – 1500 V
15	20.0	"	36	0.1	MBM – 1000 V
16	50.0	"	37	0.1	MBM – 1500 V
17	20.0	K50 – 3 – 6V	38	0.25	MBM – 500 V
18	1.0	MBM – 160 V	39	0.25	"
19	1.0	"	40	1.0	MBGCh – 750 V
20	1.0	"	41	2.0	MBGCh – 250 V
21	4700	BM – 200 V			

III. RESISTORS

No.	R	Type	No.	R	Type
1	1000G	KVM	25	33k	MLT – 0.5
2	330G	"	26	33k	"
3	100G	"	27	33k	"
4	33G	"	28	33k	"
5	10G	"	29	33k	"
6	3.3G	"	30	33k	"
7	1G	"	31	33k	"
8	330.0	"	32	158.5Ω	wire
9	100.0	"	33	161	"
10	33.0	"	34	187	"
11	10.0	MBM – 1000 V	35	0.36	MLT – 0.5
12	100G	KLM	36	0.1	"
13	330.0	KIM – 0.125	37	1k	"
14	330.0	"	38	1k	"
15	4.7	"	39	3.6k	"
16	1.5	"	40	12k	"
17	4.7	"	41	36k	"
18	1.0	"	42	0.12k	"
19	1.0	"	43	4.7	"
20	1k	"	44	100	wire
21	33k	"	45	900	"
22	33k	"	46	500	"
23	33k	"	47	600	"
24	33k	"	48	3.6k	MLT – 0.5

III. RESISTORS (cont.)

No.	R	Type	No.	R	Type
49	0.148	MVSG – 0.5	73	2.4 k	MLT – 0.5
50	0.24	MLT – 0.5	74	2.4 k	"
51	1 k	"	75	3.6 k	"
52	1 k	"	76	3.6 k	"
53	15.0	KIM 0.125	77	1.0	"
54	3.6 k	MLT – 0.5	78	4.58**	MVSG – 0.5
55	0.47	"	79	3.64**	"
56	0.36	"	80	2.89**	"
57	0.12	"	81	2.29	"
58	2.0	"	82	1.82	"
59	0.36	"	83	1.445	"
60	0.27*	"	84	1.149	"
61	0.36	"	85	0.911	"
62	0.36*	"	86	0.725	"
63	2.4 k	"	87	2.80	"
64	1 k	"	88	20.0**	"
65	220	SPO – 0.5	89	2.47	"
66	100	MLT – 0.5	90	20.0**	"
67	100	"	91	2.47	"
68	1 k	"	92	1.5	"
69	1 k	"	93	9.4**	MLT – 0.5
70	1 k	SPO – 0.5	94	2.0	"
71	1 k	MLT – 0.5	95	4.0**	"
72	1 k	"	96	0.1	"

IV. ELECTROMAGNETIC ELEMENTS

R – relay built from RP-4, 6 kohm windings
L – winding of the dynamic capacitor
M – synchronous electric motor G – 31 A
A – instrument M 265, 100 μA

V. WINDINGS OF THE TRANSFORMER

1 – 2400 × PEL 0.21
2 – 46 × PEL 0.51
3 – 700 × PEL 0.07
4 – 700 × PEL 0.07
5 – 750 × PEL 0.10
6 – 46 × PEL 0.25 × 2
7 – 3000 × PEL 0.05
8 – 25 × PEL 0.25 × 3

The designations are given in order of spacing of the windings.

Between the windings 1 – 2, 4 – 5, 6 – 7, 7 – 8, a fluoroplastic insulator was placed.

* More accurate upon adjustment.
** Two equal resistors in series.

LIST OF SYMBOLS

(The section defining the quantity or the defining formula is indicated in parentheses)

A — Relative adsorption (24.10).
C — Effective capacitance (§4).
C — Capacitance of edge effect (§14).
C_p — Parasitic capacitance.
C_0 — Total capacitance of the insulated system.
D — Coefficient of diffusion.
E — Electric field strength.
G — Kernel of the integral equation of an aspiration counter (§3).
I — Current intensity. *
K — Boltzmann constant.
L — Maximum value $\lambda_{\pm} \Phi/k_0/(k_0)$ (§32).
N — Electric flux. *
P — See Greek P.
Q — Charge. *
R — Resistance.
R_p — Leakage resistance (§26). R_p
$\bar{R}$ — Relative effective scale of turbulence (§20). $\bar{R}$
Re — Reynold's number (15.1), (21.7), (§34).
S — Surface area.
T — Absolute temperature.
U — Voltage between the collector and repulsive plate. *
U — Equilibrium voltage of the collector plate (§16). *
V — Volume.
a and b — Constants of the measuring capacitor (16.6), (16.7), (16.8), (16.18).
d — Differential; distance between the plates of a parallel-plate measuring capacitor.
e — Elementary charge.
g — Acceleration due to gravity.
h — Mesh width of grid.
h_ψ — Operator $1 - \psi \frac{\partial}{\partial \psi}$ (5.1).
j — Current density.
$\dot{k}$ — Mobility (1.1). *
$\dot{k}_0$ — Limiting mobility (4.3). *
$\dot{k}'$ — Characteristic mobility (16.14), (16.21). *
l — Length of measuring capacitor.
ln — Natural logarithm.
lg — Logarithm to the base 10.
m — Mass of air-ion; subscript, taking on integral numbers.
n — Subscript, taking on integral numbers.
q — Charge of air-ion. *
r — Distance from the axis of the capacitor.
r_0 — Wire radius.
r_2 and r_1 — Radii of the outer and the inner plate of a cylindrical capacitor.
s — Relative standard deviation.

* For footnote, see p.160.

$s_{\Delta UC}$ and $s_{\vartheta UC}$ — Relative standard deviation, characterizing the stability of the voltage supply and the effective capacitance of the measuring capacitor, respectively (§28).
s_Δ and $s_{\Delta\Delta}$ — Standard deviations characterizing the stability of the conditional charge density (§30).
t — Time.
t_0 — Filling time of the measuring capacitor (13.1), (13.2).
u — Velocity of air flow.
u_0 — Velocity of the potential flux at a distance from the surface: mean velocity of the turbulent flow.
v — Velocity of air-ion.
x — Distance along the axis from the beginning of the measuring capacitor; arbitrary quantity.
y — Distance from the surface of the plate.
Δ — Difference, absolute errors.
Λ — Conditional conductivity (5.21).
P — Conditional charge density (5.14).
Φ — Flow rate (throughput rate). *
α and β — Voltage ratios (§29).
δ — δ-Function; relative deviation of some quantity; limiting relative error.
ε — Turbulent intensity (20.3).
ϑ — Dimensionless time (19.22), (27.12).
λ — Conductivity (§1).
$\lambda_{\pm}$ — Polar conductivity (§1).
$\lambda(\dot{k}_1, \dot{k}_2)$ — Partial conductivity (1.7). *
μ and μ_t — Constants of the measuring capacitor (§19); (§20).
ν — Kinematic viscosity.
ϱ — Charge density. *
$\varrho(\dot{k})$ — Charge density spectrum (§1). *
$\varrho(\dot{k}_1, \dot{k}_2)$ — Partial charge density (1.5). *
σ — Standard deviation.
σ_{QK} — Standard deviation of the charge, generated the moment the switch is opened (§28).
σ_{UE} — Mean-square error in measuring the voltage with the aid of an electrometer.
σ_{UR} — Mean-square value of the emf of the insulator (§28).
τ — Time constant.
ψ — Arbitrary parameter of the measuring capacitor C, U, or Φ.
$\omega = 1/\dot{k}_0$. *

In the figures a square with the letter U denotes a voltage source, a circle with the letter I an ammeter, a circle with the letter E an electrometer.

* The symbol without a dot denotes the absolute value of the considered quantity: $x = |\dot{x}|$ (§1).

APPENDIX I

Special Factors in Measurement at High Altitudes

The measurement of the air-ion spectrum at high altitudes differs from ground-level measurement primarily in that the former is carried out under conditions of low pressure and correspondingly high mobility. The mobility of light ions is inversely proportional to the air density /Loeb, 1960/ over a large range and is calculated via the formula

$$k = \frac{p_n T}{p T_n} k_n, \qquad (A.1)$$

where k, p, T are respectively the mobility, pressure, and absolute temperature, and k_n, p_n, T_n are respectively the values of the same quantities under normal conditions. The first column of the summary Table A lists data on the standard model of the atmosphere CIRA 1961 and correspondingly calculated mobilities of O_2^+ ions. The initial value for the mobility of O_2^+ ions was taken from the paper /Maushart, 1968/.

We shall consider briefly some problems which specifically apply to measurements at high altitudes:

1. The uncertainty in the mobility. The mobility is in principle determined in a system, the dimensions of which are considerably larger than that of the free mean path of the particles. Therefore, particles of normal dimensions are not suitable for measuring the mobility of molecular ions at altitudes higher than 90 kilometers, where the mean free path is of the order of 1 cm or more. Values for the mean free path length l_o at different altitudes are listed in Table A.

2. Permissible field strengths. If the energy transferred to the air-ions by the electric field is of the same order of magnitude as the mean energy of thermal motion, then the law describing the proportionality of velocity to field strength is no longer valid.

An estimate on the basis of the formula $KT \approx m(kE)^2$ and experimental data /Mitchell, Riedler, 1934; Balog, 1944/ indicate that under normal conditions a field strength exceeding 10 kV/cm is inadmissible. Results of the calculation of E_{max} at different altitudes are shown in Table A.

3. Permissible air velocity. At high altitudes the kinematic viscosity of air increases. Quantitative data are given in Table A. It is easier, therefore, to maintain a laminar flow. Table A gives the velocity u_{cr}, at which $Re = ur/\nu$ in a tube with diameter d cm reaches the value 100 d. At an altitude of 50 km u_{cr} exceeds the speed of sound. The operation of aspiration counters under ultrasonic conditions has not been studied. Using conventional instruments and computation methods, a velocity of 200 m/sec should not be exceeded (the sound speed at an altitude of 80 km equals 270 m/sec).

4. Measurement of the air flow rate. No convenient methods are known for the direct measurement of the air flow rate through a measuring capacitor at high altitudes. In practice, the flow rate is determined by calculation from the velocity at which the instrument moves. This imposes additional limiting demands on the counter design and introduces an element of uncertainty into the measurement results. To increase the accuracy the instrument must be calibrated with the aid of a complex device /Oster, Dolezalek, 1966/.

5. Air-ion distribution. In the range of high mobilities the linear dispersion dx/dk (x is the settling coordinate of an ion entering the measuring capacitor at the edge of the repulsive plates) of air ions in a measuring capacitor is small, which distorts the distribution of air ions over the mobilities in the differential measuring capacitor /Dolezalek, 1962b; Dolezalek, Oster, 1965, 1965b/.

The dispersion depends on the angle between the air-ion trajectories and the flow lines of the air flow. Table A lists values of the field strength E_{cr}, at which the slope of the trajectories of O_2^+ ions in a flow of velocity u_{cr} or 200 m/sec (if $u_{cr} > 200$ m/sec) equals 45°. A comparison of the values listed under E_{max} and E_{cr} shows that at $H \geq 50$ km, $E = E_{max}$ and $u = 200$ m/sec the slope of the trajectories of the O_2^+ ions is close to 45°

6. Volta effect. The induced decrease in the working voltage of the measuring capacitor increases the relative value of the contact potentials between the plates of the measuring capacitor as well as the corresponding error in the determination of the limiting mobility. The contact potential between the plates of a standard measuring capacitor is of the order of 0.1 V, which at a height of 80 km causes a serious error. The contact potential is very unstable, and, consequently, it is difficult to make allowance for it. For this it would be necessary to plot the characteristics in the mobility range /Bordeau, Whipple, Clark, 1959/. In order to suppress the Volta effects the plates of the measuring capacitor are covered with a homogeneous, chemically stable substance. From experience in the manufacture of oscillating capacitors for electrometers it is known that the best results are obtained by gold plating. This is considered in the design of special measuring capacitors for operation at low pressures /Dolezalek, Oster, 1965, 1966a/.

7. Diffusion of air ions. The limiting resolving power of the spectroscopic instrument (Formula (34.21)) depends primarily on the voltage of the measuring capacitor. A decrease in the voltage limits the resolving power. Table A gives values of the maximum possible resolving power for an ideal capacitor geometry ($\mu = 1$) and the condition $U = E_{cr}$ 5 cm. The limiting resolving power R_d and the dispersion dx/dk are inversely proportional to each other. The maximum obtainable resolving power is achieved for a compromise of the operating conditions.

8. Electrode effect. An increase in the mobility with altitude causes an increase in the electrode effect inside the measuring capacitor. Data on the conductivity /Coroniti, Nazarek, Stergis, Kotas, Seymour, Werme, 1954; Bordeau, Whipple, Clark, 1959/ are given in Table A. An adjacent column lists values of the relative error δ, calculated from formula (18.6), assuming $l = 10$ cm, $u = u_{cr}$ or 200 m/sec.

The electrode effect causes a decrease in the current in the measuring capacitor. The assumption that under the limiting operating conditions $I_{max} = (n_+ + n_-)\, e\, \phi$ /Bragin, 1965, 1966/ is unfounded.

9. Free electrons. From results of direct measurements /Bragin, 1966/ the negative charge carriers are ions at heights up to 70 km and electrons at heights exceeding 80 km. The aspiration method is not suitable for the study of free electrons. The presence of free electrons complicates the evaluation of the electrode effect.

10. Possibility of using a magnetic field. The magnetic force $\frac{v}{c}qB$ (c is the light speed, B is the magnetic induction) equals the electric field E when

$$B = B_{cr} = \frac{c}{k}. \qquad (A.2)$$

If c and k are expressed in cgs units, then B_{cr} is given in G (gauss). The values of B_{cr} are listed in the last column of Table A.

In practice, we can readily achieve a magnetic induction of the order of 10^4 G. Consequently, starting at an altitude of approximately 50 km magnetic forces can be used to deflect air ions.

The above-mentioned factors (1—9) render the measurements difficult. Positive factors are only the possibility of increasing the flow rate and the high polar charge density in the mesosphere and the ionosphere. This enables us to relax the demands on the sensitivity of the electrometer and to shorten the time required for the counts.

The simplest instruments are those which are intended to measure only the mobility or the polar charge density /Hok, Spencer, Dow, 1953; Bordeau, Whipple, Clark, 1959; Pedarsen, 1964; Bragin, 1965/. In these instruments supersonic operating conditions are possible. Notwithstanding the simplicity of the instrument, the accuracy of measurement results requires additional analysis. One must consider the ratio of the mean free path length of the ions to the dimensions of the measuring capacitor and the ratio of the employed field strength to E_{max} (Table A). In the ionosphere certain phenomena leading to distortions are encountered /Kagan, Perel', 1956/.

More complicated are the measurements for determining the spectrum. To increase the spectral dispersion of the measuring capacitor a new method was proposed and developed /Dolezalek, 1962b; Dolezalek, Oster, 1965, 1966a, b/, which uses an alternating field. The essence of the method of Dolezalek is explained in Figure A, taken from the paper /Dolezalek, Oster, 1965b/. The lower arrangement corresponds to the new method. The ions enter the measuring capacitor via a narrow slit only during a defined phase of the alternating voltage; the remaining air is de-ionized. The instrument is a differential counter of the second order. To obtain an increasing amplitude of the alternating field along the axis the repulsive plate is divided. The manufactured measuring capacitors /Dolezalek, Oster, 1965, 1966a, b/ are cylindrical.

The method of Dolezalek is also used for integral measurement /Oster, Coroniti, 1968/.

Starting at a height of 50 km most spectrographic measurements seem to be possible /Narcisi, Bailey, 1965/. At the same height the method of grid stops is also effective /Bragin, 1962, 1963/.

Above 80 km the aspiration method is no longer applicable for spectrum measurements. A review of the results obtained in a study of the ionization in the higher atmospheric layers can be found in the paper /Sagalyn, 1965/.

TABLE A. Air-ion trajectories in a differential measuring capacitor with a constant and alternating field

H	p	T	l_0	$k(O_2^+)$	E_{max}	ν	u_{cr}	E_{cr}	R_d	λ_+	δ	B_{cr}
0	1020	289	$6.6 \cdot 10^{-6}$	2.3	10000	0.15	0.3	13	18	0.0001	0.02	$4 \cdot 10^7$
10	270	222	$1.9 \cdot 10^{-5}$	6.8	3400	0.35	0.7	10	18	0.0022	0.2	$1.5 \cdot 10^7$
20	55	217	$9.1 \cdot 10^{-5}$	32	740	1.6	3.2	10	18	0.014	0.3	$3 \cdot 10^6$
30	12	228	$4.4 \cdot 10^{-4}$	160	150	8.1	16	10	18	0.06	0.2	600000
40	2.9	248	$2.0 \cdot 10^{-3}$	700	33	39	78	11	18	0.55	0.4	140000
50	0.79	270	$7.9 \cdot 10^{-3}$	2800	8.3	170	330	7	14	1.8	0.6	35000
60	0.23	258	0.027	9400	2.5	540	—	2.1	8	5.4	1.7	11000
70	0.055	217	0.092	32000	0.72	1600	—	0.6	4.5	23	7	3000
80	0.010	185	0.42	150000	0.16	6400	—	0.14	2.4	—	—	700
90	0.0016	181	2.61	920000	0.025	39000	—	0.02	1	—	—	110
km	mb	°K	cm	$cm^3V^{-1}s^{-1}$	Vcm^{-1}	cm^2s^{-1}	ms^{-1}	Vcm^{-1}	1	CGSE	%	G

APPENDIX II

Systems of Units

According to the recommendation of the IAMAP/IAGA the preferred system of units for atmospheric electricity is the SI(MKSA) system. In the present work the CGSE system is used, whereby not only units but also many formulas appear in a different form. In order to convert the formulas to the SI system, the following rules are useful:

1. The number 4π, related to the dependence of the charge on the electric field, should be replaced by $1/\varepsilon_0 \cdot \varepsilon_0 = 8.854\,\mathrm{pF/m}$.
2. The expression $\ln(r_2/r_1)$, derived from the formula for the capacitance of the coaxial capacitor, must be changed to $\ln\frac{r_2}{r_1}/4\pi\varepsilon_0$.

Examples:

Formula No.	Formula in SI system
4.3	$k = \frac{\varepsilon_0 \phi}{CU}$
4.4	$G = \begin{cases} CUk/\varepsilon_0 & \text{for } k \leqslant k_0 \\ \phi & \text{for } k_0 \leqslant k \end{cases}$
33.1	$C = 2\pi\varepsilon_0 l / \ln \frac{r_2}{r_1}$

Conversion table for units and constants

Quantity	SI	CGSE	Conversion factor
I	$1\,A$	$= 3\cdot10^{9}\ \mathrm{ESU_I}$	$= 6.24\cdot10^{18}\ e\ sec^{-1}$
U	$1\,V$	$= 3.33\cdot10^{-3}\ \mathrm{ESU_U}$	
R	$1\,\Omega$	$= 1.11\cdot10^{-12}\ \mathrm{ESU_R}$	
C	$1\,F$	$= 9\cdot10^{11}\,cm$	$= 6.24\cdot10^{18}\ eV^{-1}$
ρ, P	$1\,cm^{-3}$	$= 3\cdot10^{3}\ \mathrm{ESU_S}\ \rho$	$= 6.24\cdot10^{12}\ e\,cm^{-3}$
$\rho(k)$	$1\,kgm^{-3}\,sec^{-1}$	$= 10^{3}\,g\,cm^{-3}\,sec^{-1}$	$= 6.24\cdot10^{8}\ eV\,cm^{-5}\,sec$
k	$1\,m^2V^{-1}sec^{-1}$	$= 3\cdot10^{6}\ \mathrm{ESU_k}$	$= 10^{4}\,cm^2V^{-1}\,sec^{-1}$
λ	$1\,sec\,m^{-1} = 1\,\Omega^{-1}m^{-1}$	$= 9\cdot10^{9}\ \mathrm{ESU_\lambda}$	$= 10^{-2}\,\Omega^{-1}cm^{-1}$
e	$= 1.602\cdot10^{-19}\,C$	$= 4.803\cdot10^{-10}\ \mathrm{ESU_Q}$	$= 1\,e$
K	$= 1.38\cdot10^{-23}\,J\,deg^{-1}$	$= 1.38\cdot10^{-16}\,erg\,deg^{-1}$	$= 8.62\cdot10^{-5}\,eV\,deg^{-1}$

Bibliography

Publications in Russian

Al'tberg, V. Molekulyarnye iony v gazakh i novyi metod izmereniya razmerov molekul (Molecular Ions in Gases and a New Method for Measuring the Sizes of Molecules). — ZhRFKhO, fiz., 44(8):41—458. 1912. (7)*

Al'tberg, V. See Altberg, W.

Arabadzhi, V. I. and I. K. Rudik. Ob elektrizatsii pyli v atmosfere (On the Electrification of Dust in the Atmosphere). — Izvestiya Vyssh. Uch. Zav., Fizika, No. 1:85—88. 1963. (26, 35).

Balog, I. I. Podvizhnost' otritsa tel'nykh ionov pri vysokikh napryazhennostyakh elektricheskogo polya (Mobility of Negative Ions at High Electric Field Intensities). — Uch. Zap. MGU, Vol. 74:123—134. 1944. (1)

Baranov, V. I. Vliyanie medlennykh ionov na izmerenie elementov atmosfernogo elektrichestva (Influence of Intermediate Ions on the Measurement of the Elements of Atmospheric Electricity). — Zh. Russk. fiz.-khim. obshchestva, ch. fiz., 57(1/2):151—170. 1925. (25—29)

Baranov, V. I. See Baranov, W. J.

Baranov, V. I. and M. D. Kravchenko. O bystrykh izmeneniyakh ionizatsii vozdukha (On the Rapid Measurement of Air Ionization). — Geofiz., 4(3):379—385. 1934. (30)

Berezina, I. I. See Milin, V. B.

Bragin, Yu. A. O vozmozhnosti izmereniya podvizhnostei i kontsentratsii zaryazhennykh chastits v atmosfere metodom zatvorov (On the Possibility of Measuring the Mobility and Concentration of Charged Particles in the Atmosphere by Means of the Screening Method). — Trudy Tsentr. Aerol. Observ., Vol. 42:109—115. 1962. (0)

Bragin, Yu. A. O metode izmereniya kontsentratsii zaryazhennykh chastits vozdukha (On the Method of Measuring the Concentration of Charger Air-particles). — Trudy Tsentr. Aerol. Observ., Vol. 46:96—100. 1963. (0)

* The numbers in brackets indicate the paragraph of the text in which the work is cited; (0) indicates the Introduction.

Chernyavskii, E.A. Novaya konstruktsiya pribora dlya opredeleniya chisla i unipolyarnosti ionov (New Design of Instrument for the Determination of the Number and Unipolarity of Ions).— Inf. Sbornik po zemn. magn. i elektrichestvu, Vol. 4:96—98. Leningrad-Moskva. 1937.
(35)

Chernyavskii, E.A. Elektricheskoe pole Srednei Azii. Ionizatsionnye kharakteristiki atmosfery (The Electric Field of Soviet Central Asia. Ionization Characteristics of the Atmosphere).— Trudy Tashkentskoi Geofiz. Observatorii, Vol. 13:162—203. 1957.
(35)

Chernyavskii, E.A. Metod i pribor dlya opredeleniya ob"emnogo zaryada pri gidroaeroionizatsii (A Method and Instrument for the Determination of the Space Charge in Hydroair Ionization).— In Sbornik: "Aeroionizatsiya i gidroaeroionizatsiya v meditsine," pp. 226—228, Tashkent, Gosmedizdat UzSSR. 1962.
(0)

Dunskii, V.F. and A.V.Kitaev. Osazhdenie unipolyarno zaryazhennogo aerozolya v zakrytom pomeshchenii (Precipitation of Unipolar Charged Aerosols in a Closed Room).— Kolloidnyi Zhurnal, 22(2): 159—167. 1960.
(2)

Fedorov, E.K. Novyi metod issledovaniya ionnogo spektra v atmosfere (A New Method for the Investigation of the Ionic Spectrum in the Atmosphere).— Doklady AN SSSR, 82(5):717—718. 1952.
(0)

Fuks, N.A. Mekhanika aerozolei (Mechanics of Aerosols).— Moskva, Izd. AN SSSR. 1955.
(0, 24, 29)

Furman, A.M. Raspredelenie po podvizhnosti i kontsentratsii legkikh i srednikh ionov v atmosfere (The Distribution According to Mobility and Concentration of Small and Intermediate Ions in the Atmosphere).— Trudy Glavnoi Geofiz. Observ., Vol. 97:106—116. 1960.
(15)

Gerasimova, M.N. Proekt pribora dlya izmereniya chisla ionov v atmosfere (Project of an Instrument for Measuring the Number of Ions in the Atmosphere).— Inf. sbornik po zemn. magn. i elektr., Vol. 3:50—51. 1937.
(35)

Gerasimova, M.N. K metodike izmereniya soderzhaniya ionov v atmosfere i o novom schetchike ionov (On Methods of Measuring the Ion Content in the Atmosphere and on a New Ion Counter).— Trudy Glav. Geofiz. Observ., Vol. 30:86—112. 1939.
(5, 29, 34, 35)

Gerasimova, M.M. Soderzhanie malykh i bol'shikh ionov v atmosfernom vozdukhe po nablyudeniyam v Slutske (The Small- and Large-Ion Contents in Atmospheric Air According to Observations in Slutsk).— Trudy NIU GMS SSSR, Ser. 1, 5, pp. 3—23. 1941a.
(35)

Gerasimova, M.N. K metodike izmereniya soderzhaniya malykh i srednikh ionov (On Methods for Measuring the Small- and Intermediate-Ion Concentrations).— Trudy NIU GMS SSSR, Ser. 1, 5, pp. 24—40. 1941b.
(10, 24)

Grachev, V.I. Opredelenie kontsentratsii legkikh ionov u gornykh rek i vodopadov v raione El'brusa (The Determination of the Concentration of Light Ions on Mountains at Rivers and near Waterfalls in the Elbrus Area).— Vopr. Kurortol., Vol. 5, pp. 87—96, Riga. 1959.
(35)

Grachev, V.I. Portativnyi schetchik ionov dlya proverki raboty ionizatorov (A Portable Ion Counter for Checking the Operation of Ion Generators).— In Sbornik: "Aeroionizatsiya i gidroaeroionizatsiya v meditsine," pp. 236—237, Tashkent, Gosmedizdat UzSSR. 1962.
(35).

Grinberg, G.A. Izbrannye voprosy matematicheskoi teorii elektricheskikh i magnitnykh yavlenii (Selected Problems from the Mathematical Theory of Electric and Magnetic Phenomena).— Moskva-Leningrad, Izd. AN SSSR. 1948.
(32)

Gubichev, V.A. Izmerenie ionnogo spektra v vozdukhe g. Rostov-na-Donu (Measurements of the Ion Spectrum in the Air of Rostov-on-Don).— Uchenye Zapiski Rostovskogo Universiteta, 32(4):183—189. 1955.
(25)

Gubichev, V.A. Ob izmerenii ionizatsii atmosfery (On the Measurement of Atmospheric Ionization).— Izvestiya Vysshikh Uchebnykh Zavedenii, Fizika, No.1:57—59. 1960.
(0, 34)

Gutman, L.N. See Tsvang, L.R.

Imyanitov, I.M. Dinamicheskie metody izmereniya malykh tokov (Dynamic Methods for the Measurement of Weak Currents). — Trudy Glav. Geofiz. Observ., Vol. 35:42—57. 1952.
(9)

Imyanitov, I.M. Sposob izmereniya ob"emnykh zaryadov (A Method for Measuring Space Charges).— Byulleten' Izobret. No.7, Patent No. 91089. 1957.
(11)

Imyanitov, I.M. Pribory i metody dlya izucheniya elektrichestva atmosfery (Instruments and Methods for Studying the Electricity of the Atmosphere).— Moskva, Gostekhteoretizdat. 1957.
(5, 29, 35).

Imyanitov, I.M. Konstruktsiya schetchikov ionov i vozmozhnosti ikh primeneniya v meditsine (Designs of Ion Counters and Possibilities to Apply them in Medicine).— In Sbornik: "Materialy nauchn. konf. po prob. "Aeroionizatsiya v gigiene truda," 11—15 noyabrya 1963, pp. 19—20, Leningrad. 1963.
(9)

Imyanitov, I.M., S.I.Zachek, B.K.In'kov, and K.A.Semenov. Pribor dlya izmereniya elektricheskoi provodimosti vozdukha u poverkhnosti zemli (An Instrument for Measuring the Electric Conductivity of Air at the Earth's Surface).— Trudy Glav. Geofiz. Observ., Vol. 110:53—66. 1960.
(14, 15)

In'kov, V.K. Izmerenie plotnosti ob"emnykh zaryadov elektrostaticheskim flyuksmetrom (Measurement of the Density of Space Charges with the Aid of an Electrostatic Fluxmeter).— Uchenye Zapiski Kirovskogo Gosudar. Pedagog. Instituta, Vol. 15:73—80. 1958.
(11)

In'kov, V.K. See Imyanitov, I.M., Milin, V.B.

Istomin, K.G. Mass-spektrometricheskie izmereniya ionnogo sostava verkhnei atmosfery na tret'em iskusstvennom sputnike zemli (Mass Spectrometric Measurement of the Ionic Composition of the Upper Atmosphere on the Third Satellite of the Earth). — Doklady AN SSSR, 129(1):81— 84. 1959.
(0)

Ivanov, N.M., G.M.Kuklina, and Yu.G.Sedunov. Metodika izmerenii ionnogo spektra s vysotnoi machty (The Method of Ion-Spectrum Measurement from a High Mast).— In Sbornik: "Issledovaniya nizh. 300 metr. sloya atmosf.," pp. 92—101, Moskva, Izd. AN SSSR. 1963.
(13)

Izergin, A.M. Issledovanie ekraniruyushchikh svoistv setki (Investigation of the Screening Properties of a Grid).— Uchenye Zapiski Kirovskogo Gosudarstvennogo Ped. Instituta, Vol. 15:45—56. 1958.
(6)

Kagan, R.L. K uchetu inertsii pribora pri meteorologicheskikh izmereniyakh (Calculation of the Inertia of Instruments for Meteorological Measurements).— Izv. AN SSSR, Ser. Geofiz., No. 2:302— 308. 1964.
(30)

Kitaev, A.V. K primeneniyu ionizirovannogo vozdukha i unipolyarnykh aerozolei (Application of Ionized Air and the Unipolar Aerosols).— Zhurnal Fiz. Khim., 36(6):1136—1139. 1962.
(2, 11)

Kitaev, A.V. and L.N.Kloiz. Spektrometr ionov i elektroaerozolei (Spectrometer of Ions and Electroaerosols).— Trudy Vsesoyuznogo Nauchno-Issledov. Instituta Med. Instr. i Oborud., Vol. 1:131—134. 1963.
(35)

Kitaev, A.V. See Dunskii, V.F.

Kloiz, L.N. See Kitaev, A.V.

Kochin, N.E., I.A.Kibel', and N.V.Roze. Teoriticheskaya gidromekhanika (Theoretical Hydromechanics). Part 2.— Moskva, Fizmatgiz. 1963.
(23)

Komarov, N.N. Voprosy rascheta neustanovivshikhsya tokov v izmeritel'nykh kondensatorakh schetchikov ionov i ionnykh spektrometrov (Problems of Calculating the Nonsteady Currents in Measuring Capacitors of Ion Counters and Ionic Spectrometers).— Izv. AN SSSR, Ser. Geofiz., No. 2:309—317. 1960a.
(0, 13, 16)

Komarov, N.N. Nekotorye rezul'taty issledovanii neustanovivshikhsya tokov v schetchikakh ionov (Some Investigation Results on Nonsteady Currents in Ion Counters).— Izv. AN SSSR, Ser. Geofiz., No. 3: 459—466. 1960b.
(0, 13, 16, 17).

Komarov, N.N. Metody i nekotorye rezul'taty izmereniya ionizatsionnogo sostoyaniya svobodnoi atmosfery (Methods and Some Results in Measuring the Ionization State of the Free Atmosphere).—In Sbornik: "Issledovanie oblakov osadkov i grozovogo elektrichestva," pp. 295—265 [sic], Moskva, Izd. AN SSSR. 1961.
(32)

Komarov, N.N. and M.D.Kuz'menko. Schetchik atmosfernykh ionov (A Counter of Atmospheric Ions).— Byulleten' Izobret., No. 4, Patent No. 126287. 1960.
(31, 35)

Komarov, N.N., M.D.Kuz'menko, and A.A.Seredkin. Izmereniya ionizatsionnogo sostoyaniya svobodnoi atmosfery v usloviyakh antitsiklona (Measurements of the Ionization State of the Free Atmosphere under Conditions of an Anticyclone).—Izv. AN SSSR, Ser. Geofiz., No. 10:1534—1540. 1960.
(0)

Komarov, N.N., M.D.Kuz'menko, and A.A.Seredkin. Schetchik atmosfernykh ionov (Counter of Atmospheric Ions).— Izv. AN SSSR, Ser. Geofiz., No. 12:1875—1881. 1961.
(31, 32, 34, 35)

Komarov, N.N. and A.A.Seredkin. Schetchik tyazhelykh ionov (A Counter of Heavy Ions).— Izv. AN SSSR, Ser. Geofiz., No. 11:1663—1670. 1960.
(0, 4, 34, 35)

Komarov, N.N. See Tsvang, L.R.

Korsunskii, M.M., M.V.Reznik, and R.M.Truten'. O metode scheta ionov generiruemykh gidroionizatorom (On the Method of Counting Ions Generated by a Hydroionizator).— In Sbornik: "Aeroionizatsiya i gidroaeroionizatsiya v meditsine," pp. 295—301, Tashkent, Gosmedizdat UzSSR. 1962a.
(0)

Korsunskii, M.M., M.V.Reznik, and R.M.Truten'. O vozmozhnom metode izmereniya kontsentratsii ionov generiruemykh gidroionizatorami (On a Possible Method for Measuring the Concentration of Ions Generated by Hydroionizators).— Izvestiya Vysshikh Uchebnykh Zavedenii, Fizika, No. 6:152—156. 1962b.
(0)

Krasnogorskaya, N.V. and A.A.Serekin. Ob ob"emnom zaryade nizhnikh sloev atmosfery (On the Space Charge of the Lower Atmospheric Air Layer).— Izv. AN SSSR, Ser. Geofiz., No. 4: 587—595. 1964.
(11)

Kravchenko, M.D. See Baranov, V.I.

Kuklina, G.M. See Ivanova, N.M.

Kuz'menko, M.D. See Komarov, N.N.

Landau, L.D. and E.M.Lifshits. Mekhanika sploshnykh sred (Mechanics of Continuous Media).— Moskva, Gostekhteoretizdat. 1954.
(34)

Landau, L.D. and E.M.Lifshits. Elektrodinamika sploshnykh sred (Electrodynamics of Continuous Media).— Moskva, Gostekhteoretizdat. 1957.
(23)

Lëb, L. See Loeb, L. B.
Lebedev, V. L. Sluchainye protsessy v elektricheskikh i mekhanicheskikh sistemakh (Random Processes in Electrical and Mechanical Systems). — Moskva, Fizmatgiz. 1958.
(26)
Lesgaft, E. E. K izucheniyu ionizatsii vozdukha (A Contribution to the Study of Air Ionization). — In: Sbornik rabot Nauchno-issled. lab. kommunal'noi gigieny Lengorzdravotdela, Vol. 2:66—73. 1938.
(35)
Levin, L. M. O zabore prob aerozolya (On Taking Aerosol Samples). — Izv. AN SSSR, Ser. Geofiz., No. 7:914—925. 1957.
(2)
Levin, L. M. Elektrostaticheskoe osazhdenie chastits aerozolya iz potoka na bol'shie tela (Electrostatic Precipitation of Particles of an Aerosol from a Flux on Large Bodies). — Izv. AN SSSR, Ser. Geofiz., No. 7:1073—1075. 1959.
(2, 4)
Litvinov, V. F. Pribor dlya izmereniya tyazhelykh ionov v atmosfere (An Instrument for Measuring Heavy Ions in the Atmosphere). — Uchenye Zapiski Kazakhskogo Gos. Universiteta, Vol. 2:73—80. 1938.
(35)
Litvinov, V. F. Ionnoe sostoyanie nizhnikh sloev atmosfery po nablyudeniyam v gor. Alma-Ata i ego gornykh okrestnostyakh (Ionic State of the Lower Layer of the Atmosphere According to Observations in the City Alma-Ata and its Mountainous Surroundings). — Uchenye Zapiski Kazakhskogo Gos. Universiteta, Vol. 6:21—89. 1941.
(35)
Litvinov, V. F. and N. N. Litvinova. Elektrofiltr dlya polucheniya prob atmosfernoi pyli (An Electrostatic Filter for Obtaining Samples of Atmospheric Gases). — Gigiena i sanitariya, No. 9: 16—18. 1955.
(0)
Litvinova, N. N. See Litvitov, V. F.
Livshits, M. N. and V. N. Moiseev. Elektricheskie yavleniya v aerozolyakh i ikh primenenie (Electrical Phenomena in Aerosols and their Application). — Moskva-Leningrad, "Energiya." 1965.
(35)
Loĭtsyanskii, L. G. Mekhanika zhidkosti i gaza (Mechanics of Fluids and Gases). — Moskva, Fizmatgiz. 1959.
(18, 21, 34)
Makhotkin, L. G. and B. L. Sushchinskii. Plotnost' ob"emnogo zaryada v Sestroretske (The Space Charge Density in Sestroretsk). — Trudy Glavnoi Geofiz. Observatorii, Vol. 110:33—39. 1960.
(35)
Matulyavichene, V. K voprosu opredeleniya spektra mass radioaktivnogo aerozolya v atmosfere (The Problem of Determining the Mass Spectrum of Radioactive Aerosol in the Atmosphere). — Nauchnye Trudy Vysshikh Uchebnykh Zavedenii Lit. SSR, Geografiya i Geologiya, Vol. 1:145—153. 1962.
(0, 20)
Mikheev, M. A. Osnovy teploperedachi (Foundations of Heat Transfer). — Moskva-Leningrad, Gosenergoizdat. 1956.
(24)

Milin, V. B., I. I. Berezina, and B. K. In'kov. Avtomat-indikator anomalii ionizatsii atmosfery (An Automatic Indicating Device for Anomalies of Atmospheric Ionization). — Uchenye Zapiski Kirovskogo Gos. Ped. Instituta, 1(8):55—60. 1954.
(35)
Minkh, A. A. Ionizatsiya vozdukha i ee gigienicheskoe znachenie (Ionization of Air and its Hygienic Significance). — Moskva, Medgiz. 1963.
(0, 35)
Moiseev, V. N. See Livshits, M. N.
Monin, A. S. and A. M. Yaglom. Statisticheskaya gidromekhanika (Statistical Hydromechanics), Part 1. — Moskva, "Nauka." 1965.
(20)
Nichkevich, O. N. See Polovko, I. K.
Otto, A. N. See Tverskoi, P. N.
Pavlyuchenkov, G. See Imyanitov, I. M.
Polonnikov, D. E. Elektronnye usiliteli avtomaticheskikh kompensatorov (Electronic Amplifiers of Automatic Compensators). — Moskva, Fizmatgiz. 1960.
(26)
Polovko, I. K. and O. N. Nichkevich. K metodike izmereniya chisla srednikh ionov (On Methods of Measuring the Number of Intermediate Ions). — Trudy Nauchno-Issledov. Gidrometeorol. Instituta, Vol. 1:42—44, Kiev. 1937.
(6)
Portnov, F. G. Aeroionoterapiya bol'nykh gipertonicheskoi bolezn'yu (Air-Ion Therapy of Patients Suffering from a Hypertonic Illness). — Riga, Izd. AN. Latv. SSR. 1960.
(0)
Reinet, Ya. Yu. Kombinirovannyi schetchik atmosfernykh ionov (A Combined Counter of Atmospheric Ions). — Trudy Glavnoi Geofiz. Observatorii, Vol. 58:23—30. 1956.
(29, 35)
Reinet, Ya. Yu. Novaya apparatura i metodika dlya opredeleniya kontsentratsii aero- i gidroionov v atmosfere (A New Apparatus and Method for the Determination of the Density of Air and Water Ions in the Atmosphere). — Uchenye Zapiski Tartuskogo Gos. Universiteta, Vol. 59:41—70. 1958.
(9, 25)
Reinet, Ya. Yu. Novaya apparatura i metodika dlya opredeleniya kontsentratsii aero- i gidroionov v atmosfere (A New Apparatus and Method for the Determination of the Concentration of Air and Water Ions in the Atmosphere). — Voprosy Kurortol., Vol. 5:45—52, Riga.1959a.
(9, 25)
Reinet, Ya. Yu. Schetchik aero- i gidroionov (A Counter of Air and Water-Ions). — Byulleten' Izobret., No. 11, Patent No. 120272. 1959b.
(35)
Reinet, Ya. Yu. Novyi portativnyi schetchik gidro- i aeroionov, prigodnyi dlya opredeleniya zaryadov elektroaerozolei (A New Portable Counter of Water and Air Ions Suitable for the Charge Determination of Electroaerosols). — In Sbornik: "Aeroionizatsiya i gidroaeroionizatsiya v meditsine", pp. 232—235, Tashkent, Gosmedizdat UzSSR. 1962a.
(35)

Reinet, Ya. Yu. Spektrometr atmosfernykh ionov (A Spectrometer of Atmospheric Ions).— Byulleten' Izobret., No. 11, Patent No. 197822. 1962b.
(35)

Reinet, Ya. Yu. Nekotorye trebovaniya otnositel'no uslovii izmereniya spektra atmosfernykh ionov aspiratsionnym metodom (Some Demands Relating to the Conditions of Measurement of the Spectrum of Atmospheric Ions by the Aspiration Method).— Trudy Vses. Nauchn. Meteorol. Soveshchaniya, Vol. 9:313—321, Leningrad, Gidrometeoizdat. 1963.
(35)

Reinet, Ya. Yu. See Reinet, J.

Reinet, Ya. Yu., H. F. Tammet, and Ya. I. Sal'm. K metodike izucheniya ionizatsii vozdukha v kurortologii i fizioterapii (Method of Study of Air Ionization in Health Resort Treatment and Physiotherapy).— In Sbornik: "Materialy I resp. s"ezda fizioterapevtov i kurortologov USSR, posvyashch. 100 letiyu so dnya rozhd. prof. A. E. Shcherbaka," pp. 124—124, Kiev, Gosmedizdat USSR. 1963.
(35)

Reznik, M. V. See Korsunskii, M. M.

Rudik, K. I. See Arababzhi, V. I.

Saks, O. V. O konstruktsii dinamicheskogo kondensatora dlya schetchikov atmosfernykh ionov (On the Construction of a Dynamic Capacitor for Counters of Atmospheric Ions).— Trudy Vses. Nauchn. Meteorol. Soveshchaniya, Vol. 9:303—306, Leningrad, Gidrometeoizdat. 1963.
(35)

Saks, O. V. See Saks, O.

Sal'm, Ya. I. See Reinet, Ya. Yu.

Sedunov, Yu. G. See Ivanova, N. M.

Segal', R. B. Raspredelenie malykh ionov vozdukha po ikh velichine (The Size Distribution of Small Air Ions).— Uchenye Zapiski Cherepovetskogo Gos. Ped. Instituta, 3(3):3—12; Izvestiya Vysshikh Uchebnykh Zavedenii, Fizika, No. 6:16—21. 1962.
(1)

Semenov, K. A. See Imyanitov, I. M.

Seredkin, A. A. See Komarov, N. N., Krasnogorskaya, N. V.

Sergieva, A. P. Ob elektricheskikh zaryadakh oblachnykh chastits (On Electric Charges of Particles Contained in Clouds).— Izv. AN SSSR, Ser. Geofiz., No. 3:347—357. 1953.
(0)

Shchepot'eva, E. S. O podvizhnosti ionov v atmosfere (On the Mobility of Ions in the Atmosphere).— Zhurnal Geofiz. i Meteorol., 6(2):85—100. 1929.
(29)

Shchepot'eva, E. S. See Baranov, W. J.

Shepsenvol, M. A. See Shul'man, A. R.

Shul'man, A. R. and M. A. Shepsenvol. Ob izmerenii slabykh tokov (On the Measurement of Weak Currents).— In: Sbornik posvyashchennyi semidesyatiletiyu akad. A. F. Ioffe, pp. 510—522, Moskva, Izd. AN SSSR. 1950.
(26)

Speranskii, A. A. Instruktsiya k upotrebleniyu aspiratsionnogo pribora Eberta (Operating Instructions for an Ebert Aspiration Counter).— Kurortnoe Delo, No. 6:1—13. 1926.
(35)

Styro, B. I. and A. I. Yurgelionis. O chisle ionov v Palange (On the Number of Ions in Palanga).— Trudy AN Lit. SSR, Vol. 413:51—54. 1956.
(35)

Sushchinskii, B. L. See Makhotkin, L. G.

Tammet, H. F. K teorii aspiratsionnykh schetchikov aeroionov (On the Theory of Aspiration Counters of Air Ions).— Izv. AN SSSR, Ser. Geofiz. No. 8:1263—1270. 1960.
(2, 7, 8)

Tammet, H. F. K voprosu sozdaniya aeroionizatorov i ionometrov dlya shirokogo vnedreniya aeroionoterapii (The Problem of Manufacturing Air Ionizators and Ionometers for a Widespread Application of Air Ionotherapy).— In Sbornik: "Aeroionizatsiya i gidroaeroionizatsiya v meditsine," pp. 250—256, Tashkent, Gosmedizdat UzSSR, 1962a.
(0)

Tammet, H. F. Schetchik aeroionov (Counter of Air Ions).— Byulleten' Izobret., No. 20, Patent No. 151071. 1962b.
(31)

Tammet, H. F. Iskazhayushchie effekty v aspiratsionnykh schetchikakh aeroionov (Distorting Effects of Air Ions in Aspiration Counters).— Izv. AN SSSR, Ser. Geofiz. No. 6:845—853. 1962c.
(14, 16, 19, 20, 25, 34)

Tammet, H. F. Analiticheskii metod obrabotki nablyudenii pri izuchenii raspredeleniya aeroionov po podvizhnostyam (An Analytical Method for Evaluating the Observations in the Study of the Air-Ion Distribution According to Mobility).— Trudy Glav. Geofiz. Observatorii, Vol. 136:103—110. 1962d.
(29)

Tammet, H. F. Vozdeistvie ob"emnogo zaryada v aspiratsionnykh schetchikakh aeroionov (The Effect of Space Charge in Aspiration Counters).— Uchenye Zapiski Tartuskogo Gos. Universiteta, Vol. 140:46—61. 1963a.
(16, 17)

Tammet, H. F. K voprosu o skhemakh vklyucheniya aspiratsionnykh schetchikov aeroionov (On the Problems of Circuit Arrangements for Aspiration Counters of Air Ions).— Trudy Glav. Geofiz. Observatorii, Vol. 146:71—74. 1963b.
(31)

Tammet, H. F. Optimal'nye parametry aspiratsionnykh schetchikov aeroionov (Optimum Parameters of Aspiration Counters of Air Ions).— Trudy Vsesoyuz. Nauchn. Meteorol. Soveshchaniya, Vol. 9:322—328. 1963c.
(34)

Tammet, H. F. Opredelenie deistvuyushchei emkosti tsilindricheskogo izmeritel'nogo kondensatora aspiratsionnogo schetchika aeroionov (The Determination of the Effective Capacitance of a Cylindrical Measuring Capacitor of an Air-Ion Aspiration Counter).— Izv. AN SSSR, Ser. Geofiz., No. 3:436—436 [sic]. 1964a.
(33)

Tammet, H. F. Aspiratsionnyi metod izucheniya ionizirovannogo vozdukha i aerozolei (Aspiration Method for Studying Ionized Air and Aerosols). Author's Summary of Thesis, Tartu. 1964b.
(2)

Tammet, H. F. See Reinet, Ya. Yu.

Targ, S. M. Osnovnye zadachi teorii laminarnykh techenii (Basic Problems in the Theory of Laminar Flow).— Moskva-Leningrad, Gostekhteoretizdat. 1951.
(18)

Terekhov, Yu. V. Portativnyi schetchik gidroaeroionov (A Portable Counter of Hydroair Ions).— In Sbornik: "Aeroionizatsiya i Gidroaeroionizatsiya v meditsine," pp. 302—303, Tashkent, Gosmedizdat UzSSR. 1962.
(35)

Teverovskii, E. M. O diffuzii i koagulyatsii chastits aerozolya v turbulentnom potoke v atmosfere (On the Diffusion and Coagulation of Aerosol Particles in a Turbulent Stream in the Atmosphere).— In Sbornik: "Novye idei v oblasti izucheniya aerozolei," pp. 108—127. Moskva-Leningrad, Izd. AN SSSR. 1949.
(20)

Truten', R. M. See Korsunskii, M. M.

Tsvang, L. R. Impul'snyi metod izmereniya spektra legkikh ionov v atmosfere (Pulse Method of Measuring the Spectrum of Light Ions in the Atmosphere).— Izv. AN SSSR, Ser. Geofiz., No. 2:202—209. 1956.
(0)

Tsvang, L. R. and L. N. Gutman. Izmerenie spektra legkikh atmosfernykh ionov (Measurement of the Spectrum of Light Atmospheric Ions).— Izv. AN SSSR, Ser. Geofiz., No. 7:891—902. 1958.
(0)

Tsvang, L. R. and N. N. Komarov. Issledovanie spektra legkikh ionov v svobodnoi atmosfere (Investigation of the Spectrum of Light Ions in the Free Atmosphere).— Izv. AN SSSR, Ser. Geofiz., No. 8:1167—1176. 1959.
(0)

Tverskoi, P. N. Kurs meteorologii (Course of Meteorology).— Leningrad, Gidrometeoizdat. 1962.
(0)

Tverskoi, P. N. and A. N. Otto. Pribor dlya scheta ionov v atmosfere i ot iskusstvennykh ionizatorov (Instrument for Counting Ions in the Atmosphere and Ions Generated by Artificial Ionizers). — In Sbornik: "Aeroionizatsiya i gidroaeroionizatsiya v meditsine," pp. 229—231, Tashkent, Gosmedizdat UzSSR. 1962.
(35)

Valta, Z. F. Priroda i podvizhnost' vozdushnykh ionov (The Nature and Mobility of Air Ions).— Geofiz. i meteorol., 6(3):197—215. 1929.
(8)

Yurgelionis, A. I. See Styro, B. I.

Zacheck, S. I. Ustroistvo dlya izmereniya i registratsii elektroprovodimosti vozdukha v atmosfere (A Device for Measuring and Recording the Electrical Conductivity of Atmospheric Air).— Byul. Izobret., No. 8, Patent No. 146547. 1962.
(13)

Zachek, S. I. Pribor dlya izmereniya provodimosti vozdukha v svobodnoi atmosfere (An Instrument for Measuring the Conductivity of Air in the Free Atmosphere).— 5-ya nauchno-tekhnicheskaya konferentsiya po novoi geofizike i gidrometeorologii, meteorologii i priboram, 21— 25 aprelya 1964g., pp. 74—75, Synopses of Reports, Leningrad. 1964a.
(13)

Zachek, S. I. Teoriya differentsial'nogo dinamicheskogo elektrometra (Theory of Differential Dynamic Electrometer).— Trudy Glav. Geofiz. Observ., Vol. 157:87—93. 1964b.
(9)

Zachek, S. I. K voprosu ob izmerenii elektricheskoi provodimosti vozdukha v svobodnoi atmosfere s samoleta (The Problem of Measuring the Electrical Conductivity of Air in the Free Atmosphere from an Airplane).— Trudy Glav. Geofiz. Observ., Vol. 157:94—120. 1964b.
(13, 20, 24)

Zachek, S. I. See Imyanitov, I. M.

Publications in Other Languages

Adkins, C. J. The Small Ion Concentration and Space-charge Near the Ground.— Quart. J. Roy. Meteorol. Soc., 85(363):237—252. 1959.
(35)

Altberg, W. Über monomolekulare Elektrizitätsträger in Gasen und eine neue Messmethode der Molekulardurchmesser.— Ann. Physik, Vol. 37:849—880. 1912.
(7)

Altberg, W. See Al'tberg, V.

Antonescu, V. I. See Neaga, V. G.

Aoki, T. and K. Kato. Ratio of Atmospheric Ion.— Bull. Electrotechn. Lab., 18(8):561—575, 628. 1954.
(29)

Aselmann, E. Über Elektrizitätsträger, die durch fallende Flüssigkeiten erzeugt werden.— Ann. Physik, Vol. 19:960—984. 1906.
(6, 11)

Awbery, J. H. See Griffits, E.

Bailey, A. D. See Narcisi, R. S.

Baranow, W. J. and E. S. Stschepetjewa. Über die Anwendung des Ebertschen Ionenzählers zur Bestimmung der Zahl und der Beweglichkeit der kleinen Ionen in der Atmosphäre.— Phys. Z., Vol. 29:741—750. 1928.
(29)

Baranow, W.J. See Baranov, V.I.
Beau, G., L. Blanquet, and P. Blanquet. L'enregistrement continu de la charge spatiale atmosphérique.—Ann. Inst. hydrol. et climatol., Vol. 24(74/75):1—17. 1953.
(35)
Beau, G., L. Blanquet, P. Blanquet, and A. Fourton. Contribution à l'étude de l'enregistrement de la charge spatiale atmosphérique.—C.r. Acad. Sci. Vol. 243(10):784—786. 1956.
(35)
Becker, A. Neuer Zylinderkondensator zur Untersuchung leitender Gase.—Z. Instrumentenkunde, Vol. 29:258—261. 1909.
(4, 15, 25)
Becker, A. Über die Träger der Quecksilberfallelektrizität.—Ann. Physik. Vol. 31:98—126. 1910.
(2, 11, 16, 19, 22)
Beckett, J.C. Air Ion Measurement.—Proc. Internat. Conf. Ioniz. Air, Sect. 3, Vol. 1:1—15, Philadelphia, Pa. 1961.
(25, 35)
Benndorf, H. Über ein mechanisch registrierendes Elektrometer für luftelektrische Messungen.—Phys. Z., Vol. 7:98—101. 1906.
(35)
Benndorf, H. Zur Theorie luftelektrischer Registrierungen I.—Sitzungsber. Akad. Wiss. IIa, Vol. 118:1163—1195, Wien. 1909.
(13)
Benndorf, H. Zur Raumladungmessung in der freien Atmosphäre.—Phys. Z., Vol. 27:576—578. 1926.
(13)
Bent, R.B. The Testing of Apparatus for Ground Fair-weather Space-charge Measurements,—J. Atmos. and Ferr. Phys., 26(2):313—318. 1964.
(35)
Bergstedt, B.A. Application of the Electrostatic Precipitator to the Measurement of Radioactive Aerosols.—J. Sci. Instr., 33(4):142—148. 1956.
(0)
Bessa, F.I. See El Nadi, A.F.
Billard, F. See Fontan, J.
Blackwood, O. The Existence of Homogeneous Groups of Large Ions.—Phys. Rev., Vol. 16:85—101. 1920.
(7, 29)
Blanc, D. See Fontan,J.
Blanquet, L. See Beau, G.
Blanquet, P. See Beau, G.
Bloch, E. Sur la measure de la mobilité des ions dans les gaz par une methode de zéro.—C.r. Acad. Sci., Vol. 138:1492—1494. 1904.
(25)
Bordeau, R.E., E.C.Whipple, and J.F.Clark. Analytic and Experimental Electrical Conductivity between the Stratosphere and the Ionosphere.—J. Geophys. Res., 64(10):1363—1370. 1959.
(35)
Boylan, R.K. The Mobilities of Atmospheric Large Ions.—Proc. Roy. Irish Acad., A 40(4):76—84. 1931.
(29)
Boylan, R.K. See Nolan, J.J.

Brackett, F.S. See Daniel, J.H.
Bricard, J. See Fontan, J.
Brown, J.C. The Relation of Space-charge and Potential Gradient to the Diurnal System of Convection in the Lower Atmosphere.—Terr. Magn., 35(1):1—15. 1930.
(11)
Cagniard, L. Sur le rôle de la ventilation dans les appareils utilisés pour mesurer les conductibilités électriques de l'air atmosphérique.—C.r. Acad. Sci., Vol. 217:574—576. 1943.
(2, 4)
Cagniard, L. Sur les principes de la mesure des conductibilités ioniques de l'air à l'aide des appareils de déperdition.—Ann. Géophys., Vol. 1:25—36. 1944.
(2, 4)
Cagniard, L. and C. Lévy. Un nouvel appareil du type de Gerdien pour la mesure correcte et précise des conductibilités électriques de l'air atmosphérique.—Ann. Géophys., Vol. 2:19—24. 1946.
(33)
Calinicenco, N. See Vasiliu, Ch.
Callahan, R. and G.A. Faucher. Aircraft Investigation of the Large Ion Content and Conductivity of the Atmosphere and their Relation to Meteorological Factors.—J. Atmos. and Terr. Phys., 5(5/6): 253—272. 1954.
(35)
Callahan, R.C., S.C.Coroniti, A.J.Parziale, and R.Patten. Electrical Conductivity of Air in the Troposphere.—J. Geophys. Res., 56(4):545—551. 1951.
(35)
Callahan, R.C. See Coroniti, S.C.
Callahan, R.C. See Sagalyn, R.C.
Carson, J. See Schilling, G.T.
Challande, R. and B.David. Nouvelle méthode de prélévement des particules solides dans la stratosphere.—C.r. Acad. Sci., 250(8):1520—1521. 1960.
(0)
Chalmers, J.A. Atmospheric Electrical Conductivity Near the Earth Surface.—J. Atmos. and Terr. Phys., 3(4):223—224. 1953.
(13)
Chalmers, J.A. See Higazi, K.A.
Chapman, S. Carrier Mobility Spectra of Spray Electrified Liquids.—Phys. Rev., Vol. 52:184—190. 1937.
(25, 35)
Clark, J.F. See Bordeau, R.E.
Clark, W.E. See Whitby, K.T.
Cobb, W.E. See Woessner, R.H.
Collin, H.L., K.N.Groom, and K.A.Higazi. The "Memory" of the Atmosphere.—J. Atmos. and Terr. Phys., 28(6/7):659—697. 1966.
(30)
Coroniti, S.C. Airborne Conductivity Meter.—Geofis. pura e. appl., Vol. 47:79—83. 1960.
35
Coroniti, S.C., A.J.Parziale, R.C.Callahan, and R.Patten. Effect of Aircraft Charge on Airborne Conductivity Measurements.—

J. Geophys. Res., 57(2):197—205. 1052.
(13)

Coroniti, S.C. See Callahan, R.C.

Coroniti, S.C., A.Nazarek, C.G.Stergis, D.E.Kotas, D.W. Seymour, and T.V.Werme. Balloon Borne Conductivity Meter.—Instrumentation for Geophysical Research No. 3, AFCRC-TR54-206. 1954.
(35A)

Csanady, G.T. Concentration Fluctuations in Turbulent Diffusion.— J. Atmos. Sci., 34(1):21—28. 1967.
(30)

Curtis, H.O. and M.C.Hyland. Aircraft Measurements of the Ratio of Negative to Positive Conductivity, In: "Recent Advances in Atmospheric Electricity," pp. 111—117, London—New York—Paris—Los Angeles, Perg. Press. 1958.
(35)

Dalla Valle, J.M. See Hinkle, B.L.

Daniel, J.H. and F.S.Brackett. An Electrical Method for Investigating the Nature and Behavior of Small, Airborne, Charged Particles.— J. Appl. Phys., 22(5):542—554. 1951.
(25, 35)

Daunderer, A. Luftelektrische Messungen.—Phys. Z., Vol. 8:281—286. 1907.
(11)

Daunderer, A. Über die Beziehung zwischen Dichte und Mittelpunkts-Potential im Innern eines würfelförmigen von elektrisch leitenden Wänden begrenzten Raumes.—Z. Math. und Phys., Vol. 57:293—301. 1909.
(11)

David, B. See Challande, R.

Davis, A.H. Convective Cooling in Liquids—Some Thermal Conductivity Data.—Philos. Mag., Vol. 47:972—977. 1924.
(24)

De Broglie, M.M. Recherches sur les centres électrisés de faible mobilité dans les gaz.—J. Phys. théor. et appl., Vol. 8:869—888. 1909.
(35)

Deignan, J. See Nolan, P.J.

Dessauer, F., W.Graffunder, and J. Laub. Beobachtungen über Ionenschwankungen im Freien und in geschlossenen Räumen.— Ann. Meteorol., 7(3/4):173—185. 1955—1956.
(30)

Dessauer, F. See Wolodkewitsch, N.

Dolezalek, H. Freiluft-Isolator mit über 10^{14} Ohm Widerstand für alle Klimate.—Geofis. pura e appl., Vol. 33:223—228. 1956.
(35)

Dolezalek, H. Der Freiluftisolator mit 10^{14} Ohm; Verbesserungen und Ergänzungen.—Geofis. pura e appl., 49(2):249—254. 1961.
(35)

Dolezalek, H. Die luftelektrische Station, Teil 2: Beschreibung der Station, Gerlands Beitr.—Geophys., 71(3):161—171. 1962a.
(35)

Dolezalek, H. On the Measurement of Mobility and Conductivity in the Mesosphere.—Z. Geophys., 28(H5):239—243. 1962b.
(A)

Dolezalek, H. See Israël, H.

Dolezalek, H. and A.L.Oster. Spectrometer for Atmospheric Ions in Their Uppermost Range of Mobility (Project: Measuring Ionic Mobilities in the Terrestrial Upper Stratosphere and Mesosphere, Phase II).—Final Report Contract DA-19-020-AMC-0058 (X), AVSSD-0200-66-RR, Wilmington, Mass. 1966a.
(A)

Dolezalek, H. and A.L.Oster. Ion-Spectrometer for the Terrestrial Mesosphere and the Atmosphere of Mars.—Z. Geophys., 32(H3): 163—172. 1966b.
(A)

Dow, W.G. See Hok, G.

Dowling, J.J. and C.J.Haughey. On the Electrification of Phosphorus Smoke Nuclei.—Proc. Roy. Irish Acad. A36(3):50—59. 1922.
(35)

Ebert, H. Aspirationsapparat zur Bestimmung des Ionengehalts der Atmosphäre.—Phys. Z., Vol. 2:662—664. 1901.
(25, 35)

Ebert, H. Eine neue Form des Ionen-Aspirations-Apparates.—Verhandl. Deutsch. phys. Ges., Vol. 7:34—37. 1905.
(25, 35)

Eichmeier, J. Beweglichkeitsspektren natürlicher atmosphärischer Ionen im Klein- und Mittelionenbereich.—Z. Angew. Phys., 23(4): 256—260. 1967.
(34)

Eichmeier, J. Die theoretischen Grundlagen und das Auflösungsvermögen von Aspiration-Beweglichkeit spektrographen für atmosphärische Ionen.—Z. Geophys., 34(HI): 69—96. 1968.
(34)

Eichmeier, J. See Siksna, R.

El Nadi, A.F. and I.F.Bessa. Small Ion Characteristics.—Proc. Math. and Phys. Soc., Vol. 22:27—42. Egypt. 1958.
(34)

El Nadi, A.F. and N.Farag. The Mobility Spectrum and the Ion Concentration of Large Ions in Air Mixed with N_2O Gas.—Geofis. pura e appl., 47(3):114—122. 1960.
(29)

El Nadi, A.F. and N.Farag. The Effect of Light on the Mobility and Concentration of Large Ions in Air Mixed with N_2O Gas.—J. Atmos. and Terr. Phys., Vol. 22(1):23—31. 1961.
(29)

El Nadi, A.F. See Ortner, G.

Elster, J. and H.Geitel. Über einen Apparat zur Messung der Elektrizitätszerstreuung in der Luft.—Phys. Z., Vol. 1:11—14. 1899.
(25)

Erikson, H.A. The Change of Mobility of the Positive Ions in Air with Age.—Phys. Rev., Vol. 18:100—101. 1921.
(8, 25, 31)

Erikson, H.A. The Change of Mobility of the Positive Ions with Age in Oxygen and Nitrogen.—Phys. Rev., Vol. 19:275—276. 1922.
(8, 25)

Erikson, H. A. On the Nature of the Ions in Air and in Carbon Dioxide.— Phys. Rev., Vol. 24:502—509. 1924.
(8, 25)

Erikson, H. A. Factors Affecting the Nature of Ions in Air.— Phys. Rev., Vol. 34:635—643. 1929.
(8, 25)

Farag, N. See El Nadi, A. F.

Faucher, G. A. A Study of Air-Flow in a Large-Ion Chamber.— In: "Recent Advances in Atmospheric Electricity," pp. 55—60, London—New York—Paris—Los Angeles. Perg. Press. 1958; J. Atmos. and Terr. Phys., 12(4):288—292. 1958.
(20)

Faucher, G. A. See Callahan, R. and Sagalyn, R.

Fischer, H. J. See Mühleisen, R.

Fontan, J., F. Billard, D. Blanc, J. Bricard, M. L. Huertas, and A. M. Marty. Etude de la mobilité des ions radioactifs formés sur les atomes de recul provenant de la désintegration du thoron dans l'air et différents gaz.— C. r. Acad. Sci., Vol. 262(19): B1315 B1317. 1966.
(0)

Fontell, N. Über die Ionenbeweglichkeit in Luft-Azeton and Luft-Essigsäuregemischen.— Soc. Sci. Fennica, Comm. Phys.— Math., 6(6):1—27. 1932.
(23)

Forster, W. W. Deposition of Unipolar Charged Aerosol Particles by Mutual Repulsion.— Brit. J. Appl. Phys., 10(5):206—213. 1959.
(2)

Fourton, A. See Beau, G.

Franck, J. Über die Beweglichkeit der Ladungsträger der Spitzenentladung.— Ann. Physik, Vol. 21:972—1000. 1906.
(16)

Fraser, D. A. See Mendenhall, A. L.

Frenkiel, F. N. Turbulent Diffusion: Mean Concentration Distribution in a Flow Field of Homogeneous Turbulence.— Adv. Appl. Mech., Vol. 3:61—107. 1953.
(20)

Fuchs, N. A. On the Stationary Charge Distribution on Aerosol Particles in a Bipolar Ionic Atmosphere.— Geofis. pura e appl., 56(3):185—193. 1963.
(0)

Fuks, N. A. See Fuchs, N. A.

Funder, L. Ermittlung, Ursachen und Bedeuten des Ionengehaltes der Grubenwetter.— Gerlands Beitr. Geophys., Vol. 54:370—449. 1939.
(34, 35)

Funder, L. Die Luftelektrizität, eine vernachlässigte Grösse in den Grubenwettern.—Glückauf, 76(17):237— 243. 1940.
(35)

Gadomski, J. The High Resistance Insulator Adapted to the Exploitation in Different Climatic Circumstances.— Cha-Pa Observ. Atmosph. and Radioactiv, pp. 139—142, Lódź. 1958—1959.
(35)

Gagge, A. P. and I. M. Moriyama. The Annual and Diurnal Variation of Ions in an Urban Community.— Terr. Magn. and Atmos. Electr., 40(3):295—306. 1935.
(35)

Geitel, H. See Elster, J.

Gerdien, H. Die absolute Messung der elektrischen Leitfähigkeit und der spezifischen Ionengeschwindigkeit in der Atmosphäre.— Phys. Z., Vol. 4:632—635. 1903.
(35)

Gerdien, H. Demonstration eines Apparates zur absoluten Messung der elektrischen Leitfähigkeit der Luft.— Phys. Z., Vol. 6:800—801. 1905a.
(25, 34, 35)

Gerdien, H. Die absolute Messung der spezifischen Leitfähigkeit und der Dichte des verticalen Leitungsstromes in der Atmosphäre.— Terr. Magn. and Atmos. Electr., Vol. 10:65—79. 1905b.
(25, 35)

Gerdien, H. Untersuchungen über die atmosphärischen radioaktiven Induktionen.— Abhandl. Ges. Wiss., 5(25):1—74, Göttingen. 1907.
(0)

Giese, W. Experimentelle Beiträge zur Kenntis von elektrischen Leitungsvermögen der Flammengase.— Ann. Physik, Vol. 17:1—41, 236—257, 519—550. 1882.
(0, 1)

Gillespie, T. Electric Charge Effects in Aerosol Particle Collision Phenomena.— Internat. J. Air Pollution, 3(1/3):44—49. 1960.
(0)

Gillespie, T. and G. Langstroth. An Instrument for Determining the Electric Charge Distribution in Aerosols.— Canad. J. Chem., 30(12):1056—1068. 1952.
(0)

Giorgi, M. Apparecchiature "CENFAM" per la registrazione continua di parametri della elettricità atmosferica, Atti 13.— Conv. annuale, Ass. geofis. Ital. pp. 355—362. Roma, s. a. 1963.
(35)

Gish, O. H. Systematic Errors in Measurements of Ionic Content and the Conductivity of the Air.— Gerlands Beitr. Geophys., Vol. 35:1—5. 1932.
(14)

Gish, O. H. Effects of Turbulent Air-Flow in some Apparatus Used in Atmospheric-electric Measurements.— Terr. Magn. and Atmos. Electr., 38(3):257—259. 1933a.
(20)

Gish, O. H. Bemerkungen zur Arbeit: H. Graziadei, "Studie über die Methodik der Ionenzählung."— Phys. Z., Vol. 34:712—713. 1933b.
(20)

Gish, O. H. and K. L. Sherman. Electrical Conductivity of Air to an Altitude of 22 kilometers.— Nat. Geogr. Soc. Contrib. Techn. Papers, Stratosphere Ser. No. 2:94—116. 1936.
(35)

Gockel, A. Luftelektrische Beobachtungen im Schweizerischen Mittelland, im Jura und in den Alpen.—Neue Denkschriften Schweizerisch. Naturforsch. Ges., Appendix 1, Vol. 54:1—75. 1917.
(11, 35)

Godefroy, A. Appareil enregistreur pour la mesure des résistances élevées et variables. Application à la mesure de la conductibilité électrique de l'air.—Ann. géophys., 5(2):164—166. 1949.
(35)

Gonsior, B. Messungen der luftelektrischen Raumladung mit Schwebestoff-Filtern.—In: "Luftelektrizität im AGJ", pp. 17—23, Aachen. 1957.
(35)

Graffunder, W. See Dessauer, F.

Graziadei, H. Th. Studie über die Methodik der Ionenzählung.—Phys. Z., Vol. 34:82—88. 1933.
(14)

Graziadei, H. Th. Zur Turbulenz bei Ionenzählern.—Phys. Z., Vol. 36: 181—182. 1935.
(20)

Green, H. L. and W. R. Lane. Particulate Clouds: Dusts, Smokes and Mists.—E. and F. N. SPON LTD, London. 1957.
(0)

Greinacher, H. and W. Klein. Über einen Apparat zur Dauerregistrierung der spezifischen Ionenzahl der Atmosphäre.—Gerlands Beitr., Geophys., Vol. 51:298—307. 1937.
(35)

Grieger, H. Ein neuer Apparat zur Messung des Ionenspektrums.—Z. Instrumentenkunde, Vol. 55:116—122. 1935.
(35)

Griffits, E. and J. H. Awbery. The Dependence of the Mobility of Ions in Air on the Relative Humidity.—Proc. Phys. Soc., Vol. 41:240—247. 1929.
(7)

Gröber, H. and S. Erk. Die Grundgesetze der Wärmübertragung, 3rd fully revised edition by U. Grigull.—Berlin u. a., Springer. 1955.
(24)

Groom, K. N. See Collin, H. L.

Gunn, R. Electrification of Cloud Droplets in Nonprecipitating Cumuli.—J. Meteorol., 9(6):397—402. 1952.

Gunn, R. Measurements of the Electricity Carried by Precipitation Particles.—In: "Thunderstorm Electricity" (ed. H. R. Byers), pp. 193—206. Chicago. 1953.
(11)

Gunn, R. Improved Apparatus for the Measurement of Atmospheric Electrical Conductivity.—Rev. Sci. Instrum., 36(5):594—598. 1965.
(35)

Gunn, R. See Woessner, R. H.

Gupta, B. K. See Venkiteshwaran, S. P.

Hansen, W. W. On the Origin of the Space-charge in the Atmosphere.—Terr. Magn. and Atmos. Electr., 40(3):277—279. 1935.
(11)

Harris, J. T. See Nolan, J. J.

Hasenclever, D. and H. Chr. Siegmann. Neue Methode der Staubmessung mittels Kleinionenanlagerung.—Staub, 20(7):212—218. 1960.
(4)

Hatakeyama, H., J. Kobayashi, J. Kitaoka, and K. Uchikawa. A Radiosonde Instrument for the Measurement of Atmospheric Electricity and its Flight Results.—In: "Recent Advances in Atmospheric Electricity," pp. 119—135, London—New York—Paris—Los Angeles, Perg. Press. 1958.
(35)

Haughey, C. J. See Dowling, J. J.

Hess, V. F. Neue Untersuchungen über die Ionisierungsbilanz der Atmosphäre auf Helgoland.—Gerlands Beitz., Geophys., Vol. 22: 256—314 und Sitzungsber. Akad. Wiss. IIa, Vol. 138:169—221. Wien. 1929.
(35)

Hess, V. F. See O'Donnel, G. A.

Hewitt, G. W. The Charging of Small Particles for Electrostatic Precipitation.—Commun. and Electronics, Vol. 31:300—306. 1957.
(25, 35)

Hewlett, C. W. Investigation of Certain Causes Responsible for Uncertainty in the Measurement of Atmospheric Conductivity by the Gerdien Conductivity Apparatus.—Terr. Magn. and Atmos. Electr., 19(4):219—233. 1914.
(35)

Higazi, K. A. and J. A. Chalmers. Measurements of Atmospheric Electrical Conductivity near the Ground.—J. Atmos. and Terr. Phys., 28(3):327—330. 1966.
(13)

Higazi, K. A. See Collin, H. L.

Hinkle, B. L., C. Orr, and J. M. Dalla Valle. A New Method for the Measurement of Aerosol Electrification.—J. Colloid Sci., 9(1):70—80. 1954.
(0)

Hinze, J. O. Turbulence.—New York—Toronto—London, McGraw-Hill Book Company, Inc. 1959.
(20)

Hock, A. and H. Schmeer. Über ein Gerät zur störfeldfreien Luftionenmessung und einen Impulszähler zur direkten Anzeige der Windgeschwindigkeit.—Z. angew. Phys., 14(H7):398—404. 1962.
(25, 35)

Hock, A. Messgeräte zur Bestimmung der Verteilung atmosphärischer Kleinionen und Kondensationskerne in bodennahen Schichten der Atmosphäre.—Arch. Techn. Messen, Vol. 373:29—34. 1967.
(35)

Hoegl, A. Messung von Konzentration und Beweglichkeit atmosphärischer Ionen.—Z. angew. Phys., 16(H4):252—258. 1963.
(4, 18, 29, 34, 35)

Hoegl, A. Messtechnik zur Bestimmung von Konzentration und Beweglichkeit atmosphärischer Ionen.—Elektromedizin, 8(3):148—152. 1963a.
(35)

Hogg, A. R. Atmospheric Electric Observations.— Gerlands Beitr. Geophys., Vol. 41:1—31. 1934.
(35)

Hogg, A. R. The Intermediate Ions in the Atmosphere.— Proc. Phys. Soc., Vol. 51:1014—1027. 1939.
(7)

Hok, G., N. W. Spencer, and W. G. Dow. Dynamic Probe Measurements in the Ionosphere.— J. Geophys. Res., 58(2):235—242. 1953.
(A)

Holl, W. See Mühleisen, R.

Hoppel, W. A. The Ions of the Troposphere: Their Interactions with Aerosols and the Geoelectric Field.— Diss. Cath. Univ., America, Washington. 1968.
(34)

Hoppel, W. A. and J. H. Kraakevik. The Mobility of Tropospheric Ions Above the Exchange Layer.— J. Atmos. Sci., 22(5):509—517. 1965.
(7, 14, 29)

Huddar, B. B. See Venkiteshwaram, S. P.

Huertas, M. L. See Fontan, J.

Hyland, M. C. See Curtis, H.

Ishikawa, H. See Takeuti, T.

Israël, H. Ein transportables Messgerät für schwere Ionen.— Z. Geophys., Vol. 5:342—350. 1929.
(35)

Israël, H. Zur Theorie und Methodik der Grössenbestimmung von Luftionen.— Gerlands Beitr., Geophys., Vol. 31:173—216. 1931.
(5, 6, 9, 10, 20, 25)

Israël, H. Zum Problem der Randstörungen bei Ionenmessungen, Gerlands Beitr., Geophys., Vol. 35:341—348. 1932a.
(14)

Israël, H. Ergänzungen zu meiner Arbeit: Zur Theorie und Methoden der Grössenbestimmung von Luftionen.— Gerlands Beitr., Geophys., Vol. 36:24—37. 1932b.
(14)

Israël, H. Der Wegersche Kleinionen-Aspirator als selbständiges Messgerät.— Meteorol. Z., Vol. 54:487—488. 1937.
(25)

Israël, H. Verzeichnis der luftelektrisch arbeitenden Stationen.— In: "Luftelektrizität im IGJ," pp. 111—114b., Aachen. 1957a.
(0)

Israël, H. Atmospharische Elektrizität, T. 1.— Leipzig, Akad. Verlagsges. Geest und Portig K.-G. 1957b.
(1, 5, 10, 14, 29, 35)

Israël, H. Atmosphärische Elektrizitat, T. 2.— Leipzig, Akad. Verlagsges. Geest und Portig K.-G. 1961.
(11)

Israël, H. and H. Dolezalek. Zur Methodik luftelektrischer Messungen IV: Störspannungen in luftelektrischen Messfühlern und ihre Verhütung, Gerlands Beitr. Geophys., 66 (H2), 129—142. 1957.
(13)

Israël, H. and L. Schalz. The Mobility-Spectrum of Atmospheric Ions.— Principles of Measurements and Results.— Terr. Magn. and Atmos. Electr., 38(4):285—300. 1933.
(10)

Itawa, A. See Takeuti, T.

Itawara, Yo. Zur Methodik der Ionenzählung in der freien Atmosphäre.— Phys. Z., Vol. 32:97—106. 1931.
(14)

Johnstone, H. F. See Kraemer, H. F.

Jonassen, N. Om mâling afatmosfaerisk lufts iontaethed.— Teknisk forl., Kopenhavn. 1962.
(31, 35)

Jones, O. C., R. S. Maddever, and J. K. Sanders. Radiosonde Measurement of Vertical Electric Field and Polar Conductivity.— J. Sci. Instrum., 36(1):24—28. 1959.
(35)

Junge, C. E. Air Chemistry and Radioactivity.— New York— London, Acad. Press. 1963.
(0)

Junge, Chr. The Size Distribution and Aging of Natural Aerosols as Determined from Electrical and Optical Data in the Atmosphere.— J. Meteorol., 12(1):13—25. 1955.
(0)

Junod, A., R. Sänger, and J. Chr. Thams. Enregistrement direct du spectre des petits ions atmosphériques.— Z. angew. Math. und Phys., 13(3):272—278. 1962.
(12)

Kaden, H. Die elektromagnetische Schirmung in der Fernmelde- und Hochfrequenztechnik.— Berlin, Springer. 1950.
(6, 32)

Kähler, K. Über die durch Wasserfälle erzeugte Leitfähigkeit der Luft.— Ann. Physik, Vol. 12:1119—1141. 1903.
(6, 25, 35)

Kähler, K. Einführung in die atmosphärische Elektrizität.— Berlin, Verlag Bornträger. 1929.
(35)

Kähler, K. Über die Verteilung der Elektrizitätsträger in der Atmosphäre.— Meteorol. Z., Vol. 47:57—68. 1930.
(35)

Kato, K. See Aoki, T.

Kawano, M. See Wilkening, M. H.

Kennedy, H. The Large Ions in Atmosphere.— Proc. Roy. Irish Acad., Vol. A32(1):1—6. 1913.
(35)

Kennedy, H. See McClelland, J. A.

Kenny, P. J. See Nolan, P. J.

Kern, W. See Riezler, W.

Kilinski, E. Ein neues Verfahren zur Registrierung der luftelektrischen Leitfähigkeit.— Z. Meteorol., Vol. 3:174—175. 1949.
(35)

Kilinski, E. Die neuen Registrieranlagen im luftelektrischen Hause des Hauptobservatoriums in Potsdam.—Z. Meteorol, Vol. 7:146—150. 1953.
(35)

Kitaoka, T. See Hatakeyama, H.

Klein, W. See Greinacher, H.

Knoll, M., J. Eichmeier, and R.W. Schön. Properties, Measurement and Bioclimatic Action of "Small" Multimolecular Atmospheric Ions.—In: "Advances in Electronics and Electron Physics," Vol. 19:177—254, New York, Acad. Press. 1964.
(35)

Kobayashi, J. See Hatakeyama, H.

Koenigsfeld, L. La mesure de la conductibilité par radiosonde.—Publs. ser. B. Inst. roy. Metéorol. No. 18:1—8, Belgique. 1955.
(35)

Koenigsfeld, L. La mesure du gradient du potentiel et de la conductibilité par radiosonde.—In: "Luftelektrizität im IGJ," pp. 84—90, Aachen. 1957.
(35)

Kohlrausch, K.W.F. Über elektrostatische Kapazität und Widerstandskapazität.—Verk. Deutsch. Phys. Ges., Vol. 8:151—156. 1906.
(4)

Kohlrausch, K.W.F. Zur Methodik der Beweglichkeits-und Wiedervereinigungsmessungen an Ionen in strömender Luft.—Sitzungsber. Akad. Wiss. IIa, Vol. 123:1929—1954, Wien. 1914.
(6)

Kotas, D.E. See Coroniti, S.C.

Kraakevik, J.H. The Airborne Measurement of Atmospheric Conductivity.—J. Geophys. Res., Vol. 63(1):161—169. 1958.
(35)

Kraemer, H.F. and H.F. Johnstone. Collection of Aerosol Particles in Presence of Electrostatic Fields.—Industr. and Engng. Chem., Vol. 47(12):2426—2434. 1955.
(4)

Kroening, J.L. Ion-density Measurements in the Stratosphere.—J. Geophys. Res., Vol. 65(1):145—151. 1960.
(14, 35)

Kurz, K. Über die scheinbaren Unterschiede der Leitfähigkeit der Atmosphäre bei positiver and negativer Ladung des Plattenelektrometers.—Phys. Z., Vol. 7:771—775. 1906.
(13)

Kurz, K. Die Beeinflussung der Ergebnisse luftelektrischer Messung durch die festen radioaktiven Stoffe der Atmosphäre.—Ann. Physik, Vol. 24:890—930. 1907.
(13)

Lamb, H. Hydrodynamics.—Cambridge University Press, 6th edition. 1957.
(18)

Lane, C. See Wilkening, M.H.

Lane, W.R. See Green, H.L.

Langevin, M.P. Sur les ions de l'atmosphère.—C.r. Acad. Sci., Vol. 140:232—234. 1905a.
(1, 5)

Langevin, M.P. Sur un enregistreur des ions de l'atmosphère.—C.r. Acad. Sci., Vol. 140:305—307. 1905b.
(1)

Langevin, M.P. and M. Moulin. Electrométre enregistreur des ions de l'atmosphère.—Le Radium, Vol. 4:218—229. 1907.
(35)

Langstroth, G. See Gillespie, T.

Laub, J. See Dessauer, F.

Lautner, P. See Mecklenburg, W.

Leckie, A.J. Luftelektrische Messungen an Bosschalaboratorium der Technischen Hochschule in Bandoeng.—Gerlands Beitr. Geophys., Vol. 52:280—333, Java. 1938.
(35)

Lenard, P. Über die Elektrizitätszerstreuung in ultraviolett durchstrahlter Luft.—Ann. Physik, Vol. 3:298—319. 1900.
(1)

Lenard, P. and C. Ramsauer. Über Bildung grosser Elektrizitätsträger.—Sitzungsberg. Akad. Wiss. Math-naturwiss. Kl. Abh., Vol. 32:1—31. Heidelberg. 1910.
(14, 25)

Lévy, C. See Cagniard, L.

Lindsay, R. See Siksna, R.

Lipscomb, W.N., F.R. Rubin, and J.H. Sturdivant. An Investigation of a Method for the Analysis of Smokes According to Particle Size.—J. Appl. Phys., Vol. 18(1):72—79. 1947.
(0, 23)

Loeb, L.B. Effect of the Gauze in the Franck Modification of the Rutherford Alternating Current Method for Measuring Ionic Mobilities.—J. Franklin Inst., Vol. 196:771—778. 1923.
(6)

Loeb, L.B. See Leb, L.

Loeb, L.B. Basic Processes of Gaseous Electronics.—Berkeley—Los Angeles, Univ. Calif. Press. 1960.
(0, A)

Lonsdale, T. The Flow of Water in the Annular Space between Two Coaxial Pipes.—Philos. Mag., Vol. 46:163—169. 1923.
(34)

Lutz, C.W. Eine neue Form des Ebertschen Aspirations—Apparates.—Sitzungsber. math.—naturwiss. Kl. Bayerischen Akad. Wiss., Vol. 14:1—17, München. 1909.
(25, 35)

Lutz, C.W. Aufzeichnung der elektrischen Raumladung der Luft.—Gerlands Beitr. Geophys., Vol. 41:416—428. 1934.
(35)

Lutz, C.W. Aufzeichnung der elektrischen Leitfähigkeit der Luft.—Gerlands Beitr. Geophys., Vol. 47:241—251. 1936.
(35)

Mache, H. Eine einfache Methode, die Geschwindigkeit von Gasionen zu bestimmen, welche weder hohes Molisierungs- noch Regenerierungsvermögen besitzen.—Phys. Z., Vol. 4:717—721. 1903.
(6, 19)

Mackell, J. F. Influence of the Earth's Potential Gradient Upon the Measurement of the Atmospheric Ionic Density by the Ebert Ion Counter.— Phys. Rev., Vol. 17:390—391. 1921.
(13)

Mackell, J. F. The Influence of the Earth's Potential Gradient upon Measurements of the Mean Ionic Density of the Atmosphere by the Ebert Ion-counter.— Phys. Rev., Vol. 21:436—448. 1923.
(13)

Maddever, R. C. See Jones, O. C.

Mallahan, F. J. See Moore, C. B.

Marty, A. M. See Fontan, J.

Masson, H. See Salvador, O.

Mateicine, V. See Vasĭlin, Ch.

Maushart, R. Über die Beweglichkeit positiver Ionen in extrem reinen Gasen und Gasgemischen.— Ann. Phys., Vol. 1(H 4/5):246:280. 1958.
(A)

McClelland, J. A. On the Conductivity of the Hot Gases from Flames.— Philos. Mag., Vol. 46:29—42. 1898.
(0, 6, 11, 25, 35)

McClelland, J. A. and H. Kennedy. The Large Ions in the Atomsphere.— Proc. Roy. Irish Acad., Vol. A, 30:72—91. 1912.
(4, 25)

McFarland, A. R. See Whitby, K. T.

Mecklenburg. W. and P. Lautner. Zur Messung des Potentialgradienten und der Raumladung in der freien Atmosphäre.— Z. Phys., Vol. 115(H 9/10):557—570. 1940.
(11)

Mendenhall, A. L. and D. A. Fraser. A Continuously Recording Instrument to Measure Air-Borne Ion Concentration.— Americ. Industrial Hygiene Ass. J., 24(6):555—562. 1963.
(35)

Metnieks, A. See Siksna, R.

Metnieks, A. L. and L. W. Pollak. Tables and Graphs for Use in Aerosol Physics. Part I. Mobility v. Radius and Vice Versa.— Geophys. Bull. Dublin Inst. Advanced Studies School Cosmic Phys., No. 16, 6, pp. 1—37. 1961.
(0)

Misaki, M. A. A Method of Measuring the Ion Spectrum.— Papers Meteorol. and Geophys., Vol. 1:313—318. 1950.
(7)

Misaki, M. A. Determination of Air Flow in an Ion Chamber. Preliminary Examination for the Study of Ion Spectrum.— Papers Meteorol. and Geophys., Vol. 11:348—355. 1960.
(4, 18, 20)

Misaki, M. Studies on the Atmospheric Ion Spectrum I. Procedures of Experiments and Data Analysis.— Papers Meteorol. and Geophys., Vol. 12:247—260. 1961.
(35)

Mitchell, J. H. and K. E. W. Riedler. The Speed of Positive Ions in Nitrogen.— Proc. Roy. Soc., Vol. A, 146:911—921. 1934.
(1)

Moore, C. B., B. Vonnegut, and F. J. Malahan. Airborne Filters for the Measurement of Atmospheric Space Charge.— J. Geophys. Res., 66(10):3219—3226. 1961.
(35)

Moriyama, I. M. See Gagge, A. P.

Moulin, M. See Langevin, M. P.

Mühleisen, R. Vorschläge für die Auswahl, Einrichtung und Zusammenarbeit luftelektrischer Stationen im internationalen Geophysikalischen Jahr.— In: "Luftelektrizität im IGJ," pp. 72—75. Aachen. 1957a.
(11)

Mühleisen, R. Atmosphärische Elektrizität.— In: "Handbuch der Physik," B. 48, pp. 541 — 607, Berlin—Gott. — Heidelberg. 1957b.
(35)

Mühleisen, R. and H. J. Fischer. Radiosonden für luftelektrische Messungen.— Arch. techn. Messen, No. 274:229—232. 1958.
(35)

Mühleisen, R. and H. J. Fischer. Luftelektrische Aerologie.— Beitr. Phys. Atmos., 34(1/2):3—14. 1961.
(14)

Mühleisen, R. and W. Holl. Eine neue Methode zur Messung der elektrischen Raumladungsdichte der Luft.— Geofis. pura e appl., Vol. 22:189—194. 1952.
(11)

Narcisi, R. S. and A. D. Bailey. Mass Spectrometric Measurements of Positive Ions at Altitudes from 64 to 112 kilometers.— J. Geophys. Res., 70(15):3687—3700. 1965.
(0, A)

Nazarek, A. See Coroniti, S. C.

Neaga, V. G. and V. I. Antonescu. Realizarea unui aparat pentru inregistrarea automată a conductibilităti electrice a aerului.— Studii si cercetări fiz. Acad. RPR, 9(3):389—391. 1958.
(35)

Neher, H. V. An Automatic Ionization Chamber.— Rev. Sci. Instrum., Vol. 24:99—102. 1953.
(35)

Nitta, M. See Yaita, T.

Nolan, J. J. The Mobilities of Ions Produced by Spraying Distilled Water.— Proc. Roy. Irish Acad., A33(2):9—23. 1916.
(29)

Nolan, J. J. The Nature of the Ions Produced in Air by Radio-active Bodies.— Proc. Roy. Irish Acad., A35(4):38—45. 1919.
(7, 25)

Nolan, J. J. Ionic Mobilities in Air and Hydrogen.— Proc. Roy. Irish Acad., A36(5):74—92. 1923.
(29)

Nolan, J. J., R. K. Boylan, and G. P. Sachy. The Equilibrium of Ionization in the Atmosphere.— Proc. Roy. Irish Acad., A37(1): 1—12. 1925.
(25)

Nolan, J. J. and J. T. Harris. Ionization in Moist and Dry Air.— Proc. Roy. Irish Acad., A36(2):31—49. 1922.
(7, 25)

Nolan, J.J. and P.J.Nolan. Preliminary Account of Observations on Atmospheric Electricity in Country Air.—Gerlands Beitr. Geophys., Vol. 25:414—428. 1930.
(4, 25)

Nolan, J.J. and P.J.Nolan. Observations on Atmospheric Ionization at Glencree, Co. Wielow.—Proc. Roy. Irish Acad., A40(2):11—59. 1931.
(25)

Nolan, J.J. and P.J.Nolan. A New Method for Counting Atmospheric Ions and Determining Their Mobilities.—Proc. Roy. Irish Acad., A42(3):15—19. 1935.
(25)

Nolan, J.J. and G.P.Sachy. Atmospheric Ionization.—Proc. Roy. Irish Acad., A37(7):71—94. 1927.
(29)

Nolan, P.J. See Nolan, J.J.

Nolan, P.J. Evidence for the Existence of Homogeneous Groups of Large Ions.—Phys. Rev., Vol. 18:185—198. 1921.
(29)

Nolan, P.J. The Character of the Ionization Produced by Spraying Water.—Philos. Mag., 1(2):417—428. 1926.
(35)

Nolan, P.J. and J.Deignan. Observations on Atmospheric Condensation Nuclei in Stored Air.—Proc. Roy. Irish Acad., A51(18):239—249. 1948.
(6)

Nolan, P.J. and P.J.Kenny. A Modified McClelland Method for Measuring Ionic Mobilities.—J. Atmos. and Terr. Phys., 2(5):266—271. 1952.
(5)

Nolan, P.J. and T.C.O'Connor. Size, Mobility and Charge of Multiply Charged Large Ions.—Proc. Roy. Irish Acad., A57(10):161—171. 1955.
(6)

Nordmann, Ch. Méthode pour l'enregistrement continu de l'état d'ionisation des gas.—Ionographe, C.r. Acad. Sci., Vol. 138:1418—1420. 1904a.
(25)

Nordmann, Ch. Enregistrement continu de l'ionisation gazeuse et de la radioactivité par les méthodes de déperdition.—C.r. Acad. Sci., Vol. 138:1596—1599. 1904b.
(25)

Norinder, H. Investigation with Regard to the Induced Charge from Electrical Fields on the Ebert Ion Counter.—Ark. mat. astron. och fys. 15, H1, No. 2:1—19. 1921.
(13)

Norinder, H. and R.Siksna. Mobility of Atmospheric Small Ions during Summer Night at Uppsala.—J. Atmos. and Terr. Phys., Vol. 4:93—105. 1953.
(30)

Obolensky, W.N. Über elektrische Ladungen in der Atmosphäre.—Ann. Physik, Vol. 77:644—666. 1925.
(11)

O'Connor, T.C. See Nolan, P.J.

O'Donnel, G.A. Electric Conductivity and Small Ion Concentration of the Atmosphere at One Metre above Ground and Conductivity at Ground Level.—J. Atmos. and Terr. Phys., Vol. 2(4):201—215. 1952.
(13)

O'Donnel, G.A. and V.F.Hess. A Comparative Study of Atmospheric Conductivity at Ground Level and One Meter Above Ground.—Arch. Meteorol. Geophys. und Bioklimatol., Vol. A4:351—367. 1951.
(34)

Onu, Const. See Vasiliu, Ch.

Orr, C. See Hinkle, B.L.

Ortner, G. and A.F.El Nadi. Intermediate and Large Atmospheric Ions at Cairo-Giza.—J. Atmos. and Terr. Phys., 7(1/2):31—39. 1955.
(9)

Oster, A.L. See Dolezalek, H.

Oster, A.L. and S.C.Coroniti. A Method of Measuring Electron and Ion Densities in the Region of 40—80 kilometers.—J. Geophys. Res., 73(13):4421—4424. 1968.
(A)

Oster, A.L. and H.Dolezalek. Laboratory Instrumentation for Testing and Calibration of in situ Probes for Lower Ionosphere, Mesosphere and Stratosphere.—Rev. Sci. Instrum., 37(4):407—411. 1966.
(A)

Pai, S.I. Viscous Flow Theory II—Turbulent Flow. Princeton a.o., D. Van Nostrand Company. 1957.
(20)

Paltridge, G.W. Experimental Measurements of the Small-Ion Density and Electrical Conductivity of the Stratosphere.—J. Geophys. Res., 70(12):2751—2761. 1965.
(4, 35)

Paltridge, G.W. Stratospheric Small-Ion Density Measurements from a High-Altitude Jet Aircraft.—J. Geophys. Res., 71(8):1945—1952. 1966.
(35)

Papp, M. See Stierstadt, K.

Parziale, A.J. See Callahan, R.C., Coroniti, S.C.

Patten, R. See Callahan, R.C., Coroniti, S.C.

Pedersen, A. Measurement of Ion Concentrations in the D Region of the Ionosphere with a Gerdien Condenser Rocket Probe.—Res. Inst. of Nat. Defence, Electr. Dep., Stockholm, Sweden, FOA—3—A607. 1964.
(A)

Pflügel, D. Über die Teilflächenmethode zur Bestimmung der Kapazität beliebiger Leiter.—Z. angew. Phys., 23(H2):89—94. 1967.
(33)

Phillips, B.B. A Discussion of the Sampling Problem during Aspiration Type Ionic Measurements.—Trans. Amer. Geophys. Union, 44(1):52—52. 1963.
(13)

Pluvinage, Ph. Etude théorique et experimentale de la conductibilité électrique dans les nuages nonorageux II.—Ann. géophys., Vol. 2:160—178. 1946.
(35)

Pollak, L.W. See Metnieks, A. L.
Prüller, P. and J. Reinet. Long-Term Investigations of Atmospheric Ionization in Tartu, Estonian SSR. — Int. J. Biometeorol., 10(2): 127—133. 1966.
(29, 30)
Ramsauer, C. See Lenard, P.
Ramsauer, C. — See Metnieks, A. L.
Reimers, H. Messungen der kleinen Ionen der Luft mit einem neuen Messgerät. — Berlin. 1944.
(20, 32)
Reinet, J. — see Reinet, Yu. A.
Reinet, J. Atmosfääri ionisatsiooni muutustest Tartus aastase perioodi vältel. — Tartu Riikliku Ülikooli Toimetised, Vol. 59:71—107. 1958.
(11)
Reinet, J., H. Tammet, and J. Salm. On the Methods of Counting Air Ions. — In: Biometeorology, Vol. 2:1037—1046, London, Pergamon Press. 1967.
(35)
Rich, T. A. The Average Size of Submicron Particles. — Internat. J. Air. Pollut., 1(4):288—292. 1959.
(4)
Richardson, L. F. Atmospheric Diffusion Shown on a Distance-Neighbour Graph. — Proc. Roy. Soc., Vol. A110: 709—737. 1926.
(20)
Riecke, E. Beiträge zu der Lehre von der Luftelektrizität. — Ann. Physik, Vol. 12:52—84. 1903.
(4)
Riedler, K. E. W. See Mitchell, J. N.
Riezler, W. and W. Kern. Ein Elektrofilter zur Abscheidung radioaktiver Aerosole. — Nukleonic, 1(5):191—195. 1959.
(0)
Rohmann, H. Methode zur Messung der Grösse von Schwebeteilchen. — Z. Phys., Vol. 17:253—265. 1923.
(0)
Rubin, T. R. See Lipscomb, W. N.
Rutherford, E. See Thomson, J. J.
Rutherford, E. Uranium Radiation and Electrical Conduction Produced by it. — Philos. Mag., Vol. 47:109—163. 1899.
(0, 25)
Sachy, P. J. See Nolan, J. J.
Sagalyn, R. C. See Callahan, R. C.
Sagalyn, R. C. and G. A. Faucher. Space and Time Variations of Charged Nuclei and Electrical Conductivity of the Atmosphere. — Quart. J. Roy. Meteorol. Soc., 82(354):428—445. 1956.
(30)
Sagalyn, R. C. and G. A. Faucher. Time Variations of Charged Atmospheric Nuclei. — In: "Artific. Stimulat. Rain," pp. 97—120. London — New York — Paris. 1957.
(30)
Salagyn, R. C. Space Electricity: Physical Problems and Experimental Techniques. — In: Probl. Atmos. Space Electr., pp. 548—565, Amsterdam a. o., Elsevier. 1965.
(A)

Saks, O. Automaatne fotograafiline ioonide loendaja. — Tartu Riikliku Ulikooli Toimetised, Vol. 42; 84—93. 1956.
Saks, O. See Saks, O. B.
Salles, E. Mesure de la conductibilité électrique de l'atmosphère à l'Observatoire de la Chambon-la-Forêt, 1939. — Ann. Inst. phys. globe Univ. Paris, Vol. 20:54—59. 1942.
(35)
Salm, J. See J. Reinet.
Salvador, O. and H. Masson. Enregistrement continu de la conductibilité ionique de l'air au voisinage du sol. — J. phys. et radium, 19(12):124A—128A, Suppl. 1958.
(35)
Sanders, J. K. See Jones, O. C.
Sänger, R. See Junod, A.
Schaffhauser, J. Messung von kurzperiodigen Schwankungen der Luftionisation. — Arch. Meteorol. Geophys. und Bioklimatal., A., Vol. 5:179—186. 1952.
(25, 30)
Schiller, L. Strömung in Rohren. — Handbuch Experimentalphysik Wien—Harms, 4(4): 1—207, Leipzig, Akad. Verlagsges, M. B. H. 1932.
(34)
Schilling, G. T. and J. Carson. On the Electrical Conductivity of Air Inside Buildings. — Arch. Meteorol. Geophys. und Bioklimatol., Vol. 5:52—58. 1953.
(30)
Schlichting, H. Entstehung der Turbulenz. — In: Handbuch der Physik, Vol. 8/1, Strömungmechanik 1, Berlin u. a., Springer. 1959.
(34)
Schmeer, H. See Hock, A. and R. Siksna.
Schmeer, H. R. Untersuchung über die Messbarkeit der elektrischen Leitfähigkeit und der Dichte der Kleinionen in der Atmosphäre. — Arch. Techn. Messen, Vol. 361:31—36, 55—56. 1966.
(9, 13, 14, 32, 33)
Scholz, J. Über die Messmethoden der elektrischen Leitfähigkeit der Atmosphäre. — Phys. Z., Vol. 32:130—139. 1931a.
(13)
Scholz, J. Gegenfelduntersuchungen und Beweglichkeitsmessung kleiner Ionen. — Gerlands. Beitr. Geophys. Vol. 29:226—238. 1931b.
(4, 14, 15)
Scholz, J. Luftelektrische Messungen auf Franz-Josephs-Land während des II internationalen Polarjahres 1932—1933. — Trudy Arkticheskogo Instituta, Vol. 6:1—169. 1935.
(14)
Schön, R. W. See Knoll, M.
Schulz, L. See Israël, H.
Sekiyama, M. The Measurement of the Aerosol by Using an Ion-Detector. — J. Fac. Ibaraki Univ., 7(3):81—84. 1959.
(4)
Seymour, D. W. See Coroniti, S. C.
Sheppard, P. A. Character of Atmospheric Ionisation. — Nature, Vol. 129:169—169. 1932.
(30)

Sherman, K. L. See Gish, O. H.
Shimizu, T. Dissipation Coefficient of Electricity of Fine Wire.— Mem. Fac. Liber. Arts Fakui Univ., Ser. 1, No. 6:43—50. 1956.
(4)
Shimizu, T. Distribution of Ions Around Charged Fine Wires. — J. Geomagn. and Geolectr., 9(2):116—118. 1957.
Shimizu, T. A Study on the Capture of Atmospheric Ions by Charged Wire Rings.— Mem. Fac. Liber. Arts Fukui, Univ., Ser. 2, Part 4, No. 10:81—117. 1960.
(4)
Siegmann, H. Chr. See Hasenclever, D.
Siksna, R. See Norinder, H.
Siksna, R. Measurements of Large Ions in the Atmospheric Air at Uppsala.— Ark. geofys., Vol. 1 : 483—518. 1950.
(5, 14)
Siksna, R. Some Topics Concerning Experimental Investigation of Air Ions.— Proc. Internat. conf. ioniz. air, Philadelphia, Pa., Sect. 9, Vol. 1:25. 1961a.
(4, 25, 35)
Siksna, R. An Ionometric Counter for Condensation Nuclei.— Geofis. pura e appl., Vol. 50:23—36. 1961b.
(4)
Siksna, R. and J. Eichmeier. Fluctuations in the Concentration of Artificially Produced Air Ions in Closed Room.— Ark. geofys., Vol. 3:299—313. 1961.
(30)
Siksna, R. and J. Eichmeier. Continuous Recording of Small Air Ions in Closed Rooms.— Ark. geofys., 4(6)563—576. 1966.
(35)
Siksna, R. and Ya. Lindsay. Air Ions Produced by a Tritium-ion Generator. II. Measurement of Ions in a Room. Mobility. — Ark, geofys., Vol. 3:141—154. 1961.
Siksna, R. and A. Metnieks. Aufladung eines isolierten Rohrs bei Durchströmen von ionisierter Luft und Adsorption der Ionen.— Z. angew. Phys., 5(12):454—461. 1953.
(16, 20, 24)
Siksna, R. and H. Schmeer. On the Recording of Rapidly Fluctuating Concentrations of Air Ions.— Ark. geofys., Vol. 3:315—330. 1961.
(30)
Spencer, N. W. See Hok, G.
Steinmauer, R. See Weiss, R.
Stergis, C. G. See Coroniti, S. C.
Stierstadt, K. and M. Papp. Aerosole als Träger der natürlichen Radioaktivität.— Atomkernenergie, 5(12):459—481. 1960.
(0)
Stschepotjewa, E. S. See Baranow, W. J. and E. C. Shchepot'eva.
Sturdivant, J. H. See Lipscomb, W. N.
Swann, W. F. G. The Measurement of Atmospheric Conductivity, Together with Certain Remarks on the Theory of Atmospheric Radioactive Measurements.— Terr. Magn. and Atmos. Electr., Vol. 19:23—37. 1914a.
(4)

Swann, W. F. G. The Theory of Electrical Dispersion into the Free Atmosphere, with the Discussion of the Theory of the Gerdien Conductivity Apparatus, and of the Theory of the Collection of Radioactive Deposit by a Charged Conductor.— Terr. Magn. and Atmos. Electr., Vol. 19:81—92. 1914b.
(4, 33)
Swann, W. F. G. On Certain New Atmospheric-electric Instruments and Methods.— Terr. Magn. and Atmos. Electr., Vol. 19:177—185. 1914c.
(14, 25, 32, 35)
Swann, W. F. G. On Certain Matters Relating to the Theory of Atmospheric-electric Measurements.— Terr. Magn. and Atmos. Electr., Vol. 19: 205—218. 1914d.
(4, 13)
Swann, W. F. G. The Theory of the Action of the Earth's Potential-gradient in Measurements with the Ebert Ion-counter.— Phys. Rev., Vol. 21: 449—455. 1923.
(13)
Takeuti, T., H. Ishikawa, and A. Iwata. Preliminary Balloon Measurement of Negative Small Ion Density.— J. Geomagn. Geoelectr., 18(4):493—494. 1966.
(35)
Tammet, H. See Reinet, J. and H. F. Tammet.
Thams, J. Chr. See Junod, A.
Thellier, O. Mésure de la conductibilité électrique de l'air par une mèthode de zero.— C. r. Acad. Sci., 196(22):1684—1686. 1933.
(35)
Thellier, O. Mésure de la conductivité électrique de l'air à Paris.— Ann. Inst. phys. globe Univ. Paris, Vol. 14:71—76. 1936.
(35)
Thellier, O. Sur l'ionisation de l'air dans une atmosphère pure (campagne) et polluée (grande ville).— Ann. Inst. phys. globe Univ. Paris, Vol. 19:107—179. 1941.
(35)
Thomson, J. J. and E. Rutherford. On the Passage of Electricity through Gases Exposed to Röntgen Rays.— Philos. Mag., Vol. 72: 392—407. 1896.
(0, 1, 25)
Thomson, W. Courants terrestres et électricité atmosphèriqué.— Conf. internat. pour la détermination des unités électriques, 16—26 Oct. 1882. Procés-verbaux, Paris, pp. 84—91. 1882.
(11)
Torreson, O. W. Instruments Used in Observations of Atmospheric Electricity.— In: Terr. Magn. and Electr. New York, pp. 231—269. 1949.
(35)
Torreson, O. W. and G. R. Wait. Measurements of Total Nuclei, of Uncharged Nuclei and of Large Ions in the Free Atmosphere at Washington.— Terr. Magn. and Atmos. Electr., Vol. 39:47—64. 1934.
(35)
Torreson, O. W. See Wait, G. R.

Townsend, J.S. Electrical Properties of Newly Prepared Gases.—Philos. Mag., Vol. 45:125—151. 1898.
(1, 2)

Uchikawa, K. On the Improvement of the Atmospheric Radiosonde.—Geophys. Mag., Vol. 31:705—714. 1963.
(35)

Uchikawa, K. Atmospheric Electricity Radiosondes for the IQSY.—Geophys. Mag., 33(2):163—177. 1966.
(35)

Uchikawa, K. See Hatakeyama, H.

Ulsamer, J. Wärmeabgabe eines Drahtes oder Rohres an einem senkrecht zur Achse strömenden Gas- oder Flüssigkeitsstrom. — Forsch. Geb. Ingenieurwesens, Vol. 3:94— 98. 1932.
(24)

Vasiliu, Ch., N. Calinicenco, Const Onu. Determinări de conductibilităti ale aerului in regiuni de munte.—Bul. stiint. Acad. RPR Sec. mat. şi fiz., 6(2):397—405. 1954.
(35)

Vasiliu, Ch., N. Calinicenco, and V. Mateiciuc. Contributiuni relativ la metodele intrebuintate in măsurarea conductibilităţii electrice a aerului. — Bul. Inst. Politehn. Iasi, 2(1/2):67— 80. 1956.
(35)

Venkiteshwaran, S.P. Measurement of the Electrical Potential Gradient and Conductivity by Radiosonde at Poona, India. — In: Recent Advances in Atmospheric Electricity, pp. 89—100, London—New York—Paris—Los Angeles, Perg. Press. 1958.
(35)

Venkiteshwaran, S.P., B.K. Gupta, and B.B. Huddar. Measurement of the Electrical Conductivity in the Upper Air by Radiosonde.—Proc. Indian Acad. Sci., A, 38(2):109—115. 1953.
(35)

Vogler, G. Über den Einfluss eines Emissionseffektes auf das Messergebnis der elektrischen Leitfähigkeit der Luft. — Geofis. pura e appl., Vol. 43:250—254. 1959.

Vogler, G. Einfluss der Auflagerung radioaktiver Substanzen an Aerosole auf den Emissionseffekt bei der Messung der elektrischen Leitfähigkeit der Luft. —Z. Naturforsch., a15(1):89—89. 1960.
(13)

Vonnegut, B. See Moore, C.B.

Wait, G.R. Report on Ion-Counters, Methods of Use and Results.—C.r. Assemblée de Lisbonne, 1933.—Union Géod. Géophys. Internat. Ass. Magn. Electr. Terr. Bull., No. 9:143—147, Copenhagen. 1934.
(13, 20)

Wait, G.R. and O.W. Torreson. The Large-ion and Small-ion Content of the Atmosphere at Washington.—Terr. Magn. and Atmos. Electr., 39(2):111—119. 1934.
(35)

Wait, G.R. See Torreson, O.W.

Weger, N. Eine Verbesserung der Methodik der Kleinionen—Zählung.—Phys. Z., Vol. 36:15—20. 1935a.
(4, 25)

Weger, N. Über einige bei Ionenmessungen mit Zylinderkondensatoren auftretende Störungen.—Gerlands Beitr. Geophys., Vol. 45:195—201. 1935b
(28)

Weiss, R. and R. Steinmauer. Messungen der Luftionen.—In: Innsbruck. Gerlands Beitr. Geophys., Vol. 50:238—251. 1937.
(25)

Werme, J.V. See Coroniti, S.C.

Whipple, E.C. An Improved Technique for Obtaining Atmospheric Ion Mobility Distributions.—J. Geophys. Res., 65(11):3679—3684. 1960.
(7)

Whipple, E.C. See Bordeau, R.E.

Whitby, K.T. and W.E. Clark. Electric Aerosol Particle Counting and Size Distribution Measuring System for the 0.015 to 1 m Size Range.—Tellus, 18(2/3):573—586. 1966.
(35)

Whitby, K.T. and A.Ya. McFarland. The Decay of Unipolar Small Ions and Homogeneous Aerosols in Closed Spaces and Flow Systems.—Proc. Internat. Conf. Ioniz. Air, I. Sect. 7, Philadelphia, Pa. 1961.
(2)

Wiedemann, G. Die Lehre von der Elektrizität, Vol. 4, Sect. 2—Braunschweig, Vieweg und Sohn. 1885.
(1, 25)

Wigand, A. Measurements of the Electrical Conductivity in the Free Atmosphere up to 9000 Meters in Height.—Terr. Magn. and Atmos. Electr., Vol. 19:93—101. 1914.
(35)

Wigand, A. Aerophysikalische Forschungen mit dem Flugzeuge.—Naturwissenschaften, Vol. 7:487—491. 1919.
(35)

Wigand, A. Messungen der Ionisation und Ionenbeweglichkeit bei Luftfahrten.—Phys. Z., Vol. 22:36—46. 1921.
(35)

Wilkening, M.H. Natural Radioactivity as a Tracer in the Sorting of Aerosols According to Mobility.—Rev. Sci. Instrum., Vol. 23:13—16. 1952.
(0)

Wilkening, M.N., M. Kawano, and C. Lane. Rodondaughter Ions and their Relation to Some Electrical Properties of the Atmosphere.—Tellus, 18(2/3): 679—684. 1966.
(0)

Woessner, R.H., W.E. Cobb, and R. Gunn. Simultaneous Measurements of the Positive and Negative Light-ion Conductivities to 26 Kilometers.—J. Geophys. Res., 63(1):171—180. 1958.
(35)

Wolodkewitsch, N. Über die elektrische Diffusion der Ionen in Gasen bipolarer Beladung.—Z. Phys., Vol. 84:593—609. 1933a.
(2)

Wolodkewitsch, N. Untersuchungen über die "elektrische Diffusion" der Ionen in Gasen unipolarer Beladung.—Ann. Physik, Vol. 16: 7—43. 1933b.
(2)

Wolodkewitsch, N. and F. Dessauer. Weitere Entwicklung der Apparatur zur Erzeugung unipolar beladener Luftströmung und Messung der Luftladungsdichte. — In: Zehn Jahre Forschung auf dem physikalischmedizinischen Grenzgebiet, pp. 34—51, Leipzig, Verlag G. Thieme. 1931a.
(35)

Wolodkewitsch, N. and F. Dessauer, Beweglichkeit und Grösse der Ionen. — In: Zehn Jahre Forschung auf dem physikalischmedizinischen Grenzgebiet, pp. 52—81, Leipzig, Verlag G. Thieme. 1931b.
(20, 35)

Yaita, T. and M. Nitta. The Effects of Turbulence upon the Measurements of Atmospheric Ions. — Bull. Electrotechn. Lab., 19(4):272—284, 308. 1955.
(20, 21, 34)

Young, W. M. Mobility of the Ions in the Corona Discharge. — Phys. Rev., Vol. 28:129—141. 1926.
(35)

Yunker, E. A. The Mobility Spectrum of Atmospheric Ions. — Terr. Magn. and Atmos. Electr., 45(2):127—132. 1940.
(32, 35)

Zelenyi, J. On Air Electrified by the Discharging Action of Ultra-violet Light. — Philos. Mag., Vol. 45:272—273. 1898a.
(11)

Zelenyi J. On the Ratio of the Velocities of the Two Ions Produced in Gases by Röntgen Radiation, and on Some Related Phenomena. — Philos, Mag., Vol. 46:120—154. 1898b.
(6, 7)

Zelenyi, J. The Velocity of the Ions Produced in Gases by Röntgen Rays. — Philos. Trans. Roy. Soc., A, Vol. 195:193—234. 1901.
(0, 7, 25)

Zelenyi, J. The Distribution of Mobilities of Ions in Moist Air. — Phys. Rev., Vol. 34:310—334. 1929.
(8, 19)

LIST OF USSR ABBREVIATIONS APPEARING IN THE BIBLIOGRAPHY

Abbreviation	Full name (transliterated)	Translation
AN SSSR	Akademiya Nauk SSSR	Academy of Sciences of the USSR
Dokl.	Doklady	Proceedings
Izd.	Izdatel'stvo	Publishing House
Izv.	Izvestiya	Bulletin
MGU	Moskovskii Gosudarstvennyi Universitet	Moscow State University
NIU GMS SSSR	Nauchno-Issledovatel'skoe Upravlenie Gidrometeorologicheskoi Sluzhby SSSR	Scientific Research Board of the Hydrometeorological Service of the USSR
ZhRFKhO	Zhurnal Russkogo Fiziko-Khimicheskogo Obshchestva	Journal of the Russian Physicochemical Society